Development of biochemical tools to characterise human H3K27 histone demethylase JmjD3



Ka Hing Che

Wolfson College

Nuffield Department of Orthopaedics,

Rheumatology and Musculoskeletal Sciences

University of Oxford

Thesis submitted for the degree of Doctor of Philosophy

Trinity Term, 2013

Development of biochemical tools to characterise human H3K27 histone demethylase JmjD3

Ka Hing Che

Wolfson College

Nuffield Department of Orthopaedics, Rheumatology and Musculoskeletal Sciences

Abstract

Covalent modifications of histone tails play essential roles in mediating chromatin structure and epigenetic regulation. JmjD3 is a JumonjiC domain containing histone demethylase, belongs to the KDM6 subfamily, and catalyses the removal of methyl groups on methylated lysine 27 on histone 3 (H3K27), a critical mark to promote polycomb mediated repression and gene silencing. The importance of JmjD3 has been implicated in development, cancer biology and immunology.

In this thesis, I report the recombinant production of active human JmjD3, development of two in vitro screening assays, a cell-based assay, and structural determination of JmjD3 in complex with the inhibitor 8-hydroxy-5-carboxyquinoline (8HQ). A highly selective and potent small molecule inhibitor GSK-J1 was subsequently identified. The inhibitor is active in HeLa cells and promotes a dose-dependent increase of global H3K27 methylation.

The inhibitor GSK-J1 was used in two different cell assay systems related to inflammation and differentiation, to understand how H3K27 demethylation controls cellular functions.

By inhibiting H3K27me3 demethylation, it is demonstrated that tumor necrosis factor (TNF) and other pro-inflammatory cytokines are regulated by H3K27 demethylase inhibition in M1- type macrophages derived from healthy volunteers and rheumatoid arthritis patients. It is also shown that inhibition of H3K27me3 demethylation abrogates cellular fusion of M2- type macrophages.

During RANKL induced osteoclast differentiation, JmjD3 is up-regulated and promotes the expression of the key transcription factor NFATc1. By inhibiting JmjD3, NFATc1 expression is reduced and osteoclastogenesis is inhibited. This mechanism demonstrates a novel anti-resorptive principle of potential utility in conditions of excess bone resorption such as osteoporosis, bone erosion in inflammatory arthritis or cancer of the bone.

These experiments further resolve the ambiguity between scaffold and catalytic function associated with the H3K27 demethylase in these biological systems, and demonstrate that its enzymatic activity is crucial for epigenetic regulation of macrophage and osteoclast function.

Acknowledgements

This dissertation would not have been possible without the help, support and guidance of many people. My greatest thanks to my supervisor Professor Udo Oppermann, whose expertise, guidance and generous support have enabled me to achieve the works in this thesis. From the initial structural studies of JmjD3 to the identification of its inhibitors, and application of the inhibitors to various cell-based systems, these would not have been happened without his support and guidance. I am also indebted to my co-supervisor Dr. Wyatt Yue who spent a lot of time to review my written work, taught me crystallography techniques and encouraged me during my DPhil studies.

I thank Professor Chris Schofield, Dr. Susanne Muller-Knapp, Dr. David Wilson and Dr. Laurens Krudiener for their support in the JmjD3 inhibitor project. Thank to Dr. Fernando Martinez for his teachings in macrophage and microarray analysis.

I am grateful to the following people for their support and friendship in the lab: Dr. Peter Cain, Ms Kelly Rooke, Ms Anneke Kramm, Mr Laurynas Pliuskys and Dr. James Dunford in Udo's team. Dr. Stan Ng, Ms Carina Gileadi, Ms Michelle Daniel, Dr. Grazyna Kochan and Ms Alice Grabbe in Structural Genomics Consortium (Oxford). Special thank to Dr. Clarence Yapp for being a good friend and company in many late nights' lab work.

I would like to express my gratitude and appreciation to the scientists in the Botnar Institute, Structural Genomics Consortium (Oxford), GlaxoSmithKline (Stevenage, UK) and Institut Génétique Biologie Moléculaire Cellulaire (Strasbourg) who taught and helped me during my DPhil studies.

I cannot thank these people enough for their friendship and love: Hin Lun Chu, Christine Yan, Bolton Chau, Lincoln Tsui, Petrina Lau, Chris Choy, Tony Chan, Paul Luk, Sunny Wong, Karven Kwan, Wendy Chan and so many people who are not named here. For they have given me wonderful memory in the beautiful and historical town of Oxford.

Lastly, I would like to thank my parents Mr Chung Po Che and Ms Yau Lai Fung, and my sister Ms Kai Yin Che for their incessant love and confidence in my abilities. From them I have the strength to complete this DPhil, and strived to make the world a better place.

Attributions

The compound collections used for inhibition studies in this thesis were collected and managed at Structural Genomic Consortium (SGC). Routine JmjD3 inhibitor screening was performed by Anthony Tumber.

The crystallography team in SGC helped in data collection and structure determination of JmjD3 in the studies. I thank Wyatt Yue and Tobias Krojer for their help in crystallography.

The specific JmjD3 inhibitor GSK-J1 was identified by GlaxoSmithKline, and further characterized by myself and SGC. I thank John Liddle and David Wilson for their work in the chemistry of GSK-J1; Laurens Kruidenier, Palwinder Mander, Julia Smith and Catriona Sharp for their work in the macrophages studies; Chun-wa Chung and her crystallography team in producing the JmjD3/GSK-J1 complex structure; Zhongjun Cheng and Dinshaw Patel for their contribution to the JmjD3/H3K27me3-peptide structure.

For osteoclast studies, quantitation of resorption pits on dentin discs was performed by Clarence Yapp. Scanning electron microscopy images were produced by Nick Athanasou.

Healthy donor blood was sourced ethically, collected and used in accordance with the terms of the informed consents. Blood from rheumatoid arthritis patients was obtained under the NHS ethical permission COREC06/Q1606/139 ("Immune function in inflammatory arthritis") and informed consent was obtained from all patients.

Associated Publications

Che, K.H., Martinez, F.O., Yapp, C., Cain, P., Wells, G., Rooke, K., Kashima, T., Kruidenier, L., Prinjha, Rab., Gordon, S., Gronemeyer, H., Athanasou, N., Oppermann, U. Histone H3K27me3 demethylases control RANKL and IL-4 programs required for formation and function of human osteoclasts and giant cells . *Manuscript in preparation.*

Hopkinson, R. J, Tumber, A., Yapp, C., Chowdhury, R., Aik, W., **Che, K. H.**, Li, X. S., Kristensen, J. B. L., King, N. F., Chan, M. C., Yeoh, K. K., Choi, H., Walport, L. J., Thinnes, C. C., Bush, J. T., Lejeune, C., Rydzik, A. M., Rose, N. R., Bagg, E. A., McDonough, M. A., Krojer, T., Yue, W. W., Ng, S. S, Olsen, L., Brennan, P. E., Oppermann, U., Muller-Knapp., S., Klose, R. J., Ratcliffe, P. J., Schofield, C. J., Kawamura, A. 5-Carboxy-8-hydroxyquinoline is a Broad Spectrum 2-Oxoglutarate Oxygenase Inhibitor which Causes Iron Translocation. *Journal of the American Chemical Society*, in press.

Kruidenier, L.*, Chung, C.-w.*, Cheng, Z.*, Liddle, J.*, **Che, K.H.***, Joberty, G., Bantscheff, M., Bountra, C., Bridges, A., Diallo, H., Eberhard, D., Hutchinson, S., Jones, E., Katso, R., Leveridge, M., Mander, P. K., Mosley, J., Ramirez-Molina, C., Rowland, P., Schofield, C. J., Sheppard, R. J., Smith, J. E., Swales, C., Tanner, R., Thomas, P., Tumber, A., Drewes, G., Oppermann, U., Patel, D. J., Lee, K., and Wilson, D. M. (2012). A selective jumonji H3K27 demethylase inhibitor modulates the proinflammatory macrophage response. *Nature*, 488(7411):404408.

* Equally contributing authors.

Rose, N. R., Woon, E. C. Y., Tumber, A., Walport, L. J., Chowdhury, R., Li, X. S., King, O. N. F., Lejeune, C., Ng, S. S., Krojer, T., Chan, M. C., Rydzik, A. M., Hopkinson, R. J., **Che, K. H.**, Daniel, M., Strain-Damerell, C., Gileadi, C., Kochan, G., Leung, I. K. H., Dunford, J., Yeoh, K. K., Ratcliffe, P. J., Burgess-Brown, N., Von Delft, F., Müller, S., Marsden, B., Brennan, P. E., Mcdonough, M. A., Oppermann, U., Klose, R. J., Schofield, C. J., and Kawamura, A. (2012). Plant Growth Regulator Daminozide Is a Selective Inhibitor of Human KDM2/7 Histone Demethylases. *Journal of Medicinal Chemistry*, 55(14):66396643.

Luo, X., Liu, Y., Kubicek, S., Myllyharju, J., Tumber, A., Ng, S., **Che, K. H.**, Podoll, J., Heightman, T. D., Oppermann, U., Schreiber, S. L., and Wang, X. (2011). A selec- tive inhibitor and probe of the cellular functions of Jumonji C domain-containing histone demethylases. *Journal of the American Chemical Society*, 133(24):94519456.

Contents

Acknowledgements **2**

Attributions **3**

Associated publications **4**

1 Introduction **15**

1.1 Epigenetics: an introduction . . . 15

1.2 The structure of chromatin . . . 16

1.3 Histone Demethylases and JmjD3 . . . 18

1.3.1 Peptidyl arginine deiminase . . . 18

1.3.2 Lysine demethylases . . . 19

1.4 Transcriptional regulation by JmjD3 . . . 20

1.5 Role of JmjD3 in health and disease . . . 23

1.5.1 Role of JmjD3 in development . . . 23

1.5.2 Role of JmjD3 in inflammation . . . 25

1.5.3 Role of JmjD3 in cancer . . . 26

1.6 Small molecule inhibitors of KDM enzymes . . . 27

1.7 Aim and outline of the thesis . . . 32

2 Cloning, Expression and Purification of JmjD3 **33**

2.1 Introduction . . . 33

2.2 Cloning . . . 33

2.3 Expression . . . 34

2.4 Purification of JmjD3-c023 . . . 37
2.5 Purification of JmjD3-c031 . . . 39
2.6 Conclusion . . . 42

3 Development of in vitro assay platforms for identification of selective JmjD3 inhibitors 43

3.1 Introduction . . . 43
3.1.1 Immunodetection assay . . . 43
3.1.2 Matrix-Assisted Laser Desorption/Ionization Time Of Flight (MALDI-TOF) mass spectrometry . . . 45
3.1.3 Formaldehyde dehydrogenase (FDH) coupled assay . . . 47
3.2 Differential Scanning Fluorimetry . . . 47
3.2.1 DSF screening of a focused library of oxygenase inhibitors . . . 48
3.3 Amplified Luminescent Proximity Homogeneous Assay . . . 53
3.3.1 Screening results from AlphaScreen . . . 56
3.4 Correlation between DSF and AlphaScreen data . . . 59
3.5 Inhibition of UTX by GSK-J1 . . . 59
3.6 Summary . . . 61

4 Structure determination of JmjD3 62

4.1 Introduction . . . 62
4.2 Crystallisation and structure determination of JmjD3 . . . 62
4.3 Overall structural description . . . 64
4.4 Comparison of JmjD3-c023 with JmjD3-GSK . . . 67
4.5 Comparison with UTX structure . . . 69
4.6 Substrate recognition . . . 72
4.7 Structural basis for specificity of the GSK-J1 inhibitor . . . 75
4.8 Structural basis of GSK-J1 specificity towards JmjD3. . . . 77
4.9 Summary . . . 78

5 Development of a high-content imaging platform for screening of JmjD3 inhibitors 80

5.1 Introduction 80

5.2 Overexpressing JmjD3 in mammalian cells 81

5.2.1 Transient expression of JmjD3 in mammalian cells 81

5.2.2 Stable transfection of JmjD3 in mammalian cells 84

5.3 Quantification of Fluorescence intensity 86

5.4 Screening of JmjD3 inhibitors 90

5.5 Summary 93

6 H3K27 demethylase inhibitors as chemical tools to understand macrophage biology 94

6.1 Introduction 94

6.1.1 Chromatin modification and control of macrophage functions 95

6.2 Epigenetic regulation of M1 macrophage 97

6.2.1 Molecular pathways of M1 macrophage activation 97

6.2.2 Effect of JmjD3 inhibitors on classically activated macrophages 98

6.2.3 Effect of JmjD3 inhibitor on chronically activated macrophages 101

6.3 Epigenetic regulation of M2 macrophage 104

6.3.1 Molecular pathways of M2 macrophage fusion 104

6.3.2 Effect of H3K27 demethylase inhibition in alternatively activated macrophages 104

6.3.3 Gene expression studies in M2 macrophages 105

6.4 Summary 109

7 H3K27 demethylase inhibition as novel anti-resorptive mechanism in osteoclast function 110

7.1 Overview of bone remodelling 110

7.2 Osteoclast biology and NFATc1 pathways 111

7.3 Generation of active human osteoclasts in cell culture 113

7.4 Defining osteoclast criteria in cell culture 114

7.5 Effect of KDM6 demethylase inhibition in osteoclast differentiation 114

7.5.1 Morphology and osteoclast numbers . . . 114
7.5.2 Bone resorption . . . 117
7.6 Comparison with other known anti-resorptive mechanisms . . . 119
7.7 Microarray analysis . . . 121
7.7.1 Early RANKL stimulation (Day 8) . . . 121
7.7.2 Differentiating osteoclasts (Day 14) . . . 123
7.7.3 Mature osteoclasts . . . 124
7.8 Chromatin analysis . . . 129
7.9 Conclusion . . . 132

8 Discussion and future perspectives **133**

9 Materials and Methods **140**

9.1 Cloning . . . 140
9.1.1 Ligation independent cloning (LIC) of JmjD3 into pNIC28 vector . . . 140
9.1.2 Cloning of Flag-JmjD3 into pcDNA5/FRT/TO vector . . . 140
9.1.3 Transformation of plasmid into competent cell XL-1 (Blue) or BL21(DE3) . . . 141
9.1.4 Screening of colonies by restriction digestion analysis . . . 141
9.2 Expression of JmjD3 in *E.coli* . . . 141
9.3 Purification of JmjD3 expressed in *E.coli* . . . 142
9.3.1 Cell lysis . . . 142
9.3.2 Immoblized metal affinity chromatography (IMAC) . . . 142
9.3.3 JmjD3-c023 ion-exchange chromatography . . . 142
9.3.4 JmjD3-c031 ion exchange chromatography . . . 142
9.3.5 Size exclusion Chromatography . . . 143
9.4 Crystallization and structure determination of JmjD3 . . . 143
9.5 Differential scanning fluorimetry . . . 144
9.6 MALDI-TOF mass spectrometry . . . 144
9.7 AlphaScreen . . . 145
9.8 Immunofluorescence (IF) assay . . . 145

9.9 Macrophage experiments . . . 146
9.9.1 M1 macrophage cell culture . . . 146
9.9.2 M2 macrophage cell culture . . . 146
9.10 Osteoclast methods . . . 147
9.10.1 Osteoclast cell culture . . . 147
9.10.2 Immunofluorescence microscopy . . . 147
9.10.3 TRAP and Bone resorption assays . . . 147
9.10.4 Quantification of collagen fragments . . . 148
9.11 RNA isolation, Reverse Transcription and Real-Time Quantitative PCR (qPCR) . . . 148
9.12 Chromatin Immunoprecipitation (ChIP) Assay . . . 149

References **150**

Appendices **175**

List of Figures

1.1 Organization of DNA in eukaryotic cell. 17

1.2 Cartoon representation of a nucleosome showing DNA 17

1.3 Mechanism of arginine demethylation by Peptidyl arginine deiminase. 19

1.4 Mechanism of lysine demethylation by lysine specific demethylase 1. 19

1.5 Mechanism of lysine demethylation by JmjD3. 20

1.6 Nomenclature, domain architecture and substrate specificity of the KDM family. . . . 21

1.7 Schematic diagram showing a model of transcription regulation by JmjD3 at the transcription start site. 22

1.8 a) Chemical structures of reported KDM inhibitors. 29

1.8 b) Chemical structures of reported KDM inhibitors. 30

1.8 c) Chemical structures of reported KDM inhibitors. 31

2.1 Schematic diagram showing 25 subcloned JmjD3 constructs emcompassing the JmjC domain 34

2.2 Purification of JmjD3-c023. 38

2.3 Purification of JmjD3-c031. 41

3.1 44

3.2 Domain boundary of JmjD3-c023 and JmjD3-c031 45

3.3 Demethylase activity of JmjD3-c023 and JmjD3-c031 - Mass Spectrometry 46

3.4 Principle of formaldehyde dehydrogenase (FDH)-coupled assay 47

3.5 Differential scanning fluorimetry assay 49

3.6 Comparison of T_m shift values of JmjD3-c023 and JmjD3-c031 towards 8HQ 49

3.7 Bar graph showing 37 compounds having T_m shifts of more than 2°C. 51
3.8 Chemical structures of a selected panel of compounds having T_m shifts of more than 2°C in DSF screen 52
3.9 Heat map highlighting five compounds from DSF screen with selectivity towards JmjD3 against other histone demethylases. 52
3.10 Comparison of T_m shift values of JmjD3-c023 and JmjD3-c031 towards 8HQ 53
3.11 Specificity of anti-H3Kme2 to peptides of different methylation states. 54
3.12 Formation of H3K27me2 product over time under different concentration of JmjD3 enzyme. 55
3.13 Potent compounds identified from AlphaScreen 57
3.14 Chemical structures of 10 compounds having lowest IC_{50} values by in the library screen by AlphaScreen. 58
3.15 Heat map showing IC_{50} values of selected compounds against different class of histone demethylases 58
3.16 Scatter plots showing T_m shift values from DSF assay versus IC_{50} values from AlphaScreen assay. 59
3.17 Inhibition of UTX by GSK-J1 60

4.1 JMJD3 crystals 64
4.2 Cartoon representation of JmjD3 JmjC domain 65
4.3 JmjD3-c023 active site. 66
4.4 Comparison of JmjD3-c023 with JmjD3-GSK 68
4.5 Comparison of JmjD3 and UTX. 71
4.6 Substrate recognition of H3K27me3 peptide by JmjD3 and UTX. 74
4.7 Structural basis for specificity of the GSK-J1 inhibitor. 76
4.8 Structural basis of GSK-J1 specificity towards JmjD3 as compared with other histone demethylases. 78

5.1 Cloning of Flag-JmjD3 mammalian expression construct. 82
5.2 Treatment of Flag-JmjD3 transfection complex in HeLa cells. 83

5.3 Excitation and Emission spectra of DAPI, Alex Fluor 488 , Alex Fluor 594. 84
5.4 Transient transfection of Flag-JmjD3 in HeLa cells. 85
5.5 Stable transfection of Flag-JmjD3 in HeLa cells. 86
5.6 Flow chart of the image quantification process. 88
5.7 Fluorescence intensities of Flag-JmjD3 transfected cells. 89
5.8 Chemical structures of JmjD3 inhibitors tested in the immunofluorescence assay. . . . 91
5.9 Dose responsive plot of JmjD3 inhibitors tested in the Immunofluorescence Assay. . . 92

6.1 Mechanisms of macrophage polarization. 96
6.2 Toll Like Receptor Activation. 97
6.3 LPS induces JmjD3 expression in human macrophage 98
6.4 Effect of JmjD3 inhibitors on primary human macrophages in classically activated pathway. 100
6.5 Effects of GSK-J4 and GSK-J5 on macrophages derived from peripheral blood of rheumatoid arthritis patients. 102
6.6 ChIP analysis of the association of H3K27me3with the TNFα transcription start site in LPS-stimulated human primary macrophages. 103
6.7 Effect of JmjD3 inhibitors on IL-4 induced giant cell formation. 105
6.8 Gene expression studies in M2 macrophages. 106
6.9 Quantitative PCR analysis of a panel of genes implicated in M2 macrophage functions. 108

7.1 Bone remodelling 111
7.2 Morphology of osteoclast under GSK-J4 treatment. 116
7.3 GSK-1 inhibits bone resorption. 118
7.4 Comparison of GSK-J4 with known anti-resorptive compounds. 121
7.5 An overview of the experimental procedure with activities indicated. 121
7.6 Osteoclast microarray analysis 123
7.7 Venn diagram showing number of genes regulated by RANKL and GSK-J4. 123
7.8 Gene expression analysis of key osteoclast development genes. 129
7.9 NFATc1 ChIP-qPCR 130

7.10 Chromatin analysis of selected osteoclast genes. 131

9.1 Effect of temperature and different constructs to the solubility of JmjD3 177

Chapter 1

Introduction

1.1 Epigenetics: an introduction

The word "Epigenetics" was coined by C.H. Waddington in 1942 , to initially describe the causal mechanism how genes give rise to different phenotypes (Waddington, 1957). However, the definition of epigenetics has changed over the last half century and is now used to describe how cells with the same genotype exhibit different phenotypes for many generations (Berger et al., 2009). Nowadays, the definition of epigenetics is specific and described as "the study of mitotically and/or meiotically heritable changes in the gene function that can not be explained by changes in DNA sequence" (Russo, 1996); or similarly "An epigenetic trait is a stably heritable phenotype resulting from changes in a chromosome without alterations in the DNA sequence" (Berger et al., 2009). The definition of epigenetics is still not uniformly agreed upon, and many researchers use the term loosely to describe nearly any chromatin mechanism that somehow relates to the coordination and regulation of gene transcription, DNA repair or nuclear function, and involves DNA, histone or chromatin protein modifications, as well as non-coding RNAs. Whatever the precise definition is, epigenetics offers possibly important clues to understand the interactions between genetic make-up of an individual, environmental cues and relation to phenotype such as disease susceptibility.

In recent years, it was suggested that epigenetic processes involve three different players: the "Epigenators, Initiators and Maintainers" (Berger et al., 2009). In a cellular context, the "Epigenator" senses environmental signals and transduces them into the nucleus. An "epiginator" can be a

cell surface receptor that is activated by a cytokine, or a signalling pathway that transduces extracellular signals to the transcription factors in the nucleus. The "Initiator" designates the position on chromatin where the epigenetic state can be established. It can be a transcription factor that binds to specific DNA sequences and activates or inhibits transcription, or a noncoding RNA that modulates transcription. The "Maintainer" sustains epigenetic memory in the cell, and examples are DNA methylations and certain histone modifications. These chemical modifications on the biomolecules introduce signals that define the epigenetic state. These signals are established by epigenetic modifiers enzymes that introduce or remove chemical groups from the biomolecules. In this thesis, an epigenetic modifier, called JmjD3, which belongs to a class of enzymes called histone lysine demethylase (KDM), will be investigated. A number of biochemical tools were developed to characterise JmjD3, providing insight into biological functions of this demethylase enzyme.

1.2 The structure of chromatin

The underlying mechanism of epigenetic control is dependent on the manner in which DNA is compactly organized into the higher order chromosome structure in eukaryotic cells (Fig. 1.1). The chromosome is composed of packed chromatin, where the basic repeating unit is a nucleosome formed by 146 base pairs of DNA wrapped around a core histone octamer containing two copies each of histone subunit H2A, H2B, H3 and H4. In general, two different types of modification are found to occur on the eukaryotic chromosome that mediate gene expression and result in phenotypic changes, namely DNA methylation and histone modification.

Each of the four histone subunits (H2A, H2B, H3 and H4) that make up the protein component of the nucleosome contains structurally a core histone fold responsible for assembling into the histone octamer, as well as an N-terminal flexible region that protrudes from the nucleosome (Fig. 1.2).

These 'N-terminal tails' do not have defined secondary structure and are subjected to a variety of post-translational modifications (PTMs). These PTMs include for example acetylation of lysine residues, phosphorylation of serine, threonine and tyrosine residues, and methylation of lysine and arginine residues. Other less common PTMs include sumoylation and ubiquitylation of lysine residues. The functional consequence of PTMs on gene expression and transcription can be two-fold: First,

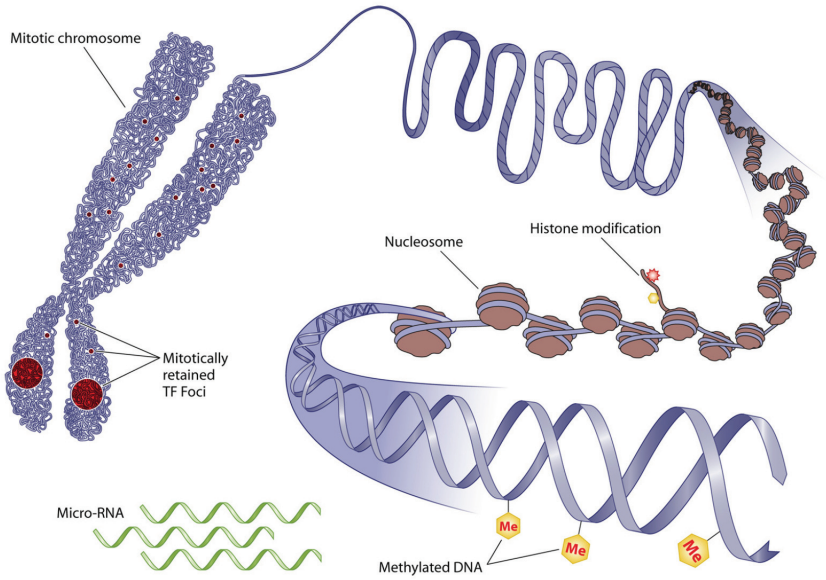


Figure 1.1: Organization of DNA in eukaryotic cell. The figure is from an original artwork from (Zaidi et al., 2010), reprinted with permission.

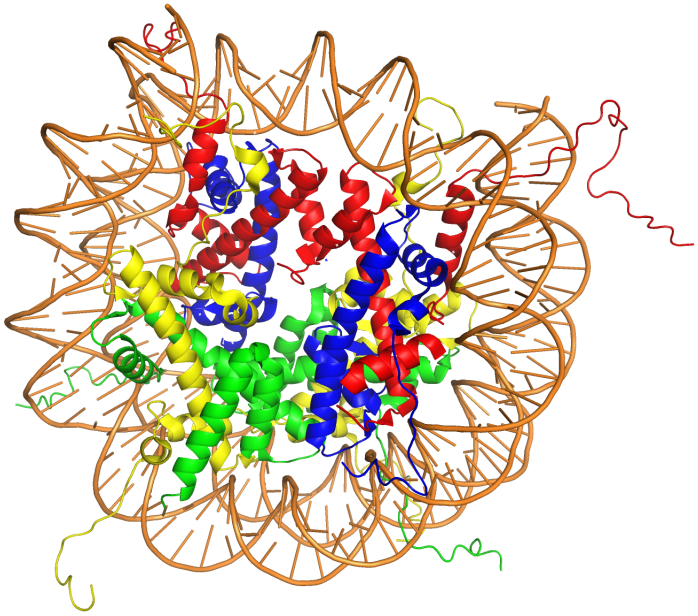


Figure 1.2: Cartoon representation of a nucleosome showing DNA (orange), Histone H2A (yellow), H2B (green), histone H3 (red), H4 (Blue). Histone tails can be seen protruding from the core (pdb: 1EQZ)(Harp et al., 2000).

PTMs can have a direct impact on the physical properties of individual nucleosomes which in turn results in more global changes in the chromatin structure. For example the phosphorylation of serine, threonine or tyrosine residues on histone tails introduces profound negative charges that will alter chromatin structure (Bannister and Kouzarides, 2011). A second, and probably more powerful effect of PTMs, is the recruitment of specialized 'reader' domains to recognize the specific modifications and mediate downstream biological effects (Allis, 2007).

1.3 Histone Demethylases and JmjD3

Lysine and arginine methylation of histones was identified early on and its importance was hypothesized by Allfrey in the 1960s (Allfrey et al., 1964). Histone methylation, especially of lysine residues, was long believed to be a permanent and irreversible modification, and it was thought that the methylated histone tail could only be replaced by newly synthesized histones. In 2004, two research groups reported the first histone arginine demethylase, namely peptidyl arginine deiminase 4 (PADI4) (Cuthbert et al., 2004; Wang et al., 2004)). However, this arginine demethylation reaction results in a citrulline residue, which is different from the native arginine (Fig. 1.3). The first lysine specific demethylase (named LSD1) was also identified during the same period (Shi et al., 2004; Metzger et al., 2005), an enzyme whose function was later on shown to be of critical importance in regulating key transcriptional events. LSD1 and its paralogue LSD2 belong to the enzyme family of amine oxidases (Fang et al., 2010), and in 2006, a significantly larger and distinct class of lysine demethylases, belonging to the Jumonji C (JmjC)-domain-containing family was characterised (Clissold and Ponting, 2001; Tsukada et al., 2005; Klose et al., 2006a,b).

1.3.1 Peptidyl arginine deiminase

Peptidylarginine deiminase 4 (PADI4) converts monomethylated arginine to citrulline by removing the imine on arginine (Fig. 1.3) (Cuthbert et al., 2004). It specifically acts on Arg2, Arg8, Arg17 and Arg26 residues on the histone H3 tail. The end product is citrulline instead of arginine which is not a direct reversal of arginine methylation. Such arginine deimination antagonizes the transcription induction mediated by arginine methylation (Cuthbert et al., 2004).

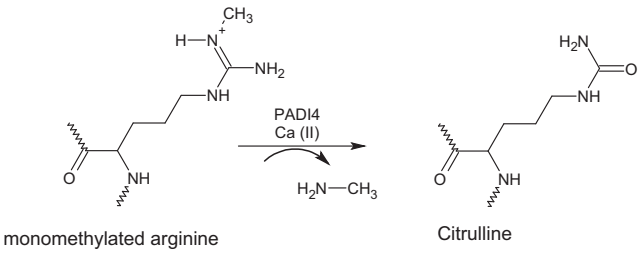


Figure 1.3: Mechanism of arginine demethylation by Peptidyl arginine deiminase.

1.3.2 Lysine demethylases

As mentioned, LSD1 was the first reported histone lysine demethylase (KDM). It catalyzes the demethylation of H3K4me1 and H3K4me2 as well as H3K9me1 and H3K9me2 by an oxidative demethylation reaction (Fig. 1.4) (Shi et al., 2004; Metzger et al., 2005). The reaction uses FAD as cofactor while an imine intermediate is generated. The imine is subsequently hydrolysed, formaldehyde is released and a demethylated mono methyl or lysine residue is formed. Only mono- and dimethylated lysine can be demethylated by LSD1 because the reaction requires a protonated nitrogen for catalysis. Non-histone targets were also reported to be substrate of LSD1 such as DNA methyltransferase I, E2F1 and p53 (Wang et al., 2008; Kontaki and Talianidis, 2010; Huang et al., 2007).

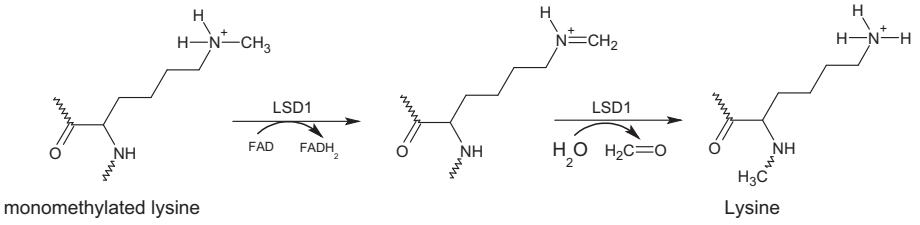


Figure 1.4: Mechanism of lysine demethylation by lysine specific demethylase 1.

The third class of histone demethylases are JmjC-domain-containing lysine demethylases. The Jumonji C (JmjC) domain utilises iron(II) and 2-oxoglutarate as cofactors and catalyses lysine demethylation of histones through an oxidative reaction (Fig. 1.5) (Tsukada et al., 2005). So far 28 different Jumonji C domain candidates have been identified in the human genome, 15 of which have been

reported to promote demethylase activity at the H3 tail (Lohse et al., 2011). A list of KDMs and identified substrates are illustrated in Figure 1.6.

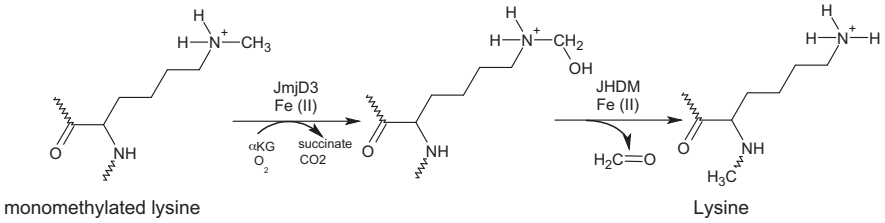


Figure 1.5: Mechanism of lysine demethylation by JmjD3.

JmjD3 belongs to the class of histone lysine demethylase (KDM) 6 family. It has a JmjC domain essential for the catalytic function of the enzyme, and was reported to demethylate H3K27me3 and H3K27me2 in vitro (Xiang et al., 2007). It shares high sequence homology with its nearest KDM6 family namely ubiquitously transcribed tetratricopeptide repeat X and Y (UTX, UTX) though lacking the tetratricopeptide repeat (TPR) domains in the N-terminus as found in UTX/UTY (Fig. 1.6). Several CxxC motifs were identified in JmjD3 at the C-terminus immediately after the JmjC domains which are proposed to be crucial for demethylase activity (Chapter 4).

1.4 Transcriptional regulation by JmjD3

In eukaryotic cells, H3K4me3 and H3K27me3 are maintained by the trithorax Group (TrxG) and Polycomb Group (PcG) proteins respectively (Allis, 2007). The TrxG genes maintain gene expression and activation. They methylate H3K4 which is an activation mark for transcription. The human homologue of TrxG is Myeloid/lymphoid or mixed-lineage Leukemia (MLL) (Schuettengruber et al., 2007). PcG proteins are responsible for transcription repression. They can be biochemically characterised into Polycomb repressive complex 1 and 2 (PRC1 and PRC2). The Enhancer of zest homolog 1 (Ezh1) and Ezh2 are components of the PRC2 complex that contain histone H3K27 methylating activities. H3K27me3 marks are associated with repressed genes. In embryonic stem cells, it was found that H3K4me3 and H3K27me3 coexist in the promoters of genes that are involved in development (Bernstein et al., 2006). These genes are "bivalently marked", and RNA Polymerase II (RNAPII) is stalled at the transcription start site of these bivalently marked genes. Such transcription state

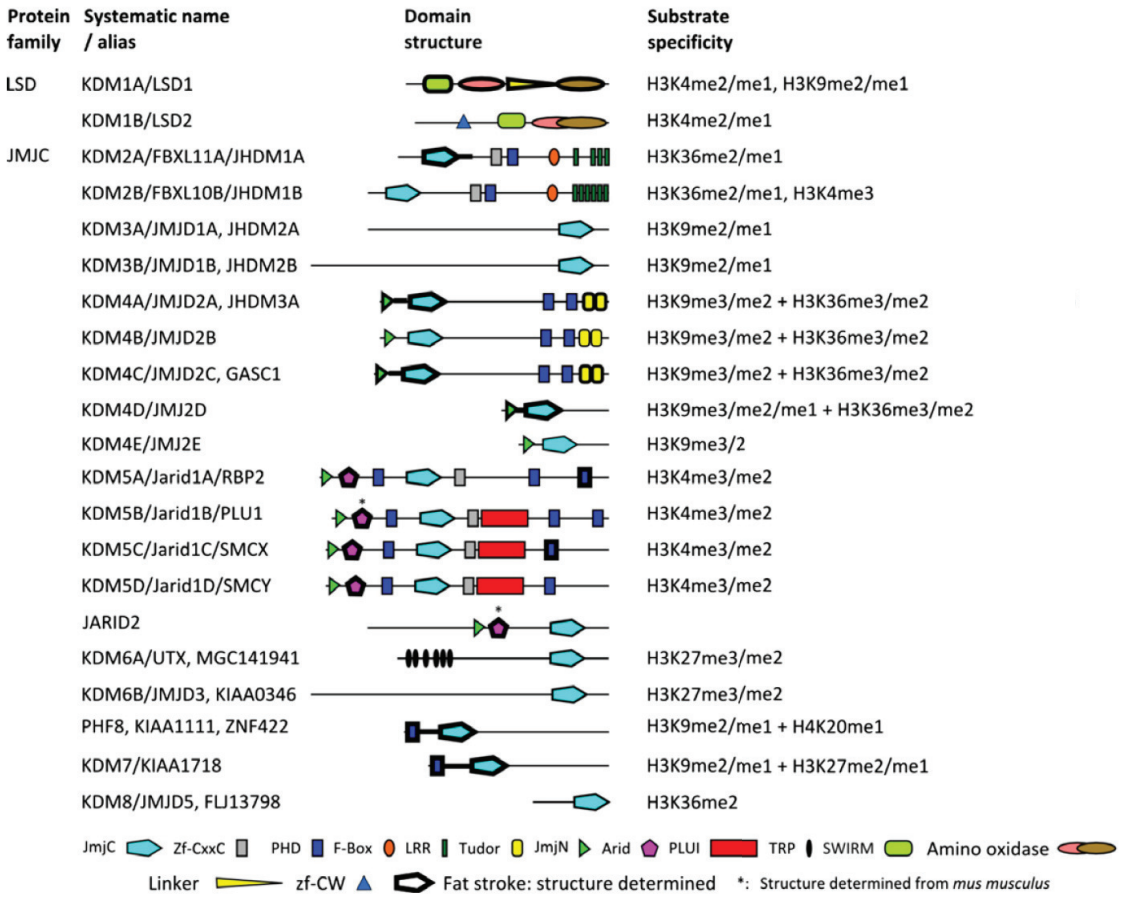


Figure 1.6: Nomenclature, domain architecture and substrate specificity of the KDM family. The figure is modified from an original artwork from (Lohse et al., 2011), reprinted with permission.

is said to be "poised" and ready for transcription (Fig. 1.7). A second stimulation is required for transcription elongation (Core and Lis, 2008).

One proposed role of JmjD3 in transcription regulation is to promote elongation (Chen et al., 2012). JmjD3 is associated with many proteins involved in transcriptional elongation including KIAA1718, SPT6, SPT16 and CDC73. In promyelocytic leukemia cell line HL-60, JmjD3 is associated with KIAA1718 and binds to many target genes. A fraction of these genes are bivalently marked by H3K4me3 and H3K27me3 and associated with promoter-proximal, poised RNAPII before activation. For example, 12-O-tetradecanoyl-phorbol 13-acetate (TPA) stimulation of HL-60 cells leads to upregulation of JmjD3 and demethylates H3K27me3 at the promoters of these genes, and RNAPII were found in the gene bodies, suggesting the occurrence of transcription elongation (Chen et al., 2012). Similar results have also been found in transforming growth factor beta (TGFβ)

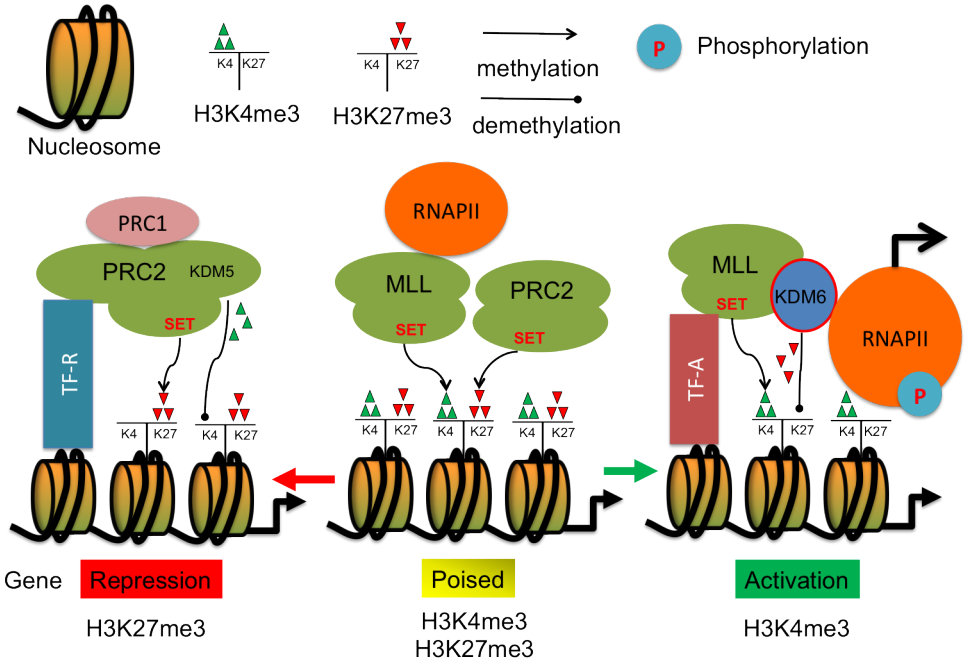


Figure 1.7: Schematic diagram showing a model of transcription regulation by JmjD3 at the transcription start site. PRC1/2: Polycomb Repressive complex 1/2. MLL: Myeloid/lymphoid or mixed-lineage Leukemia. SET: SET domain-containing protein. TF-A: Transcription factor activator. TF-R: Transcription factor repressor. RNAPII: RNA Polymerase II.

simulated neuronal stem cells, where JmjD3 demethylates H3K27me3 along gene bodies of TGFβ responsive genes, and transcription elongation was observed (Estarás et al., 2013). However, it is unclear whether demethylation of H3K27me3 by JmjD3 is a cause or consequence of the transcription repression. It was suggested that PRC1 and PRC2 which bind to the H3K27me3 regions can block transcription elongation (Margueron et al., 2008).

However, an unanswered question is, how does JmjD3 remove the PRCs and demethylate H3K27me3? Similarly, unanswered questions in the role of trithorax in H3K4me3 associated transcription activation exist, since in vitro data suggest that H3K4me3 has no effect on transcription activation (Pavri et al., 2006; Kim and Buratowski, 2009), and there are promoters carrying H3K4me3 in the absence of active transcription (John W Edmunds, 2008); Accordingly, the development of biochemical tools such as histone demethylase inhibitors can be instrumental to understand the underlying transcription mechanism.

1.5 Role of JmjD3 in health and disease

Since the identification of Jmjd3 as the H3K27 demethylase in 2007 (De Santa et al., 2007; Xiang et al., 2007), there have been over 100 publications associated to date (April, 2013) describing the characterised functions of JmjD3 in many biological themes, mainly development, inflammation and cancer biology.

1.5.1 Role of JmjD3 in development

JmjD3 is involved in the early development of mammalian cells. JmjD3 is highly expressed in human, rhesus monkey and mouse oocytes at metaphase II (Awe and Byrne, 2013). Upregulation of JmjD3 followed by H3K27me3 decrease was observed in the process of oocyte preimplantation in bovine fertilisation. Knockdown of JmjD3 in oocytes inhibited H3K27me3 demethylation and reduced blastocyst development (Canovas et al., 2012). Furthermore, JmjD3 controls the endoderm and mesoderm commitment in early embryo. Early embryo development is modulated by Wnt and Nodal signalling pathways, and in both pathways JmjD3 counteracts the PcG-mediated repression by erasing H3K27me3 at the promoters of bivalently marked (H3K4me3 and H3K27me3) target genes. Examples of these genes include WNT3 and DKK1 of the Wnt pathway, as well as SMAD2/3, SMAD4 and FOXH1 of the Nodal pathway. Removal of H3K27me3 results in leaving only the H3K4me3 activation marks, thus enabling expression of these genes (Jiang et al., 2013; Kim et al., 2011).

In later stages of embryo development, JmjD3 is largely involved in regulation of genes responsible for body and limb morphogenesis, including Homeobox (HOX) and T-box transcription factors (Agger et al., 2007; Lan et al., 2007; Gao et al., 2010; Miller and Weinmann, 2009), although here the enzymatic function of JmjD3 appears to be at least in part dispensable.

In mouse embryonic fibroblasts (MEFs) derived induced pluripotent stem cells (iPSC), the silencing of JmjD3 in MEFs produced significantly more iPSC colonies than the control, and ectopic expression of JmjD3 inhibited reprogramming. The inhibitory effect is mediated through both demethylase-dependent and demethylase-independent pathways (Zhao et al., 2013). The demethylase-dependent function mediates removal of H3K27me3 repressive marks on genes involved in reprogramming such as INK4A/ARF. The demethylase-independent pathway involves plant homeodomain finger protein

20 (PHF20) targeted by JmjD3 for ubiquitination by E3 ligase, Trim, leading to degradation. Accordingly, it was suggested that the JmjD3-PHF20 axis critically controls the cellular reprogramming process (Zhao et al., 2013).

Other work has shown that JmjD3 is implicated in bone cell differentiation. In mesenchymal stem/stromal cells (MSCs) which were induced through BMP treatment to differentiate into bone-forming osteoblasts, the silencing of JmjD3 caused significantly reduced osteogenic differentiation and increased adipogenic differentiation (Ye et al., 2012). Another study suggested that JmjD3 is also involved in differentiation of osteoclasts (the sole bone resorbing cells). In mouse bone marrow macrophages (BMMs), JmjD3 is induced by Receptor Activator of NF-κB Ligand (RANKL) and erases H3K27me3 at the promoter of NFatc1(Yasui et al., 2011), a key gene that regulates differentiation of macrophages to osteoclasts (Takayanagi et al., 2002). In both studies, the authors suggested that JmjD3 is a potential therapeutic target in metabolic bone diseases such as osteoporosis.

A number of studies indicated that JmjD3 plays an important role in neural differentiation and commitment (Jepsen et al., 2007; Burgold et al., 2008). JmjD3 is one of the early neural differentiation regulators modulated by Bone morphogenetic protein 4 (BMP4) in neural stem cells. It is recruited by phosphorylated Smad3 and is crucial to activate TBFβ-responsive genes (Estarás et al., 2012; Fei et al., 2010). In retinoic acid (RA) induced neural differentiation, there was an increased expression level of HOX genes and JmjD3 was shown to remove H3K27me3 at the HOX gene regulatory elements (Shahhoseini et al., 2013). Mash1, a key gene induced by RA for neuronal differentiation, is also regulated by JmjD3 through a similar mechanism (Dai et al., 2010). Silencing of a RNA binding protein KSRP induces expression level of JmjD3 in RA stimulated neurogenesis of P19 cells (Giovarelli et al., 2013).

Importantly, a JmjD3 knockout in mouse results in perinatal lethality. The pre-Botzinger complex (PBC) complex, which is the pacemaker of the respiratory rhythm generator, was disrupted. It is believed that JmjD3 is important for the maintenance of the PBC, structure and function of the neuronal networks (Burgold et al., 2012).

Histone H3K27me3 may not be the only demethylation substrate for JmjD3. Sola et al. reported that during mouse neural stem cell differentiation, the N-terminal region, but not JmjC domain, of JmjD3 interacts with and stabilises p53 in a demethylase-independent manner and contributes to

nuclear localization of p53 (Solá et al., 2011). Thus JmjD3 may have physiological functions other than the control of methylated lysine 27 in histone H3.

1.5.2 Role of JmjD3 in inflammation

JmjD3 is implicated in certain aspects of the inflammatory response. It was shown that JmjD3 affected downstream of NF-κB signalling pathway in lipopolysaccharide (LPS) stimulated pro-inflammatory macrophages. JmjD3 associates with 70% of LPS-inducible genes (Wei et al., 2009; Das et al., 2012), though it was disputable whether JmjD3 is directly involved in transcription of these genes (De Santa et al., 2009). Stimulation of anti-inflammatory mouse macrophages by IL-4 induces JmjD3 via the STAT6 pathway and leads to activation of several anti-inflammatory genes (Ishii et al., 2009b). In addition, the polarization of mouse anti-inflammatory macrophages during helminth infection is modulated by JmjD3 (Satoh et al., 2010). Furthermore, it was shown that JmjD3 is also involved in the lethal toxin intoxication resistance of macrophage RAW 264.7 cells (Das et al., 2010).

In T cells, JmjD3 is involved in T-helper cell lineage commitment (Miller and Weinmann, 2010). It also regulates expression of hematopoietic progenitor kinase 1 (HPK1/MAP4K1), a kinase that negatively regulates T-cell immune response. Expression of HPK1 is influenced by Jmjd3-mediated demethylation of H3K27 at the promoter region (Zhang et al., 2011). Overexpression of JmjD3 causes upregulation of HPK1, which in turn suppresses T-cell response. Hence, blocking of JmjD3 activity could be a potential therapeutic approach for the treatment of T-cell related disease such as systemic lupus erythematosus (SLE) (Zhang et al., 2011).

JmjD3 is involved in the function of a number of cell types in wound healing. JmjD3 and UTX are markedly upregulated at the wound site and control epidermal differentiation (Shaw and Martin, 2009; Sen et al., 2008). JmjD3 is downregulated in lipopolysaccharide (LPS) stimulated keratinocyte HaCaT cells (de Camargo Pereira et al., 2012). JmjD3 regulates expression of regulatory genes Itaga2b and Mpl in megakaryocyte (Dumon et al., 2012). Jmjd3-mediated H3K27me3 demethylation is crucial for IL-6 gene activation in endothelial cells of injured spinal cord. (Lee et al., 2012).

1.5.3 Role of JmjD3 in cancer

Jmjd3 is implicated in the pathogenesis of many types of cancer, and it is suggested that increased levels of JmjD3 are usually associated with pathogenesis, for example JmjD3 is expressed higher in renal cell carcinoma than normal tissue (Shen et al., 2012). In vitro, overexpression of JmjD3 in A549 lung cancer cells was found to promote cell proliferation and decrease the G1 phase cell number (Tian et al., 2012). High JmjD3 expression is also seen in Epstein-Barr virus (EBV) related Hodgkin's Lymphoma. EBV infection in B cells was shown to induce JmjD3 expression, where the majority of the JmjD3 target genes in B cells promote plasma cell differentiation (Anderton et al., 2011). High level of JmjD3 was also found in human papillomavirus E7 (HPV) associated cervical cancer. A profound increased expression level of homeobox (HOX) genes suggested that HPV uses JmjD3 to reprogram host epithelial cells (McLaughlin-Drubin et al., 2011). JmjD3 is also overexpressed in myelodysplastic syndromes (MDS) of CD34+ cells (Wei et al., 2013). Knockdown of JmjD3 increased the number of erythroid colonies in vitro, and it was suggested that blocking JmjD3 may be of a potential therapeutic value in MDS Leukemia. Lastly, in estrogen-responsive breast cancer MCF7 cells, the activation of anti-apoptotic B-cell lymphoma 2 (BCL2) is dependent on both methylation of H3K27 methyltransferase EZH2 and demethylase JmjD3. Knockdown of JmjD3 caused apoptosis in MCF7 cells (Svotelis et al., 2011). These examples show that JmjD3 promotes cancer growth by activating cell proliferative genes or anti-apoptotic genes.

However, JmjD3 is also regarded as a tumour suppressor gene because of its counteracting action on the function of oncogenic PcG proteins. The INK4A/ARF locus comprises tumour suppressor genes $p16^{INK4A}$ and $p14^{ARF}$ which are repressed by PcG proteins in normal growing cells, through deposition of H3K27me3 repressive marks at the promoter. When the cells undergo oncogenic stress, JmjD3 is induced by RAS-RAF signalling pathway and activates $p16^{INK4A}$ and $p14^{ARF}$, causing p53-dependent cell cycle arrest (Barradas et al., 2009; Agherbi et al., 2009; Agger et al., 2009). In prostate cancer, androgen receptor (AR) is stimulated by androgen and represses transcription of the miR-99a/let7c/125b-2 microRNA clusters. These clusters can inhibit expression of IGF1R, which promote androgen-mediated growth of prostate cancer. JmjD3 was shown to activate miR-99a/let7c/125b-2 clusters even in the absence of androgen (Sun et al., 2013).

Furthermoree, the JmjD3 mediated epithelial-mesenchymal transition (EMT) has been studied in details. JmjD3 is expressed more highly in invasive beast carcinoma than normal breast tissue. Knockdown of JmjD3 stopped breast cancer invasion, and overexpression of JmjD3 affected the expression of a range of adhesion molecules, including downregulation of E-cadherin and upregulation of N-cadherin and fibronectin. Detailed analysis revealed that in TGFβ stimulated EMT, JmjD3 removes H3K27me3 at the promoter of an EMT inducer gene SNAI1, thus allowing transcription of the gene (Ramadoss et al., 2012). However, it was shown that JmjD3 knockdown causes upregulation of SNAI1 in a different study. In SW480-ADH colon cancer cells, calcitrol 1,25(OH)(2)D(3) induced JmjD3 expression and JmjD3 regulates target genes that are of epithelial adhesive phenotype. Knockdown of JmjD3 induced SNAI1-mediated EMT, upregulation of mesenchymal markers and downregulation of epithelial proteins. Expression of JmjD3 correlates with expression of Vitamin D receptor but is inversely correlated with expression of SNAI1 in 96 human colon tumours (Pereira et al., 2011, 2012). These studies indicated that JmjD3 may play a role in cancer metastasis.

Other reports of JmjD3 in cancer are also available. Dysregulation of JmjD3 seems to contribute to the aberrant H3K27 methylation patterns in brain tumour medulloblastoma (Dubuc et al., 2012; Bunt et al., 2012), and mutation of JmjD3 gene was found in lymophoblastic leukaemia cell line MHH-CALL-2 (Chen et al., 2013).

Taken together, the importance of JmjD3 in cancer biology has been indicated in these studies. Hence, there is a great medical and scientific interest to further characterise JmjD3. Specifically, the development of small molecule inhibitors to block JmjD3 demethylase activity is desirable to probe its biological function.

1.6 Small molecule inhibitors of KDM enzymes

Selective inhibitors are important for understanding the biological functions of histone lysine demethylases (KDMs). Many investigators rely on the use of RNA silencing to study the functions of KDMs. However, such methods may be undesirable because the phenotypic changes may be due to the loss of the protein by silencing rather than the loss of the demethylase activity. Secondly, the KDM itself may be an important part of a transcription complex, hence knocking it down may have disastrous

effects to the complex and transcriptional machinery, leading to cell death. Development of a small molecule inhibitor allows the blockage of the demethylase activity while retaining the integrity of the protein in the cell. To further understand the therapeutic potentials of JmjD3 inhibitors in e.g. oncology, development of specific and cell active inhibitors is mandatory. In the following section, I will discuss the current knowledge of KDM inhibitors.

Small molecule inhibitors for the KDM1 family have been studied extensively in the past few years. The KDM1 family comprises LSD1 and LSD2 which demethylate H3K4me2/me1 substrate. These amine oxidases are inhibited by MAO inhibitors derived from pargyline (Fig. 1.8, compound 1) (Metzger et al., 2005), phenelzine (Ki= 17.6μM) (2) and Tranylcypromine (Ki=477 μM) (3) (Lee et al., 2006). However, later on it was reported that pargyline was not able to inhibit LSD1 in vitro (Lee et al., 2006). Since MAO inhibitors are used for the treatment of depression, tranylcypromine based compounds were modified to inhibit LSD1 but not MAOs. These include compounds 4 - 6, displaying K_i values of 1.1 μM, 1.3 μM and 1.9 μM against LSD1 respectively (Binda et al., 2010; Ueda et al., 2009). Compound 5 has been shown to inhibit growth of NB4 leukemia blast cells in vitro (Binda et al., 2010). The fluorine-containing Trans-2-phenylcylopropylamine (2-PCPA) (7) has a K_i value of 0.61 μM (Mimasu et al., 2010) against LSD1. It has been shown to increase H3K4me2 level in HEK293T cells. CB1007 (8) has K_i value as low as 0.05 μM and was shown to be active in inhibiting the proliferation of pluripotent cancer cells (Wang et al., 2011).

The KDM2 to KDM7 subfamilies utilise the JmjC domain to demethylate sequence-specifically lysine residues of histone H3 tails. A number of generic inhibitors have been identified to inhibit these KDMs. These include analogues of 2OG (Fig. 1.8), namely N-oxalylglycine (NOG, 10), or 2,4-pyridinedicarboxylic acid (2,4-PDCA, 11), hydroxamic acids and 8-hydroxy-5-carboxyquinoline (8HQ, 16). NOG inhibits KDM4A (Jmjd2A), KDM4C (JmjD2C), KDM4E (JmjD2E) as well as many other Fe(II) and 2OG dependent oxygenases such as hypoxia-inducible factor (HIF) prolyl hydroxylase (PHD) and asparaginyl hydroxylase factor-inhibiting-HIF (FIH). 2,4-PDCA is a potent inhibitor against KDM4 with IC_{50} values that range from 0.6 μM to 2.4 μM against KDM4A, KDM4C and KDM4E (Rose et al., 2008; Kristensen et al., 2011a). It also inhibits a range of 2OG oxygenases including FIH, KDM5B, PHD and PHF8 (Kristensen et al., 2012; Rose et al., 2011). Hydroxamic acids are known to inhibit histone deacetylases (HDAC), and SAHA (12) is clinically used for treating

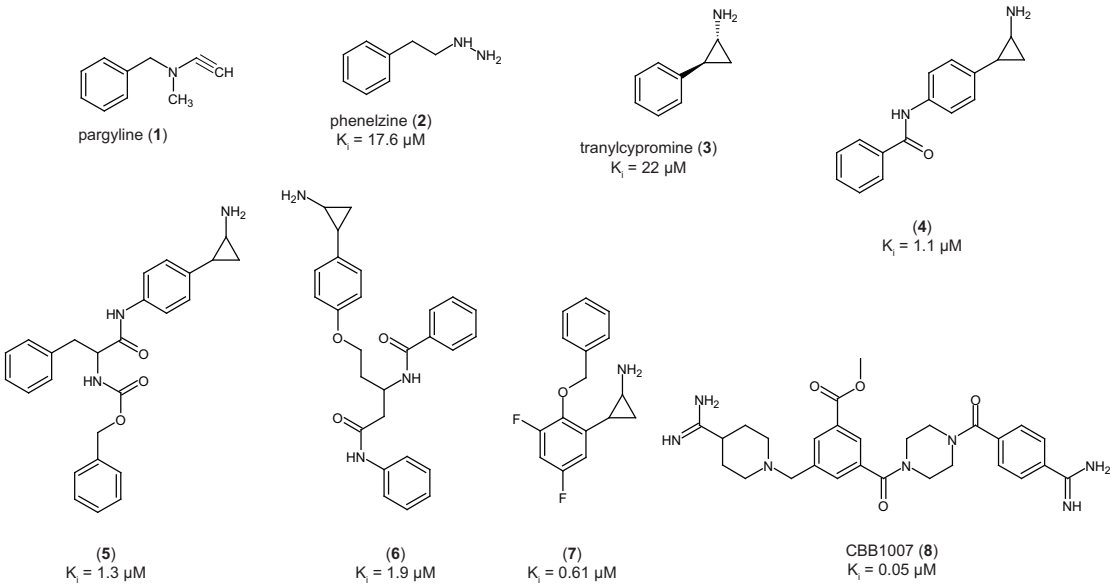


Figure 1.8: Chemical structures of reported KDM inhibitors.

certain types of lymphoma. Extensive research has been done on modifying the hydroxamate core (13) to achieve higher potency and selectivity. The best hydroxamate derived so far was the one conjugated with a methylated lysine mimic resulting in compound 14 and Methylstat (15). Compound 14 has IC_{50} values of 1.3 - 2.0 against KDM4A and KDM4C and showed no inhibition on PHD enzymes (Hamada et al., 2010). Methylstat (15) has IC_{50} values of 3.4 - 5.9 μM against KDM4A, KDM4C and KDM4E, 10 μM against PHF8, 43 μM against KDM6B and over 10 fold IC_{50} values against PHD, FIH and LSD1 thus suggesting some degree of specificity towards demethylases (Luo et al., 2011). 8HQ (16) is a quinoline-containing compound that exhibits inhibition to both the KDM2 and KDM4 family. As it will be shown in later chapters (Chapter 3), it also inhibits KDM6B (JmjD3). It has been reported to have an IC_{50} value as low as 0.2 μM against KDM4A in vitro and increases H3K9me3 level in HeLa cells (King et al., 2010). Bipyridyls (17) and N-oxalyl-D-tyrosine (18) have been shown to inhibit KDM4E (Chang et al., 2011; Rose et al., 2010a).

Nickel (II) was also reported to inhibit KDM3A (JmjD1A), and excessive iron (II) is not able to reactivate nickel (II) bound KDM3A (Chen et al., 2010). However, since most 2OG oxygenases utilise Iron (II) as cofactor for catalysis, nickel (II) would likely to have widespread impacts on other KDMs.

Two specific inhibitors have been identified for the KDM2-7 subfamilies so far. Daminozide (19)

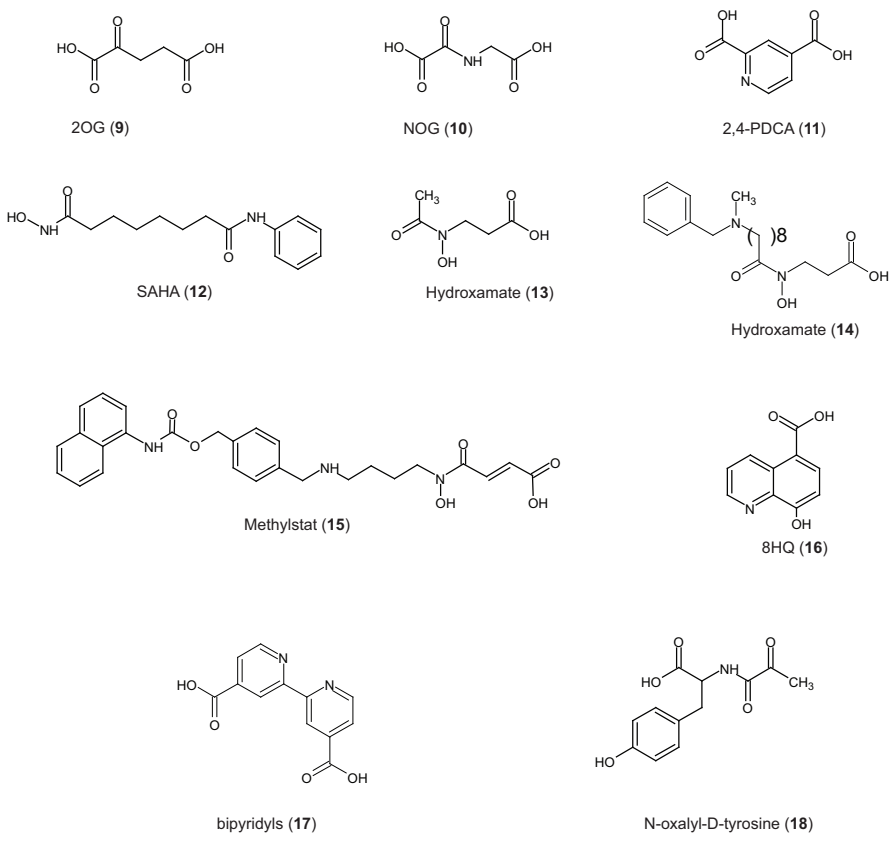
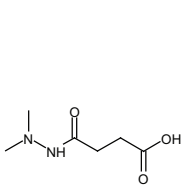


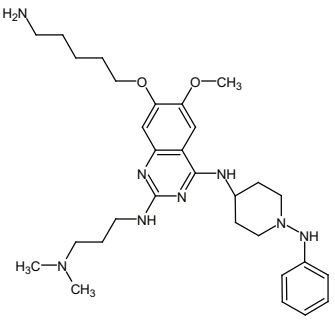
Figure 1.8: continue. Chemical structures of reported KDM inhibitors.

is specific to KDM2A (FBXL11) and KDM7A (KIAA1718), displaying a K_i value of 1.97 μM and IC_{50} value of 2.1 μM respectively (Rose et al., 2012). However, no cell-based data are available at the moment and it is very likely that daminozide is cell impermeable due to its polar carboxylic group. E67 (20) is a H3K9 peptide-mimetic compound that can inhibit KDM7 (KIAA1718) and H3K9 methyltransferases G9a. It has a K_i value of 2.5 μM against KDM7A (Upadhyay et al., 2012) and appears to be selective against KDM5C (Jarid5C)

To conclude, inhibitors with some degree of specificity have been developed for the KDM1 family, however, they cross react with other members of the monoamine oxidase family. Furthermore, their in vitro potency is still fairly low. Several generic inhibitors have been developed to inhibit KDM2 and KDM4 enzymes, and there is a very limited number of inhibitors that can inhibit JmjD3 of the KDM6 family, namely methylstat and 8HQ. Both of them show a broad, and varying degree of inhibition against other KDMs. A specific, potent and cell-active inhibitor for the KDM6 family is therefore much needed, would be of great interest to the scientific community and could possibly advance the understanding of JmjD3 in biology.



Daminozide (**19**)



E67 (**20**)

Figure 1.8: continue. Chemical structures of reported KDM inhibitors.

1.7 Aim and outline of the thesis

The overall objectives of my research project were to develop biochemical tools to characterise JmjD3 in biological systems. The specific goals towards this objective were therefore as follows:

• Development of an expression system for human JMJD3 to obtain sufficient amounts of soluble recombinant protein suitable for protein crystallization studies and activity assays.

• Crystal structure determination of human JMJD3, which can be used for understanding the molecular basis of their enzymatic mechanism and specificity, as well as for rational inhibitor design.

• Development of a demethylase enzymatic assay which can be adapted for high throughput screens to identify small molecule inhibitors.

• Development of a cell-based assay, suitable for the profiling of inhibitors.

• Identification of potent, selective and cell active inhibitors for JmjD3 and other members of the KDM6 subfamily.

• Use of the above identified inhibitor(s) to investigate the roles of lysine 27 demethylation in cellular contexts, particularly macrophages/inflammation, and osteoclast differentiation/bone resorption.

Chapter 2

Cloning, Expression and Purification of JmjD3

2.1 Introduction

A pre-requisite for any enzymatic and structural studies is the availability of milligram quantities of purified, homogenous protein sample. At the initial stage of my D.Phil work, one of my primary objectives is to establish a recombinant expression system to obtain sufficient amounts of JmjD3 protein, at which time there has been no documented procedures. The *E.coli* system was first chosen, because of its robustness and convenience in setup, and also its tractability in obtaining good yields of stable functional proteins for other Jumonji domain containing proteins (Ng et al., 2007; Hong et al., 2010; Del Rizzo et al., 2012).

2.2 Cloning

In order to maximize the probability of obtaining stable, soluble fragments of recombinant JmjD3 proteins, a total of 24 JmjD3 construct sequences encompassing the JmjC domain but each with different pairings of the N- and C-terminal were designed (JmjD3-c001 to JmjD3-c031) (Fig. 2.1). There are 4 different N-terminal boundaries and 6 different C-terminal boundaries. Full length JmjD3 construct (180 kDa) was not created, as the probability of obtaining soluble protein expressed in *E.coli* often decreases with increasing molecular weight (Francis and Page, 2001).

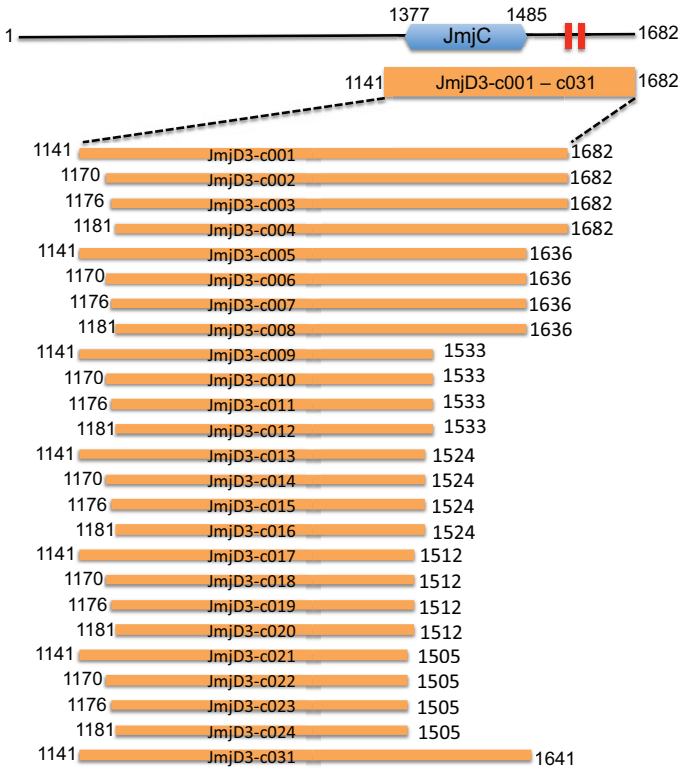


Figure 2.1: Schematic diagram showing 25 subcloned JmjD3 constructs encompassing the JmjC domain. Red boxes indicate the positions of predicted CxxC motifs.

These DNA fragments were PCR amplified and subcloned into the pNIC28-Bsa4 bacterial expression vector using the Ligation Independent Cloning (LIC) method. This expression vector is a pET-based plasmid using a T7 promoter and *lac* operon where gene expression is inducible by Isopropyl β-D-1-thiogalactopyranoside (IPTG). The plasmid incorporates an N-terminal hexahistidine (His6)-tag followed by a Tobacco Etch Virus (TEV) protease recognition site, which allows His6-tag removal by proteolysis. An additional construct (JmjD3-c031) was subcloned into the pNH-TrxT vector which incorporates an N-terminal His6-tag followed by a thioredoxin fusion protein, to enhance protein solubility and yield.

2.3 Expression

Recombinant protein production in *E.coli* has been shown to be very robust and high in yield for many studied proteins. However, in some cases the use of *E.coli* in heterologous expression can produce misfolded and insoluble proteins that accumulate as inclusion bodies when the protein is overex-

pressed, partly due to the inability of *E.coli* to mediate the required post-translation modifications (e.g. glycosylation, phosphorylation) for eukaryotic proteins (Francis and Page, 2001). Solubility of proteins can be improved by synchronizing the processes of protein synthesis and folding. This can be achieved by varying experimental conditions such as growth temperature, inducer concentration and type of growth medium. Initial expression and purification test for the 25 JmjD3 constructs was carried out in 50 ml scale, at three temperatures (18°C, 25°C and 37°C) using 0.5 mM IPTG and Terrific Broth (TB) as growth medium. Cells were harvested after 16 hours (18°C, 25°C) or 4 hours (37°C) post - induction, lysed by ultra-sonication, and subjected to immobilized metal affinity chromatography (IMAC). Protein expression and solubility is then evaluated by SDS-PAGE detection of target protein bands from cell lysate and IMAC elution samples.

A summary of the expression and solubility results for all JmjD3 constructs is shown is Table 2.1. All JmjD3 constructs were highly expressed at both 37°C and 25°C (as seen in Total cell lysate of Appendix 1a & b), but the expressed protein was predominantly insoluble. At 18°C the expression level was lower than at 25°C or 37°C (Appendix 1c), but the proportion of soluble proteins was significantly higher. Interestingly, doublet and triplet bands were observed in constructs c017 - c020, suggesting partial degradation of the protein.

In general, a higher expression and solubility level was observed for the shorter constructs (c009 - c023), among which construct c023 resulted in the highest level of soluble protein at 18°C and was chosen for use in structural studies (Chapter 4). Subsequently a longer construct c031 (1141 - 1641), which extends the C-terminus of c023 (1176 - 1505) by further 136 residues (1506 - 1641), was designed to evaluate the importance of this C-terminal region on enzyme activity (Chapter 3).

Construct ID	Solubility at 37°C	Solubility at 25°C	Solubility at 18°C	Comments
JMJD3A-c001	N	low	low	
JMJD3A-c002	N	low	low	
JMJD3A-c003	N	N	N	
JMJD3A-c004	N	N	N	
JMJD3A-c005	N	low	low	
JMJD3A-c006	N	low	low	
JMJD3A-c007	N	N	N	
JMJD3A-c008	N	N	N	
JMJD3A-c009	N	low	medium	
JMJD3A-c010	low	low	medium	
JMJD3A-c011	low	low	medium	
JMJD3A-c012	N	low	medium	
JMJD3A-c013	low	low	medium	
JMJD3A-c014	N	N	N	
JMJD3A-c015	low	low	medium	
JMJD3A-c016	low	low	medium	
JMJD3A-c017	low	low	medium	protein degradation
JMJD3A-c018	low	low	medium	protein degradation
JMJD3A-c019	low	low	medium	protein degradation
JMJD3A-c020	N	low	medium	protein degradation
JMJD3A-c021	low	low	low	
JMJD3A-c022	low	low	low	
JMJD3A-c023	low	low	medium	Not active, structure solved
JMJD3A-c024	N	N	N	
JMJD3A-c031	Not available	Not available	medium	very active

Table 2.1: Solubility of JmjD3 in 50 *ml* test expression. Protein solubility is defined by density of JMJD3 band of IMAC elution fractions on SDS-PAGE. The more dense the JMJD3 band, the higher the solubility and yield of the protein. N represents protein being not soluble at all. The boundaries of each construct can be found in (Fig. 2.1).

2.4 Purification of JmjD3-c023

The soluble construct of JmjD3-c023, identified in the small scale expression test, was expressed in 30-litre scale for structural and inhibitor studies, using similar growth condition as defined in the small scale. Purification of the recombinant JmjD3 constructs was attempted using a two-step procedure consisting of IMAC and size exclusion chromatrography (SEC).

In IMAC, recombinant His6-tag proteins were captured by immobilized metal ion (e.g. Ni^{2+}) on the resin and eluted by high concentration of imidazole (250 mM). Using IMAC as the first purification step, JmjD3 protein was enriched to about 50% purity as judged from SDS-PAGE (Fig. 2.2A). TEV protease was then added to in the pooled eluent samples of construct c023 in order to remove the N-terminal hexahistidine tag. TEV-mediated cleavage efficiency was usually over 90% using a 1:30 mass ratio of TEV protease to recombinant proteins as judged by SDS-PAGE (Fig. 2.2B). The cleavage reaction was carried out at 4°C overnight.

In order to polish the IMAC-purified protein sample, a second SEC size exclusion chromatography step was performed using a Superdex 200 gel filtration column in the Akta Fast protein liquid chromatography (FPLC) system, to separate proteins by molecular mass. The chromatogram revealed three peaks were obtained with elution volume (V_e) = 46 mL, 57 mL and 80 mL (total column volume = 120 mL) (Fig. 2.2C, red, green and blue box.) The peak at V_e = 46 mL contains high molecular weight aggregates which eluted in the void volume of the column (Fig. 2.2C, red box). The peak at V_e = 57 mL likely contains proteins or complexes greater than 70 kDa (Fig. 2.2D, green box). The peak at V_e = 80 mL contains JmjD3-c023 (Fig. 2.2D, blue box). The purified proteins were concentrated, flash frozen in liquid nitrogen and stored at -80°C freezer, and was used for inhibitor binding assay (Chapter 3) and protein crystallization (Chapter 4). The average yield for this purification is 2 mg/L culture.

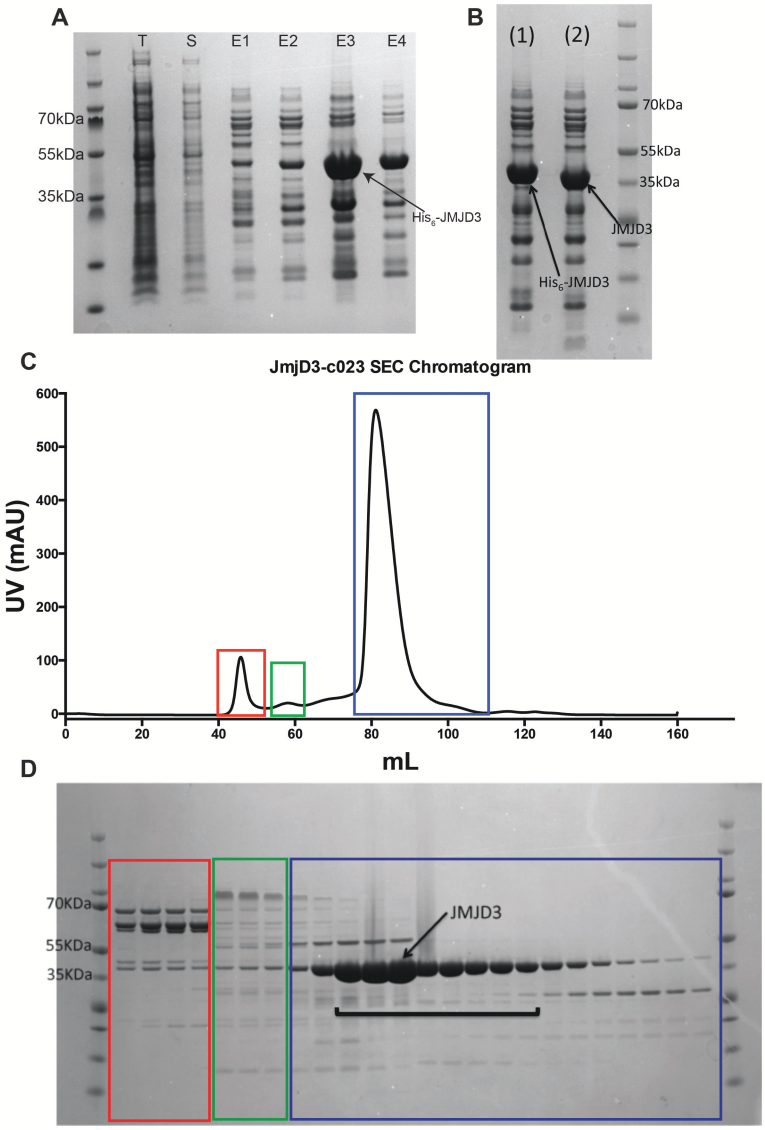


Figure 2.2: Purification of JmjD3-c023.

A) SDS-PAGE showing JmjD3-c023 (40.1 kDa) eluted from a IMAC column. T: Total cell lysate, S: Clarified supernatant, E1-E4 IMAC elutions.

B) SDS-PAGE showing JmjD3-c023 cleaved by TEV. Lane 1: His_6-tag-JmjD3 eluted from IMAC (40.1 kDa). Lane 2: TEV treated JmjD3 (37.7 kDa).

C) Chromatogram showing JmjD3-c023 eluted from gel filtration column. Red, green and blue boxes correspond to the samples in D.

D) SDS-PAGE showing JmjD3-c023 eluted from gel filtration column. Red, green and blue boxes correspond to the peaks in C. Black square bracket indicates pooled fractions.

2.5 Purification of JmjD3-c031

The soluble construct of c031, containing His6-thioredoxin-tag, was expressed in 30-litre scale for structural and enzymatic studies, using similar growth condition as JmjD3-c023. Purification of the JmjD3-c031 was attempted using a three-step procedure consisting of IMAC, ion exchange chromatrograghy (IEX) and SEC.

Purification of JmjD3-c031 by IMAC was performed as before. JmjD3-c031 was enriched to about 20% purity as judged from SDS-PAGE (Fig. 2.3A). TEV protease was then added to the pooled eluent samples. TEV-mediated cleavage efficiency was over 90% using a 1:30 mass ratio of TEV protease to recombinant proteins (Fig. 2.3B). The cleavage reaction was carried out at 4°C overnight, in a reaction buffer supplemented with 1 mM EDTA to chelate any nickel ion leaked from the column that may affect subsequent assay activity.

The partially purified, TEV-treated protein was then subjected to IEX. Although the theoretical isoelectric point (pI) of JmjD3-c031 is 6.4, the protein was found to bind to cation exchange resins at 20 mM HEPES pH 7.5 and was sufficient to separate JmjD3 from His_6-thioredoxin and low molecular weight proteins (Fig. 2.3C). Bound Protein was eluted with a linear salt gradient of NaCl as implemented in FPLC. JmjD3-c031 was eluted between 100 - 150 mM NaCl, yielding a final purity of 90% as judged by SDS-PAGE (Fig. 2.3C).

In order to polish the IEX-purified protein sample, a final SEC step was performed using a Superdex 200 gel filtration column to separate proteins by molecular mass. Two peaks were obtained with Ve = 120mL and 200 ml (total column volume = 320ml). The first peak (Ve = 120 ml) may contain high molecular weight aggregates as it eluted near the void volume of the column (110 mL) (Fig. 2.3D, red). The second peak corresponds to JmjD3-c031 as revealed by SDS-PAGE (Fig. 2.3D, blue). The purified proteins were concentrated, flash frozen in liquid nitrogen and stored at -80°C and was used for activity assay (Chapter 3). The average yield for this purification is 0.5 mg/L culture.

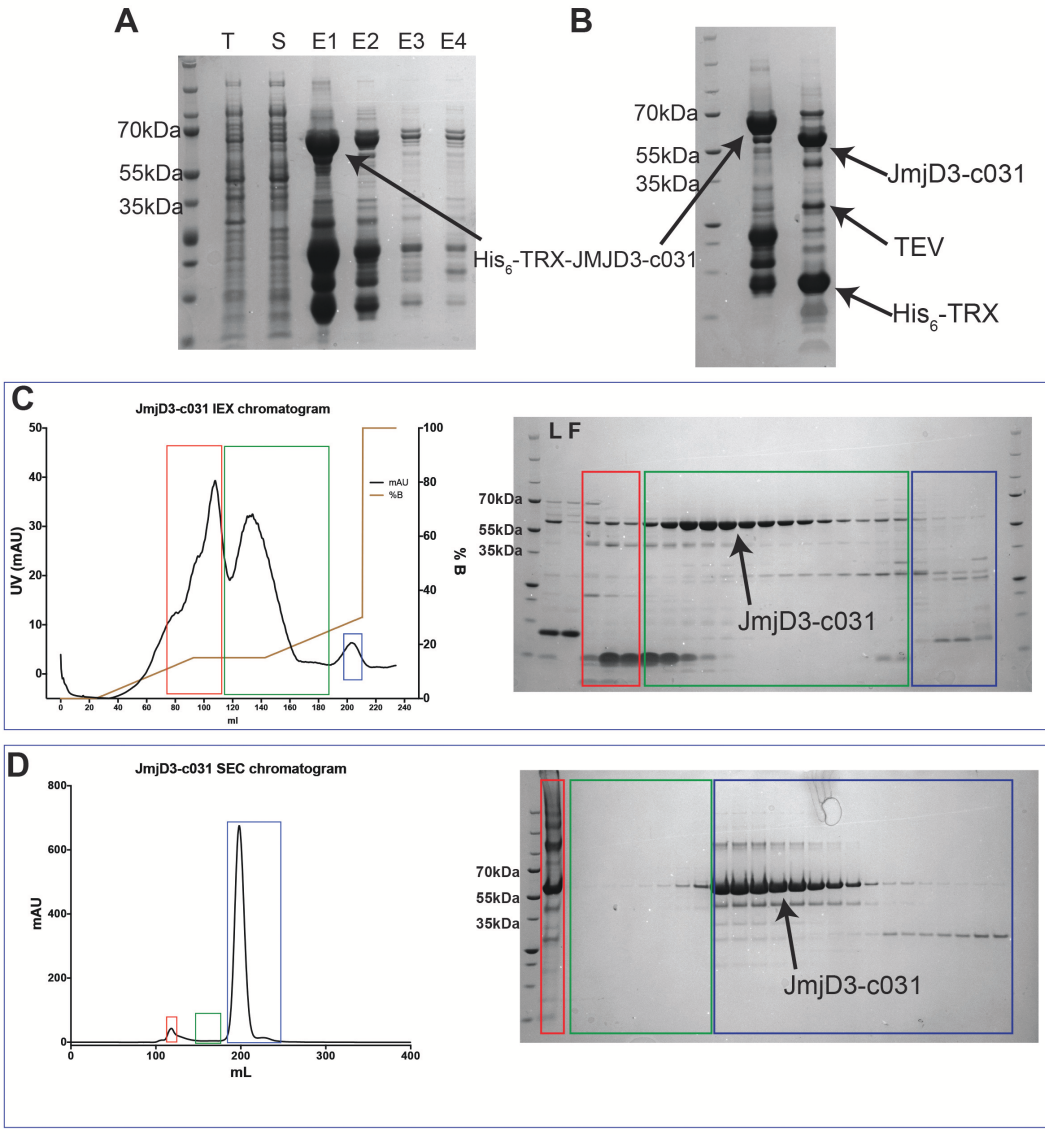

A
T
S
E1
E2
E3
E4
70kDa
55kDa
35kDa
His6-TRX-JMJD3-c031
B
70kDa
55kDa
35kDa
JmjD3-c031
TEV
His6-TRX
C
JmjD3-c031 IEX chromatogram
UV (mAU)
%B
mAU
%B
ml
L F
70kDa
55kDa
35kDa
JmjD3-c031
D
JmjD3-c031 SEC chromatogram
mAU
mL
70kDa
55kDa
35kDa
JmjD3-c031

Figure 2.3: (previous page) Purification of JmjD3-c031.

A) SDS-PAGE showing His6-thioredoxin-JmjD3-c031 (71.1 kDa) eluted from an IMAC column. TRX: Thioredoxin, T: Total cell lysate, S: Clarified supernatant, E1-E4 IMAC elutions.

B) SDS-PAGE showing JmjD3-c031 cleaved by TEV. Lane 1: His_6-thioredoxin-JmjD3-c031 eluted from IMAC (71.1 kDa). Lane 2: TEV treated JmjD3 (57.2 kDa).

C) FPLC chromatogram and the corresponding SDS-PAGE showing JmjD3-c031 eluted from HiTrap SP column. L: sample before IEX, F: flow through. Red, green and blue boxes are peaks correspond to the bands in SDS-PAGE. Brown line indicates the change in NaCl concentration during the IEX purification

D) FPLC chromatogram and the corresponding SDS-PAGE showing JmjD3-c031 eluted from size exclusion column (HiLoad Superdex 200 26/60). Red, green and blue boxes are peaks corresponding the bands in SDS-PAGE.

2.6 Conclusion

25 JmjD3 constructs harbouring hexahistidine tag at their N-terminus were subcloned into pNIC28 vector and expressed in *E.coli*. Expression was first tested in small scale and it was found that the majority of the expressed proteins were insoluble when expressed at 25°C or 37°C. Best solubility was obtained for short constructs (JmjD3-c009 - JmjD3-c023) when expressed at 18°C. Two constructs, JmjD3-c023 and JmjD3-c031, were chosen and the purification procedures were optimized. The resultant proteins have in general greater than 90% purity as judged by SDS-PAGE. In JmjD3-c023, a two step purification was implemented. These include IMAC and SEC. In JmjD3-c031, an addition IEX chromatography was used after IMAC. The purified proteins were subject to functional and structural studies in the following chapters.

Chapter 3

Development of in vitro assay platforms for identification of selective JmjD3 inhibitors

3.1 Introduction

Over the past few years, several methods have been developed for quantifying histone demethylase activity in vitro. These include immunodetection of reaction products by specific antibodies, several mass spectrometry methods such as matrix-assisted laser desorption/ionisation-time of flight (MALDI-TOF) mass spectrometry, and formaldehyde detection by a formaldehyde dehydrogenase (FDH)-coupled assay. The drawbacks of these assays are low throughput, often a prerequisite of expensive equipment, and high protein and reagent consumption, making them less well suited for high throughput screening. This chapter describes the characterisation of JmjD3 activity using the above methods, as well as the development of two assay platforms that allow profiling of chemical candidates in a medium-throughput fashion.

3.1.1 Immunodetection assay

Immunodetection of histone demethylase activity by antibody has been used since the discovery of the first histone demethylase LSD1 (Shi et al., 2004; Metzger et al., 2005). It has also been used to detect

JmjD3 activity. JmjD3 was incubated with mammalian cell nuclear extracts and histone modifications were detected by western blot, where the disappearance of the H3K27me3 mark indicated demethylase activity (Swigut and Wysocka, 2007).

During the early stage of my studies, an immunodetection assay was used to measure purified recombinant JmjD3 activity. Recombinant proteins harbouring the catalytic region (JmjD3-c023 and JmjD3-c031) were incubated with calf thymus bulk histones to assay for demethylase activity (Fig. 3.1). Ammonium iron (II) sulfate and 2-oxoglutarate were used as cofactors in the reaction. Ammonium iron (II) sulfate was used instead of iron (II) sulfate as it is less inclined to oxidation to iron (III). The reaction products were dot-blotted on a membrane and probed by anti-H3K27me3 antibody. JmjD3-c031 was found to be enzymatically active as the histone H3K27me3 marks in bulk histones were removed (Fig. 3.1). The JmjD3-c023 construct was inactive (Fig. 3.1). Although it has a preserved JmjC domain, it lacks the C-terminal 177 residues. Inspection of the sequence reveals that this C-terminal region contains two CxxC signature motifs (Fig. 3.2). These are zinc-binding motifs crucial for the catalytic activity of JmjD3 (Chapter 4). The immunodetection assay is a robust method providing a qualitative determination of demethylase activity, but it lacks any quantitative information.

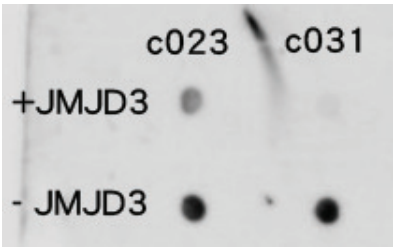


Figure 3.1: Dotblot showing that JmjD3-c031, but not JmjD3-c023, has histone demethylation activity in vitro. 10 μg of calf thymus bulk histones were incubated with 1 μg of recombinant JmjD3 proteins, 1 mM 2-oxoglutarate, 1 mM ascorbic acid, 100 μM ferrous ammonium sulphate and 50 mM HEPES pH 7.5. The presence of H3K27me3 marks was detected by anti-H3K27me3 antibody.

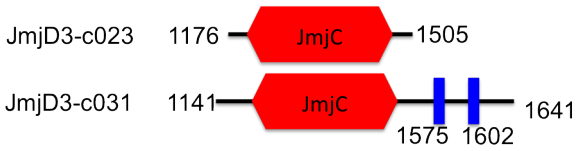


Figure 3.2: Schematic diagram showing domain organization of JmjD3-c023 and JmjD3-c031 construct. Blue boxes indicate the positions of predicted CxxC motifs.

3.1.2 Matrix-Assisted Laser Desorption/Ionization Time Of Flight (MALDI-TOF) mass spectrometry

MALDI-TOF is a mass spectrometry method to detect different species in a mixture of biomolecules by their mass to charge ratios (m/z). The biomolecules are prepared by mixing with α-cyano-4-hydroxycinnamic acid matrix and spotted on a stainless steel plate to allow crystallisation. In the mass spectrometer, a laser is fired to the crystal under vacuum, the matrix absorbs the laser energy, ionizes the analyte molecule with an added proton $[M+H]^+$, and the charged ions are accelerated in an electric field. Depending on the mass to charge ratio of the molecules, they travel at different rates in the electric field and hit the mass detector at different times, allowing the mass of the molecule to be determined. MALDI-TOF can be used to evaluate whether a demethylation reaction has occurred or not, by determination of mass shifts between substrate and product. Figure 3.3 shows the demethylation of H3K27me3 peptide by JmjD3-c031, with appearance of peaks corresponding to the demethylated species (red asterisks), while JmjD3-c023 was inactive as expected. As a semi-quantitative method, MALDI-TOF can be used to calculate the IC_{50} values of identified inhibitors by incubating the protein with H3K27me3 peptide in the presence of varying concentrations of inhibitors. The drawback of MALDI-TOF is that relatively high protein and peptide concentrations are used. Mass spectra were sometimes noisy, and can be very sensitive towards small fluctuations in the protein, substrate peptide and reaction conditions used. To accommodate this, ZipTip, a specially designed pipette tip which is filled with reversed- phase resin C18, was used to desalt the reaction mixture prior to mass spec detection, in order to increase the signal to noise ratio in peptide detection. This is a laborious procedure, but can be automated and thus provides a platform that is amenable to increased thoughput approaches.

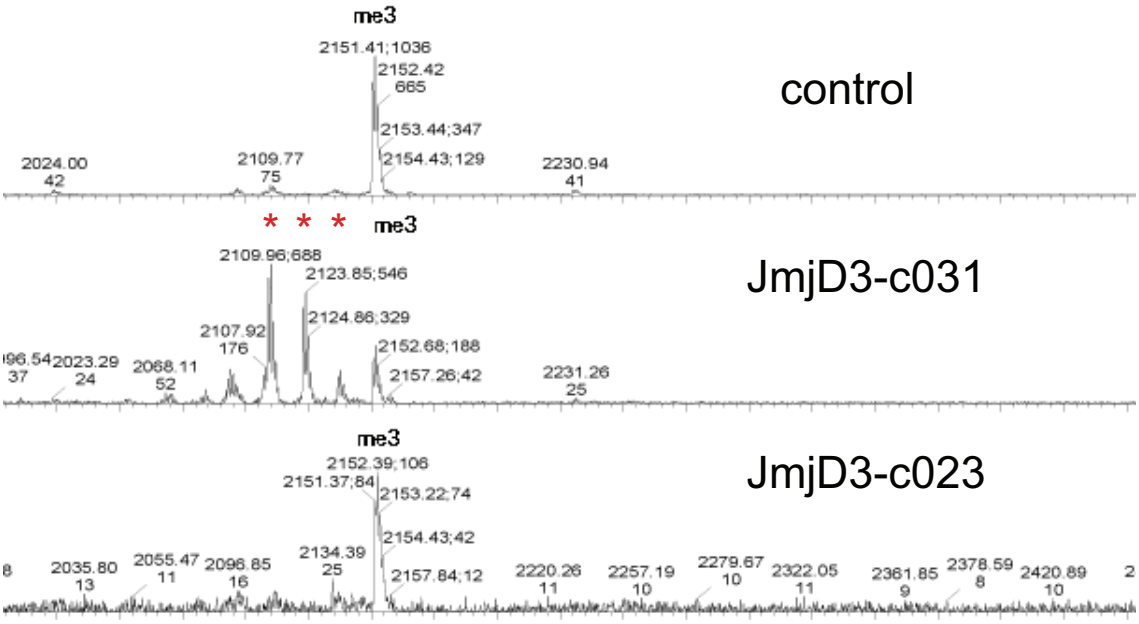


Figure 3.3: Mass spectrometry showing JmjD3-c031 has H3K27 demethylation activity. H3K27me3 peptide (KAPRKQLAKAARK(me3)SAPATGG) was incubated with recombinant JmjD3 and analyzed by mass spectrometry. The masses of tri-, di-, mono-, and un-methylated H3K27 peptides were 2151, 2137, 2123 and 2109 Da respectively. Red asterisks indicate the peaks of demethylated products.

3.1.3 Formaldehyde dehydrogenase (FDH) coupled assay

The FDH-coupled assay was developed to study steady state kinetics of some histone demethylases. (Rose et al., 2010b; King et al., 2010; Kristensen et al., 2011a). The principle of the assay is illustrated in Figure 3.4. Briefly, FDH is an NAD^+-dependent enzyme that converts formaldehyde, a by-product during the demethylation reaction (Chapter 1), into formic acid, with the concomitant formation of NADH. The change of NADH concentration can be detected by a fluorescence detector ($\lambda_{excitation}$ 340 nm, $\lambda_{emission}$ 450 nm).

The FDH assay consumes large amount of enzyme and peptide. Up to 1 μM of enzyme and 100 μM of peptide are required in a single reaction (70μL) (King et al., 2010). Attempts to miniaturize the assay have not been feasible, because if the concentration of the reactants is too low, very little NADH will be generated that falls below the detection limit of the equipment, thus it is not ideal for a high-throughput screening strategy.

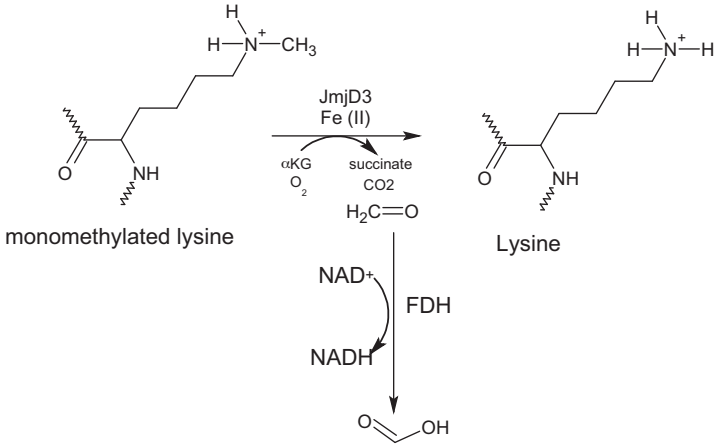


Figure 3.4: Schematic diagram showing mechanism of formaldehyde dehydrogenase (FDH)-coupled assay. Formaldehyde formed from the demethylation reaction is converted to formic acid by FDH. A NADH molecule is produced which is detected by spectrophotometry.

3.2 Differential Scanning Fluorimetry

Differential scanning fluorimetry (DSF) is a rapid screening method to identify small molecules that bind and stabilise proteins. The protein of interest is subjected to increasing temperature in a

thermocycler, and gradually unfolds thus exposing the hydrophobic core of the protein. Flourescence intensity is monitored as a function of temperature with a reporter dye SYPRO ORANGE. The fluorescence of the dye was quenched in an aqueous environment, but becomes highly fluorescent when bound to the hydrophobic regions of the unfolded protein. The melting temperature (T_m), defined as the transition mid-point at which the folded and unfolded protein concentrations are equal, is determined (Fig. 3.5). Inclusion of a protein-binding ligand in the assay stabilises the protein and shifts the unfolding process, causing a change in T_m. Therefore comparison of the T_m values of the protein with or without ligands can be used to imply ligand binding (Niesen et al., 2007).

It should be noted that the compactness of the protein structure can influence T_m values. Ideally the protein construct should contain only one structurally compact domain for the binding of a small molecule ligand. Multiple domains or flexible components outside the domain of interest may interfere with the binding of SYPRO ORANGE, which results in lower fluorescence signal or different folding transitions, hence complicate analysis. In the case of JmjD3, it is found that JmjD3-c023, but not JmjD3-c031, gives higher T_m shift value in DSF assay when incubated with a potent histone demethylase inhibitor 8-hydroxyquinoline-5-carboxylic acid (8HQ) (Fig. 3.6). Although JmjD3-c023 is enzymatically inactive due to the lack of C-terminal domain compared with JmjD3-c031, JmjD3-c023 is a more favourable construct to screen for small molecule binders in DSF assay.

The advantage of the DSF method is that it is very robust, and large amounts of samples can be screened in a day. 94 compounds can be tested in a 96-well plate including controls. However, this method only identifies ligand binding, with no indication of whether the small molecules would affect enzyme activity or bind to the active site of the enzyme. Therefore further experimental approaches are needed to validate each hit from a DSF experiment.

3.2.1 DSF screening of a focused library of oxygenase inhibitors

Having established that ligand binding to JmjD3 can be detected by DSF, JmjD3-c023 was subsequently screened in the DSF assay against a focused library containing 1046 compounds obtained from the NIH Chemical Genomics Center (NCGC), GlaxoSmithKline (GSK) and Prof. Chris Schofield's research group. These compounds are derived from previously identified KDM inhibitors (Rose et al., 2008, 2010a). There were 37 unique compounds yielding T_m shifts of more than 2°C (Fig. 3.7). Top

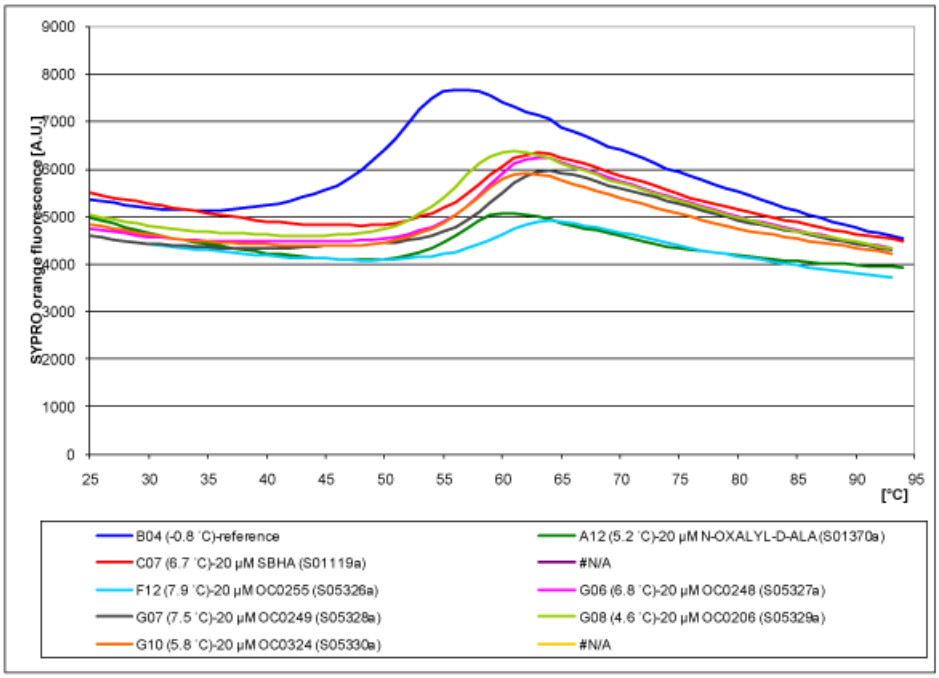


Figure 3.5: A typical result from the differential scanning fluorimetry assay using JmjD3-c023. Compounds are screened in 96 well plate format. Several hits were identified above, showing rightward (positive) T_m shifts of 4 - 8°C compared to control with no compounds (Blue).

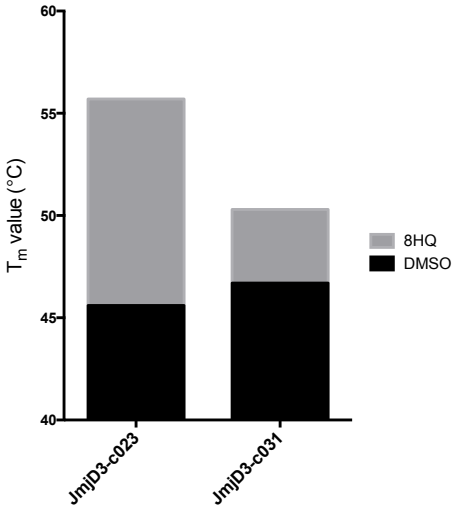


Figure 3.6: Comparison of T_m shift values of JmjD3-c023 and JmjD3-c031 towards 8HQ. The fact that both JmjD3-c023 and JmjD3-c031 constructs lead to T_m shift may suggest that 8HQ binds to the catalytic Jumonji domain.

10 hits are shown in Figure 3.8. Examination of these compound structures revealed that many are generic 2OG oxygenase inhibitors. These include quinolines (1, 3), oxalyl-tyrosine (2), hydroxamic acid (7) and bipyridines (4, 5, 6, 8, 9, 10) (Chapter 1).

The largest T_m shift was observed with 5-carboxyl-8-hydroxyquinoline (8HQ), which was previously reported as a potent JmjD2 inhibitor (King et al., 2010). It has a 10.1°C T_m shift in JmjD3. Such high T_m shift value indicated that 8HQ greatly stabilises JmjD3. Four out of the ten top hit compounds contain the 2,2-bipyridine group that can form a complex with the transition metal by bidentate interactions. It is possible that these compounds chelate the metal ion in the core of the JmjC domain (as seen in Chapter 4), thus stabilising the protein by occupying the space in the active site. They could be potential competitive inhibitors against the natural substrate 2OG. Interestingly, many of these compounds also contain a bulky aromatic or cyclo-hydrocarbon group branching from the main metal chelating centre. These bulky groups (Fig 3.8. square boxes) may occupy the space next to the metal centre, which is very likely the opening of the active site.

Five out of the 37 top hits showed some degree of selectivity towards JmjD3 when they were cross-profiled against other histone demethylases in DSF (Fig. 3.9). These include 8HQ with a three-fold stabilising effect in JmjD3 (10.1 °C) than in JmjD2 family members (3.6°C). These compounds were selected for subsequent inhibition studies.

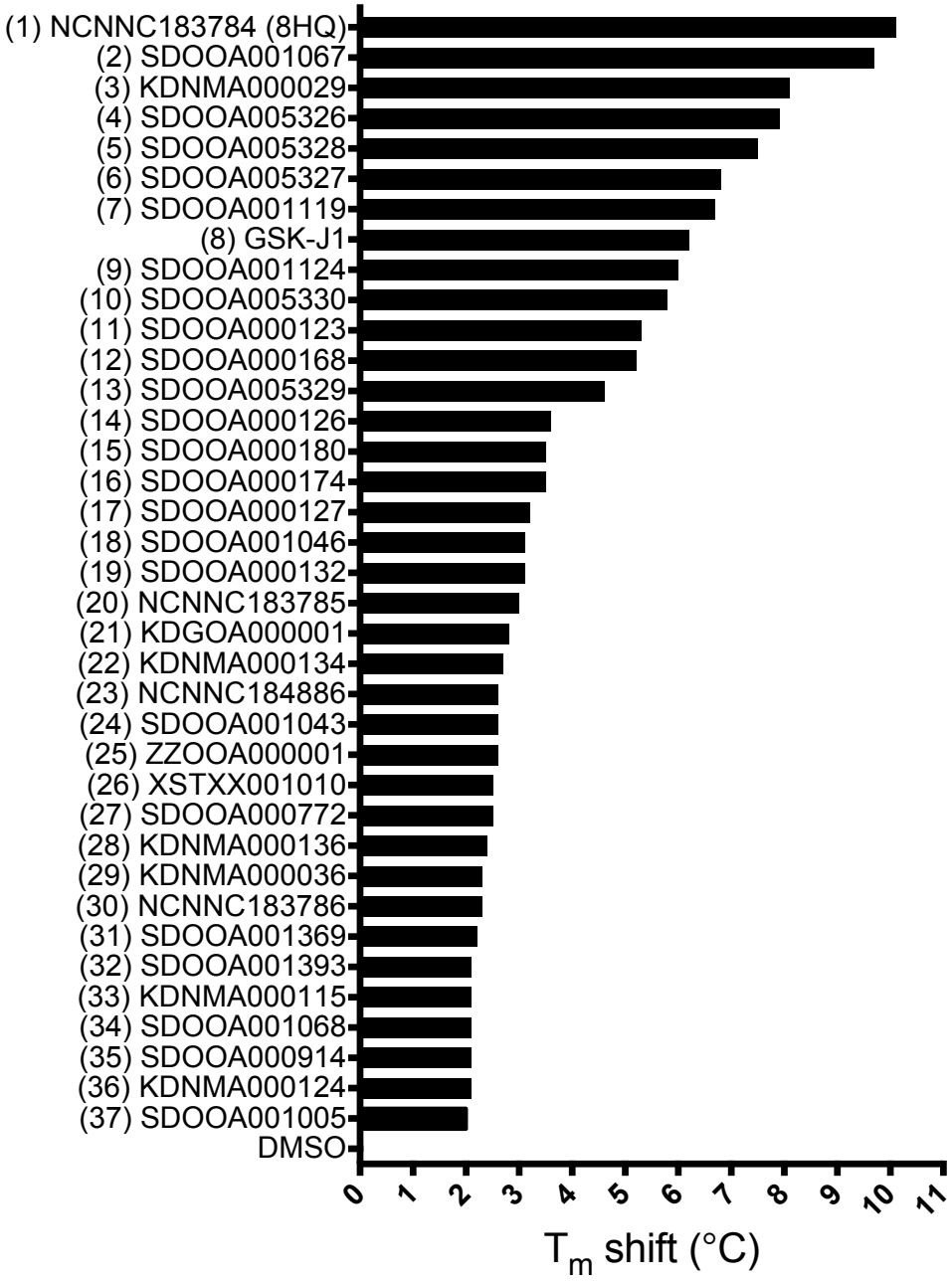


Figure 3.7: Bar graph showing 37 compounds having T_m shifts of more than 2°C towards JmjD3-c023, in decreasing order of shift value.

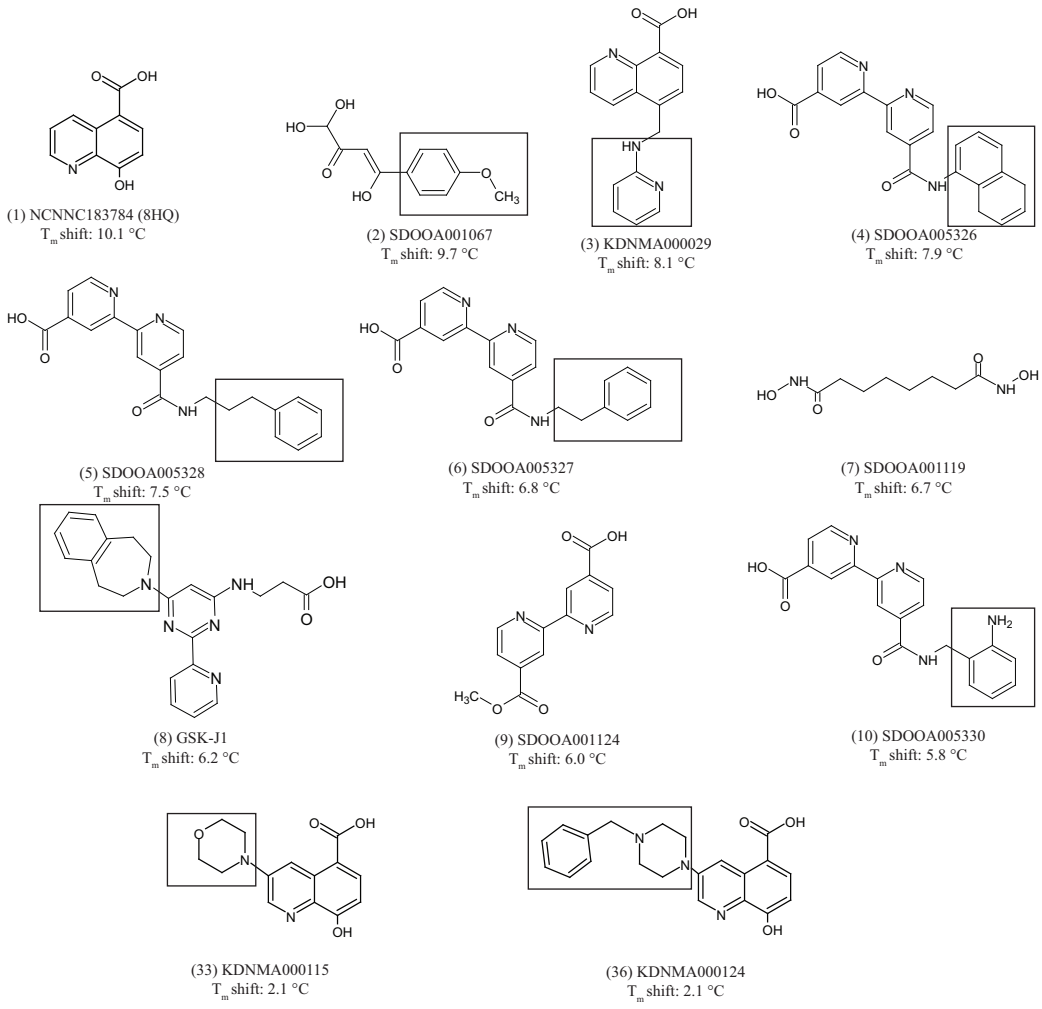


Figure 3.8: Chemical structures of a selected panel of compounds having T_m shifts of more than 2°C. Boxes indicate a bulky chemical group branching from the metal chelating centre.

	JmjD1A Tm Shift (°C)	FBXL11 Tm Shift (°C)	JmjD3 Tm Shift (°C)	JmjD2 Tm Shift (°C)	JmjD2B Tm Shift (°C)	JmjD2C Tm Shift (°C)	JmjD2D Tm Shift (°C)	Jmj2E Tm Shift (°C)	NO66 Tm Shift (°C)	MINAB Tm Shift (°C)
(1) NCNNC183784 (8HQ)	N/A	0.3	10.2	3.6	0.2	3.8	0.5	2.4	-2.0	-1.6
(2) KDNMA000029	N/A	-0.1	8.2	-4.4	-1.1	-8.7	-0.3	-1.2	-2.8	-1.6
(8) GSK-J1	-0.6	-2.4	6.2	-1.0	-3.1	-2.0	-1.0	-1.0	0.0	-1.1
(33) KDNMA000115	N/A	-0.1	2.1	N/A	N/A	0.1	N/A	-0.1	0.1	-0.4
(36) KDNMA000124	N/A	0.0	2.1	N/A	N/A	0.4	N/A	0.1	N/A	-0.2

Figure 3.9: A heat map highlighting five compounds from DSF screen with selectivity towards JmjD3 against other histone demethylases. The numbers are coloured according to their magnitude, ranging from highest T_m shift (red) to lowest (green) for each compound.

3.3 Amplified Luminescent Proximity Homogeneous Assay

Amplified luminescent proximity homogeneous assay screen (AlphaScreen) is a bead-based proximity assay which could be used to study interactions between biomolecules. This method can be developed to detect a demethylation reaction, relying on the use of two kinds of alpha beads. One is the streptavidin-coated donor bead that binds to a biotinylated peptide substrate. The other one is the protein A-coated acceptor bead that binds to anti-H3K27me2 antibody. When a demethylation reaction occurs, the H3K27me3 mark on a biotinylated substrate peptide is converted to H3K27me2 and the anti-H3K27me2 antibody binds to H3K27me2 peptide, bringing the donor and acceptors beads into close proximity. Upon laser excitation at 680 nm, the donor beads emit short-lived singlet oxygen which emits light photons at 520-620 nm when reaching the acceptor bead (Fig. 3.10). The absorbance is therefore correlated to the quantities of H3K27me2 produced.

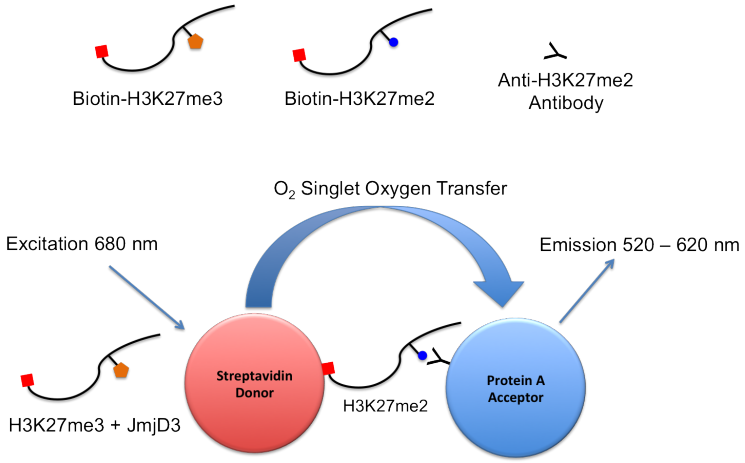


Figure 3.10: Schematic diagram of the AlphaScreen mechanism. Biotin-H3K27me3 peptide is demethylated to H3K27me2 by JmjD3. The biotinylated peptide binds to Streptavidin donor beads and the H2K27me2 epitope is recognized by anti-H3K27me2 antibody coated on Protein A acceptor beads. Excitation of the reaction mixture with 680 nm laser induces O2 oxygen transfer and emits photons at 520 - 620 nm.

Selection of a high-quality antibody is crucial to the design and execution of this experiment. Since JmjD3 catalyzes three stepwise reactions leading to different methylation states (Kme3 to Kme2, Kme2 to Kme1, and Kme1 to Kme0), and hence three choices of antibodies, each detecting a specific methylation state, can be used. Anti-H3K27me3 antibody can be used to detect substrate

depletion. Anti-H3K27me2 and anti-H3K27me1 antibodies can be used to detect product formation. The ideal antibody should have high specificity because it is only detecting small differences on the epitope.

To test the specificity of an antibody, anti-H3K27me2 antibody was tested against H3 peptide at different K27 methylation states (Fig 3.11). The highest signal to noise ratio for product (H3K27me2) to substrate (H3K27me3) is 111 at 50 nM (Fig. 3.11). In the subsequent screening assay, 60 nM peptide will be used to produce adequate signal (>1000000 unit) with minimal peptide consumption.

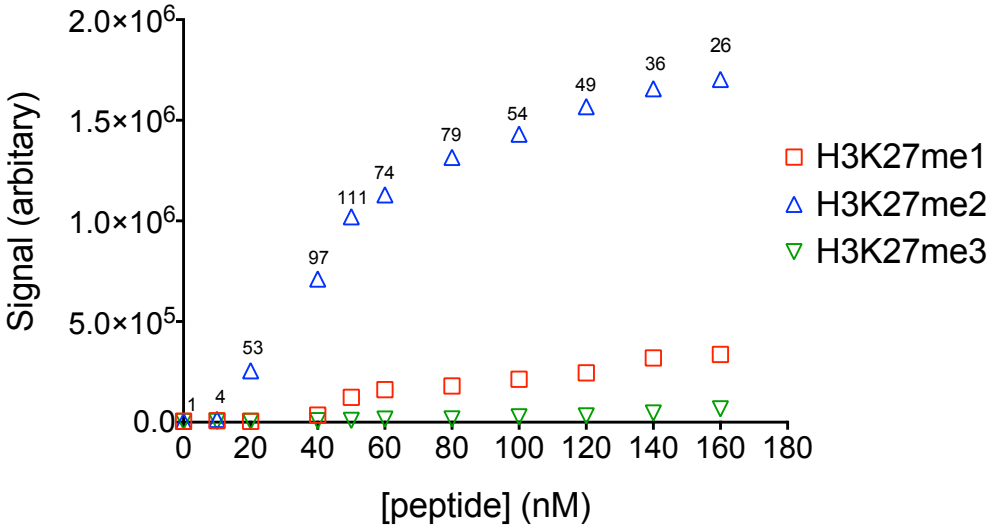


Figure 3.11: Specificity of anti-H3Kme2 to peptides of different methylation states. The numbers above H3K27me2 data points are the signal to noise ratio of product (H3K27me2) and substrate (H3K27me3). The sequence of the peptides used is Biotin - KAPRKQLATKAARK(me1/2/3)SAPATGG

The conversion of Kme3 to Kme2 is the fastest step in the JmjD3-catalyzed reaction (Kristensen et al., 2011b). The initial velocity measured for the enzyme should therefore reflect this step. However, Kme2 to Kme1 or Kme2 to Kme1 reactions are also occurring simultaneously. The complexity of these reactions leads to two problems that may affect measurement of the enzyme kinetics. First, accumulation of Kme2 will cause production inhibition when it competes with Kme3 for substrate binding. Therefore the rate of the Kme3 to Kme2 step will be underestimated. Second, there is also signal loss due to depletion of Kme2 in the Kme2 to Kme1 reaction. Both problems can be tackled by

minimizing the reaction time and the concentration of JmjD3 enzyme, thus reducing the occurrence of Kme2 to Kme1 or Kme1 to Kme0 reactions.

To illustrate the concentration and time dependence, Figure 3.12 shows the formation of H3K27me2 product over time under different concentration of JmjD3 at room temperature. Formation of H3K27me2 occurred at a rate of 19887 unit / min in 0.5 nM JmjD3. When 10 times more JmjD3 was used (5 nM), H3K27me2 is formed 10 times faster (216258 unit / min) but lost rapidly due to demethylation of Kme2 to Kme1. When 2 nM JmjD3 was used, signal loss of Kme2 product was seen after three minutes of incubation. The optimal JmjD3 concentration is 1 nM as it produced adequate signal (30945 unit / minute) for measurement of initial velocity. The reaction rate reaches a plateau after 5 minutes without any signal loss, suggesting that the Kme2 to Kme1 reaction is dependent on the enzyme concentration. To conclude, JmjD3 is used at 1nM and the reaction is stopped after 3 minutes.

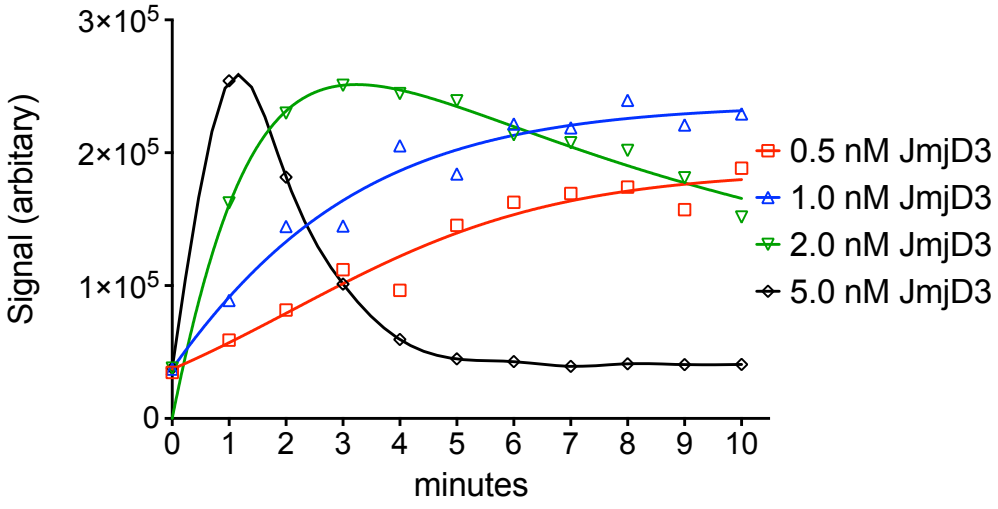


Figure 3.12: Formation of H3K27me2 product over time under different concentration of JmjD3 enzyme at room temperature. 60 nM H3K27me3 peptide was used as substrate.

The AlphaScreen is very sensitive in detecting an enzyme reaction down to concentrations of 60 nM peptide and 1 nM enzyme concentration in a 10 μL format, thus consuming very little reagents. However, the assay is very sensitive to ambient light and temperature, which results in occasionally inconsistent readings across a 384-well plate. These issues can be improved by proper control of laboratory environment such as the use of a light insulated box. Despite these drawbacks, it is adapted

as the main platform for screening of JmjD3 inhibitors in the Structural Genomic Consortium, where parts of this work were carried out.

3.3.1 Screening results from AlphaScreen

Using the above assay conditions, JmjD3 was screened against a library containing 6734 compounds to identify potential JmjD3 inhibitors. These compounds were obtained from collaborators of the Structural Genomics Consortium, including NIH Chemical Genomics Center (NCGC), GlaxoSmithKline (GSK) and Prof. Chris Schofield's research group. The screening experiments were performed with assistance from Dr Anthony Tumber at the SGC who also helped with determining the majority of the following IC_{50} values against JmjD3.

49 unique compounds were found to yield IC_{50} values of less than 1 μM (Fig. 3.13). Figure 3.14 shows 10 inhibitors having the lowest IC_{50} with available chemical structures, of which four were previously identified to have selectivity for JmjD3 in the DSF screen. Nine out of the top ten compounds are 8HQ derivatives and the other one is a pyridyl-pyrimidine containing compound. 8HQ itself has the lowest IC_{50} value (0.03 μM), consistent with the previous DSF result. As mentioned before, all these potent compounds were found to have a bulky chemical group branching from the C-2 position of the quinoline group. For example, GSK-J1 (Fig. 3.14, (3)) contains a benzazepine ring. These bulky groups are likely to play similar roles in binding, as exemplified by co-crystallisation studies of these compounds with JmjD3 as described in Chapter 4. These bulky groups may therefore be chemically modified to enhance potency and selectivity of the compound against JmjD3.

GSK-J1 (3) has the highest potency against JmjD3 among the histone demethylase family (Fig. 3.15). It is over 1000 fold more selective towards JmjD3 than other histone demethylases (Kruidenier et al., 2012). KDNMA000124 (8) is the second most selective compound, although it inhibits JmjD1A at IC_{50} of 1 μM. KDNMA000115 and 8HQ also inhibit JmjD1A and JmjD2A with IC_{50} value less than 1 μM in vitro, thus not selective among the histone demethylase family. To conclude, GSK-J1 is the most selective inhibitor of JmjD3 in this study.

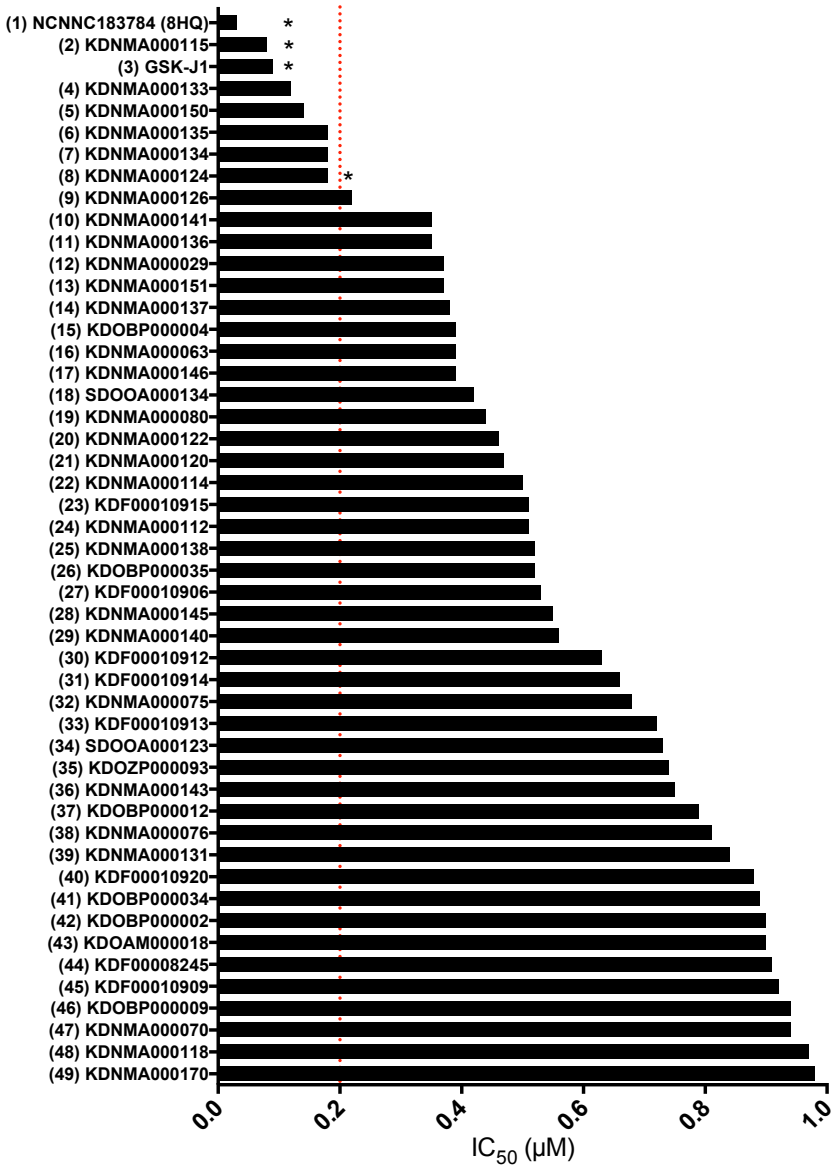


Figure 3.13: Bar graph showing 49 compounds having IC_{50} value lower than 1.0 μM, as determined from the AlphaScreen. The red dotted line indicates the position of 0.2 μM, chosen as the threshold. The black dotted line indicates compounds that were previously identified in DSF screen to have selectivity in the histone demethylase family.

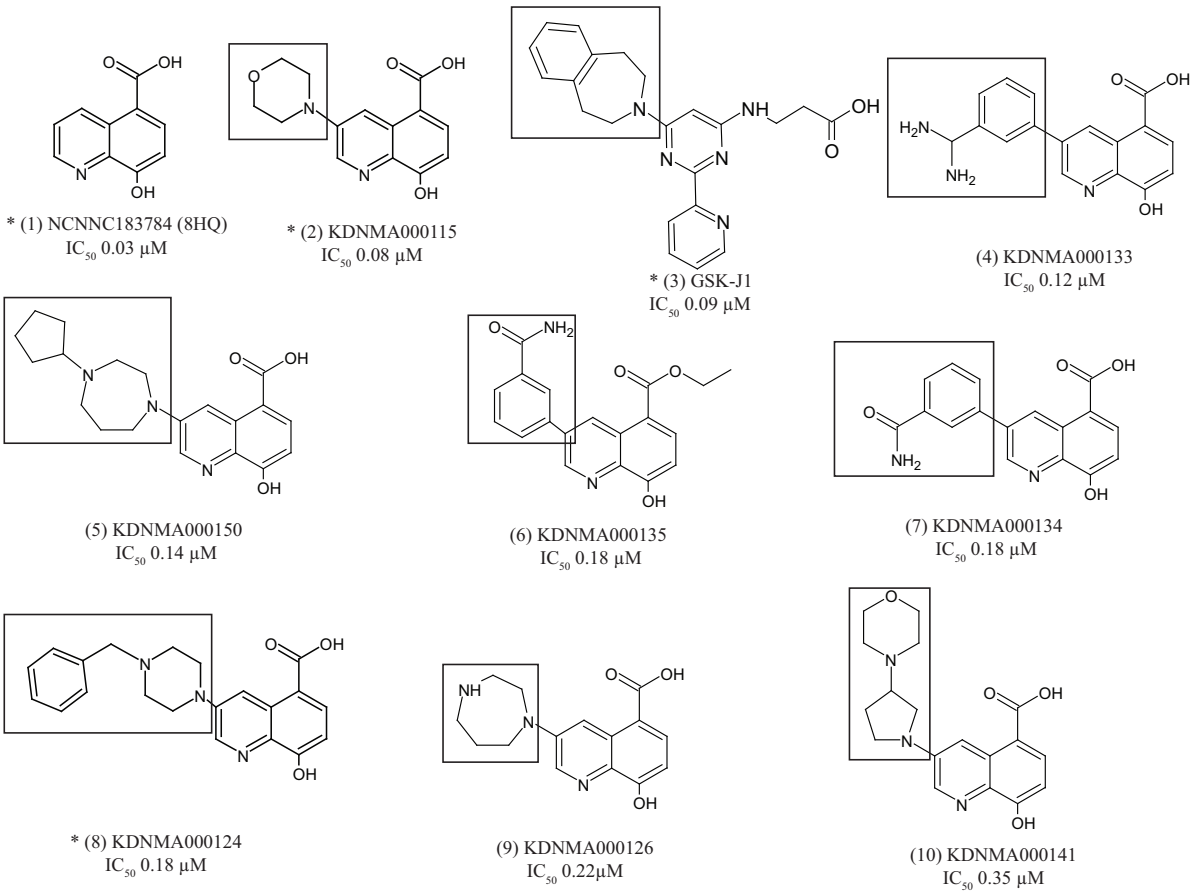


Figure 3.14: Chemical structures of 10 compounds having lowest IC_{50} values in the library screen by AlphaScreen. Asterisks indicate compounds previously identified in DSF screen to have selectivity towards JmjD3 in the histone demethylase family. Square boxes indicate bulky chemical group likely to be involved in binding specificity.

	FBXL11 IC_{50} (μM)	JmjD1 IC_{50} (μM)	JmjD2C IC_{50} (μM)	JmjD2E IC_{50} (μM)	JmJD3 IC_{50} (μM)	Jarid1C IC_{50} (μM)
NCNNC183784 (8HQ)	5.21	0.17	0.56	0.30	0.03	18.77
KDNMA000115	19.94	0.44	0.23	0.35	0.08	11.62
KDNMA000124	N/A	1.05	4.19	1.84	0.18	18.30
GSK-J1	62% inhibition at 100 μM	38.00	N/A	15.15	0.09	16.02

Figure 3.15: A heat map showing IC_{50} values of selected compounds against different class of histone demethylases, as determined in the AlphaScreen. GSK-J1 has the highest selectivity towards JmjD3. The numbers are coloured according to their potency, ranging from lowest IC_{50} (red) to the highest IC_{50} (green) for each compound.

3.4 Correlation between DSF and AlphaScreen data

To investigate whether there is a relationship between IC_{50} values from AlphaScreen and T_m shift values from DSF assay, 90 inhibitors that contain data from both assays against JmjD3 were compared. Of the 83 compounds that have IC_{50} values greater than 0.2 μM, 70 of them give T_m shift below 2°C (Fig. 3.16A), suggesting that less potent inhibitors will likely not have any stabilising effect on JmjD3. There are 7 compounds with IC_{50} below 0.2 μM, of which 5 compounds have T_m shift more than 2°C (Fig. 3.16B). These include the 4 compounds identified from AlphaScreen (Fig. 3.15) that display selectivity towards JmjD3. In particular the two most potent inhibitors, 8HQ (IC_{50} 0.03μM) and GSK-J1 (IC_{50} 0.09μM), give the highest T_m values of 6.2°C and 10.1°C respectively.

To conclude, an inhibitor which produces an IC_{50} below 0.2 μM would likely to have high T_m shift values in DSF. High T_m shift values in DSF may not necessarily indicate a potent inhibitor, and the magnitude of T_m shift may not be proportional to its potency.

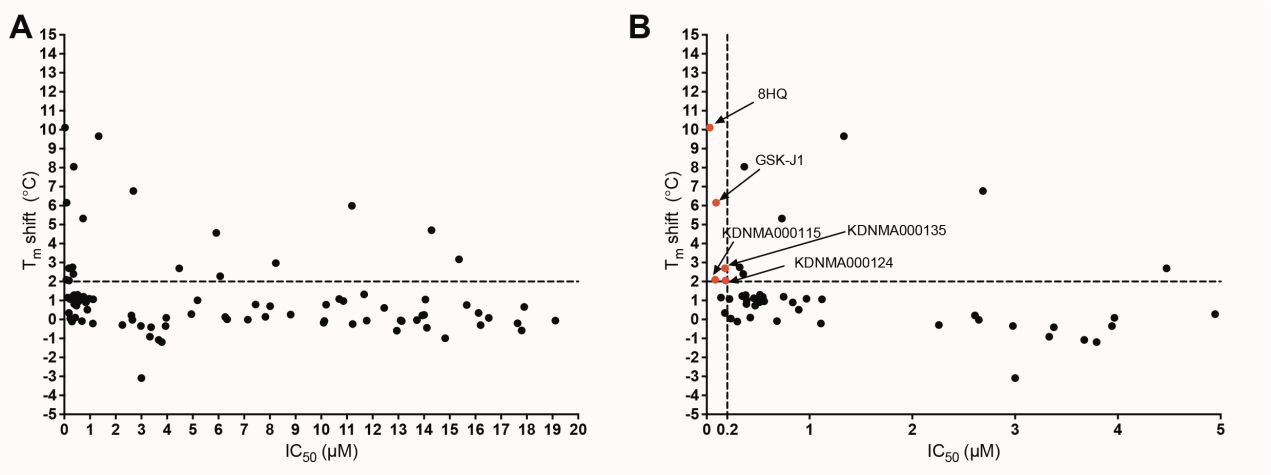


Figure 3.16: Scatter plots showing T_m shift values of JmjD3 inhibitors versus the IC_{50} values. A) IC_{50} values range from 0 to 20 μM. B) IC_{50} values range from 0 to 5 μM.

3.5 Inhibition of UTX by GSK-J1

To test whether GSK-J1 also inhibits UTX of the same KDM6 family, UTX was treated with GSK-J1 and compared with JmjD3 in a mass spectrometry assay. It is found that GSK-J1 inhibits both JmjD3 and UTX at a similar potency, with $IC_{50} = 56$ μM for UTX (3 μM enzyme) and $IC_{50} = 18$ μM

for JmjD3 (1 μM enzyme). Inhibition of UTX by GSK-J1 is not unexpected because the sequence of UTX Jumonji domain as well as the 3D structure share high homology with JmjD3 (Chapter 4).

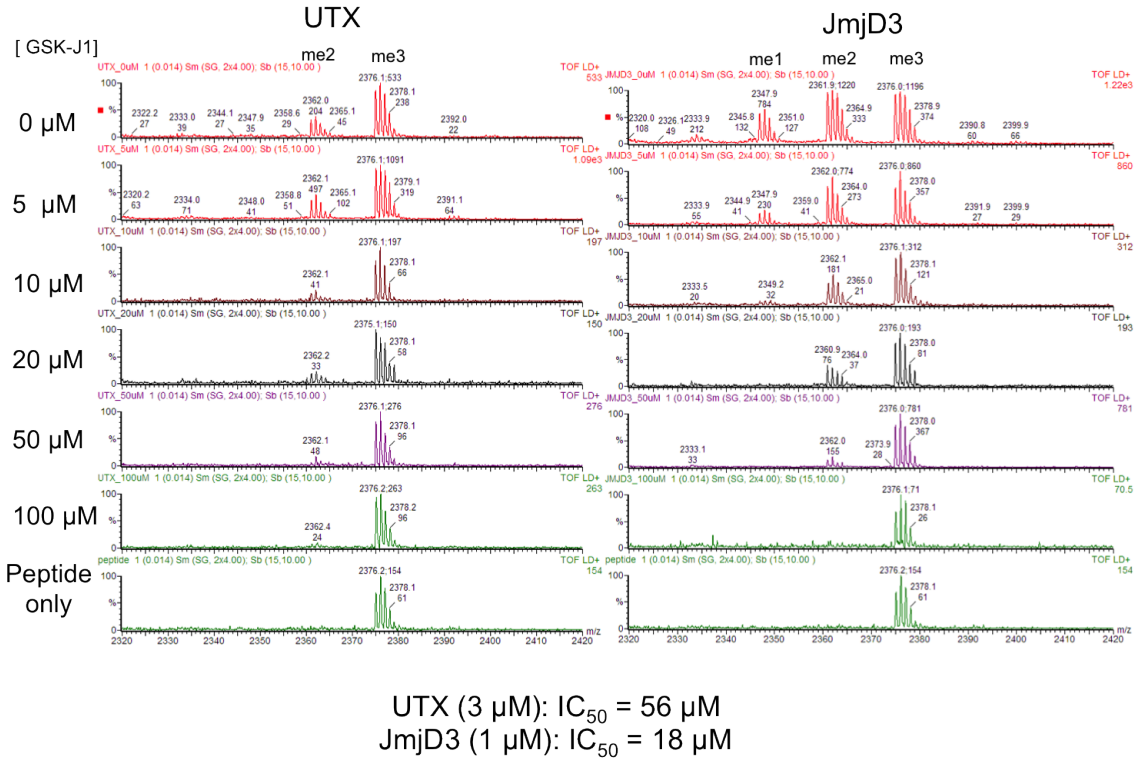


Figure 3.17: Mass spectra showing dose response inhibition of JmjD3 and UTX by GSK-J1. UTX assay condition: 3 μM UTX, 10 μM H3K27me3 peptide, 1 mM 2OG, 2 mM ascorbic acid, 50 μM ammonium iron (II) sulfate. Reaction incubated for 20 minutes at room temperature and stopped by adding EDTA to a final concentration of 10 mM. JmjD3 assay condition: 1 μM JmjD3, 10 μM H3K27me3 peptide, 1 mM 2OG, 2 mM ascorbic acid, 50 μM ammonium iron (II) sulfate. Reaction incubated for 3 minutes at room temperature and stopped by adding EDTA to 10 mM. Peptide sequence: KAPRKQLAKAARK(me3)SAPATGG

3.6 Summary

In this chapter, a number of assays for histone demethylase activity, and the different potential applications they could serve, have been discussed. The antibody based immunodetection assay and MALDI-TOF assay allow a qualitative detection of histone demethylase activity, and in particular the MALDI-TOF assay shows the actual change in mass of a histone peptide, thus giving a more confident and conclusive result to investigators. However, it is difficult to detect the mass of the histone purified from cell extracts by MALDI-TOF because of the heterogeneity of histone modifications. Instead, immunodetection assay can serve this purpose. Histone- and methylation state- specific antibodies can be used to detect the loss of substrate (H3K27me3) or the gain of products (H3K27me2 and H3K27me1). An antibody based cell assay is developed to detect demethylation of histones in cells, and will be discussed in Chapter 5.

DSF assay and AlphaScreen assays can be adopted for high throughput screening purposes. DSF is robust and yields information of which compounds can stabilise a protein, an indication of ligand binding. However, the DSF assay can also produce false positive or negative results. It is essential to confirm the hits by a second validation method such as the FDH-coupled or AlphaScreen Assay. AlphaScreen assay has the highest throughput among these approaches. It uses an antibody based detection but is more sensitive than the immunodetection assay described above. It also consumes very little enzymes and peptides therefore ideal for high throughput screening of JmjD3 inhibitors.

Both DSF and AlphaScreen assays were used to screen for a library of small molecules. GSK-J1 was identified as a potent and selective histone demethylase inhibitor. It has an IC_{50} value of 0.09 μM and is 1000 fold more potent to JmjD3 than other histone demethylase as measured by AlphaScreen. Other 8HQ-based inhibitors, namely KDNMA000115 and KDNMA000124, were also identified to have high potency towards JmjD3, though not as selective as compared to GSK-J1.

To conclude, the development of these assay platforms and the discovery of GSK-J1 as a potent inhibitor provide useful biochemical tools, paving the way for further structural and cellular experiments to characterize JmjD3 as described in latter chapters.

Chapter 4

Structure determination of JmjD3

4.1 Introduction

During the initial phase of the JmjD3 project, structural information was not available on any members of the JmjD3 / UTX (KDM6) subfamily. The use of a homology model to understand the catalytic mechanism was undesirable because JmjD3 has low sequence identity compared with other enzymes of the KDM family, whose structures have been experimentally determined. Crystallisation of JmjD3 was performed in 2010 as part of this thesis work and resulted in its structure determination. The determination of the JmjD3 crystal structure not only helps us to further characterize the enzyme, but also enables structure based inhibitor design. During the course of this thesis, several structures were determined, by myself, collaborators and external groups. Table 4.1 gives an overview of the different structures that are now available. In this chapter, we will discuss the use of X-ray crystallography technique to understand the structure-function relationship of JmjD3 and the KDM6 subfamily.

4.2 Crystallisation and structure determination of JmjD3

The two purified constructs of JmjD3 (c023 and c031), as described in chapter 2, were subjected to nano-litre scale crystallisation trial using the vapour diffusion method. In a typical 96-well experiment, purified protein (15 mg/ml) was mixed with a series of crystallisation solutions in 150 nL sitting drops that were incubated against a reservoir containing the crystallisation solutions. These solutions were

PDB code	species	protein	Cofactor / Ligand	Reference
2XXZ	human	JmjD3	Fe(II), 8HQ	this work
2XUE	human	JmjD3	Fe(III), 2OG	Kruidenier et al. (2012)
4ASK	human	JmjD3	Co (II), GSK-J1	Kruidenier et al. (2012)
4EYU	mouse	JmjD3	Ni (II), NOG	Kruidenier et al. (2012)
4EZ4	mouse	JmjD3	Ni (II), NOG	Kruidenier et al. (2012)
4EZH	mouse	JmjD3	Ni (II), NOG, H3K27me3	Kruidenier et al. (2012)
3AVR	human	UTX	Ni (II), NOG, H3K27me3	Sengoku and Yokoyama (2011)
3AVS	human	UTX	Ni (II), NOG	Sengoku and Yokoyama (2011)

Table 4.1: Available structures of the KDM6 family.

obtained from commercially available 'random-matrix' screens, which sample various combinations of precipitants, pH buffers and salt solutions from a diverse spectrum of the chemical space. Further parameters were varied to improve crystallizability include incubation temperature (20°C vs. 4°C), and the ratio of protein to crystallisation solution in the sitting drops (2:1, 1:1, and 1:2). Initial crystals for the construct c023 were observed in several conditions from the Hampton Index crystal screen. These conditions contained in common 20% (v/v) PEG 3350 as the precipitant, but with various metal ion salts. Follow-up grid screens, varying the concentrations of precipitants, pH buffers and salt solutions in small increments, were designed, and the optimal crystallisation condition was narrowed down to 0.15 - 0.2 M $MgCl_2$, 0.1 M HEPES pH 7.5, 23-25% (v/v) PEG 3350 and 2 mM $NiCl_2$. In an attempt to further improve crystal quality and morphology, and to obtain ligand-bound complexes, protein was co-crystallised with 1 mM 8-hydroxyquinoline-5-carboxylic acid (8HQ) that was identified as an inhibitor of JmjD3 in the DSF assay described in Chapter 3. Diffraction-quality crystals initially appeared after 2 days and reached a maximum dimension of 120 μm x 20 μm x 5 μm after 7 days (Fig. 4.1). Crystals were cryo-protected with 25% (v/v) ethylene glycol during crystal mounting and flash frozen in liquid nitrogen in preparation for X-ray data collection.

The structure determination of JmjD3 described henceforth was performed with assistance from Dr Tobias Krojer and Dr Wyatt Yue of the SGC, as part of the structural genomics pipeline. In brief, X-ray diffraction data were collected at the Diamond Light Source beamline I02, to a resolution limit of

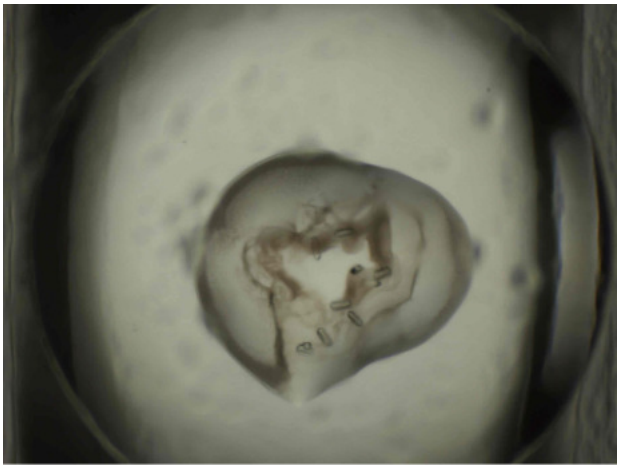


Figure 4.1: These crystals are grown in 0.1 M HEPES pH 7.5, 25% (v/v) PEG 3350 and 2mM $NiCl_2$ in a 1:1 drop ratio with 10 mg/mL protein in 20°C.

1.8 Å. The space group was determined to be P 21 21 21 with unit cell dimensions a = 56.8 Å, b = 71.4 Å, c = 159.7 Å, $\alpha = 90°$, $\beta = 90°$, $\gamma = 90°$. Attempts to solve the JmjD3 structure by the molecular replacement method, using previously reported structures from the JMJD2 demethylase subfamily (e.g. JMJD2A, JMJD2D, JMJD2E) as search models, were not successful. Therefore phases were derived from Single-wavelength Anomalous Dispersion (SAD) using a mercury derivative, thiomersal. This generated an interpretable electron density map, which was used for manual model building and refinement. The final model converged to Rfree and Rfactors of 0.216 and 0.185 respectively. Analysis of a ramachandran plot revealed no outliers in the model. The final coordinates and structure factor were deposited in the Protein Data Bank with the accession code 2XXZ.

4.3 Overall structural description

The refined structure of JmjD3-c023 contains 2 protomers in the asymmetric unit, modelled with residues 1175-1493 in chain A and residues 1175-1499 in chain B. No electron density was observed for residues 1173-1174 (chains A and B), 1494-1502 (chain A) and 1500-1502 (chain B). While present in the expression construct, these residues are likely to be disordered in the crystal. The overall architecture of JmjD3-c023 reveals the typical double stranded β-helix (DSBH) fold found in all other 2OG oxygenases for which structures have been solved (Fig. 4.2). The DSBH fold comprises eight β-strands that are grouped into a four-stranded β-sheet on one side of a deep cavity, and

another four-stranded β-sheet on the opposite side. In the active site, located at the bottom of the deep cavity of the DSBH fold, a Ni (II) ion is coordinated by the conserved triad of His1390, Glu1392 and His1470. The active site metal ion was modeled as Ni (II) which was present in the crystallisation buffer, and substituted for the endogenous Fe (II) to form a catalytically inert complex. Electron density at the active site further reveals a bound 5-carboxy-8HQ molecule that was co-crystallised with JmjD3. 5-carboxy-8HQ occupies the location of the 2OG binding site (overlay with 2OG/NOG in other structures), and coordinates the Ni (II) in a bidentate manner via its 8-hydroxyl oxygen and quinoline nitrogen atoms. The 5-carboxylic acid group further forms a salt bridge with Lys1381 (Fig. 4.3).

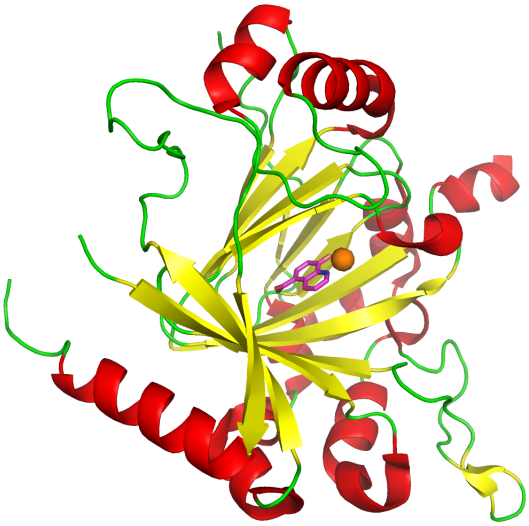


Figure 4.2: Cartoon representation of JmjD3 Jumonji domain. The bound ligand 8-hydroxyquinoline-5-carboxylic acid is shown in sticks (Cα atoms coloured magenta) and the active site Ni (II) in orange sphere. The JmjD3 protomer is coloured according to secondary structure elements (helix: red, β strand: yellow, loop: green)

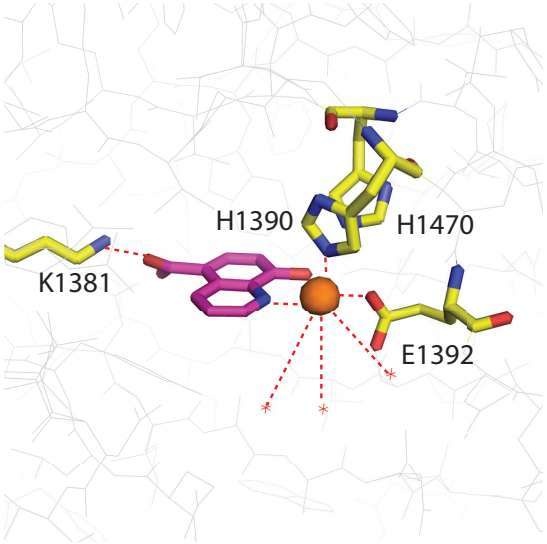


Figure 4.3: JmjD3-c023 active site. Ni (II) (orange) is coordinated by H1390, E1392, H1470 and 8-hydroxy-5-carboxyquinoline. The carboxyl group of 8-hydroxy-5-carboxyquinline forms a salt bridge with K1381. Water molecules are shown as red asterisks.

4.4 Comparison of JmjD3-c023 with JmjD3-GSK

The crystallised construct JmjD3-c023 is enzymatically inactive and unable to demethylate H3K27me3 peptide using immunodetection and MALDI-TOF assays (Chapter 3). Nevertheless, attempts to crystallise the longer construct JmjD3-c031 (aa 1141-1641), shown to be catalytically active in Chapter 3 were not successful. In the mean time, parallel efforts from our collaborator GlaxoSmithKline (GSK) to crystallise a longer JmjD3 fragment have allowed its structure determination (PDB accession code: 2XUE) (Kruidenier et al., 2012). The longer construct, encompassing residues 1157-1641 (here annotated JmjD3-GSK), has an extra C-terminal zinc binding domain (ZBD, aa 1488-1641). Superimposition of the JmjD3-c023 and JmjD3-GSK structures reveals the same overall architecture within the Jumonji domain, with root mean square deviations (RMSD) equal to 0.45 Å. Minor structural differences between the two structures are found in a flexible loop region (Glu1357 - Gly1366). In JmjD3-c023, this loop extends outward from the core DSBH fold in protomer A (Fig 4.4A, red), but adopts a similar orientation as seen in the JmjD3-GSK structure (Fig 4.4A,B) where this loop region forms a short 3_{10} helix and is stabilized by packing against a neighbouring helix in the additional ZBD, but in protomer B this loop is partially disordered.

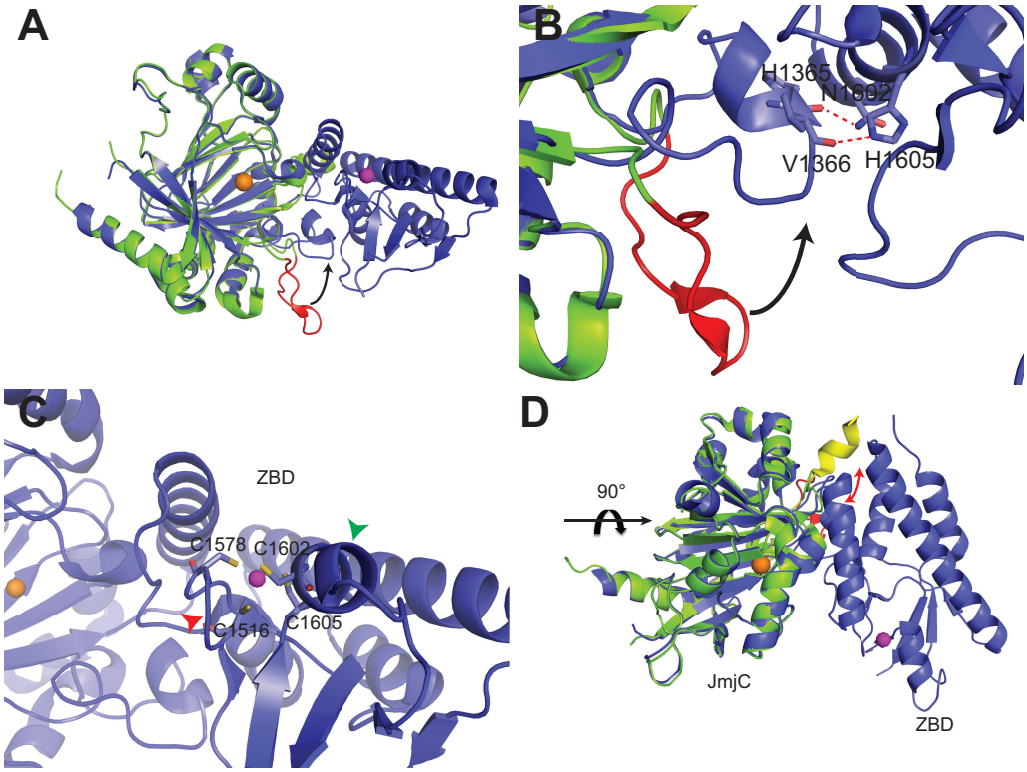


Figure 4.4: Comparison of JmjD3-c023 with JmjD3-GSK. a) JmjD3-c023 (green) protomer A superimposed with JmjD3-GSK (blue). The active-site metal Co (II) of JmjD3-GSK is depicted in orange. The additional zinc binding domain of JmjD3-GSK with Zinc ion is coloured in magenta. A flexible loop of JmjD3-c023 is coloured red (Glu1357 - Gly1366). b) A close look at the loop region. Red dash line denote the hydrogen bonds between two interacting two helix in JmjD3-GSK. c) View of the zinc binding domain. Zinc ion is coordinated by four cysteine residues (Cys1575, Cys1578, Cys1602, Cys1605). D) C-terminal residues Ala1487 to Ala1494 (yellow, JmjD3-c023) are pointing to the extracellular space in the JmjD3-c023 instead of towards the ZBD in JmjD3-GSK (red arrow). Amino acid residues Leu1395 to V1403 are missing from the C-terminal end of JmjD3-023 (yellow). Structure is rotated 90° from the structure in panel A as indicated.

The ZBD, essential for the demethylase activity of JmjD3, contains two CxxC motifs (Cys1575-xx-Cys1578, Cys1602-xx-Cys1605) to coordinate a Zn (II) ion. The function of the zinc ion is likely to stabilize the loop (Glu1570 - Asn1584) and a short helix (Cys1602 - S1610) (Fig 4.4C, loop: red arrow, short helix: green arrow) in the vicinity. A second difference between the two structures resides in the helical segment Ala1487-Ala1494, which constitutes the C-terminus for the JmjD3-c023 construct (Fig. 4.4D). This helix adopts different orientations in the two JmjD3-c023 protomers (partially disordered in protomer A), both of which are oriented outwards to the exterior solvent space. By contrast, the equivalent helix in JmjD3-GSK posits in opposite direction and forms part of a 4-helix bundle in the core ZBD (Fig. 4.4D, red arrow). Such difference is attributed to the lack of the full ZBD such that the helix is not packed in the ZBD but instead orientated towards the exterior solvent space. Half of the helix at the C-terminal end, Leu1395 to V1403, is missing from the JmjD3-c023 structure due to a lack of electron density observed in the dataset, suggesting that these regions are highly flexible.

The above two structural differences between JmjD3-c023 and JmjD3-GSK highlight the importance of the additional ZBD for optimal stability and correct orientation of certain regions. In the absence of the ZBD the conformation of the helix and loop as seen in JmjD3-c023 structure may likely be crystal packing artefact.

4.5 Comparison with UTX structure

During the course of my DPhil study, the crystal structures of human UTX in the apo form and in complex with H3K27me3 peptide (22-mer, RKQLATKAARKSAPATGGVKKP) were reported (Sengoku and Yokoyama, 2011). This allows comparison of the JmjD3 and UTX structures to understand substrate binding within KDM6 family. Superimposition of JmjD3-GSK with the apo-UTX structure revealed no large differences in their overall tertiary structures (Fig. 4.5A; r.m.s.d. $= 0.55$ Å) Sequence alignment of JmjD3 and UTX Jumonji domains reveals a non-conserved region of 32 residues in the Jumonji domain (Fig. 4.5B). The region is disordered in both JmjD3 and UTX crystal structures, suggesting its structural flexibility. In JmjD3, this region contains 8 amino acids(6 glutamates and 2 aspartates), 5 serines and 5 prolines. In UTX, it contains 11 amino acids (3 histidines, 4 lysines and 4

arginines) and serines. These amino acid compositions are unlikely to form any secondary structures and therefore may explain its intrinsic flexibility. The region is unlikely to be involved in the substrate recognition and demethylation reaction for both JmjD3 and UTX, because it is distant from the expected substrate binding site. Instead, this region may be involved in protein-protein interaction, for example with different transcription factors that distinctively require JmjD3 but not UTX (due to its basic amino acid compositions). Whether the loop is of any importance to transcription regulation remains to be experimentally determined.

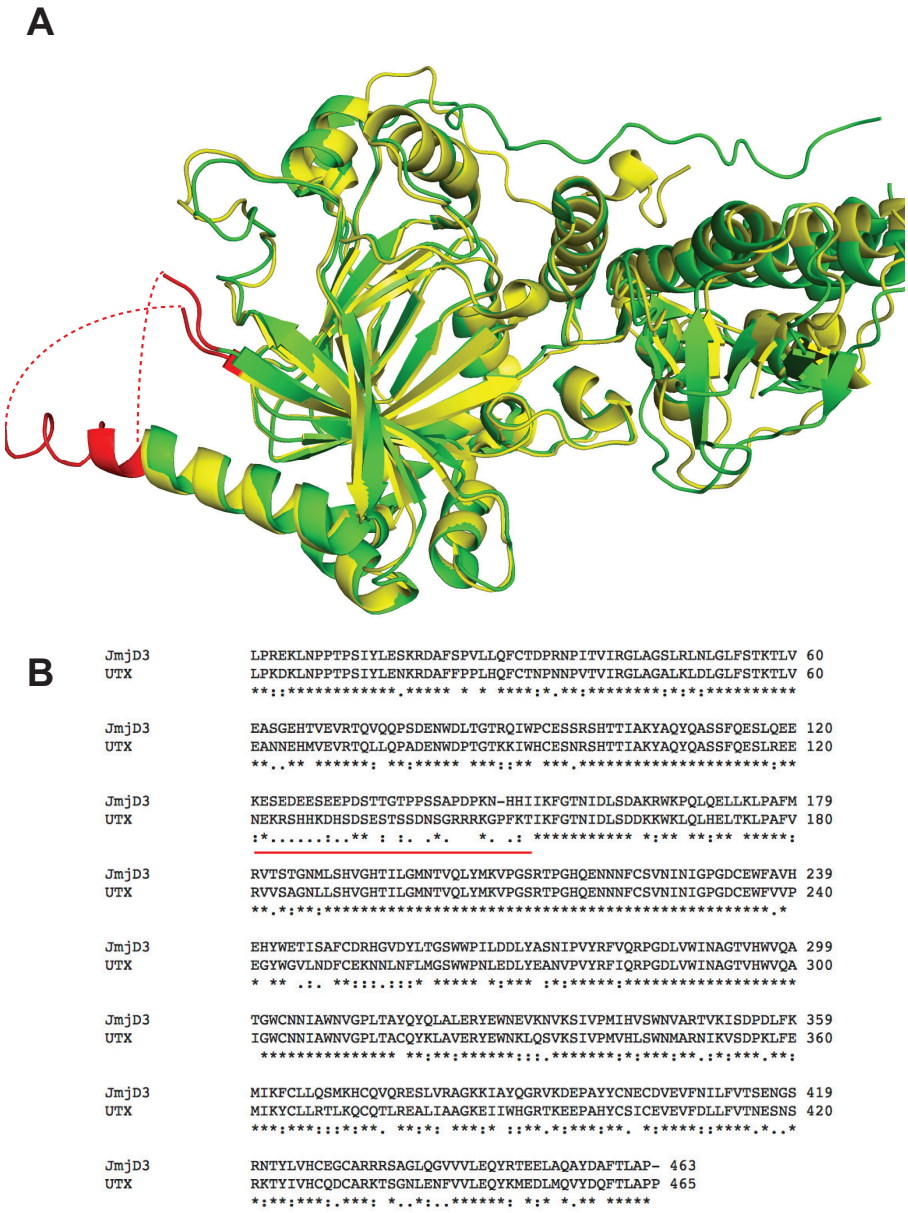


Figure 4.5: Comparison of JmjD3 and UTX. Superimposition of UTX (green) with JmjD3 (yellow) Jumonji domains and ZBD. The non-conserved region is missing in both structures. The ending residues of the non-concserved region in both are colored in red in both proteins and connected with dashed lines. B) Sequence alignment of JmjD3 and UTX showing the non-conserved region underlined in red. An asterisk indicates a conserved amino acid. A single dot indicates either size or hydropathy is conserved. A colon indicates both size and hydropathy are conserved.

4.6 Substrate recognition

The crystal structure of mouse JmjD3 (mJmjD3) in complex with H3K27me3 peptide (20-mer) was recently solved (Kruidenier et al., 2012). In the complex structure (PDB accession:4EZH), the H3K27me3 peptide (A24ARK(me3)SAPATGG34) is positioned in a cleft on the surface of the Jumonji domain(Fig. 4.6A, left). The methylated lysine is pointing inwards to the central cavity of the Jumonji domain. Arg26 of H3 forms hydrogen bonds with Asp1333 and Glu1244 of JmjD3. Pro30 of H3 forms hydrophobic interaction with P1388. The oxygen atom of P30 forms hydrogen bond with Arg1246. These interactions are crucial for substrate recognition and specificity (Fig. 4.6B), as mutation of Arg26 and Pro30 of H3 to alanine resulted in a loss of demethylase activity (Sengoku and Yokoyama, 2011)(Kruidenier et al., 2012)). Inside the catalytic pocket, the methylated lysine is placed in close proximity with the catalytic centre containing the metal ion and 2-oxoglutarate (Fig. 4.6C).

The ZBD is essential for substrate recognition. Lack of ZBD in JmjD3-c023 results in the loss of demethylation reaction (Chapter 3). The importance of ZBD cannot be illustrated in the JmjD3/H3K27me3 complex structure as the N-terminal tail of H3 was not present in the structure. In the UTX / peptide structure (Sengoku and Yokoyama, 2011), the co-crystallised peptide contains additional 7 residues in the N-terminal compared to that used in the mJmjD3 complex, hence showing vital interactions with ZBD that contributes to the binding specificity of H3K27me3 substrate (Fig. 4.6A, right). In particular, the H3R17 guanidino side-chain forms electrostatic interactions with Glu1326 of UTX (equivalent to Glu1570 of mJmjD3). H3Q19 side chain group interacts with backbone amide nitrogen of Tyr1354 of UTX (equivalent to Tyr1598 of mJmjD3). There is also a backbone H-bond interaction between H3A21 and Tyr1354 of UTX. H3K23 forms electrostatic interaction with Glu1355 (equivalent to Asp1579 of mJmjD3). The histone H3 R17, Q19, K23, R26 and P30 are the key residues exist in histone H3 tail that forms the basis of specificity of H3K27 demethylation (Fig. 4.6E).

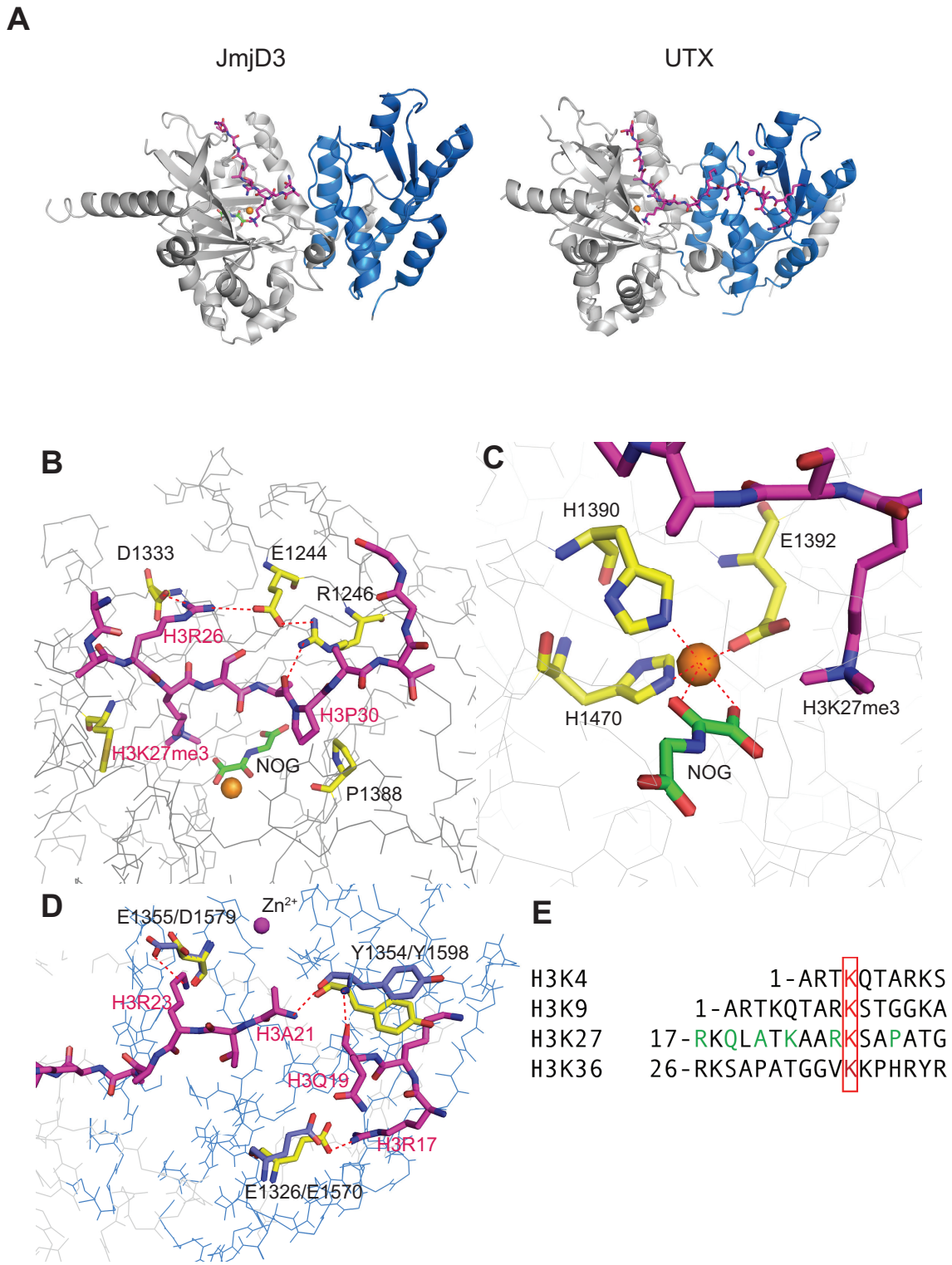

A
JmjD3
UTX
B
D1333
E1244
R1246
H3R26
H3P30
H3K27me3
NOG
P1388
C
H1390
E1392
H1470
H3K27me3
NOG
D
E1355/D1579
Zn2+
Y1354/Y1598
H3R23
H3A21
H3Q19
H3R17
E1326/E1570
E
H3K4 1-ARTKQTARKS
H3K9 1-ARTKQTARKSTGGKA
H3K27 17-RKQLATKAARKSAPATG
H3K36 26-RKSAPATGGVKKPHRYR

Figure 4.6: (Previous page) A) Structures of mJmjD3 and UTX in complex with H3K27me3 peptide. Cartoon representation of mJmjD3 (left, PDB accession code: 4EZH) with H3K27me3 peptide (magenta) lie in the cleft of the Jumonji domain (silver). In the UTX structure (right, PDB accession code: 3AVR), the H3K27me3 peptide (magenta) binds to both Jumonji domain (silver) and ZBD (Blue). B) Active site of mJmjD3 in complex with H3K27 (20-34). The H3K27me3 peptide (magenta) is in stick representation. Key residues in JmjD3 involved in peptide recognition are shown in yellow. The catalytically important 2-oxoglutarate (green) and Ni (II)(orange) are shown. Hydrogen bonds are shown as red dashed lines. C) Enlarged view of the catalytic site of mJmjD3 showing H3K27me3 peptide (magenta), 2-oxoglutarate (green) and key residues (yellow) interacting with Ni (II) (orange). D) Interaction of Histone H3 R17, Q19 A21 and K23 residues with Zinc binding domain of JmjD3 and UTX. Peptide is shown in magenta. Dash lines indicate the interaction between the peptide and UTX residues (blue) or JmjD3 residues (yellow) residues. Residues numberings are denoted for UTX / JmjD3. E) Sequence alignment of known lysine methylation sites in the histone H3 tail. Methylated lysines are colored red. Histone residues that interact with JmjD3 or UTX, as revealed in the panels B and D, are colored green.

4.7 Structural basis for specificity of the GSK-J1 inhibitor

The specific KDM6 family inhibitor GSK-J1 (Fig. 4.7A) identified as part of my D.Phil study (chapter 3) was co-crystallised with human JmjD3 (PDB accession doe: 4ASK) by our collaborator GSK (Kruidenier et al., 2012). In the structure determined at 1.86 $\AA$, a GSK-J1 molecule is bound in the catalytic site of JmjD3 (Fig 4.7B).

The GSK-J1 molecule comprises three chemical groups that contribute to its selectivity to JmjD3, namely the propanic acid, the pyridyl-pyrimidine and the tetrahydrobenzazepine (THB)(Fig. 4.7A).

The binding of GSK-J1 does not induce major structural changes to JmjD3 as revealed by comparison between the apo JmjD3-c023 and ligand-bound JmjD3-GSKJ1 structures, with the exception of a shifted catalytic ion position (described below).

Two nitrogen atoms of the pyridyl-pyrimidine of GSK-J1 form a bidentate interaction with the catalytic metal cobalt (II). This causes the position of the catalytic metal to be shifted by 2.2 $\AA$ from its original position without ligand (Fig. 4.7B) (R.M.S.D. = 0.187). The propanoic group of GSK-J1 occupies the same position as 2-oxoglutarate, and forms ionic interactions with Lys1381 and Asn1480 of JmjD3, indicating that GSK-J1 can function as a competitive inhibitor to 2-oxoglutarate. The THB ring of GSK-J1 fits into a subpocket formed between the side-chains of Arg1246 and Pro1388.

Superimposition of GSK-J1 with the 8-hydroxy-5-carboxyquinoline (8HQ) complex structure reveals that the carboxyl group of both compounds mimic the 2-oxoglutarate interaction with Lys1381. In addition, they both form bidentate interactions with the catalytic metal (Fig 4.7C). The catalytic metal is shifted by both compounds, though the displacement is more prominent with GSK-J1 than 8HQ. Such displacement of metal is believed to cause JmjD3 to be inactive for substrate catalysis. The GSK-J1 molecule also contains an additional bulky tetrahydrobenzazepine fitting into the subpocket of JmjD3 that is not explored by 8HQ, thus likely contribute to the its high selectivity towards JmjD3.

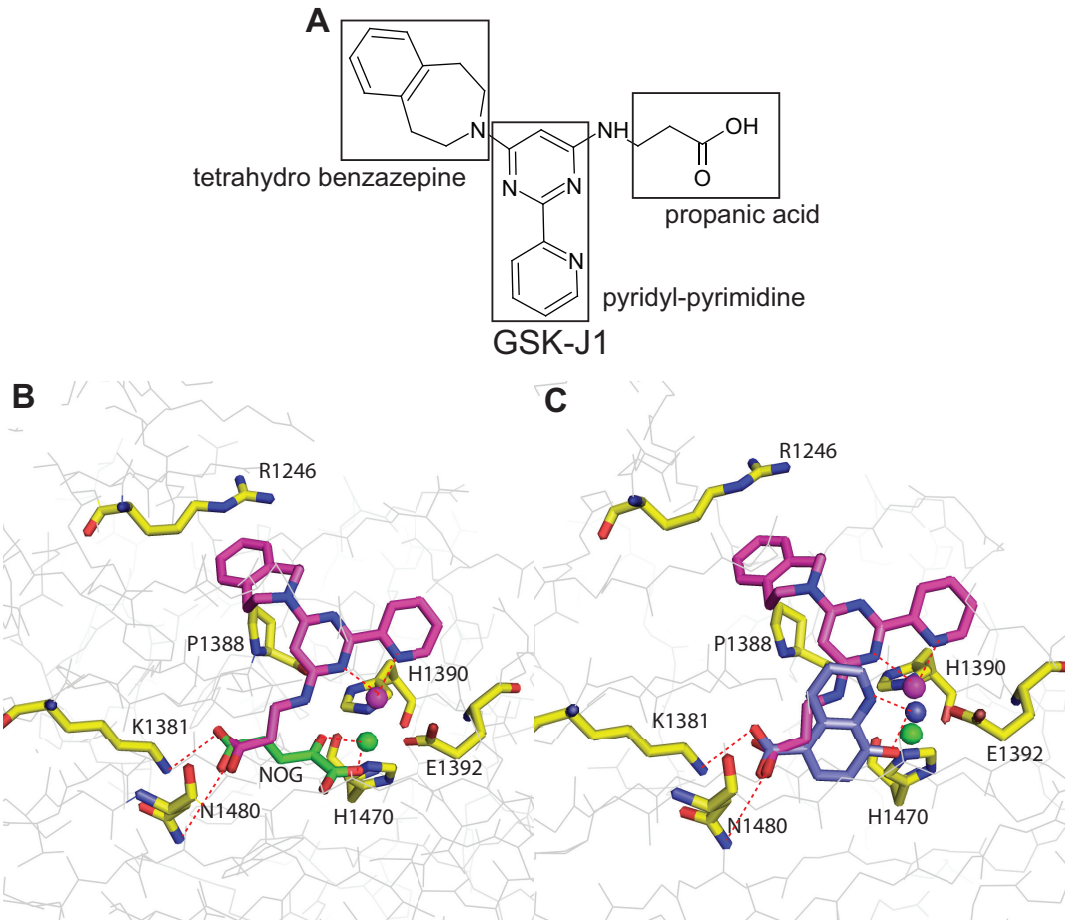


Figure 4.7: A)Chemical structure of GSK-J1

B) and C) Structures of GSK-J1 and 8HQ bound in catalytic core of JmjD3. GSK-J1 (magenta), 8HQ (blue) and core JmjD3 residues (yellow) are in stick representation. Spheres showing the position of catalytic metal without inhibitor (green), with 8HQ (blue) and GSK-J1 (magenta). Hydrogen bonds shown as dashed red lines.

4.8 Structural basis of GSK-J1 specificity towards JmjD3.

Not surprisingly, the Jumonji domain of JmjD3 shares high structural homology with the Jumonji family of histone lysine demethylases. The fact that the chemical structure of GSK-J1 is highly specific to the JmjD3/UTX subfamily, merits structural analysis in order to define the underlying molecular basis. To this end, the JmjD3-GSK/GSK-J1 structure is aligned with a selected panel of histone lysine demethylases including JMJD2A (PDB code 2OX0), JMJD1C (2YPD), and FBXL11 (2YU1), which are structural representatives from different subfamilies of histone demethylases. This structural overlay, as illustrated in Figure 4.8, reveals how the active site pocket differs in the four proteins and how the chemical structure of GSK-J1 explores unique subpockets within JmjD3 that are not present in the other Jmj proteins.

The propanoic acid group, mimicking the 2OG, will fit snugly into the catalytic pocket of all histone demethylases. The pyridyl-pyrimidine group clashes with Lys241 in JmjD2A, which is equivalent to Gly1435 in JmjD3 (Fig. 4.8B). It will also clash with His2336 in JmjD1C, which is equivalent to His1390 in JmjD3 (Fig. 4.8C).

The THB group will clash with side-chains of all the non-JmjD3 histone demethylases, indicating that the chemical group is crucial to the selectivity towards JmjD3. In JmjD2A, THB group will clash with Asn86, which is equivalent to Ser1271 in JmjD3 (Fig. 4.8B). The smaller side-chain of Ser1271 in JmjD3 provides a space for the THB group to fit in. The THB group will also clash with Lys2260 and Lys2262 in JmjD1C, which are corresponding to Phe1328 and Thr1330 in JmjD3 respectively (Fig. 4.8C). The shorter side-chains of Phe1328 and Thr1330 in JmjD3 allows space for the THB group to bind to JmjD3. Lastly, the THB group will clash with Met111 and Ile144 of FBXL11, which are equivalent to Arg1246 and Thr1330 in JmjD3 (Fig. 4.8D). Interestingly, Arg1246 of JmjD3 has a longer side-chain than Met111 in FBXL11 but it does not create any steric hindrance to the THB group. It is possible that the sulfur atom of methionine in FBXL11 restricts the flexibility of the side chain, while in Arg1246 of JmjD3, it has a higher degree of freedom so it can avoid clash with the THB group. A summary of the analysis is presented in Table 4.2.

To conclude, the GSK-J1 fits into the catalytic core of JmjD3 but not in other histone lysine

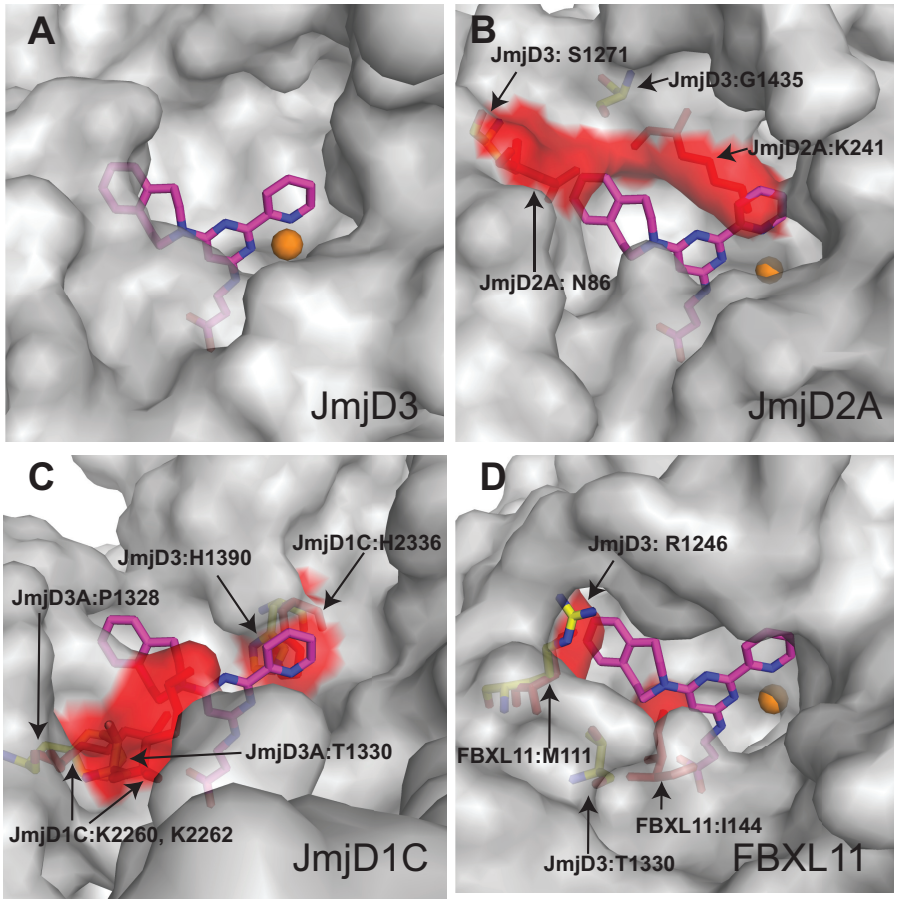


Figure 4.8: Surface representation of A) JmjD3 B) JmjD2A C) JmjD1C D) FBXL11. Active site metal is presented as orange sphere. GSK-J1 (magenta) is modelled into JmjD2A, JmjD1C and FBXL11 based on structural alignment with JmjD3. All the potential residues that clash with GSK-J1 in non-JmjD3 proteins are coloured red and corresponding JmjD3 residues are coloured yellow.

demethylases examplified above. The distance between key interacting residues and GSK-J1 are in an optimal relation without clashing and weakening the interactions.

4.9 Summary

The first crystal structure of the JmjD3 Jumonji domain was determined in complex with 8-hydroxyquinoline-5-carboxylic acid. Together with peptide/inhibitor-bound structures of JmjD3 and UTX determined by collaborators and other researchers, the current repertoire of structural information illustrates the structure function relationship of key residues for binding metal, cofactors (Iron(II) and 2-oxoglutarate) as well as the H3K27me3 substrate. The structures also demonstrate the importance

	tetrahydrobenzazepine	pyridyl-pyrimidine	propanic acid
JmjD2A	Asn86, (Ser1271)	Lys 241 (Gly1435)	no clash
JmjD1C	Lys2260, Lys2262 (Phe1328, Thr1330)	His2336 (His1390)	no clash
FBXL11	Met111, Ile144 (Arg1246, Thr1330)	no clash	no clash

Table 4.2: Amino Acid residues that could clash with GSK-J1 in JmjD1C, JmjD2A and FBXL11. The corresponding JmjD3 residues are presented in the blanket.

of a zinc binding domain in substrate recognition, and help to understand the specificity of GSK-J1 when compared with structurally related histone lysine demethylases.

Chapter 5

Development of a high-content imaging platform for screening of JmjD3 inhibitors

5.1 Introduction

The term 'high-content imaging' refers to the technique of image acquisition and analysis using an automated microscope. The automated microscope is capable of performing auto-focus imaging to the specimen and generates large amount of data of simultaneous read-outs without manual operation. Through the development of quantitative image algorithm and robust statistical analysis softwares, the results are less biased and comparable between laboratories. High-content imaging has become an ideal tool for biochemical lead identification and optimization in both industrial and academic laboratories (Zock, 2009). After identification of lead compounds for the inhibition of JmjD3 in the enzymatic assay (chapter 3), the compounds were subjected to test for activity in cells. The ideal cell assay system should preferably measure an immediate phenotypic effect of enzyme inhibition i.e. inhibition of histone H3K27 demethylation by JmjD3. However, endogenous JmjD3 only demethylates histones at very few locations in the epigenome, making it very difficult to detect locus-specific loss of H3K27 tri-methyl marks by antibody staining. This issue can be resolved by overexpressing JmjD3 in cells which erases all H3K27 tri-methyl marks in cells. The significant decrease of methylation

in histones can be detected by antibody staining and measured by quantitative immunofluorescence microscopy, thus allowing medium-throughput testing of JmjD3 inhibitors in cells. In this chapter, we will discuss the development of the immunofluorescence assay and comparison of the potency of a selected panel of JmjD3 inhibitors from previous chapters.

5.2 Overexpressing JmjD3 in mammalian cells

5.2.1 Transient expression of JmjD3 in mammalian cells

Overview

pcDNA5/FRT/TO (Invitrogen) was chosen as the vector for protein overexpression in HEK293 cells. The construct (Fig. 5.1A) has a Cytomegalovirus (CMV) promoter for transcription initiation which is commonly used for expression of recombinant proteins in mammalian cells. It also has a TetO2 sequence which prevents "leaky" expression by Tet repressors but allows induction by tetracycline. The vector contains a FLP Recombination Target (FRT) sequences which is needed for the plasmid to integrate into the cell genome and a stable selection marker (hygromycin) that allows the creation of a stable transfected cell line if needed.

Full-length Flag tagged human JmjD3 was subcloned into pcDNA5/FRT/TO vector using the *EcoRV* and *NotI* restriction sites. The insert was amplified by PCR with flanking sequences identical to the 5' and 3' end of the pre-cut vector to facilitate the subsequent cloning by recombination. The PCR product was inserted into the vector by In-Fusion Cloning strategy (See Chapter 9 for detailed methods). The plasmid was transformed into *E.coli* and clones were confirmed by restriction digestion (Fig. 5.1B). The H1390A mutant was also created by site-directed mutagenesis, for use as negative control in the experiment. The histidine residue is involved in binding of iron (II) important for catalysis (Chapter 4), and its substitution to alanine was previously reported to abolish the enzymatic activity of JmjD3 (Xiang et al., 2007). The plasmid was prepared by binding the plasmid DNA to an ion-exchange resin. After extensive washing, the endotoxin derived from *E.coli* can be effectively removed. Removal of the endotoxin in DNA sample greatly enhances transfection efficiency.

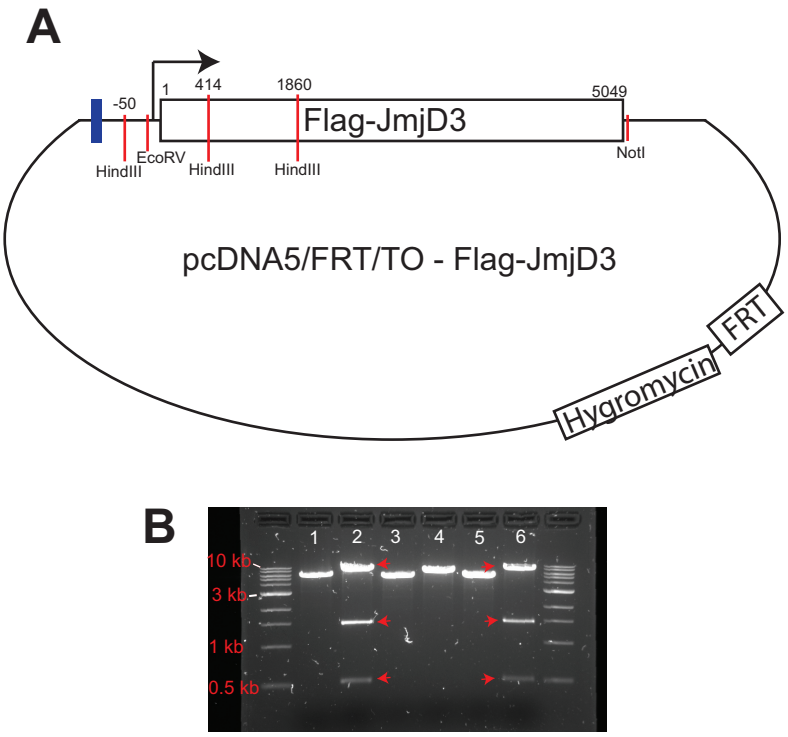


Figure 5.1: A) Schematic diagram of the Flag-JmjD3 construct showing the position of the restriction sites sed. Blue box indicates the position of the CMV promoter. Arrow indicates the direction of transcription. B) Colony screening by restriction digestion analysis. The plasmids were prepared by mini prep and digested with *HindIII*. Successful clones will contain 3 fragments (464bp, 1446bp and 9065bp). Sample 2 and 6 contain Flag-JmjD3 inserts.

Transfecting Flag-JmjD3 into mammalian cells

The HEK293 cell line was chosen as expression strain in the first attempt because they are commonly used for recombinant protein expression. However, it was found that HEK293 cells adhere poorly on cell culture vessels, which resulted in massive cell loss during subsequent staining procedures. Thus HeLa cells were used which are also commonly used for recombinant protein expression and adhere more strongly to the cell culture vessel.

To introduce DNA into HeLa cells, DNA was mixed with Fugene transfection reagent to form a liposome complex and then administrated to the cells. The treated cells remained viable under microscope observation after 24 hour incubation (Fig. 5.2). Cells treated with Flag-JmjD3 liposome complex have no noticeable morphological difference compared to the untreated control, and there was no observable cytotoxicity associated with the transfection reagent and overexpression of JmjD3

.

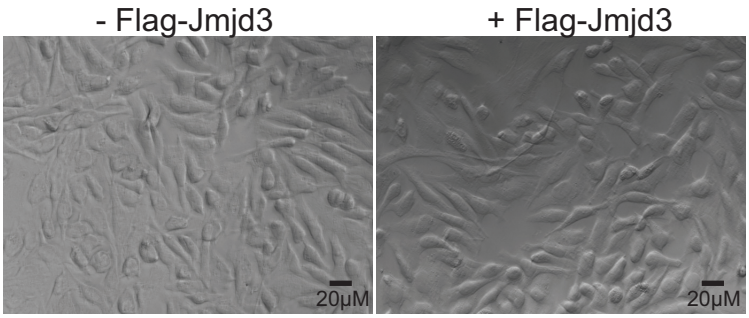


Figure 5.2: Treatment of Flag-JmjD3/liposome complex in HeLa cells. No noticeable morphological differences were observed between treated and untreated cells.

The cells were fixed in 4% paraformaldehyde after incubation for 24 hours and stained with mouse anti-Flag and rabbit Anti-H3K27me3 antibodies. Secondary antibodies were anti-mouse IgG conjugated with alexa-594 and anti-rabbit IgG conjugated with alexa-488. 4,6-diamidino-2-phenylindole (DAPI) was used to stain nucleic acids in the nucleus. The fluorophores DAPI, Alexa Fluor 488 and Alexa Fluor 594 were chosen because their excitation peaks are separated by at least 75 nm, thus avoiding false signals from neighbouring channels provided a specific optical filter is used. These fluorophores also have high photostability and intensities, thus giving consistent fluorescence sig-

nals under prolonged excitation times. Figure 5.3 shows the excitation and emission spectra of the fluorophores.

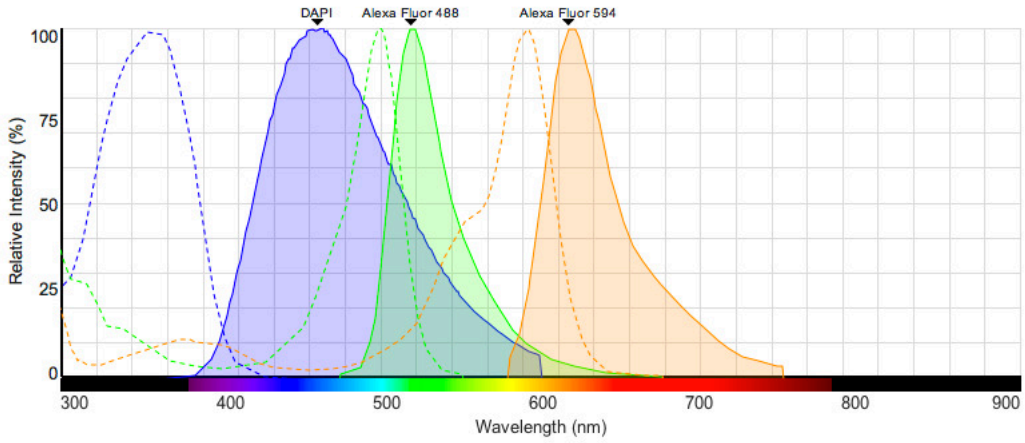


Figure 5.3: Excitation (dash lines) and Emission spectra (solid lines) of DAPI (blue), Alexa Fluor 488 (green), Alexa Fluor 594 (orange).

Flag-JmjD3 (red) and histone H3K27me3 (green) were localized in the nucleus (blue) as expected (Fig. 5.4). Tri-methyl H3K27 marks were absent in cells transfected with wild-type (WT) JmjD3. This was due to high levels of JmjD3 expressed in the cells which demethylate all the histone H3K27me3 marks. In the JmjD3/H1390A mutant, the H3K27me3 intensity remained unchanged indicating that the loss of H3K27me3 marks in wild-type was due to the histone demethylase activity of JmjD3. Altogether, these observations confirm that H3K27me3 is an in vivo substrate of JmjD3.

5.2.2 Stable transfection of JmjD3 in mammalian cells

The limitation of the transient transfection approach is that not all cells are transfected and express the protein, thus not all cells will have lost their H3K27 tri-methyl marks upon treatment with JmjD3. This increases the difficulties in image analysis because of the variability of H3K27me3 staining as well as the consumption of large amount of transfection reagents in routine screening. To this end, we attempted to create a stable cell line, using the Invitrogen Flp-In T-Rex System, so that all cells express Flag-JmjD3 constitutively. In brief, the system uses genetically engineered cells in which a specific recombination site was integrated. The plasmid containing the gene of interest can be integrated at the recombination site of the genome using the Flp recombinase. This is achieved by co-

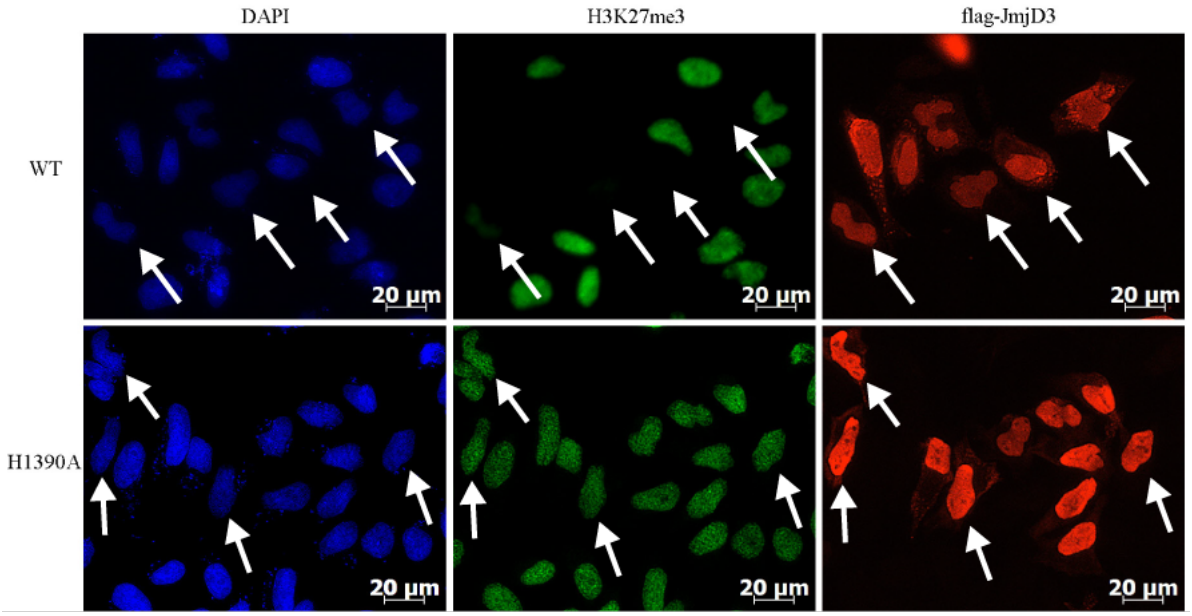


Figure 5.4: Wild-type (WT) JmjD3, but not mutant (H1390A), demethylates H3K27me3 chromatin marks(green) in Flag-Jmjd3 transfected (red, arrows) HeLa cells. DAPI staining indicates cells in the microscope field.

expressing the expression construct and a plasmid containing Flp recombinase (pOG44, Invitrogen). The cells which are stably transfected are hygromycin resistant and therefore enable positive selection of successful clones. The use of this system allows efficient integration of Flag-JmjD3 into the genome, thus greatly reducing the time for selecting stable clones.

Using this procedure, a stable cell line was created and was then tested for histone H3K27 demethylase activity. Flag-JmjD3 expression was induced by tetracycline. Fluorescence imaging results show that all cells express Flag-JmjD3 (Fig. 5.5). However, the expression level of Flag-JmjD3 was too low in the stable cell line to achieve significant H3K27 demethylation in the nucleus as evidenced in Fig 5.5. Even by using higher concentrations of inducer (10 ng/mL tetracycline), the expression level of Flag-JmjD3 still was not comparable to transiently transfected cells, though they both use the same CMV promoter. The DNA sequence was carefully verified and no mutation was found in the protein coding sequence, ruling out the possibility that the lack of demethylation was due to an error in the coding sequence. A possible explanation for the lack of demethylation in stable transfection is that a high level of expression is required for complete demethylation of histones. In stably transfected cells, there is only one copy of the Flag-JmjD3 gene existing in each

genome, thus limiting the expression level of JmjD3. In transiently transfected cells, multiple copies of Flag-JmjD3 can exist simultaneously in a cell so that the expression level is greatly enhanced, resulting in demethylation of all H3K27 tri-methyl marks in the histones.

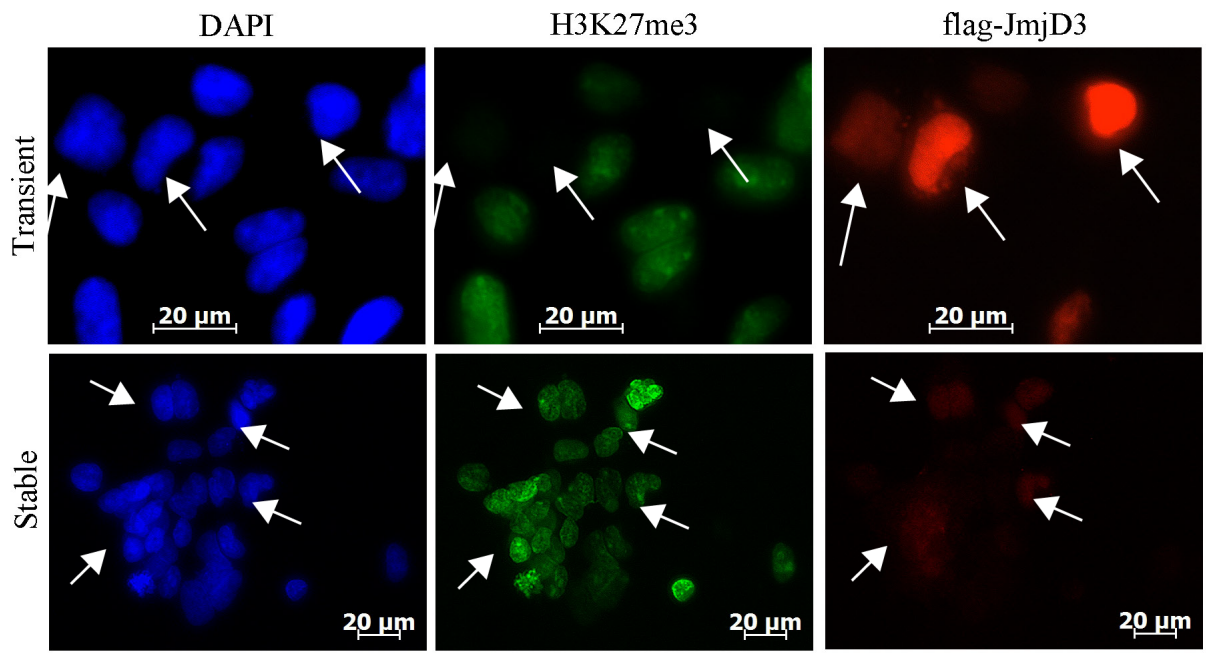


Figure 5.5: Transient transfected, but not stably transfected JmjD3 demethylates H3K27me3 (green) in HeLa cells. Arrows indicate cells expressing Flag-JmjD3.

5.3 Quantification of Fluorescence intensity

As discussed in the previous section, the transient transfection approach was used due to the lack of demethylation observed in stably transfected cells. To tackle the problem that not all cells may express Flag-Jmjd3, resulting in inconsistent H3K27me3 staining and error introduced to the measured H3K27me3 intensity values, we developed an image analysis protocol which automatically identifies transfected cells and measures H3K27me3 intensity.

To begin with, fluorescence images were taken on the BD pathway system, a high-content imaging microscope, at an optimal exposure such that all pixel intensities lie within the detection limit of the detector and hence no intensity information was lost due to overexposure. The exposure time must be constant between different samples to allow comparisons. The fluorescence images were analysed by CellProfiler (Carpenter et al., 2006), a program which can process large amount of digital images

in batch mode. Figure 5.6 shows a flow chart of the quantification process. In each sample image, there were three colour channels: blue, green and red corresponding to DAPI, H3K27me3 (alexa-488) and Flag-JmjD3 (alexa-594) respectively. First, the program uses a thresholding algorithm called Robust Background to identify all nuclei in the blue channel and labeled each nucleus as individual object. The algorithm assumes a Gaussian distribution for the image, and removes the brightest and dimmest 5% of pixels. It then calculates the mean and standard deviation of the remaining pixels. A threshold value is calculated as the mean value plus two times the standard deviation. Pixel intensities above the threshold are defined as foreground pixels and those below the threshold as background pixels. Neighbouring foreground pixels are connected and form an object; thus each object is a nucleus of a cell. Second, the program will measure the mean fluorescence intensity of every object in the red channel. The mean fluorescent intensity is calculated by summation of all pixel intensities and divided by the number of pixels in the object. Cells transfected with Flag-JmjD3 which have high fluorescence are selected (Fig. 5.7). Using this information, the mean fluorescence intensities of H3K27me3 are measured only in cells transfected with Flag-JmjD3.

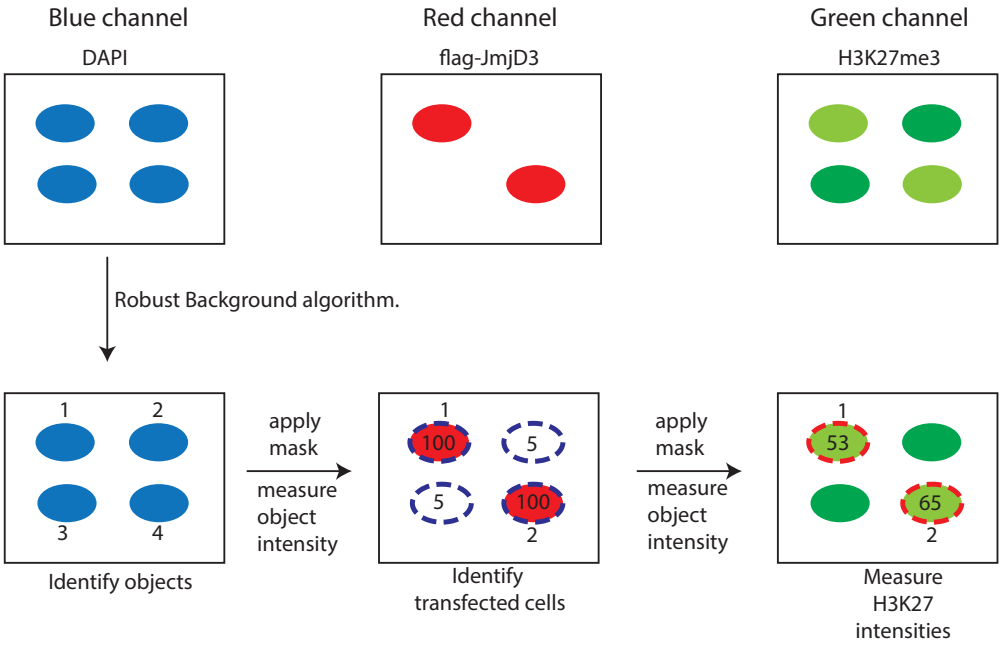


Figure 5.6: Schematic diagram of automated quantification of H3K27me3 fluorescence intensity in Flag-JmjD3 transfected cells. Nuclei are identified as individual objects in blue channel. Transfected cells which have high fluorescence intensities in nuclei are selected in red channel. The H3K27me3 intensities of selected nuclei are measured in the green channel.

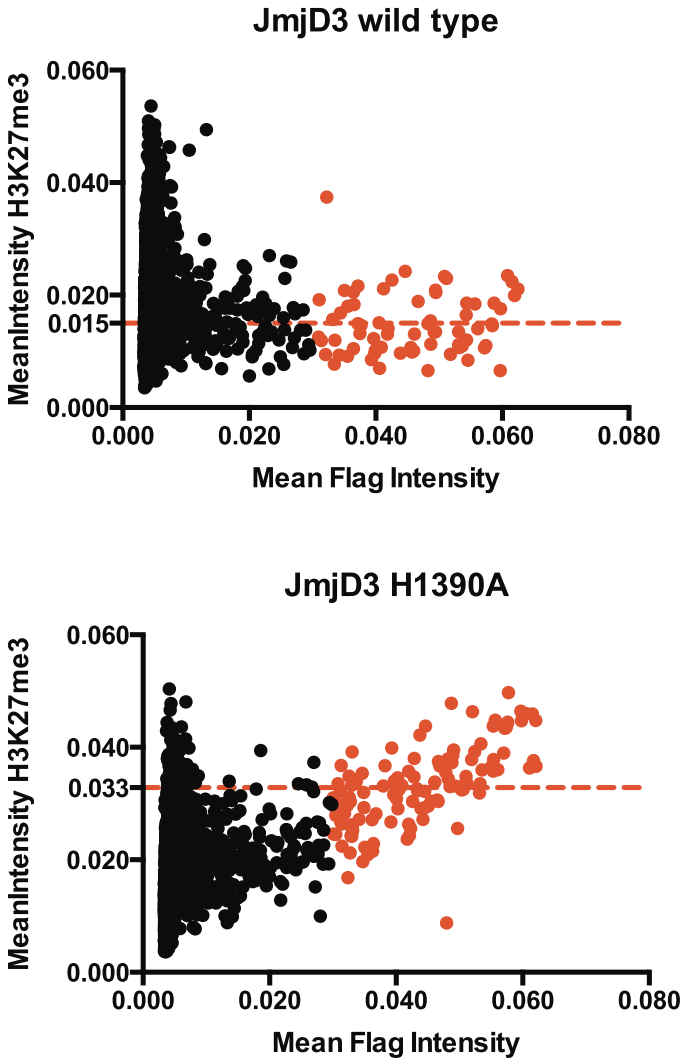


Figure 5.7: Scatter plot showing fluorescence intensities of cells transfected with Flag-Jmjd3 or Flag-JmjD3 H1390A plasmid. Red dots indicate cells expressing high level of JmjD3 (Flag intensity > 0.03). Dash lines represent the mean H3K27me3 intensity of cells expressing high level of JmjD3.

5.4 Screening of JmjD3 inhibitors

Five JmjD3 inhibitors previously identified in Chapter 3 by the AlphaScreen assay, with IC50 values below 1 μM in vitro, were subjected to testing in the immunofluorescence assay. The chemical structures for the five compounds (8HQ, 8HQ-115, 8HQ-124, GSK-J4 and GSK-J5) are shown in Figure 5.8. 8HQ is a known JmjD2 inhibitor which is active in cells (King et al., 2010), whereas 8HQ-115 and 8HQ-124 contain a morpholino group and N-benzyl- piperazine group at the C3 position of the quinoline ring respectively. It is hypothesized that these chemical groups add specificity to JmjD3. Whether these chemical groups have increased potency in cells compared to 8HQ was to be determined. GSK-J4, an ethyl-ester prodrug of GSK-J1 was provided by GSK. It was reported that the ester group in GSK-J4 increases cell permeability to the compound (Kruidenier et al., 2012). Intracellular esterases hydrolyse the ester group and convert the compound to the active form GSK-J1. GSK-J5 is a prodrug of GSK-J2, a structural isomer which is inactive towards JmjD3, therefore acting as a negative control in the assay. Although 8HQ and its derivatives contain a charged carboxyl group which may decrease membrane permeability of the compounds, previous studies in JmjD2 have shown that it is active in cells (King et al., 2010).

To begin with testing the efficacy of these compounds, cells were grown in 96-well optical graded cell culture plates. They were transfected with Flag-JmjD3 and incubated with inhibitors at varying concentrations in an attempt to determine a dose-response curve. After fixation and antibody staining, image acquisition was performed in the BD PATHWAY high content imaging system. Fluorescence intensities corresponding to H3K27me3 in the images were measured in CellProfiler. The results showed that all compounds except GSK-J5 inhibited JmjD3 below 50 μM in cells (Fig. 5.9). GSK-J4 has the strongest effect among the four active compounds, having an IC50 of 9.3 μM. The IC50 values of 8HQ, 8HQ-115 and 8HQ-124 were 26.9 μM, 25.2 μM and 24.9 μM respectively. Cytotoxicity was observed in GSK-J4 and GSK-J5 at high concentration (100 μM), indicating the concentration window for cell based experiments. Data points beyond this inhibitor concentration are discarded from calculations. Manual inspection of these conditions in the microscope show that the nuclei contained more condensed chromatin leading to increased immunofluorescence staining in DAPI and H3K27me3 channels, possibly due to apoptosis. Nevertheless, administration of compounds at such

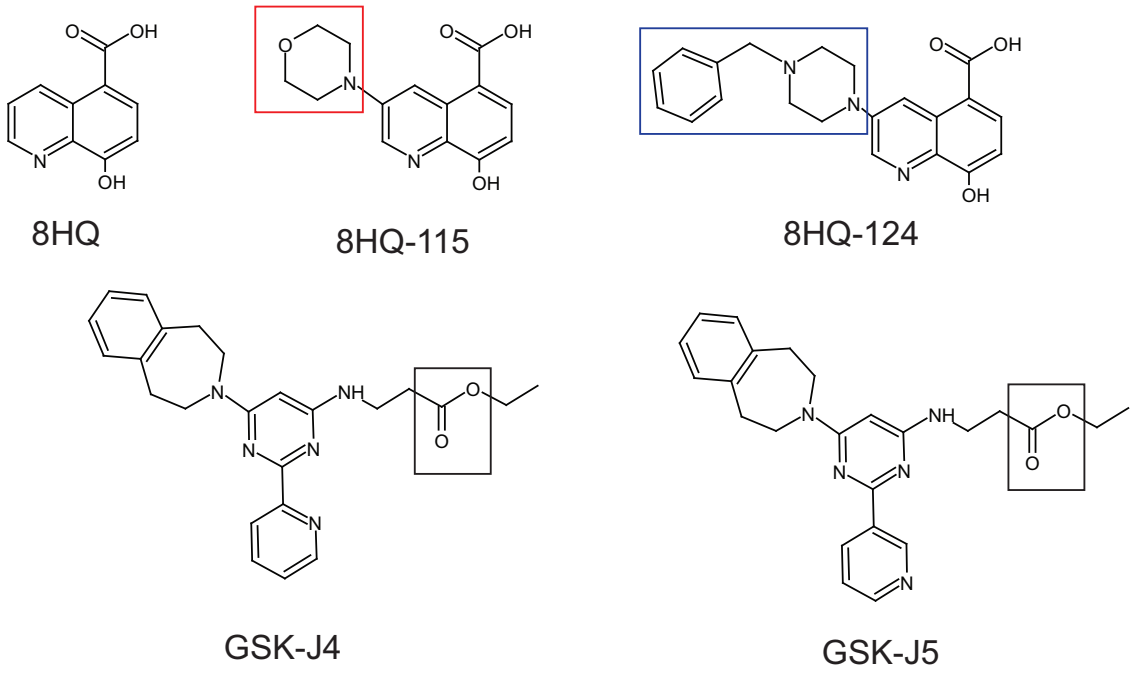


Figure 5.8: Chemical structures of JmjD3 inhibitors tested in the immunofluorescence assay. Red box indicates the morpholinyl group. Blue box indicates the N-benzy piperazine group. Black boxes indicate the ester group as mentioned in the text.

high concentrations in cell culture is not desirable as it may have non-specific target effects on other cellular pathways.

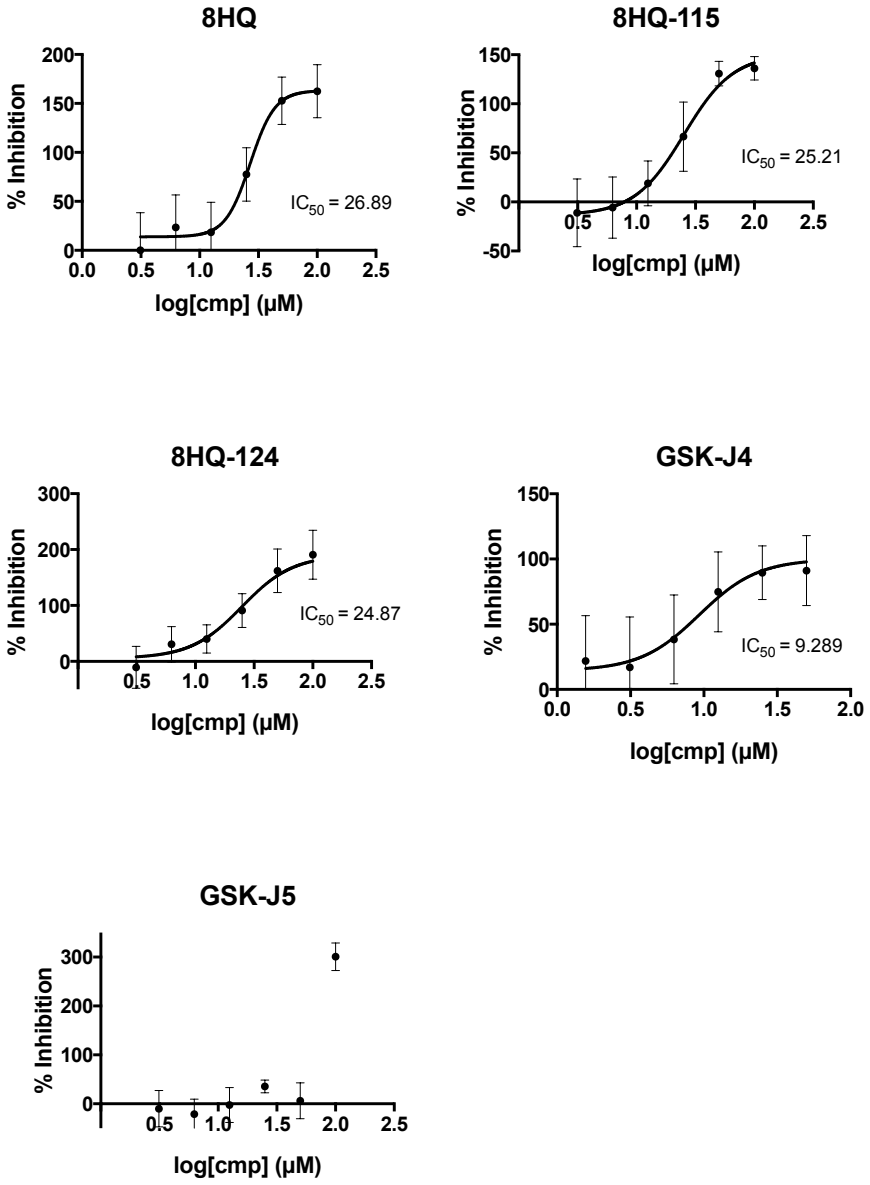


Figure 5.9: Dose responsive plot of JmjD3 inhibitors tested in the immunofluorescence assay. Data (from n=3 experiments) are presented as the mean ± s.d. Cmp, compound.

5.5 Summary

An immunofluorescence based cell assay was developed allowing routine screening of JmjD3 inhibitors. The principle of this assay is to measure H3K27me3 fluorescence intensities in cells transiently expressing Flag-JmjD3 when incubated with JmjD3 inhibitors. The assay allows screening of up to 95 different compounds in single dose or 12 compounds in 7 different concentrations on a 96-well plate. A computational method for quantifying H3K27me3 fluorescence intensities in transfected cells was developed. Together with an automated microscope, hundreds of compounds can be screened and analysed within one day. The assay is sufficiently sensitive so that a complete dose-response curve of an inhibitor can be determined, giving valuable information to compare potencies of different inhibitors in cells. Five JmjD3 inhibitors were selected and tested in the immunofluorescence assay. Four out of five compounds were able to inhibit JmjD3 in cells at low micromolar concentrations, with GSK-J4 having the highest potency among the four. Together with previous selectivity information on the histone demethylase family in Chapter 3, it can be concluded that GSK-J4 is a potent, selective and cell-active JmjD3 inhibitor.

Chapter 6

H3K27 demethylase inhibitors as chemical tools to understand macrophage biology

6.1 Introduction

Macrophages are phagocytic cells that originate from hematopoietic precursors, constitute an essential part of the innate immune system and recognize and engulf pathogens in a process known as phagocytosis. They are derived from monocytes and differentiate into macrophages upon migration into tissues under stimulation of growth factors and cytokines found in the local tissue environments. Macrophages adopt heterogeneous phenotypes in their gene expression patterns and functions (referred to asplasticity), depending on the stimuli that they are exposed to. Regarding activation macrophages are broadly divided into classically activated macrophages (termed M1) and alternatively activated macrophages (M2), mimicking the T helper cell nomenclature because of the cytokines that induce the activation stages.

The two types of macrophages are characterized by specific immune functions and cytokines they produce. The M1 macrophage is generally considered pro-inflammatory having anti-microbial activity. When mouse macrophages are stimulated with lipopolysaccharide (LPS) or interferon gamma (IFNγ), they display the following cytokine profile: high level of Interleukin-12 level (IL-12^{hi}) and Interleukin-

23(IL-23^{hi}), and low level of Interleukin-10 (IL-10^{lo}). Mouse M2 macrophages show a different type of activation and are responsible for homeostatic functions such as tissue repair. They can be stimulated by IL-4, IL-13 or immune complexes and have the following phenotypes: IL-12^{lo}, IL-23^{lo} and IL-10^{hi} (Fleetwood et al., 2009; Biswas and Mantovani, 2010) (Fig. 6.1). The exact mechanism underlying their plasticity is not fully understood, a common view is that this is driven by external stimuli such as cytokines, growth factors, interactions with immune cells/pathogens, which leads to alteration of chromatin structures and different transcription profiles.

6.1.1 Chromatin modification and control of macrophage functions

Epigenetic regulation is implicated in controlling both M1 and M2 macrophage activation states. The transcription factor PU.1 was discovered to co-localize to genomic regions prominent for histone H3K4me1 and H3K27 acetylation modifications which are markers for enhancer activity (Ghisletti et al., 2010; Heinz et al., 2010). The expression of PU.1 leads to deposition of H3K4me1 in the genome, creating small "open" DNA regions that can be accessed by transcription factors such as NF-κB and IFN regulatory factors (IRFs). PU.1 seems to be a key transcription factor that creates a macrophage-specific chromatin signature which can maintain macrophage identity.

In addition to histone modifications, another important epigenetic regulation is the methylation of DNA. CpG islands are found in the promoter of primary macrophage response genes including tumour necrosis factor (TNF), superoxide dismutase 2 (SOD2) and prostaglandin G/H synthase 2 (PTGS2). Genomic regions containing CpG islands have low nucleosome occupancy and overlap with RNA polymerase II (Pol II). In the resting state, RNAPII synthesizes unspliced transcripts starting from CpG islands containing promoters. When the macrophage is stimulated, PolII is phosphorylated and produces mature mRNA. CpG island seems to be an indication of rapidly transcribed genes in the macrophage primary response (Ramirez-Carrozzi et al., 2009; Hargreaves et al., 2009).

Histone demethylase JmjD3 also plays a role in the activation of both M1 and M2 macrophages. In LPS-stimulated M1 macrophage, JmjD3 is induced and recruited to transcription start sites (TSS) of many genes containing histone H3K4me3 and Pol II, indicating JmjD3 is associated with transcriptionally active genes (De Santa et al., 2007). It was further shown that most targets genes are unaffected by JmjD3 deletion in mouse (De Santa et al., 2009) indicating that JmjD3 may not be

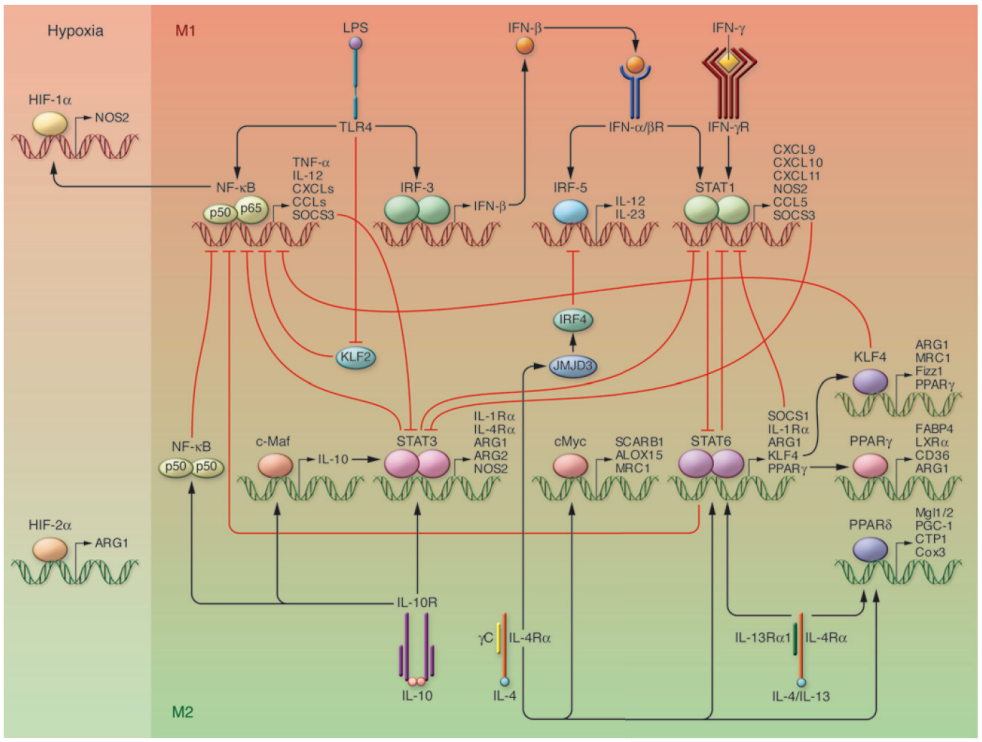


Figure 6.1: Major pathways of macrophage polarization. NF-κB promotes M1 macrophage activation. STAT3 and STAT6 are involved in M2 macrophage activation.IL-4 induces M2 macrophage activation via the JmjD3-IRF4 axis to inhibit IRF5 mediated M1 activation. The figure is original artwork from Sica and Mantovani (2012), reprinted with permission.

required for transactivation. In murine M2 macrophages, JmjD3 is up-regulated by IL-4 treatment and co-occupies genomic sites with signal transducer and activator of transcription 6 (STAT6) (Ishii et al., 2009b), an important transcription factor for M2 macrophage functions. JmjD3 demethylates histone H3K27 at the promoter of M2 marker genes including arginase (Arg1), resistin like alpha (Retnla) and chitinase 3-like 3 (Chi3l3) and promote transcription of these genes. However, despite these discoveries, the functions of Jmjd3 in both M1 and M2 macrophages are yet not fully understood. The development of the JmjD3 inhibitor GSK-J4 (see previous chapters) enables us to address an important question - that is whether these gene expression and phenotypic changes are the result of histone demethylation or due to other mechanisms such as protein - protein interaction (Solá et al., 2011). In the experiments described in this chapter, human M1 and M2 macrophages were treated with JmjD3 inhibitors in vitro and some of the important macrophage phenotypic responses and gene transcription profiles were investigated.

6.2 Epigenetic regulation of M1 macrophage

6.2.1 Molecular pathways of M1 macrophage activation

A number of in vitro models have been established to study macrophage biology. In human monocytes isolated from peripheral blood, granulocyte/macrophage colony-stimulating factor (GM-CSF) treatment leads to formation of pro-inflammatory M1-type macrophages in vitro. The macrophage is primed by GM-CSF and following LPS or IFNγ stimulation, it produces high amounts of pro-inflammatory cytokines such as tumour necrosis factor (TNF), IL-1and IL-6, compared to cells that are not GM-CSF primed. LPS is a cell wall component in gram negative bacteria that is recognized by Toll-like receptors (TLRs) on the cell surface. The activation of TLR leads to activation of Myeloid differentiation primary response 88 (MyD88) dependent or independent pathways (Akira and Takeda, 2004). In the MyD88 dependent pathway, MyD88 binds the Toll/Interleukin Receptor (TIR) domain of TLRs and phosphorylates TNF receptor associated factor 6 (TRAF6), which mediates activation of downstream NF-κB. In MyD88-independent pathway, the TIR-domain-containing adapter-inducing interferon-β (TRIF) binds to TRAP6 and phosphorylates Interferon regulatory factor 3 (IRF3). IRF3 binds to DNA and activates IFN-β (Fig. 6.2).

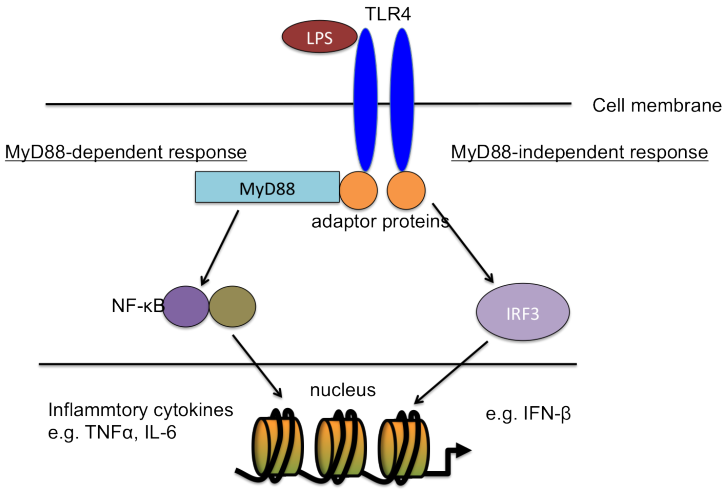


Figure 6.2: Schematic diagram showing activation of Toll Like Receptor by LPS.

NF-κB is an important transcription factor to modulate immune responses, and the activation of NF-κB leads to transcription of a set of primary response genes, most of which are pro-inflammatory cytokines such as TNFα and IL-6. TNFα in turn acts as an autocrine factor to activate the NF-κB and

the MAPK pathways. Excessive production of TNFα by macrophages results in pathogenic conditions such as tissue damage, chronic inflammation, haemorrhagic necrosis, leading to sepsis and shock. LPS stimulated macrophages in vitro become unable to reactivate many pro-inflammatory cytokines after a few hours following LPS re-stimulation, switching from pro-inflammatory M1 to an M2-like phenotype and gaining the ability to produce high level of IL-10 which is an immunosuppressive molecule (Lawrence and Natoli, 2011). This effect is known as endotoxin tolerance and is important for regulation of the immune response.

6.2.2 Effect of JmjD3 inhibitors on classically activated macrophages

Rapid induction of histone demethylase JmjD3 was reported in mouse bone marrow derived macrophages upon LPS stimulation (De Santa et al., 2007). To verify that JmjD3 is also induced in human macrophages upon LPS stimulation, human macrophages were generated using monocytes derived from healthy donors (N=3). These macrophages were primed by GM-CSF for 5 days then stimulated with LPS. Quantitative PCR was performed to measure the level of JmjD3 mRNA in cells before and after LPS treatment. An increase of JmjD3 mRNA after LPS stimulation was observed(Fig. 6.3). In this experiment the level of JmjD3 increased only by 1.5- fold in human macrophages, compared to the 5- fold in mouse macrophages (De Santa et al., 2007).

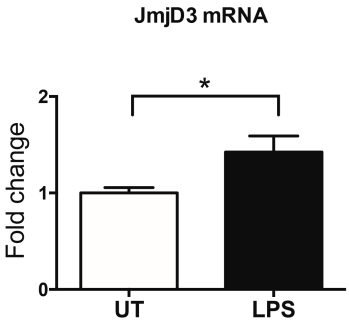


Figure 6.3: Induction of JmjD3 mRNA by LPS in classically activated macrophage. All data are mean $\pm$ s.d. N = 3. UT: untreated.

We then tested whether JmjD3 histone demethylase activity plays a role in the expression of pro-inflammatory cytokines. We measured the level of TNFα produced by macrophages. TNFα was chosen because it is the primary pro-inflammatory cytokine produced by M1 macrophages upon LPS

induction, and it is also implicated in autoimmune diseases such as rheumatoid arthritis. A panel of JmjD3 inhibitors was tested in LPS stimulated M1 macrophages. These inhibitors were previously discussed (Chapter 5) to be active in HeLa cells overexpressing JmjD3. The amount of TNFα in the medium after 6 hours of LPS stimulation was determined using the Luminex system, a sensitive multiplex protein detection platform based on immunodetection. Among the five JmjD3 inhibitors tested, only GSK-J4 was found to reduce TNFα production in macrophages (Fig 6.4A). No effect of TNFα reduction was seen in the presence of GSK-J5, 8HQ and its derivatives. The absence of cellular activity for 8HQ and its derivatives could be due to rapid degradation of the compounds e.g. by high levels of cytochrome P450 or other drug metabolising or excreting enzymes in activated macrophages (Wickramasinghe, 1987). For example, it was previously reported that the quinoline ring of 8HQ is susceptible to oxidation by the cytochrome P450 isoform CYP2E1 (Reigh et al., 1996). These results showed that only GSK-J4 can reduce TNFα expression in macrophages while 8HQ derived compounds cannot.

It is possible that treatment with exogenous compounds to the cells could affect cell viability, hence affecting TNFα production. To measure cell viability, the widely used tetrazolium salt WST-1 (Cory et al., 1991) was added to the cells after compound incubation. Viable cells which express high levels of mitochondrial dehydrogenases cleave the WST-1 to a colorimetric compound, indicating the cells are metabolically active and hence "healthy". Reduced viability (60%) was seen in macrophages treated with 30μM GSK-J4 for 6 hours (Fig. 6.4B), though previous immunofluorescence assay showed that 30 μM of GSK-J4 was not cytotoxic to HeLa cells. We could not rule out the possibility that reduction of TNFα was due to the reduced viability of the cells at this concentration, but it is also possible that GSK-J4 decreases the expression of metabolic enzymes that cleave the WST-1 substrate, thus reducing the production of colouri-metric substrates. In addition, responses to GSK-J4 were highly variable, since different donors exhibited different cell viability after GSK-J4 treatment. Therefore, to understand the variability in healthy human volunteers the sample size would need to be increased.

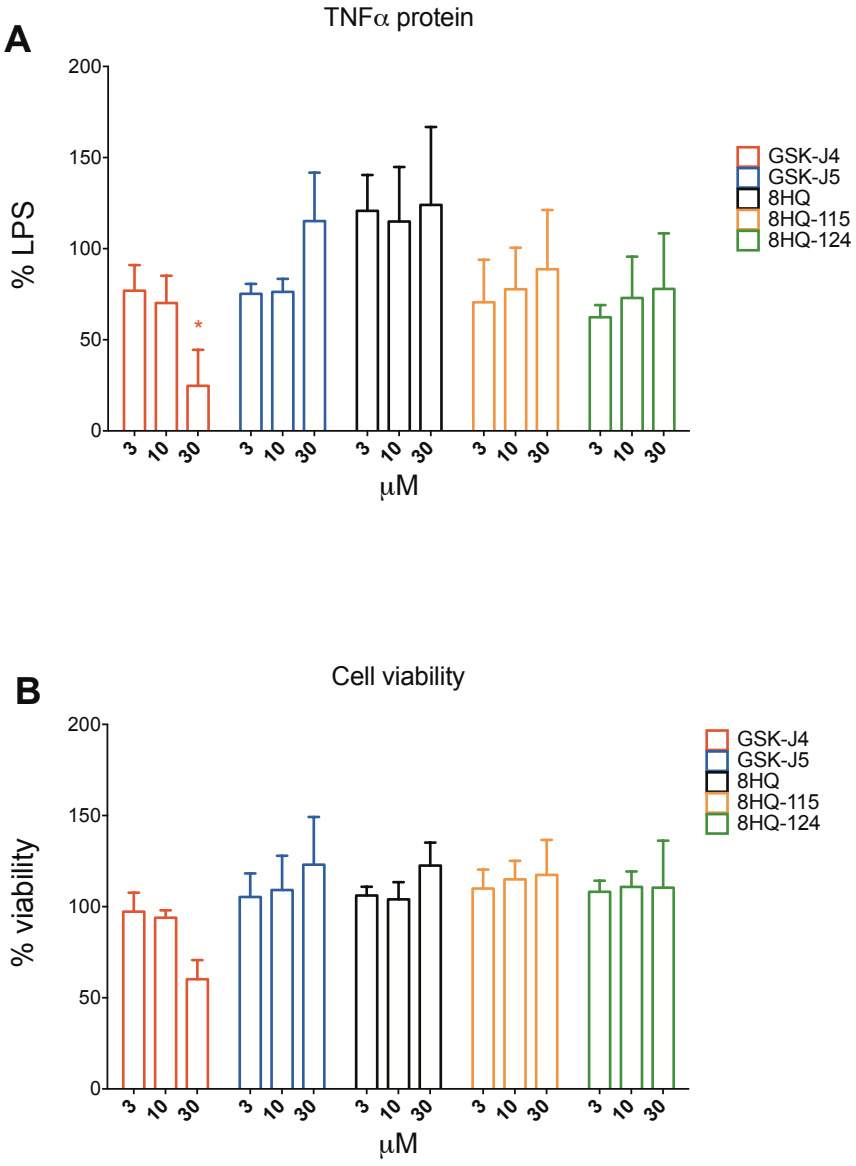


Figure 6.4: Effect of JmjD3 inhibitors on primary human macrophages on classically activated pathway. A) Quantification of TNFα level in the medium, as judged by %LPS measured by Luminex. B) Cell viability after treatment of JmjD3 inhibitors for 6 hours. All data are mean $\pm$ s.d. N = 3.

6.2.3 Effect of JmjD3 inhibitor on chronically activated macrophages

In rheumatoid arthritis patients, TNFα is constitutively produced by macrophages in inflamed tissues and is a key factor driving the destructive disease phenotype (Vasanthi et al., 2007). To test whether blocking of JmjD3 activity can lead to inhibition of TNFα production in patient derived cells, macrophages derived from rheumatoid arthritis patients were subjected to GSK-J4 or GSK-J5 treatment in vitro. Peripheral blood monocytes from six patients were isolated and M1 macrophages were prepared as described previously. TNFα in medium was measured using the Meso Scale Discovery (MSD) platform in the laboratory of EpiNova, GlaxoSmithKline (Stevenage, UK).

TNFα cytokine in culture medium was found to be significantly reduced by GSK-J4 at 10 μM and 30 μM (Fig 6.5A). A significant reduction of TNFα mRNA was also observed(Fig. 6.5B), suggesting that inhibition of TNFα production occurred at the transcriptional level. Effect of GSK-J5 on both TNFα protein expression and mRNA transcription were insignificant (Fig. 6.5), therefore it can be concluded that blocking of JmjD3 activity has a significant effect on macrophage TNFα expression. This is in contrast to the previous report that deletion of JmjD3 in mouse had no effect in mouse macrophages (De Santa et al., 2009), leading to the hypothesis that UTX may play a redundant role in TNFα expression because GSK-J4 can inhibit both JmjD3 and UTX histone H3K27 demethylases. To test the above, our collaborators at GSK performed double siRNA knockdown of both JmjD3 and UTX in human macrophages, resulting in complete abrogation of TNFα expression (Kruidenier et al., 2012) to levels found under GSK-J4 treatment. It is therefore concluded that inhibition of both JmjD3 and UTX histone demethylase activities is needed for TNFα regulation and that inhibition by GSK-J4 leads to a similar effect.

The effect of JmjD3 and UTX inhibition on H3K27 methylation has been shown by ChIP analysis (Fig. 6.6) (Kruidenier et al., 2012). LPS treated macrophages have decreased H3K27 trimethylation at the transcription start site of TNFα. GSK-J4 but not GSK-J5 increased H3K27 methylation at the region. These results confirmed that H3K27 demethylase activity of JmjD3 is associated with TNFα expression and that inhibition of the histone demethylase activity is associated with reduced production of TNFα.

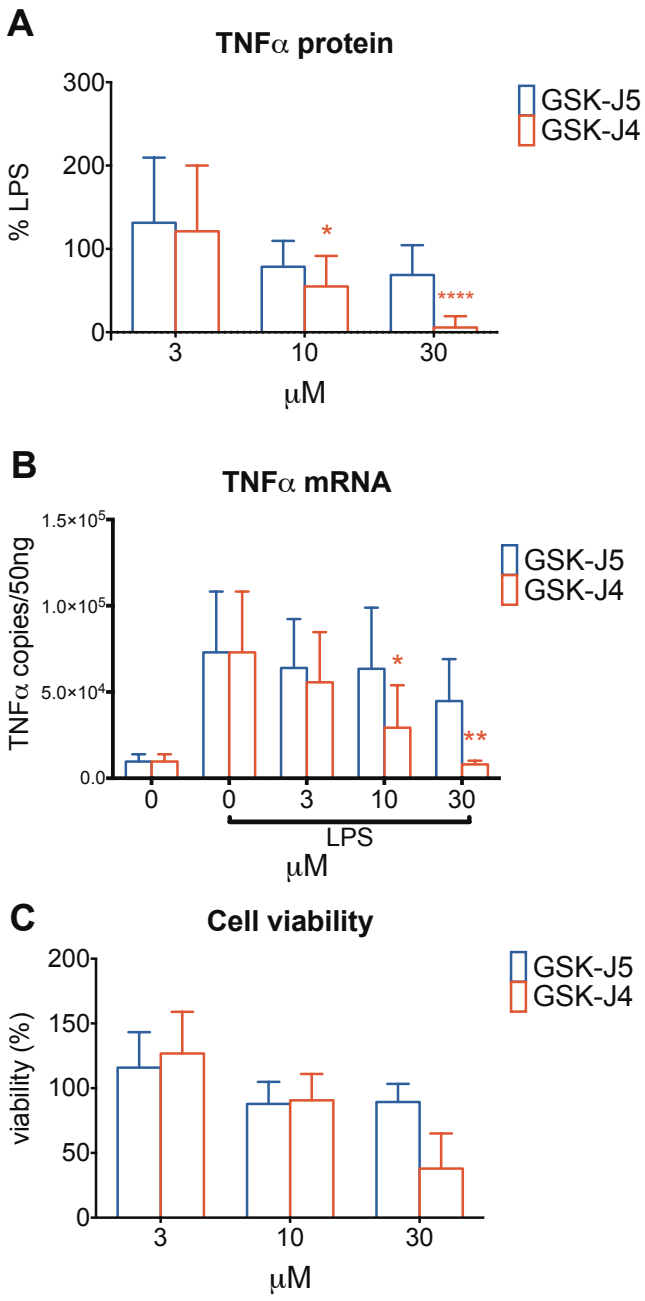


Figure 6.5: Effect of GSK-J4 and GSK-J5 in macrophages derived from peripheral blood of rheumatoid arthritis patients. A) TNFα protein level in medium, as judged by %LPS measured by MSD. B) TNFα mRNA level measured by qPCR C) Cell viability after treatment of the compounds for 6 hours. All data are mean $\pm$ s.d. N = 6.

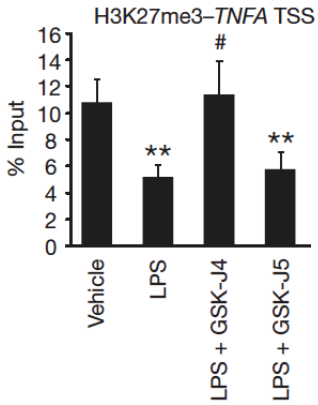


Figure 6.6: ChIP analysis of the association of H3K27me3with the TNFα transcription start site in LPS-stimulated human primary macrophages in the presence of 30 μM GSK-J4 or GSK-J5 (data are presented as the mean ± s.e.m. from n = 8 donors). P values were calculated using a two-tailed Student' s t-test. *, P <0.05 compared with vehicle; **, P <0.01 compared with vehicle; #, P <0.05 compared with LPS; ##, P <0.01 compared with LPS. This figure is modified from Kruidenier et al. (2012), reprinted with permission.

6.3 Epigenetic regulation of M2 macrophage

6.3.1 Molecular pathways of M2 macrophage fusion

Polarization of M2-like alternatively activated macrophages is induced by Th2 cells in vivo. Binding of IL-4 or IL-13 to the IL-4 receptor activates the M2 macrophage phenotype, which is activated by STAT6 through JAK. In M2 macrophages, STAT6 is a transcription factor, which regulates expression of M2 genes. M2 macrophage activation results in production of anti-inflammatory cytokines that can mediate repression of pro-inflammatory cytokines, including IL-10, transforming growth factor beta (TGF-β) and IL-1 receptor antagonist (IL-1Ra) (Gordon and Martinez, 2010). These cytokines can promote angiogenesis, fibrosis and tissue repair, and are able to suppress TNFα and IL-6 production in M1 macrophages. IL-4 and IL-13 can also induce macrophage fusion to form multinucleated giant cells (MGCs) in vitro. This phenomenon is observed in infection caused by microbial/parasitic such as *Schistosoma mansoni* and *Mycobacterium tuberculosis*. These MGCs, also so-called "Langerhans" giant cells are found in *M.tuberculosis* infection (Gordon and Martinez, 2010). The exact function of these MGCs is not fully understood, although it is hypothesized that these cells may be able to degrade large foreign body components which cannot be phagocytized by small mononuclear macrophages. Various genes have been identified involved in cell fusion, including ATP6v0d2, E-cadherin and DC-STAMP. Osteoclasts are other types of MGC related to macrophage but they are induced by the RANKL cytokine (see next chapter). Osteoclasts have specific roles in bone resorption and are functionally different from M2 macrophages.

6.3.2 Effect of H3K27 demethylase inhibition in alternatively activated macrophages

To investigate the effect of JmjD3 inhibition in alternatively activated macrophages, IL-4 induced M2 macrophages were generated using monocytes derived from human peripheral blood. These cells were cultured in 10% human serum for 4 days, then exposed to IL-4 for 72 hours. GSK-J4 or GSK-J5 was added 30 minutes before IL-4 induction. Cell fusion occurred within 72 hours and the cells exhibited giant cell morphology in the control and GSK-J5 groups (Fig. 6.7, black arrows). However, treatment with GSK-J4 led to complete abrogation of cell fusion. These cells remained mononuclear after 72

hours of IL-4 induction (Fig. 6.7). Since GSK-J4 is only selective for the KDM6 family of histone demethylases, it can be concluded from this point that inhibition of KDM6 histone demethylases does affect the IL-4 induced fusion of macrophages.

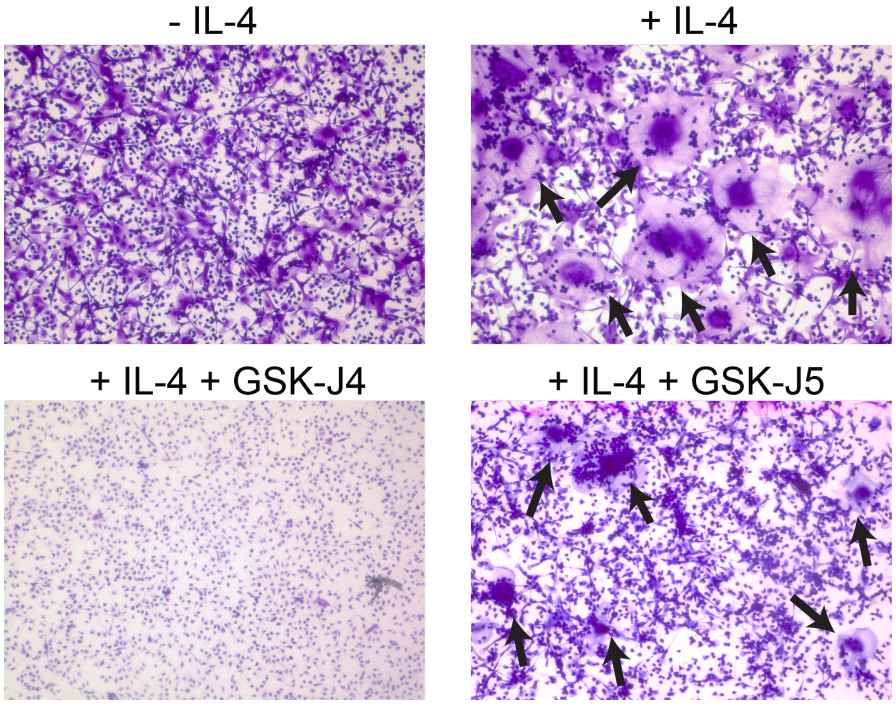


Figure 6.7: Effect of JmjD3 inhibitors on IL-4 induced giant cell formation. No giant cell formation was seen in GSK-J4 treated cells. Cells were stained by crystal violet. Black arrows indicate positions of multinucleated giant cells. Image magnification: 40x.

6.3.3 Gene expression studies in M2 macrophages

Since there are no established/published functional assays available to characterize giant cell function, microarray analysis was performed to investigate the effect of gene expression changes occurring under GSK-J4 (or GSK-J5) treatments. RNA was extracted from cells after 24 hours exposure to IL-4 with or without JmjD3 inhibitors. The microarray used was Affymetrix GeneChip Human Gene 1.0 ST array which consists of 36079 probes for 21014 annotated genes. Addition of IL-4 resulted in at least two-fold changes in 271 genes, of which 79 were upregulated and 192 were downregulated (Fig 6.8 and appendix II&III). Classical IL-4 induced genes including Fibronectin 1 (FN1), mannose receptor C type 1 (MRC1), monoamine oxidase A (MAOA), Chemokine (C-C motif) ligand 22 (CCL22), CCL26 and IL-17 receptor beta (IL-17Rb) were upregulated (Gordon and Martinez, 2010). Upregulation of

transglutaminase 2 (TGM2) was observed, which is consistent with the recent proposal that TGM2 is a selective M2 marker in human macrophages (Martinez et al., 2013). There were in total 115 IL-4 induced genes counter-regulated by GSK-J4, 27 upregulated and 88 downregulated. Amongst the classical IL-4 induced genes, FN1, MRC1, CCL22 and CCL26 were downregulated by GSK-J4 (Fig. 6.8).

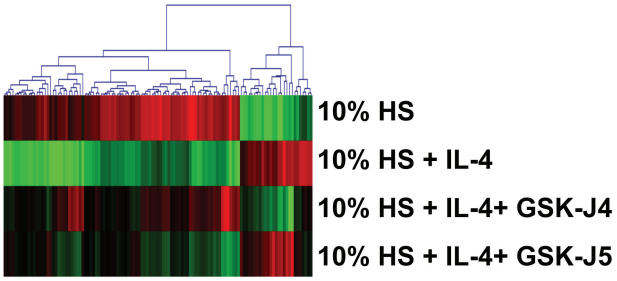


Figure 6.8: Hierarchical clustering of genes selectively counter-regulated by GSK-J4 in macrophages exposed to IL-4. HS, human serum. Red and green represents high and low expression respectively.

For follow-up experiments, ATP6v0d2, FN1, P2RY13, P2RY14, PTGS1, JMJD3 and UTX were selected for qPCR verification (Fig. 6.9A-F). These genes were chosen because they (with the exception of the two demethylases) were previously implicated in giant cell fusion and as M2 biomarkers. The qPCR results were consistent with changes of expression values in microarray. GSK-J4 caused a slight change of expression in ATP6v0d2, a gene involved in cell fusion, but the expression was not rescued by GSK-J5 (Kim et al., 2007). FN1 is a cell adhesion molecule that plays a major role in cell growth, migration, and differentiation, which is important for wound healing (Blystone et al., 1994). It was downregulated by GSK-J4 but not GSK-J5 (Fig. 6.9A). P2RY13 and P2RY14 are sugar nucleotide receptors previously reported as M2 marker genes induced by IL-4 (Martinez et al., 2006). Both of them were counter-regulated by GSK-J4 but not by GSK-J5 (Figs. 6.9B, C). P2RY14 was involved in UDP-glucose dependent dendritic cell activation (Skelton et al., 2003). However, the exact functions of these genes in macrophages are not known. Prostaglandin-endoperoxide synthase 1 (PTGS1), also known as COX-1, is involved in synthesis of prostaglandin E2 (Williams and Shacter, 1997) in activated macrophage and it is responsive to IL-4 (JI 2006). It was downregulated by GSK-J4 but not by GSK-J5 (Fig. 6.9D). Its paralogue, PTGS2 (COX-2), which is highly expressed in arthritis conditions and is a well known M1 marker, was as expected not induced by IL-4 in the

microarray dataset (data not shown). Lastly, JmjD3 was shown to be induced two fold by IL-4 (Fig. 6.9E), however no change in UTX expression was observed (Fig. 6.9F). These data suggest that JmjD3 is very likely to be involved in IL-4 induced giant cell fusion. Inhibition of JmjD3 alters the expression of a large number of IL-4 induced genes, resulting in abrogation of cell fusion.

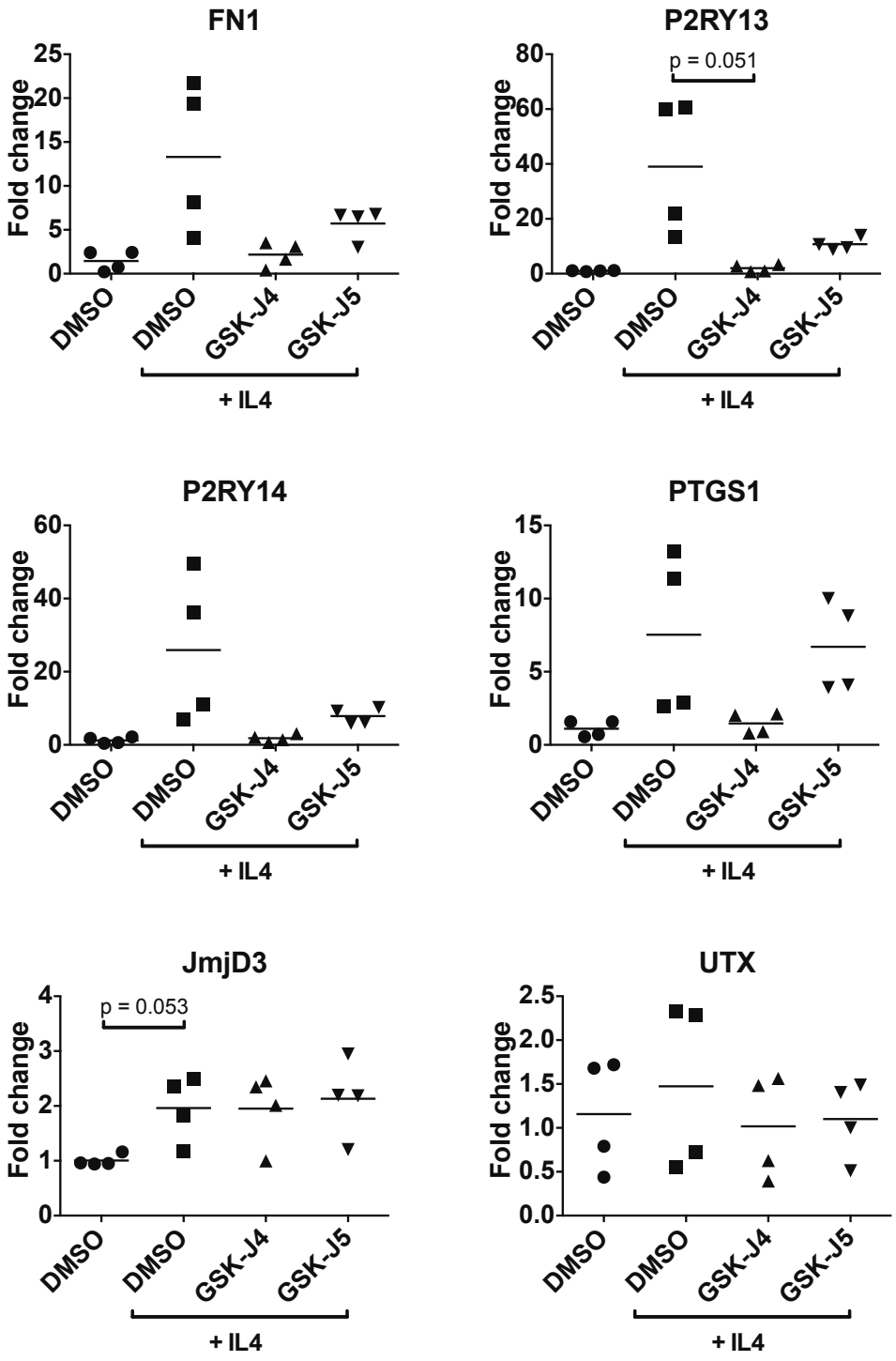


Figure 6.9: Quantitative PCR analysis of a panel of genes implicated in M2 macrophage functions. Horizontal lines represent mean of four experiments.

6.4 Summary

Macrophages are important cells in the immune system with diverse functions such as anti-microbial defence and tissue repair. They are "plastic" cells i.e. they display an enormous potential to adapt and functionally respond to changes in their environment, and can differentiate into pro-inflammatory M1 or anti-inflammatory M2 phenotypes. It is believed that epigenetic mechanisms play a major role in determining the macrophage phenotype, as demonstrated previously and the experiments described in this chapter. The H3K27 demethylase inhibitors provide a unique tool to understand the biological relevance of histone H3K27 methylation in macrophages, and among a panel of previously identified JmjD3 inhibitors, only GSK-J4 was shown to be active in reducing TNFα production in human M1 macrophages and macrophages derived from rheumatoid arthritis patients. Most of the data concerning M1 macrophage were already published in collaboration with GlaxoSmithKline during the writing of this thesis (Kruidenier et al., 2012). It is noteworthy that not only expression of TNFα was reduced upon GSK-J4 treatment but also other pro-inflammatory cytokines including IL-1, IL-6 and IFNB, suggesting that these pro-inflammatory cytokines may share a common epigenetic activation mechanism related to methylation of histone H3K27. The paper also showed that H3K27me3 demethylation occurred at the promoter of TNFα when cells were stimulated with LPS. This shows that JmjD3 is directly involved in the transcriptional regulation of TNFα expression, and possibly the other pro-inflammatory cytokines mentioned above.

In M2 macrophages, GSK-J4 completely abrogated giant cell fusion. Microarray analysis showed that a large fraction of IL-4 induced genes were counter-regulated by GSK-J4. In follow up studies on some selected genesincluding M2 biomarkers such as UDP-glucose membrane receptors and cyclooxygenase-1, this effect of H3K27 demethylase inhibition was further verified. The exact mechanism of fusion inhibition remains to be elucidated, but it is very likely that regulation of H3K27 methylation is involved as shown by a complete block of giant cell formation. Further experiments such as ChIP-seq are needed to understand the effect of Jmjd3 inhibition on the epigenome and its changes during IL-4 and inhibitor treatments. In conclusion, the data presented in this chapter have corroborated that GSK-J4 is a valuable biochemical tool to study JmjD3 function in innate immune cells.

Chapter 7

H3K27 demethylase inhibition as novel anti-resorptive mechanism in osteoclast function

7.1 Overview of bone remodelling

Bone tissue is the primary structural component of the human skeletal system. Among its functions, the bone tissue provides a framework for locomotion and protection of internal organs, is the site of hematopoiesis, and controls calcium and phosphate homeostasis (Bilezikian et al., 2008).

Bone formation and remodelling in vertebrates are highly dynamic and connected processes. They are orchestrated by three types of cells: osteoblasts, osteocytes and osteoclasts (Fig. 7.1). Osteoblasts are the bone producing cells derived from mesenchymal stem cells, actively produce collagen and mineralise the collagen matrix to form the rigid structure of bone. Osteoblast differentiation is regulated by bone morphogenetic protein (BMP) and wingless (Wnt) signalling pathways (Crockett et al., 2011). Osteocytes are mature osteoblasts "trapped" in the bone matrix after bone formation. They are able to sense mechanical stress of bone and are responsible for the maintenance of bone structures. They use the Wnt/β-catenin pathway to transmit signal of mechanical loading to the cells on the bone surface (Bonewald and Johnson, 2008). Osteoclasts are cells originated from hematopoietic stem cells that actively secrete proteolytic and matrix degrading enzymes to dissolve

the bone material. Such degradation process is known as bone resorption. Osteoclast differentiation is controlled by the RANK-RANKL pathway (Weilbaecher et al., 2011).

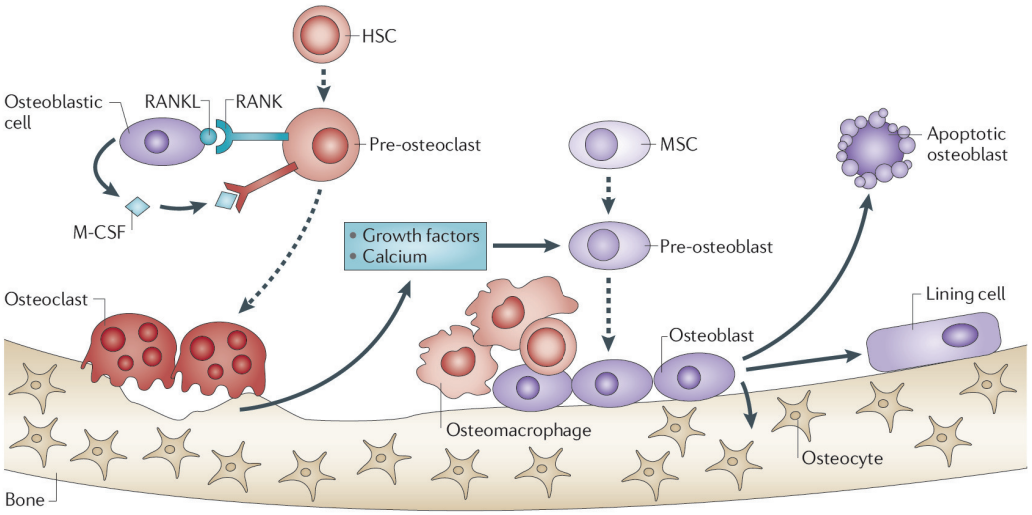


Figure 7.1: Schematic diagram showing major cell types that are involved in bone remodelling. Osteoblasts and osteoclasts are responsible for bone formation and resorption respectively. Osteocytes sense mechanical status of the bone and communicate with other bone cells. This artwork is obtained from Weilbaecher et al. (2011), reprinted with permission.

In recent years, it has emerged that epigenetic regulation affects many aspects of cell biology such as development and disease (Allis, 2007; Esteller, 2007). These mechanisms can eventually be attributed to transcriptional regulation of genes. Osteoclasts are central in bone physiology and the discovery of a histone H3K27 demethylase inhibitor has enabled us to study the functions of histone modifications in osteoclasts and to discover a new anti- resorptive mechanism with implications in bone diseases associated with excessive resorption such as osteoporosis, Paget' s disease or bone cancer.

7.2 Osteoclast biology and NFATc1 pathways

As described above, osteoclasts are cells that are capable of degrading bone. They are formed by fusion of mononuclear osteoclast precursors derived from hematopoietic cells found in the bone marrow. They are terminally differentiated cells and morphologically resemble multinucleated macrophages described in chapter 6. The key functional difference is that osteoclasts have the ability to perform

lacunar resorption on mineralised bone material. An osteoclast first forms a sealing zone with its membrane on the bone surface, and then secretes proteolytic and degrading enzymes to break down the bone matrix underneath. The degraded material is absorbed by endocytosis and released on the other side of the cells by exocytosis. The proteolyic enzymes involved include the cathepsin and matrix metalloproteases (MMP), such as Cathepsin K, MMP-9 and MMP-13 (Vaananen et al., 2000).

Early on it was found that differentiation of human osteoclast precursors into human mature osteoclasts requires macrophage colony-stimulating factor (M-CSF), 1,25-dihydroxyvitamin D3 and bone derived stromal cells (Fujikawa et al., 1996; Yasuda et al., 1998), but does not require bone substrate (Fuller et al., 2010). It was believed that ligand-receptor interactions were involved in osteoclast formation as evidenced by the requirement of bone derived stromal cells in the cell culture. The essential ligand was later identified to be the Receptor Activator of NFκB Ligand (RANKL) of the RANKL - RANK pathway (Lacey et al., 1998; Yasuda et al., 1998). RANKL (also known as TNFSF11) is a TNF superfamily cytokine expressed in (among others) bone stromal cells. The RANK receptor belongs to the TNF receptor superfamily which is expressed in osteoclast precursors. The binding of RANKL to RANK receptor activates TRAP6, a mediator of RANK that binds to three different sites on the receptor (Gohda et al., 2005). Six major signalling pathways have been identified downstream of TRAF6, including NFκB, NFATc1, JNK (Ikeda et al., 2004a), P38 (Matsumoto et al., 2004; Huang et al., 2006), ERK, src/AKT. AP-1 and NF-κB are the major transcription factors that are activated in the early stage of osteoclast differentiation. AP-1 is a dimer of c-FOS and c-Jun which is induced by the JNK1 pathway (David et al., 2002). NF-κB is a transcription factor that can be composed of different subunits including p50/105, p52/p100, p65/RelA, RelB and c-Rel. It regulates a large number of genes critical for many cellular activities in particular the immune response (Hayden and Ghosh, 2004). The subunits p50 and p52 are required for activation of osteoclastogenesis (Franzoso et al., 1997; Xing et al., 2002). NFATc1, a transcription factor originally identified in T cells, is induced by NF-κB in osteoclast precursors (Takayanagi et al., 2002; Ishida, 2002). It interacts with AP-1 and leads to the induction of a number of genes leading to cell fusion (e.g. ATP6V0D2, DCSTAMP) (Kim et al., 2007) as well as expression of proteolytic enzymes necessary for osteoclast function such as cathepsin K and TRAP.

Recently, histone modification has been implicated in osteoclast differentiation. Yasui et al.

reported that JmjD3 could be involved in mouse bone marrow derived osteoclast development (Yasui et al., 2011). JmjD3 or UTX were knocked down by siRNA in mouse osteoclast precursors and it was discovered that JmjD3 but not UTX abrogated osteoclast formation. Gene expression studies revealed that expression of NFATc1 was reduced upon JmjD3 knockdown. Chip-seq analysis showed that there were changes in H3K27me3 levels at the promotor of NFATc1. Accordingly, such H3K27me3 demethylation may be involved in the regulation of NFATc1 expression, which in turn controls the expression of key osteoclast development and functional genes such as c-FOS and Cathepsin K. However, it was unclear whether the effect of JmjD3 was due to the demethylase activity or other molecular processes and the precise mechanisms underlying the inhibition of osteoclastogenesis were not investigated. The use of small molecular inhibitor such as GSK-J1 and its cell-permeable ester derivative GSK-J4 has allowed us to study the role of demethylase activity of JmjD3 and monitor subsequent molecular events in osteoclasts and its precursor cells.

7.3 Generation of active human osteoclasts in cell culture

To investigate epigenetic regulation in human osteoclast differentiation, an osteoclast differentiation system was established in this DPhil study, and further developed for functional assays. Human osteoclasts were generated from monocytes (CD14+) which can be readily obtained from human peripheral blood. Whole blood was separated by a Ficoll - paque gradient to separate leukocytes from erythrocytes. The leukocytes were enriched in a buffy coat layer which contains all peripheral blood mononuclear cells (PBMC). The PBMCs were washed and incubated with anti-CD14 antibody conjugated with magnetic beads. A pure CD14+ population was then separated using a magnetic device.

The CD14+ cells were grown in MEM-a medium supplemented with 10% of fetal calf serum and M-CSF (25 ng/mL) for 6 days to form macrophages. This step is required for the cells to adapt to cell culture conditions in order to produce homogenous osteoclast precursors. RANKL (50 ng/mL) was then added to the medium on day 7 to initialise the osteoclast differentiation program. Osteoclast precursor cell bodies began to enlarge and fuse with neighbouring cells. The medium and cytokines were replenished every three days. At the end of three weeks, cells grew up to 200 μm in diameter and

contained up to 30 nuclei. At this stage, cells became tartrate-resistant acid phosphatase (TRAP) positive and were capable of resorbing bone substrate. To assess bone resorption, osteoclast precursor cultured on bone substrate and dentin discs produced from elephant ivory tusks were routinely used as substrate for bone resorption. The dentin discs were 5 mm in diameter and 0.5 mm in thickness. They were placed at the bottom of a culture dish to allow adhesion of osteoclast precursors on top. Mature osteoclasts were capable of forming lacunae pits on the dentins.

7.4 Defining osteoclast criteria in cell culture

After three weeks of culture, the morphology of the cells was heterogenous; it was therefore necessary to define a list of criteria for identification and quantification of mature osteoclasts, as adopted from the literature (Sabokbar and Athanasou, 2003). First, mature osteoclasts must have a cell body larger than 50 μm in diameter. Second, the cells must contain at least three nuclei. Third, they must be TRAP staining positive. Fourth, lacunae pits must be identified on dentin discs to ensure they are functionally active osteoclasts. Other criteria include a vitronectin receptor positive status (VNR+), and formation of F-actin rings indicative of a cytoskeletal organisation allowing sealing of the bone surface and subsequent resorption.

7.5 Effect of KDM6 demethylase inhibition in osteoclast differentiation

7.5.1 Morphology and osteoclast numbers

To identify the role of H3K27 histone demethylases in osteoclast differentiation, GSK-J4 and GSK-J5 were used to inhibit JmjD3 or UTX. As described in Chapters 3 and Chapter 6, GSK-J4 is the pro-drug of GSK-J1 which is the active form of the inhibitor. GSK-J5 is the pro-drug of GSK-J2, a structural isomer of GSK-J1 which has no inhibitory effect on JmjD3 or UTX in vitro or in cells but acts as a negative control in cellular assays. To begin with, human osteoclast precursors were generated from 6-day cultures in M-CSF. At day 7, the medium was changed and the cells were incubated with M-CSF and GSK-J4 or GSK-J5 for 30 minutes. RANKL was added to a final concentration of

50 ng/mL to initiate the differentiation program. The medium, cytokines and compounds were replenished every three days. After one week of RANKL treatment (Day 14), a dramatic morphological difference was observed between GSK-J4 and the control group. In the control group, osteoclast precursors changed from spindle-like shape to oval shape and began to fuse with neighbouring osteoclast precursors forming multinucleated cells (Fig. 7.2A). Immunofluorescence staining showed that these cells were vitronecin receptor (VNR) positive and showed a characteristic F-actin ring structure (Fig. 7.2A). In cells undergoing GSK-J4 treatment, there was a significantly reduced number of osteoclasts formed, cells remained mononuclear, were VNR negative and demonstrated absence of an F-actin ring structure.

Continuous treatment of the cells with RANKL provided the necessary stimulus for the osteoclasts to complete maturation. At Day 22, cells were up to 200 μm in diameter and contained up to 30 nuclei in the control group and the GSK-J5 but not the GSK-J4 group (Fig. 7.2B). GSK-J4 treated osteoclast precursors retained a spindle-like shape comparable to no RANKL treatment and the fusion event was significantly less than the control group. The number of TRAP+ multinucleated cells in GSK-J4 treatment was significantly less than the control group (Fig. 7.2C). In the GSK-J5 treatment, osteoclast formation was not inhibited and the morphology of the cells was similar to the control group.

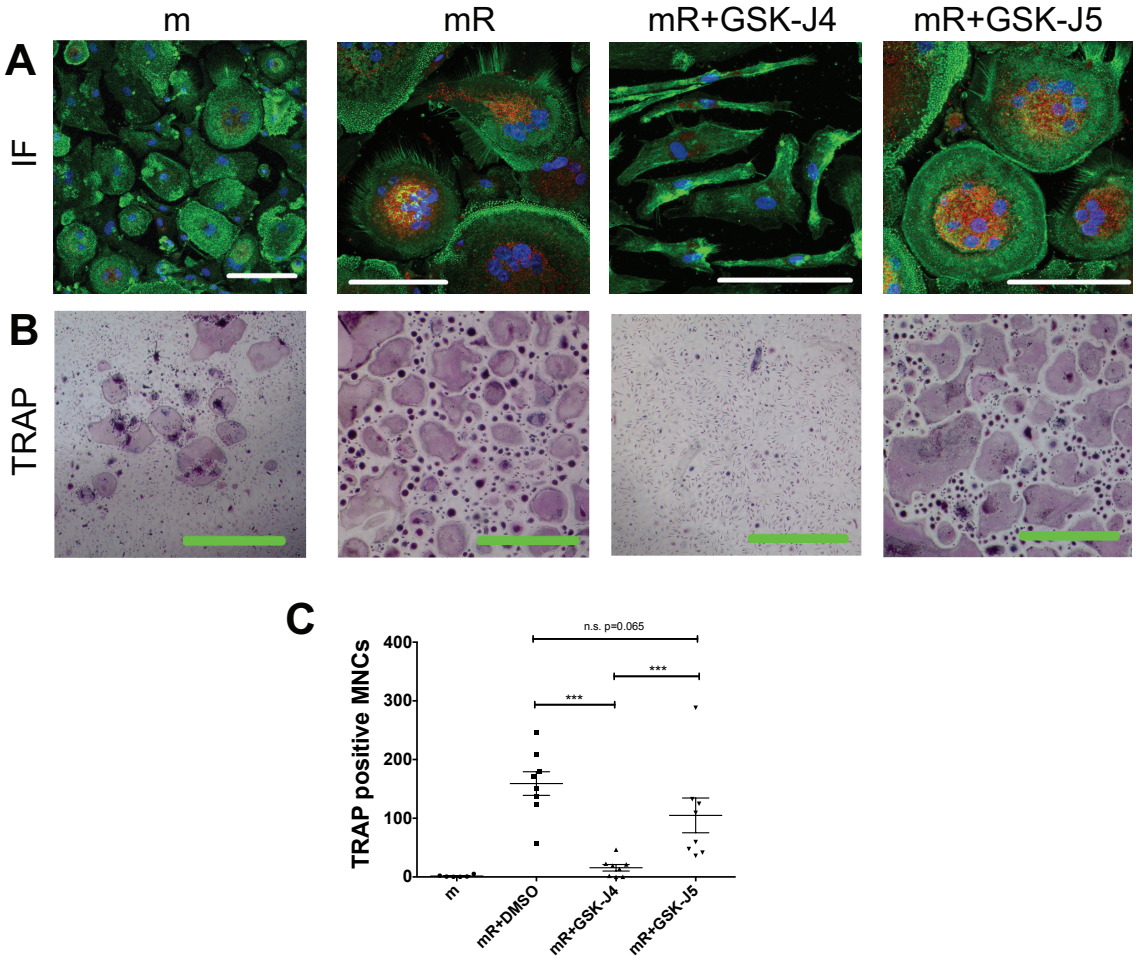


Figure 7.2: GSK-J4 inhibits human osteoclast differentiation. Abbreviations: m = M-CSF, mR = M-CSF + RANKL. A) Immunofluorescence microscopy showing nucleus (blue, DAPI stain), actin (anti-actin antibody with anti-rabbit IgG conjugated with Alex488) and VNR (red, anti VNR antibody conjugated with anti-mouse IgG conjugated with Alexa594) of osteoclasts at Day 22. White scale bar is equivalent to 50 μm. B) TRAP staining showing impaired osteoclast development under GSK-J4 treatment but not GSK-J5 at Day 14. C) Chart showing number of TRAP positive multinucleated cells was significantly reduced under GSK-J4 treatment. Green scale bar is equivalent to 100 μm. N = 8. *** $P < 0.001$ by student' s t test. All data are means $\pm$ s.e.m.

7.5.2 Bone resorption

The ability of osteoclasts to resorb bone material was tested under GSK-J4 and GSK-J5 treatment. CD14+ cells were seeded on a 24-well plate containing 4 dentin discs in each well and the cells were treated for three week as described previously. At day 22, dentin discs were retrieved, treated with ammonium hydroxide to lyse the cells and stained in 1% toluidine blue solution. Toluidine blue stains nucleic acids and polysaccharides that were found on the surface of lacunae pits, and also enhances the contrast when inspected under a light microscope. A large number of lacunae pits were found in the control group and GSK-J5 treatment (Fig. 7.3A), significantly less lacunae pits were found on dentin discs in the GSK-J4 condition. Scanning electron microscope analysis also showed a significantly reduced number of resorptive pits on the dentin disc in the GSK-J4 treated sample (Fig. 7.3B). The method of quantifying resorption volume on dentin pits was developed by Dr. Clarence Yapp (Botnar Research Institute, Oxford). Using this method it is shown that cells treated with GSK-J4 have 7 fold less resorptive potential (Fig. 7.3C).

Enzyme linked immunosorbent assay (ELISA) was performed to quantify the level of type I collagen fragments in the cell culture medium. Type I collagen fragments were produced from the breakdown of type I collagen by collagenase expressed in osteoclasts, notably Cathepsin K and MMP9. A specific antibody was used to detect collagen fragments but not the whole collagen molecule. A high level of type I collagen fragment was detected starting at day 15 (5 days after RANKL stimulation) in the control group and the GSK-J5 condition (Fig. 7.3D). Low levels of type I collagen fragment were present in the GSK-J4 condition, suggesting there was less collagen I breakdown under GSK-J4 treatment. It could be due to a decreased expression of collagenase or reduction in the activity. Major osteoclast producing collagenases such as Cathepsin K or MMP9 were reported to function in a low pH condition under the sealing zone of osteoclast (Garnero, 1998). The lack of osteoclast formation may not provide an acidic environment for the collagenase to function.

The above results showed that GSK-J4 affects not only the morphology of the osteoclasts but also their functions. Since GSK-J4 appears to be selective towards the KDM6 family of histone demethylases and no other phenotypic effect was observed in GSK-J5 compared to the control group,

it can be concluded from this point that inhibition of KDM6 histone demethylases dramatically inhibits osteoclast development.

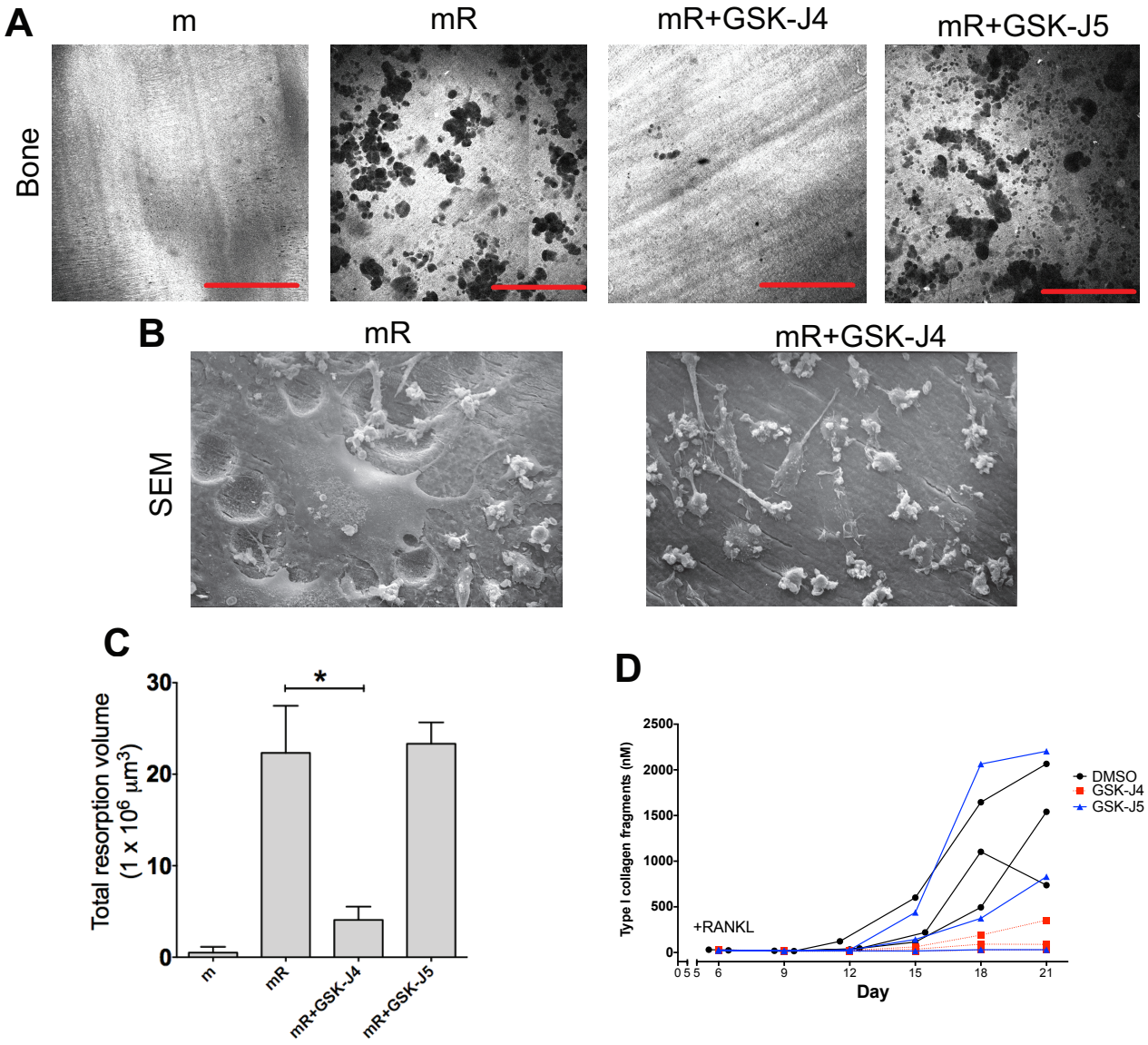


Figure 7.3: GSK-J4 inhibits osteoclast bone resorption. A) Confocal image of dentin disc surfaces showing absence of bone resorption in cells under GSK-J4 treatment but not under GSK-J5. Red scale bars indicate 100 μm. B) Scanning electron microscope (SEM) image showing absence of lacunae pits on the dentin disk upon GSK-J4 treatment. Blue scale bars indicate 10 μm. C) Total volume of resorption pits on 4 dentin discs measured by confocal microscopy. N = 3. * P $<$ 0.05 by student' s t test. All data are means $\pm$ s.d. D) Concentration of collagen I fragments in cell culture medium over time in three different donors. Samples were harvested every three day before replenishing with fresh medium. Each data point represents amount of college I fragments produced during the three day period.

7.6 Comparison with other known anti-resorptive mechanisms

To explore the possibility that inhibition of JmjD3 is a potential novel therapeutic anti-bone resorption mechanism, we compared GSK-J4 with clinically used anti-resorptive drugs such as bisphosphonates, cathepsin k inhibitors or osteoprotegerin as RANKL-scavenging mechanism. These anti-resorptive drugs were incubated with osteoclast precursors for 1 hour at which point they were induced by RANKL as described above. The number of osteoclasts was measured after two weeks of differentiation. These drugs can be divided into a few categories: Alendronate and zoledronate are nitrogen-containing pyrophosphate analogs (N-bisphosphonates, N-BP) which target isoprenoid synthesis in bone cells (Russell et al., 2008). These nitrogen-containing bisphosphonates have high affinity towards calcium in the bone matrix and are actively resorbed by osteoclasts. It is observed that they reduced osteoclast numbers upon RANKL treatment (Fig. 7.4A). Osteoprotegerin (OPG) is a decoy receptor for RANKL, binds to RANKL in solution, and prevents RANK binding and downstream NFκB activation in osteoclasts. OPG also reduced osteoclast numbers as shown in Figure 7.4B, however not as effectively as N-BPs. Cathepsin K inhibitor II, which inhibits resorption activity of mature osteoclasts, did not affect numbers of mature osteoclasts, as expected. GSK-J4 treatment appears to be as effective as conventional drugs at the given concentration to inhibit osteoclast function, whereas GSK-J5 showed no significant difference from the control group.

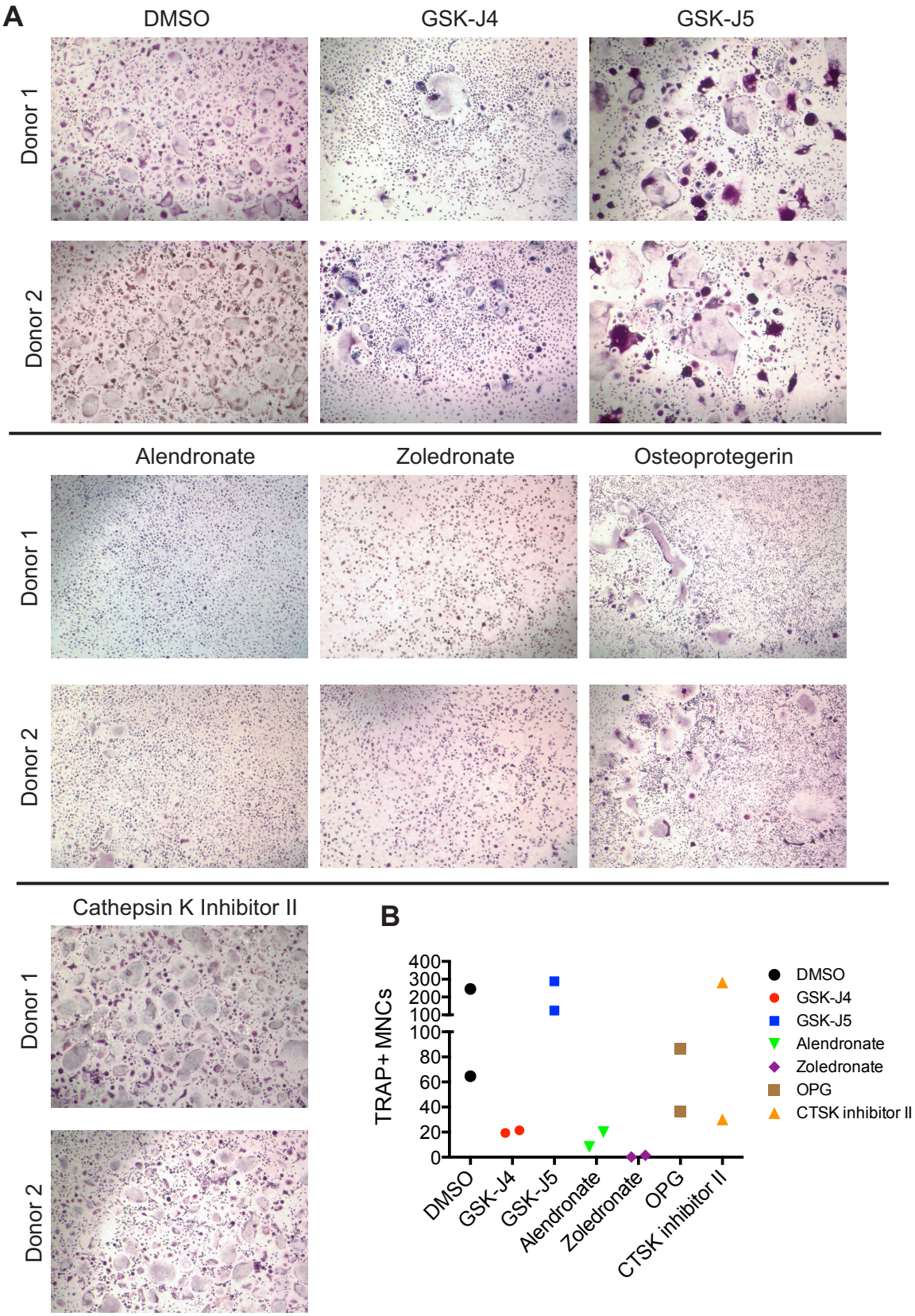

A
DMSO
GSK-J4
GSK-J5
Donor 1
Donor 2
Alendronate
Zoledronate
Osteoprotegerin
Donor 1
Donor 2
Cathepsin K Inhibitor II
Donor 1
Donor 2
B
TRAP+ MNCs
400
300
200
100
100
80
60
40
20
0
DMSO
GSK-J4
GSK-J5
Alendronate
Zoledronate
OPG
CTSK inhibitor II
DMSO
GSK-J4
GSK-J5
Alendronate
Zoledronate
OPG
CTSK inhibitor II

Figure 7.4: (Previous page) Comparison of GSK-J4 with known anti-resorptive compounds. A) TRAP staining of three-week osteoclast treated with a panel of anti-resorptive compounds. Osteoclast precursors were treated with GSK-J4 (20 μM), GSK-J5 (20 μM), Alendronate (10 μM) , Zoledronate (10 μM), OPG (25 ng/ mL), Cathepsin K (CTSK) inhibitor II (1 μM) or control (DMSO) with RANKL stimulation at Day 7. Cells were allowed to grown for two weeks with change of medium/supplement of inhibitors every three days. Cells were fixed after two weeks and TRAP stained. Images magnification: 40x B) Number of TRAP positive multi-nucleated cells (MNCs) after three weeks of culture. N = 2.

7.7 Microarray analysis

To understand the underlying molecular mechanism of osteoclast inhibition, microarray analysis was performed using the Affymetrix GeneChip Human Gene 1.0 ST array which consists of 36079 probes for 21014 annotated genes. It is hypothesized that inhibition of JmjD3 will likely cause changes in gene expression and inhibit osteoclast differentiation.

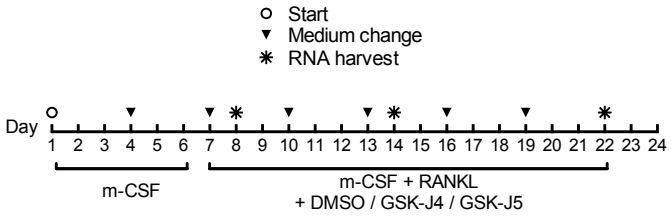


Figure 7.5: An overview of the experimental procedure with activities indicated.

7.7.1 Early RANKL stimulation (Day 8)

To identify the early gene expression events leading to fusion and multinucleation, 6-day osteoclast precursors were treated with GSK-J4 or GSK-J5 for 30 minutes and stimulated with RANKL for 24 hours. RNA samples were harvested after 24 hours (Procedures summarized in Fig. 7.5). RANKL stimulation results in at least two fold changes of mRNA level in 219 genes, 154 genes of which were up-regulated and 65 were down-regulated (Figs. 7.6, 7.7 and appendix IV&V). Among the regulated genes detected in the array analysis, ACTN2 (actinin, alpha 2) is important for monocyte/macrophage maturation and is up-regulated in osteoclast formation (Luikart et al., 1999). Chemokines that are

necessary for cell interactions, including the CC chemokines CCL5, CCL7 and CCL24, as well as the CXC chemokines CXCL5, CXCL10 and CXCL11, were induced. Gene expression of membrane receptors CLEC1A, CLEC4E, CD200R1, CD209 and CD274 (PDCD1LG1a) were also affected. These surface proteins may be important for homotypic interactions. CA2 (Carbonic anhydrase II), which catalyzes the inter-conversion of CO_2 and water to bicarbonate ions and protons, was induced, and is known for acidification and bone resorption (Riihonen et al., 2007). Expression of SLA (Src-like-adaptor), which negatively regulates differentiation of osteoclasts and proliferation of osteoclast precursors, was decreased (Kim et al., 2010). The following genes were selected and verified in qPCR: CBLB (Cas-Br-M (murine) ecotropic retroviral transforming sequence b) protects osteoclast from apoptosis (Fig. 7.8E) (Purev et al., 2009). LIF (leukemia inhibitory factor) stimulates osteoclast differentiation and is implicated in the control of osteoclast size (Fig. 7.8L) (Bozec et al., 2008; Richards et al., 2000). TGFB3 (transforming growth factor, beta 3) inhibits osteoclast differentiation by stimulating osteoprotegerin expression in osteocytes (Fig. 7.8S) (Heino et al., 2002; Thirunavukkarasu et al., 2001). TSPAN13 (Tetraspanin-13) may be involved in osteoclastogenesis (Fig. 7.8W) (Iwai et al., 2007).

The array analysis (Fig 7.6) shows that GSK-J4 has a strong effect on early RANKL profiles. Expression of 55 out of 219 RANKL induced genes was counter-regulated by GSK-J4 (52 down-regulated and 3 up-regulated). Amongst the genes important for osteoclast formation and regulated by RANKL in early hours, the following genes were found: MET (met proto-oncogene) can regulate osteoclast function by activating c-Src kinase (Fig. 7.8M) (Gaasch et al., 2006; Adamopoulos et al., 2006). NHEDC2(Na+/H+ exchanger domain containing 2) is involved in osteoclast fusion, differentiation and resorption (Ha et al., 2008a). QPCR experiments were also performed on JmjD3, UTX, NFATc1, c-FOS and c-JUN even though they were not identified in our microarray dataset. JmjD3, but not UTX mRNA was increased in the first 24 hours upon RANKL stimulation (Fig. 7.8J & K). NFATc1 expression was counter-regulated by GSK-J4 (Fig. 7.8O). Other transcription factors such as c-FOS and c-JUN were also counter-regulated by GSK-J4 within the first 24 hours of treatment.

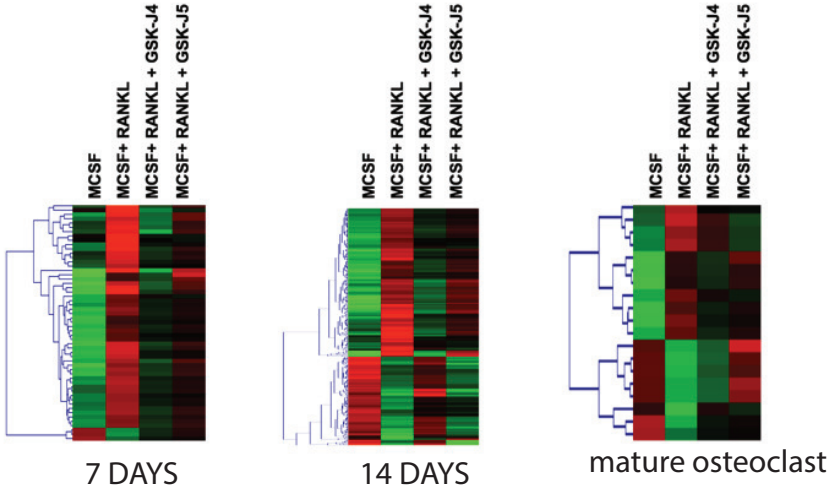


Figure 7.6: Hierarchical clustering of genes selectively counter-regulated by GSK-J4 in the RANKL transcriptome at different stages of osteoclast formation. Red and green bar represents high and low expression levels respectively.

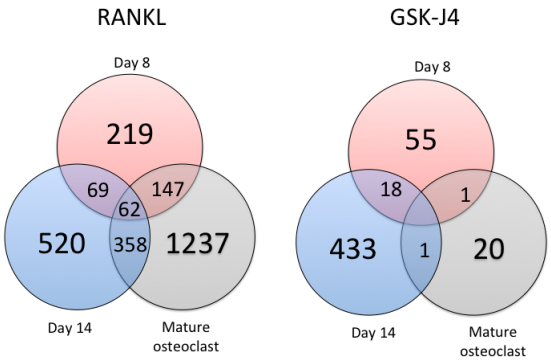


Figure 7.7: Venn diagram showing number of genes regulated by RANKL and GSK-J4 at different time point.

7.7.2 Differentiating osteoclasts (Day 14)

Continuous treatment of RANKL for 7 days had stronger effects than 24 hours in the induced gene expression program (Fig. 7.6, 7.7 and appendix VI&VII). For a total of 889 regulated genes, 424 genes were up-regulated and 465 were down-regulated. 433 genes were counter-regulated by GSK-J4, of which 270 genes were down-regulated and 163 genes were up-regulated. 124 out of 219 genes in

this dataset were also present in the day 8 dataset (see above). Several key osteoclast genes such as ATP6V0D2, DCSTAMP, NHEDC2, TMEM156 and TSPAN13 are transmembrane proteins which are involved in osteoclast fusion or proton transport (Wu et al., 2009; Yagi et al., 2006; Ha et al., 2008a; Kim et al., 2013; Iwai et al., 2007). Expression of these genes was down-regulated by GSK-J4 in day 14 (Figs. 7.8A, G, P, T and W). CTSK (Capthepsin K), ACP5 /TRAP (acid phosphatase 5, tartrate resistant), MMP9 (matrix metallopeptidase 9) are enzymes that are involved in degradation of extracellular matrix. CTSK and ACP5/TRAP were down-regulated by GSK-J4 but not in the control and the GSK-J5 groups (Figs7.8D and V). MMP9 expression was only up-regulated in Day 22 and was antagonized by GSK-J4 (Fig 7.8N). CBLB, EPHB2, LIF, MET, NFATc1 and PPARGC1A are genes that promote osteoclastogenesis, and expression of these genes was down-regulated by GSK-J4 except EPHB2 at Day 14 (Fig. 7.8E, H, M, O and Q). IRF-8, SEMA3E and TGFB3 are genes that will inhibit osteoclast formation when expressed. Interestingly, GSK-J4 induced expression of IRF-8 (Fig. 7.8I), but not SEMA3E (Fig. 7.8R) and TGFB3 (Fig. 7.8S) TNFSF13B belongs to the TNF superfamily and it is highly up-regulated in the microarray dataset but it has no reported function in osteoclasts.

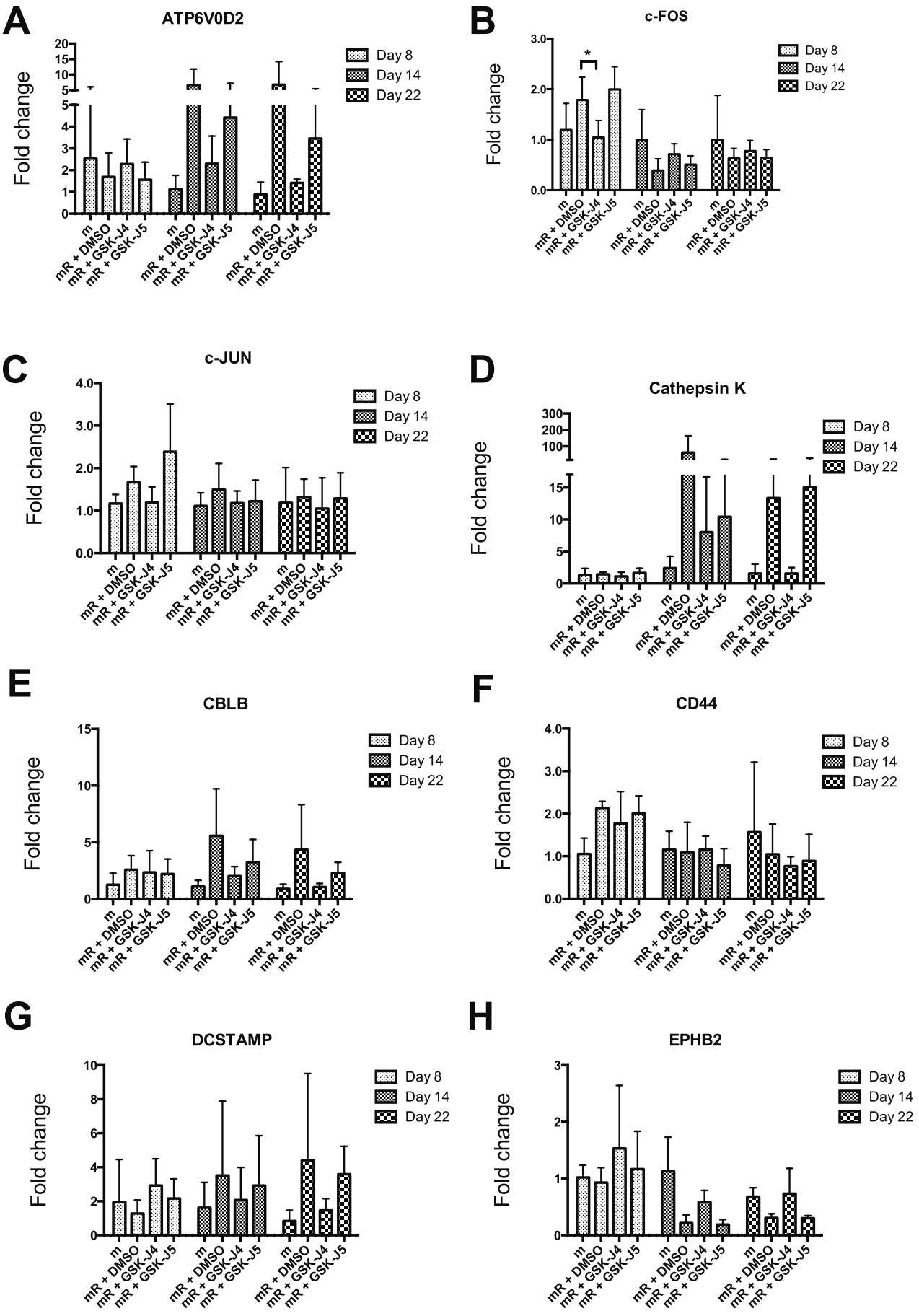
7.7.3 Mature osteoclasts

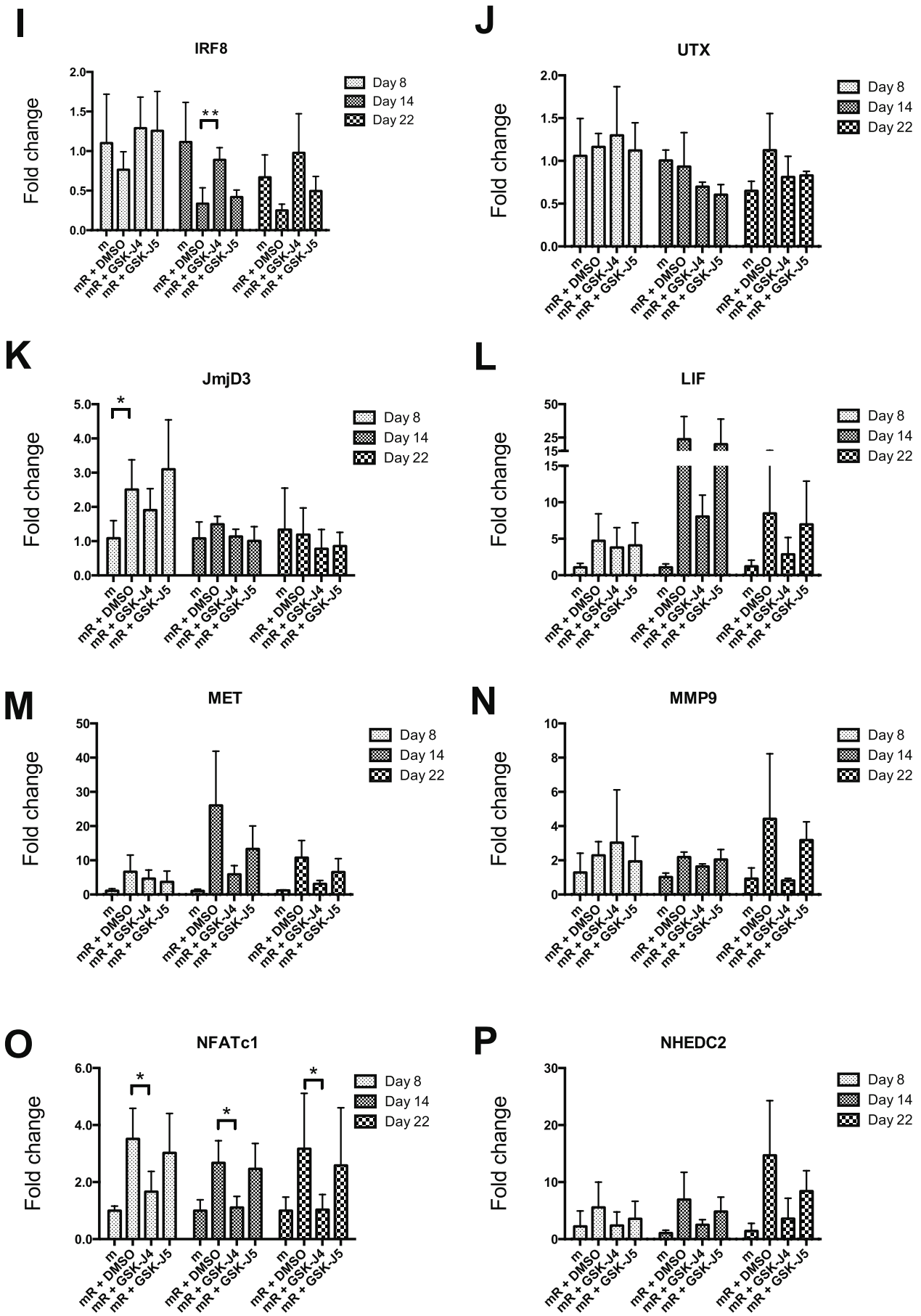
To investigate whether Jmj3 inhibition inhibits mature osteoclasts, cells were stimulated with RANKL and allowed to develop for three weeks. GSJ-J4 and GSK-J5 were treated on Day 22 and RNA samples were harvested 24 hours after. Although stimulation with RANKL alone changed expression of 1237 genes (438 up-regulated and 799 down-regulated, Fig. 7.6, 7.7 and appendix VIII&IX), GSK-J4 had relatively low impact such that only 20 genes were counter-regulated, of which 11 genes were down-regulated and 9 were up-regulated. The implications of these counter-regulated genes in osteoclast biology were less clear. Among the genes regulated were the signalling mediators RND1 from the Rho GTPase1 family, and MYOZ1(Myozenin) which interacts with Actinin, alpha 2 and other cytoskeleton proteins (Faulkner, 2000).

Altogether, these data supports that GSK-J4 inhibits osteoclast formation by interfering with the transcriptomic changes required for development, cellular fusion and bone resorption properties.

Table 7.1: Selected genes related to osteoclast differentiation and function

Gene Symbol	Gene Name	Functions related to osteoclast	Reference
ACP5	TRAP / acid phosphatase 5, tartrate resistant	Osteoclast marker, catalyzes the conversion of orthophosphoric monoester to alcohol and orthophosphate	(Matsuo, 2004)
ATP6V0D2	ATPase, H+ transporting, lysosomal 38kDa, V0 subunit d2	osteoclast-specific proton pump	(Wu et al., 2009)
CALM1	calmodulin 1 (phosphorylase kinase, delta)	osteoclast differentiation, function, and survival	(Seales et al., 2005)
CBLB	Cas-Br-M (murine) ecotropic retroviral transforming sequence b	protect osteoclasts from apoptosis	(Purev et al., 2009)
CD44	CD44	CD44 antibodies inhibit osteoclast formation	(de Vries et al., 2005; Kania et al., 1997)
CTSK	Cathepsin K	extracellular matrix degradation.	(Gelb et al., 1996)
EPHB2	EPH receptor B2	loss of EPHB2 results in in creased osteoclast differentiation	(Cheng et al., 2012)
FOS	c-FOS / FBJ murine osteosarcoma viral oncogene homolog	induce osteoclast differentiation	(Huang et al., 2006)
ILF3	NF90 interleukin enhancer binding factor 3, 90kDa	upregulated in osteoclast	(Day et al., 2004)
IRF8	interferon regulatory factor 8	suppress osteoclastogenesis	(Zhao et al., 2009)
JUN	c-JUN / jun proto-oncogene	induce osteoclast differentiation	(Ikeda et al., 2004b)
KDM6A	UTX / lysine (K)-specific demethylase 6A	Histone H3K27 demethylase	(Yasui et al., 2011)
KDM6B	JmjD3 / lysine (K)-specific demethylase 6B	Histone H3K27 demethylase involves in epigenetic regulation of osteoclast	(Yasui et al., 2011)
LIF	leukemia inhibitory factor (cholinergic differentiation factor)	osteoclast size, stimulate osteoclast differentiation	(Bozec et al., 2008; Richards et al., 2000)
MET	met proto-oncogene (hepatocyte growth factor receptor)	osteoclast differentiation	(Adamopoulos et al., 2006; Gaasch et al., 2006)
MMP9	matrix metallopeptidase 9 (gelatinase B, 92kDa gelatinase, 92kDa type IV collagenase)	extracellular matrix degradation.	(Sundaram et al., 2007)
NFATc1	nuclear factor of activated T-cells, cytoplasmic, calcineurin-dependent 1	key regulator in osteoclast differentiation	(Koga et al., 2005; Kim et al., 2007)
NHEDC2	Na+/H+ exchanger domain containing 2	inhibition of NHEDC2 inhibited osteoclast differentiation	(Ha et al., 2008b)
PPARGC1A	peroxisome proliferator-activated receptor gamma, coactivator 1 alpha	activation of osteoclastogenesis, iron uptake	(Wei et al., 2010; Ishii et al., 2009a)
SEMA3E	sema domain, immunoglobulin domain (Ig), short basic domain, secreted, (semaphorin) 3E	decrease osteoclast formation	(Hughes et al., 2012)
TGFB3	transforming growth factor, beta 3	inhibit osteoclast differentiation, stimulate osteoprotegerin expression	(Heino et al., 2002) (Thirunavukkarasu, 2001)
TM7SF4	DCSTAMP / transmembrane 7 superfamily member 4	cell fusion	(Yagi et al., 2006)
TMEM156	transmembrane protein 156	highly upregulated in microarray, maybe involved in calcium signaling	(Kim et al., 2013)
TNFSF13B	tumor necrosis factor (ligand) superfamily, member 13b	highly upregulated in microarray dataset	N/A
TSPAN13	tetraspanin 13	may be involved in osteoclastogenesis	(Iwai et al., 2007)


A
ATP6V0D2
Fold change
Day 8
Day 14
Day 22
m
mR + DMSO
mR + GSK-J4
mR + GSK-J5
B
c-FOS
*
C
c-JUN
D
Cathepsin K
E
CBLB
F
CD44
G
DCSTAMP
H
EPHB2


I
IRF8
Fold change
Day 8
Day 14
Day 22
m
mR + DMSO
mR + GSK-J4
mR + GSK-J5
J
UTX
K
JmjD3
L
LIF
M
MET
N
MMP9
O
NFATc1
P
NHEDC2

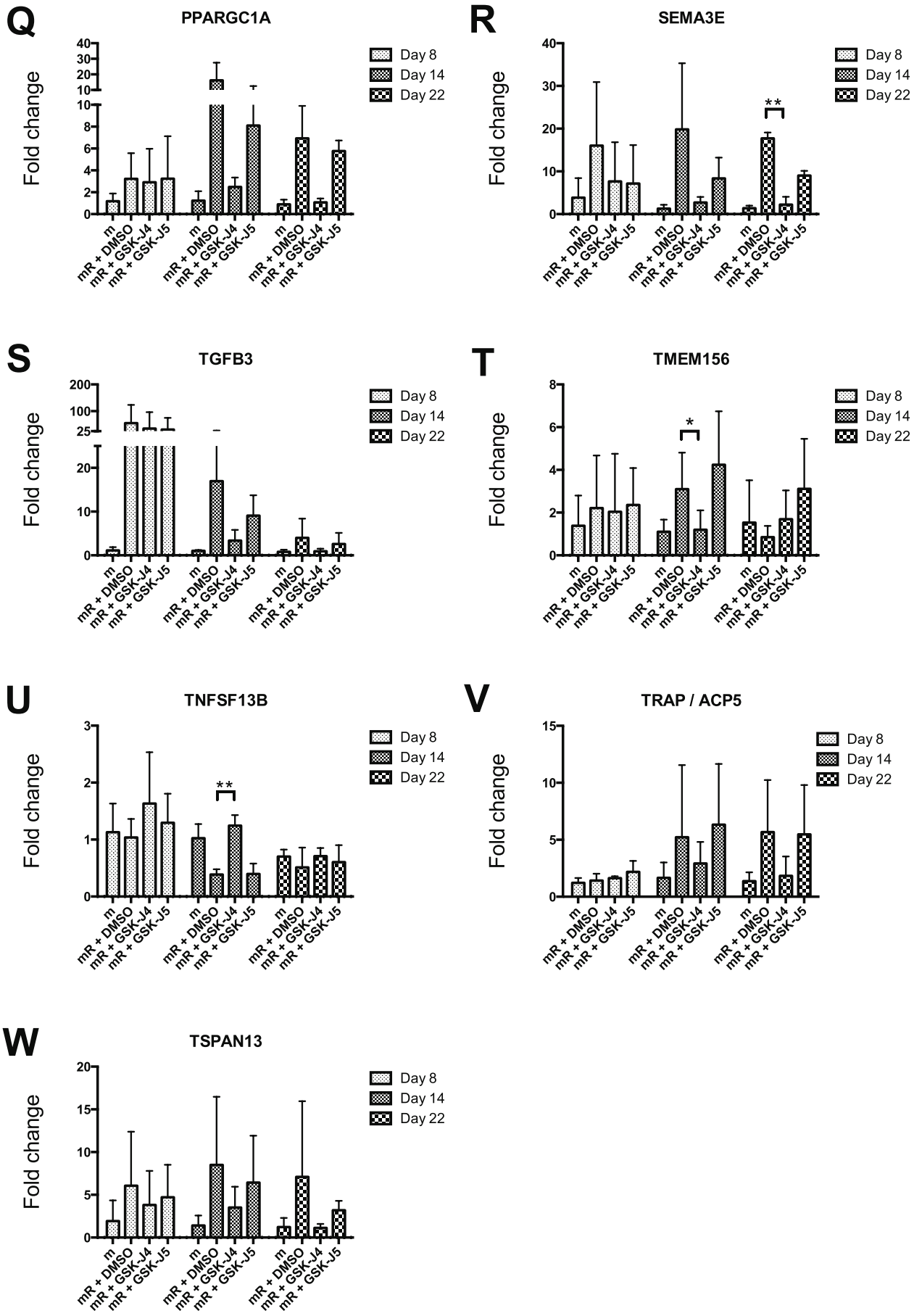

Q
PPARGC1A
Fold change
Day 8
Day 14
Day 22
m
mR + DMSO
mR + GSK-J4
mR + GSK-J5
R
SEMA3E
**
S
TGFB3
T
TMEM156
*
U
TNFSF13B
**
V
TRAP / ACP5
W
TSPAN13

Figure 7.8: (Previous pages) A panel of genes related to osteoclast development and functions were selected from microarray analysis and validated by quantitative PCR in the sybrgreen format. These genes were assayed at day 8, day 14 and day 22 during osteoclast differentiation. 18S rRNA was used as housekeeping gene to normalize the dataset. Experiments were repeated at least three times independently. * P <0.05, ** P <0.01 by student's t test. All data are means ± s.d.

x

7.8 Chromatin analysis

A chromatin immunoprecipitation assay (ChIP) was performed in order to understand the changes of histone methylation under JmjD3 inhibition in osteoclast. Differentiating osteoclasts treated with GSK-J4 at day 14 were fixed in 1% formaldehyde after 24 hours. The chromatin was sheared into small fragments (200-1000bp) by ultrasonication. Chromatins fragments containing H3K27me3 histones marks were pulled down by antibodies. The purified chromatin was de-crosslinked by heat and the DNA was further purified for subsequent qPCR.

We performed ChIP-qPCR on NFATc1, a key transcription factor for osteoclastogenesis previously reported to be downregulated upon JmjD3 knockdown in mouse osteoclast precursors. To identify loci that maybe involved in H3K27 methylation, the NFATc1 sequence was aligned with the human monocytes H3K27me3 ChIP-seq dataset available in the Gene Expression Omnibus (GEO) database (Bernstein et al., 2010). It was discovered that there is a distinctive H3K27me3 cluster at the 5' end of the gene in monocytes (Fig. 7.9A). Using the transcription factor binding site prediction program MATCH of the Transfac database (Wingender et al., 2000), a NF-κB binding site was predicted at the promoter of the NFATc1 gene. ChIP-qPCR results showed that there was an increase of H3K27 methylation upon GSK-J4 treatment at this region, suggesting that JmjD3 or UTX may be directly involved in controlling the histone methylation (Fig. 7.9B).

A number of genes which were differentially regulated by GSK-J4 in the microarray analysis dataset also contain distinctive H3K27 methylation patterns at the 5' end of the gene in monocytes, notably EPHB2, IRF8, LIF, MET, PPARGC1A, SEMA3E, TGFB3 and TSPAN13 (Fig. 7.10). Whether these histone H3K27 signatures also exist in osteoclasts and are important for transcriptional regulation have not been fully elucidated and merit further investigations.

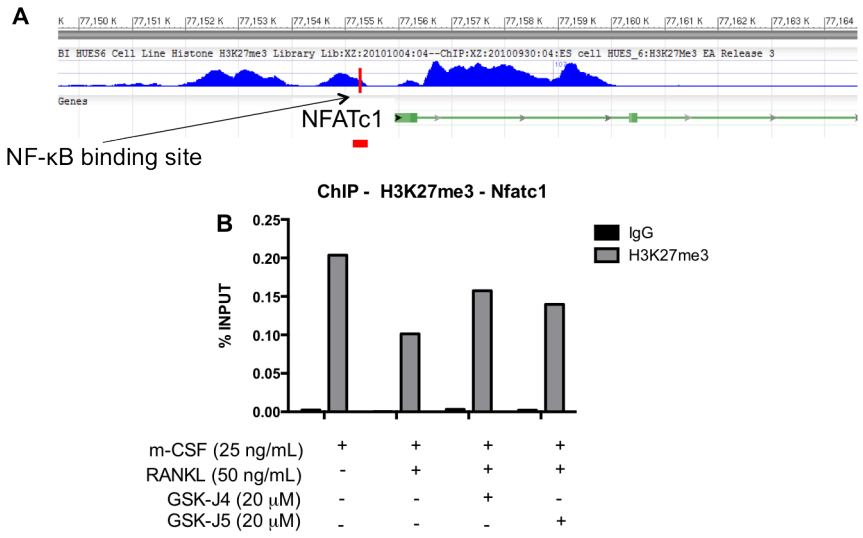


Figure 7.9: A) H3K27 trimethylation is enriched at the upstream region of NFATc1 gene in monocytes. Red box indicate the assayed region for ChIP-qPCR experiment. B) ChIP-qPCR result showing there is an increased level of H3K27me3 at the promoter of NFATc1 gene upon GSK-J4 or GSK-J5 treatment. N=1.

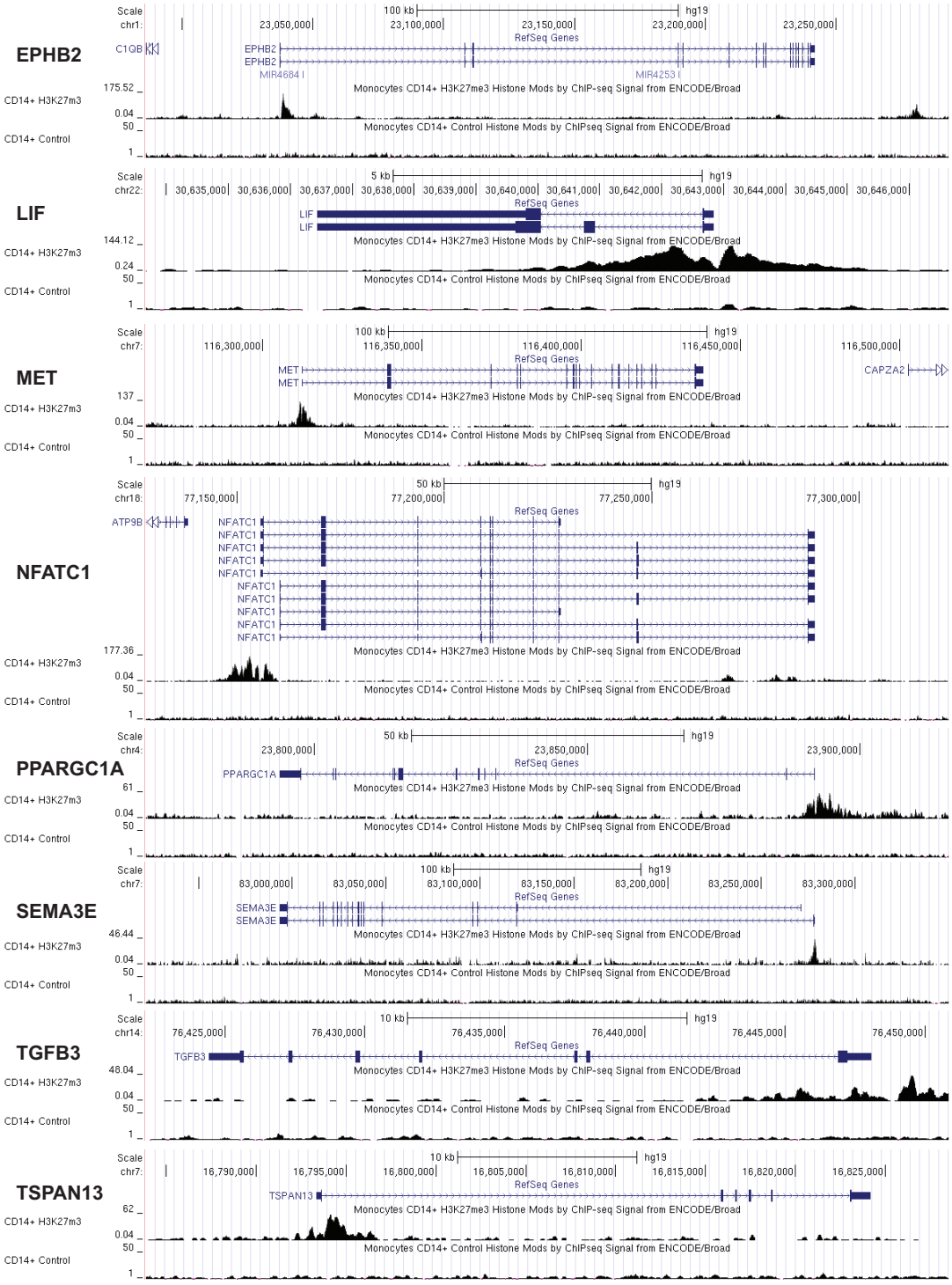


Figure 7.10: Selected genes from microarray analysis showing enriched H3K27me3 level at the 5' end of the gene in human monocytes. Arrow showing transcription direction. Data is produced by ENCODE and obtained from Gene Expression Omnibus Database. (Bernstein et al., 2010).

7.9 Conclusion

Human osteoclast differentiation and functions were abrogated by the H3K27 demethylase specific inhibitor GSK-J4. GSK-J4 reduced osteoclast numbers and bone resorption in vitro. Microarray analysis indicated that there is a large effect on gene expression under GSK-J4 treatment during the early RANKL induction (Day 8) and the rapid cell fusion (Day 14) period. Significantly less transcriptional changes were observed in mature osteoclasts treated with GSK-J4. ChIP experiments showed that there is a change of H3K27 methylation at the NFATc1 promoter region, suggesting a possible molecular mechanism of differentiation inhibition. ChIP-seq experiments are to be carried out to reveal other changes in histone methylation during osteoclast differentiation. Whether epigenetic alteration can be a therapeutic approach to inhibit osteoclast differentiation merits further experiments both in vitro and animal studies. In order for GSK-J4 to be used in animal models, chemical modification of the compound is required to increase its half life in the body as GSK-J4 is likely to be rapidly hydrolysed by serum esterases in animal experiments. A possible modification for bone targeting could be the conjugation of GSK-J4 to bisphosphonates. The drug will reside in bone tissue and only be absorbed by bone cells, thus reducing any potential side effects to other tissues.

Chapter 8

Discussion and future perspectives

As evidenced from many studies, H3K27 demethylases JmjD3 and UTX are important histone demethylases implicated in diverse aspects of biology including development, cancer biology and immunology (Chapter 1). In this thesis, a number of biochemical assays and tools were developed for the characterisation of JmjD3, including 1) the expression and purification of pure and active recombinant human JmjD3 Jumoni domain; 2) structure determination of JmjD3 to reveal its architecture and binding to small molecule ligands such as 8HQ; 3) two in vitro assays for the identification of compounds that can stabilise or inhibit JmjD3; 4) a cell-based immunofluorescence assay to test the activity of JmjD3 inhibitors in cells; 5) identification of a potent, selective and cell active inhibitor (GSK-J1 and its prodrug GSK-J4); and 6) application of the JmjD3 inhibitor on cellular systems of macrophages and osteoclasts. These achieved objectives have been instrumental to facilitate other studies, e.g. development of in vitro and cell-based screening assays have guided development of small molecule inhibitors for other demethylases (outlined briefly below). In the following sections, I will describe how the major milestones advance our knowledge on the biology of histone H3K27 demethylases:

Structure determination of JmjD3 demonstrates novel, potentially druggable features: The first crystal structure of JmjD3 Jumonji domain was determined in complex with 8HQ (Chapter 4). It revealed a double stranded β-sheet (DSBH) that is common with other 2OG oxygenases. Since then, a number of other structures have become available, e.g. in complex with GSK-J1

and histone H3K27me3 peptide. The crystal structure in complex with H3K27me3 peptide, revealed that interactions with the substrate histone H3 peptide requires not only the catalytic domain but also the ZBD, and the ZBD-histone interaction is crucial for substrate specificity of H3K27me3 histone. Similar zinc binding domains may exist in other histone demethylase e.g. JmjD2, and may be important for substrate specificity. For inhibition studies, the binding of 8HQ or GSK-J1 to JmjD3 establishes an ionic interaction with the catalytic metal ion, causing a shift of the metal position, as demonstrated by structural alignment with the apo-enzyme. The compounds also block the binding of 2-oxoglutarate, thus inhibit JmjD3 competitively. It has emerged that the specificity of GSK-J1 towards H3K27 demethylases is attributed to the tetrahydrobenzazepine group of the molecule. The chemical group occupies an additional space in the catalytic pocket, and such space is not occupied by 8HQ. This pocket does not exist in other member of the histone demethylases family as shown by computational models that fit GSK-J1 in Jumonji domains of other members of the KDM family, highlighting a novel mechanism to improve compound selectivity.

A H3K27 demethylase inhibitor can be used to distinguish between distinct demethylase protein functions: The central question in the biology of histone demethylases is whether the observed phenotype is caused by its histone demethylase activity or due to other non-enzymatic factors such as protein - protein interactions. As mentioned in chapter 1, most, if not all, Jmj-demethylases are part of transcriptional complexes. The answer in the case of KDM6 enzymes is provided where the use of a specific JmjD3 inhibitor that blocks only the demethylase activity, but retains any protein - protein interaction, allows the investigator to conclude the causality of the observed phenotype. It was reported that KDM6 enzymes exert scaffolding functions (Miller et al., 2010). The recent demonstration that chromatin protein-protein interactions can be targeted, e.g. by inhibitors of bromodomains (Filippakopoulos et al., 2010; Dawson et al., 2011), suggest that it might be also possible to develop specific chemical tools to dissect non-enzymatic (ie scaffold or protein binding) functions of histone demethylases.

GSK-J4 is the first selective and cell active histone demethylase inhibitor described so far. Since the discovery of the first histone lysine demethylase LSD1 and subsequently, JmjC- type

histone demethylases, efforts have been put into developing specific KDM inhibitors. Most reported inhibitors against Jmj-type demethylases are metal chelators that bind the active site metal, and inhibit a broad spectrum of histone demethylases and 2-oxoglutarate dependent oxygenases (Chapter 1). It was reported that bipyridyl- and daminozide-type compounds have some in vitro selectivity against histone demethylases such as KDM4 and KDM2 subfamilies, respectively, but so far no data has been demonstrated in any cell-based system. (Chang et al., 2011; Rose et al., 2012). Other types of compounds such as cyclic peptides, which are histone tail mimetics, have been developed and tested, but show a high degree of cytotoxicity (unpublished data). As discussed above and chapter 4, the tetrahydrobenzazepine group is crucial for its selectivity towards JmjD3. It may be possible to produce selective probes for other KDM by using a different chemical group attached to the pyridyl-pyrimidine scaffold instead of the tetrahydrobenzazepine group. For example, Lys2262 in JmjD1C could potentially clash with GSK-J1 in the computational model. If the tetrahydrobenzazepine group is replaced with a smaller, e.g. a carboxyl group, it could prevent the steric clash and potentially form an ionic interaction with the Lys2262, creating a JmjD1C specific probe. Nevertheless, the discovery of KDM6-specific GSK-J4 here is a proof of concept that a selective and cell active histone demethylase inhibitor can be developed, and that KDM6 enzymes and other demethylases constitute a druggable target class.

The availability of a KDM6 chemical probe enables understanding of biology and identifies possible therapeutic applications: The biological effects of KDM6 inhibition by GSK-J4 have been demonstrated in Chapters 6 and 7 of this thesis. This work defines possibly novel therapeutic options in inflammation, specifically osteoimmunology and possibly bone cancer. First, the inhibitor treatment reduces TNF and inflammatory cytokine production in proinflammatory macrophages, and constitutes a novel mechanism to control cytokine production and hence the complex inflammatory milieu. The inhibitor studies conducted here and at collaborator sites also demonstrate the importance of chemical tools in understanding biology: early knockdown studies in mice suggested that H3K27 demethylation does not necessarily play an important role in cytokine control (De Santa et al., 2009), however an important function is demonstrated here in human cells. The feature of GSK-J4 to inhibit both UTX and JmjD3 has been of advantage to dissect the macrophage

cytokine biology, since knockdown studies in human macrophages demonstrated that inhibition of both enzymes is needed to achieve cytokine suppression. This shows how chemical and molecular genetic knockdown approaches complement each other to better understand biology. Furthermore, the interactions and inhibitor susceptibilities between different cell types involved in inflammation such as T-cells, monocytes, macrophages, B-cells, dendritic cells and others, have to be carefully evaluated. There might be differences in the response to inhibitor treatment between different tissue specific immune cells. In this work, I analysed primary macrophages, derived from peripheral blood monocytes of volunteers and RA patients; however, it will be of high interest to study macrophages that are directly derived from disease tissues such as the synovium in RA patients. Second, I also established another macrophage system, namely giant cells that correspond to M2-type macrophages, where GSK-J4 treatment abrogated cellular fusion. This might be of possible therapeutic interest in understanding better the pathobiology of these cells, and it appears feasible to inhibit formation of these cells that are implicated in adverse transplant reactions, e.g. rejection of surgical implants. Lastly, the work carried out provides the foundation to postulate a novel anti- resorptive mechanism in bone biology. The work builds upon the observation that JmjD3 knockdown inhibits murine osteoclast development (Yasui et al., 2011), and the use of KDM6 inhibitors in my work goes beyond this initial result by describing the associated mechanism and molecular events in human osteoclast biology.

Targeting KDM6 family as anti- cancer approach: As reviewed in Chapter 1, JmjD3 was overexpressed in many types of cancers, including lung cancer, B cell lymphoma, cervical cancer, myelodysplastic syndrome and breast cancer and in tumour metastasis. Preliminary data produced by myself and colleagues have shown that GSK-J4 inhibits proliferation of cancer cells such as Ewing Sarcoma and multiple myeloma (data not shown). Together with the described anti-resorptive properties of KDM6 inhibition, such findings pave the way for developing epigenetic inhibitors as novel anti- cancer agents in bone oncology, where a major problem is the proliferative and invasive property of the cancer, combined with the increased bone resorption through increased amounts of osteoclasts.

KDM6 assay development will enable next-generation Jmj inhibitor efforts: Although

the discovery of the selective, potent and cell-active GSK-J4 compound is a breakthrough in Jmj inhibitor development, the molecule certainly needs improvements to be suitable for further studies such as animal models. One prerequisite of presenting an active GSK-J4 in cells is the necessity to mask the carboxylate (the free carboxylate though is necessary for on-target activity) by using ester modifications. It is expected that the ester will be rapidly cleaved by unspecific plasma esterases thus limiting its utility in in vivo models. Thus a replacement of the carboxylate function with a bioisostere is required and should be the aim of future medicinal chemistry efforts. A second, and more general issue is that epigenetic drug therapy would greatly benefit from a tissue-targeted effort - due to the central role of chromatin and epigenetic modifications in controlling transcription and development in most if not all cellular systems. It is to be expected that KDM6 inhibition would exert pleiotropic effects and eventually general toxic effects if given systemically. Methods to increase tissue specificity is possibly a conjugation of an epigenetic inhibitor to a peptide containing an endocytosis signal. The peptide will then be cleaved by proteases in the cells, rendering an active compound in target cells. Furthermore, conjugating the inhibitor to a bisphosphonate scaffold may increase bone-tissue specificity. The resulting bisphosphonate-containing epigenetic inhibitor will have high affinity to calcium and will be localized to bone tissue, where it can be actively taken up by bone cells such as osteoclasts, or released in a slow manner depending on the bisphosphonate linker chemistry. This bone targeting principle could be of great therapeutic value where inhibitions of bone resorption and anti-cancer effects can be achieved simultaneously.

Open questions and outlook: Given the above results, some questions remain unanswered: *1) how does JmjD3 modulate activity of the transcription complex through removal of H3K27me3 marks?* It was reported that JmjD3 facilitates transcriptional elongation Chen:2012hr. How does JmjD3 promote RNA polymerase II to escape transcription initiation complex and start to elongate by removing H3K27me3 marks? If there is any protein that binds to H3K27me3 marks and block elongation, JmjD3 will have to displace such protein and demethylate the H3K27me3 marks. A clear picture of molecular mechanism is yet to be drawn. *2) Is there any other specific role of the N-terminal non-JmjC region of JmjD3?* There is a long N-terminal region (300 aa) of JmjD3 without predicted secondary structure. Perhaps the N-terminal region is involved in protein protein interaction in

transcriptional complexes. A JmjD3 pull down experiment followed by mass-spectrometric analyses could be performed to identify interacting partners. It may also have a self-regulatory role on the Jumonji domain, in this case a full length JmjD3 protein is required to characterise its function. *3) Which genes does JmjD3 regulate?* Since we have not yet identified a JmjD3 antibody with less non-specific background, it was not possible to perform JmjD3 ChIP-seq experiments in the current study. I hope in the near future a good JmjD3 antibody will be available that will help investigators to understand the role of JmjD3 in chromatin biology. *4) Would it be possible to create a probe that can inhibit JmjD3 but not UTX or vice versa?* JmjD3 and UTX have different functions in cells, e.g. UTX is in general expressed ubiquitously (Agger et al., 2009), while JmjD3 is expressed for example in immune cells and can be induced, e.g. through LPS or cytokine treatments. However, the sequence and structure of JmjD3 and UTX Jumonji domain are nearly identical, so it is expected that a small molecule inhibitor that inhibits specifically JmjD3 or UTX would be difficult to make. *5) Is GSK-J5 a useful negative control?* The GSK-J5 is a prodrug of GSK-J2, a structural isomer to GSK-J4 which is inactive towards JmjD3 in cells as shown in immunofluorescence assay in Chapter 5 (Fig. 5.9). It was used as a negative control in subsequent studies. However, results from gene expression array studies showed a substantial changes in gene expression after addition of GSK-J5 to the cells (Fig. 6.8 and Fig. 7.8). A possible explanation is that a relative high concentration of GSK-J5 was used (20 μM). Although JmjD3 was not inhibited by GSK-J5 at this level, high concentration of the compound may impose stress to the cells which resulted in the expression of a subset of genes unrelated to the inhibition of JmjD3. In addition, the prodrug requires intracellular esterase to become active in cells; therefore the action of prodrug is limited by the amount of esterase in that particular cell types. If the esterase is absence or low, the prodrug will accumulate and may have an undesirable effect to cells.

Future prospective: more detailed studies can be done on the following aspects: *1) kinetic studies of JmjD3 and inhibitors.* AlphaScreen assay is a robust assay used for screening of JmjD3 inhibitors. However, it uses a relatively low substrate to enzyme ratio (60 nM H3K27me3 peptide to 1 nM enzyme) in the assay configuration, which is not ideal for studying enzyme kinetics e.g. to obtain Km values of the substrates and Ki values of the inhibitors, as the steady state assumption of Michaelis-Menten kinetics require much higher substrate to enzyme ratio ($\geq$1000). One can use

formaldehyde dehydrogenase assay, which can monitor the reaction real time with a spectrophotometer. However, it is a coupled assay and may be complicated by the necessity to carefully optimise the coupled reaction to obtain accurate and reproducible data. The other method would be the use of a high throughput mass spectrometric method such as the Rapidfire system, which automate sample purification and data acquisition. A recent paper reported the use of a fluorescence probe conjugated inhibitor to evaluate the binding affinity of several known histone demethylases to their substrates (Xu et al., 2013), such system could be of a new assay platform for kinetics studies in histone demethylases. *2) pinpoint the mechanism that governs M2 macrophage fusion.* Despite the substantial change in the transcription profile upon inhibition of JmjD3 and UTX, we have not been able to identify any known fusion related gene that is involved in this event. A large scale RNAi knockdown study of these genes could be performed to discover molecules that are important for fusion. *3) replicates in gene expression arrays.* The gene expression data presented in this thesis was a single experiment due to the cost of the studies. Although a follow up qPCR experiment can be performed to validate gene expression in biological replicates, important genes which are regulated by RANKL and affected by KDM6 inhibitors may be missed in the initial microarray studies, or results in false positive hits. The array studies shall be repeated and statistical analysis should be done. *4) more detailed chromatin analysis in macrophages and osteoclasts by chromatin-immunoprecipitation (ChIP).* Initial ChIP experiment was not successful due to the low availability of chromatin samples sourced from primary human tissues. These problems could be potentially solved by amplifying low amount of DNA from low number of cells by DNA polymerase (Liu et al., 2003; Shankaranarayanan et al., 2011). The amplified DNA can be subjected to next generation sequencing to understand regions of genome that are affected by KDM6 inhibition.

Concluding Remark. The development of the biochemical tools in my thesis has advanced our understanding of the JmjD3 biology. Using the information of this thesis as a starting point, I hope more biochemical tools and specific inhibitors for other histone modifying enzymes can be developed. This will greatly enhance our knowledge in epigenetic and chromatin mechanisms, holding promises for the future of epigenetic drug discovery.

Chapter 9

Materials and Methods

9.1 Cloning

9.1.1 Ligation independent cloning (LIC) of JmjD3 into pNIC28 vector

The recombinant expression vectors used in LIC were developed by SGC. In brief, the insert DNA was PCR amplified with pLIC-for and pLIC-rev primers (below). pNIC28 vector was digested with *BsaI* (New England Biolabs, NEB). The vector and DNA were purified and treated with 3 units of T4 DNA polymerase (Fermentas). The 3' - 5' exonuclease activity of T4 DNA polymerase generates long complementary overhangs in the vector and insert DNA. The vector and insert DNA were ligated without the use of DNA ligase.

pLIC-for: TACTTCCAATCCATG - 21 bp insert sequence

pLIC-rev: TATCCACCTTTACTG - 21 bp insert sequence

9.1.2 Cloning of Flag-JmjD3 into pcDNA5/FRT/TO vector

The construct was designed according to the manual of In-Fusion Cloning Kits (Clontech). In brief, the insert was PCR amplified using primers including 5' and 3' sequences that are homologous to the vector sequence. The pcDNA5/FRT/TO vector was digested with *EcoRV* (NEB), and the insert and digested vector were mixed and treated with In-Fusion Enzyme. The insert was then integrated into the vector.

9.1.3 Transformation of plasmid into competent cell XL-1 (Blue) or BL21(DE3)

10 ng DNA was added to 100 μL XL-1 (Blue) or BL21(DE3) competent cells and incubated in ice for 20 minutes. The mixture was "heat shocked" at 42°C for 45 seconds and immediately placed on ice for 2 minutes. 1 mL of Luria-Bertani (LB) medium was added to the cells and incubated at 37°C for 1 hour. The cells were plated on LB agar plate containing 50 ng/mL kanamycin and incubated at 37°C overnight.

9.1.4 Screening of colonies by restriction digestion analysis

Colonies was picked from agar plate and inoculated in 5 mL LB containing 100 μg/mL ampicillin overnight.

For the construct in pNIC28 vector, 1 μg plasmid was incubated with 20 units of *NdeI* (NEB) and *EcoRI* (NEB) in NEBbuffer 2 at 37°C for 1 hour. The resulting DNA was analyszed by agarose gel electrophoresis.

For the construct in pcDNA5/FRT/TO vector, 1 μg plasmid was incubated with 20 units of *HindIII* (NEB) in NEBbuffer 2 at 37°C for 1 hour,. The resultant DNA fragments were analyzed by agarose gel electrophoresis.

9.2 Expression of JmjD3 in *E.coli*

Colonies were picked from the agar plate and inoculated into a baffled flask containing 320 mL Terrific Broth (TB) with 50 ng/mL kanamycin. The starter culture was incubated at 37°C with 250 rpm rotation. The next day, 320 mL of the starter culture was inoculated into 32 L of Terrific Broth (TB) (16 flasks of 2 L each) supplemented with 50 ng/mL kanamycin.

The flasks were placed in an orbital shaker and rotated at 300 rpm and 37°C. Optical density (OD) at 600 nm was measured at hourly intervals it reached OD 1.5 at which point the incubator temperature was lowered to 18°C and Isopropyl β-D-1-thiogalactopyranoside (IPTG) was added to the medium at a concentration of 0.2 mM. The resulting cultures were harvested after 24 hours.

9.3 Purification of JmjD3 expressed in *E.coli*

9.3.1 Cell lysis

Cell paste containing recombinant protein was was resuspended in Lysis Buffer (50 mM HEPES pH 7.5, 500 mM NaCl, 20 mM imidazole, 1 mM PMSF, 1000 unit / mL Benzonase) and passed through high pressure homogeniser (EmulsiFle -C5) 2-3 times until the solution was not viscous. The homogenised lysate was centrifuged at 30,000 x g, 4°C for 1 hour.

9.3.2 Immoblized metal affinity chromatography (IMAC)

The clarified supernatant was loaded onto a 5 mL HisTrap crude column (GE Healthcare). The column was washed with 10 column volumes (CV) of wash buffer (50 mM HEPES pH 7.5, 500 mM NaCl, 40 mM imidazole). Elution was carried out by 5 CV of elution buffer (50 mM HEPES pH 7.5, 500 mM NaCl, 250 mM imidazole). Eluted fractions were analyzed by SDS-PAGE. Protein concentration was measured by absorbance at 280 nm using a Nanodrop spectrophotometer device. Fractions containing affinity-purified protein were combined, and 1 mg of tobacco etch virus (TEV) protease was added to every 30 mg of His-tagged protein for His-tag removal.

9.3.3 JmjD3-c023 ion-exchange chromatography

30mL of TEV-treated protein was diluted 10 times in IEXQ binding buffer (20 mM Tris-Cl pH 7.5, 1 mM Dithiothreitol (DTT)) to reach a salt concentration of 50 mM NaCl. The protein was loaded onto a 5 mL Hitrap Q HP column connected to an Akta purifier (GE Healthcare). The column was pre-equilibrated with 10CV of IEXQ Binding Buffer, and elution of proteins was achieved by a linear salt gradient from 50 mM to 1 M NaCl in 10 CV. JmjD3-c023 with a pI value of 5.2 was eluted at 300 mM NaCl.

9.3.4 JmjD3-c031 ion exchange chromatography

30mL of TEV-treated protein was diluted 10 times in IEXSP binding buffer (20 mM HEPES pH 7.5, 1 mM DTT) to reach a salt concentration of 50 mM NaCl. The protein was loaded onto a 5mL Hitrap SP column connected to an Akta purifier. The column was pre-equilibrated with 10CV of

IEXSP binding buffer, and elution of proteins was achieved by concentration linear salt gradient from 50 mM to 1M NaCl in 20 CV. JmjD3-c031 with a pI value of 6.4 was eluted at 120 mM NaCl.

9.3.5 Size exclusion Chromatography

A Hiload superdex 200 16/60 column (GE Healthcare) was equilibrated with 10 mM HEPES pH 7.5, 500 mM NaCl, 0.5 mM TCEP. JmjD3-c023 or JmjD3-c031 containing fractions from ion exchange chromatography were concentrated to a volume of 5 mL and loaded on to the size exclusion column. The column was run at 2 mL/min and 1 mL fractions were collected using a 2 mL 96 well block. JmjD3-c023 or JmjD3-c031 were eluted at a volume of 20 mL (over a 120 mL volume).

Purified protein was concentrated using a centrifugal device (4000rpm, 4°C) with a molecular weight cut-off at 30 kDa, to 10 mg/mL, and stored at -80°C in the size exclusion chromatography buffer.

9.4 Crystallization and structure determination of JmjD3

Crystals of JmjD-c023 were grown by the sitting drop vapour diffusion method. A typical crystallization experiment uses a 96-well 3-drop microplate (SwissCi), where protein (15 mg/ml) and crystallization solutions were dispensed using a Mosquito liquid handling robot (TTP labtech), to form 150 nL sitting drops in three different ratios of protein to crystallization solution (2:1, 1:1, 1:2). The sitting drops were incubated against a 20 μL reservoir containing the crystallization solutions. These solutions were obtained from commercially available 'random-matrix' screens, such as the Hampton Crystal, Hampton Index and Joint Center for Structural Genomics screens. The crystallization microplates were incubated in 20°C or 4°C within the Minstrel HT system (Rigaku) which consists of an automatic imaging station and temperature-controlled storage incubators.

The optimized condition to grow JmjD3 crystals involves a sitting drop mixing 100 nL protein (11 mg/mL) + 1 mM 8-hydroxyquinoline-5-carboxylic acid and 50 nL well solution was equilibrated against reservoir solution containing 0.2 M MgCl2, 0.1 M HEPES pH 7.5, 25% (w/v) polyethylene glycol 3350, 2 mM $NiCl_2$. Crystals were cryo-protected in reservoir solution supplemented with 25% (v/v) ethylene glycol and solution was equilibrated against reservoir solution containing 0.2 M MgCl2, 0.1 M HEPES pH 7.5, 25% (w/v) polyethylene glycol 3350, 2 mM $NiCl_2$. Crystals were cryo-protected

in reservoir solution supplemented with 25% (v/v) ethylene glycol and 5 mM 8-hydroxyquinoline-5-carboxylic acid and flash-frozen in liquid nitrogen. Preliminary X-ray characterization of mounted crystals were carried out in-house using a FRE x-ray generator coupled to a HTC detector (Rigaku). Diffraction data were then collected in oscillation mode at the Diamond Light Source beamline IO2.

Diffraction data were integrated and scaled using MOSFLM and SCALA from the CCP4 (Collaborative Computational Project No.4) Program Suite (Winn et al., 2011). To solve the phase problem, native crystals were soaked in 1 mM thiomersal for 20 minutes, allowing the detection of anomalous signals from mercury and subsequent phase determination by SAD. Four mercury sites were identified with the program SHELXD followed by phase refinement with SHARP and solvent flattening with SOLOMON. This generated an interpretable electron density map for manual model building using COOT (Emsley and Cowtan, 2004). The derivatized crystals were non-isomorphous to the native crystals, which diffracted to a significantly higher resolution. Thus, the resulting model from SAD was used as a search model to locate the molecule in the native structure (at higher resolution) by molecular replacement using PHASER. After further cycles of manual model building and refinement, the final model converged to Rfree and Rfactors of 0.216 and 0.185 respectively.

9.5 Differential scanning fluorimetry

1 μM of JmjD3-c023 in buffer (10 mM HEPES pH 7.4, 150 mM NaCl, 1:1000 SYBRO ORANGE (Invitrogen) as supplied, 15 μM $NiCl_2$) with 20 μM compounds from a focused KDM inhibitors in a reaction volume of 20 μL. The fluorescence change was monitored on a real time PCR machine (Agilent Mx3005p) at 610 nm by increasing temperature from 25° to 70° in 25 minutes.

9.6 MALDI-TOF mass spectrometry

1 μM of JmjD3 was incubated with JmjD3 inhibitor for 10 minutes in enzyme buffer(50 mM HEPES pH 7.5, 100 μM ascorbic acid, 10 μM ammonium ferric sulphate) in a reaction volume of 10 μL at room temperature. The reaction was started by adding substrate peptide (KAPRKQLATKAARK(me3)SAPATGG) and 2-oxoglutarate to a final concentration of 10 μM and 100 μM respectively. The reaction was stopped by adding formic acid to 1% (v/v) concentration after 3 minutes. The reaction sample was

desalted using Zip tip (Millipore) and spotted on a MALDI sample plate by mixing with α-Cyano-4-hydroxycinnamic acid (CHCA) as matrix. Samples were analysed on a MALDI-TOF system (Water Corporation).

9.7 AlphaScreen

5 μL of JmjD3-c031 (1 μM) was incubated with 100 nL various concentrations of JmjD3 inhibitors for 30 minutes in AlphaScreen buffer (50 mM HEPES pH 7.5, 0.1% bovine serum albumin, 0.001% (v/v) Tween-20) in room temperature. The reaction was started by adding 5 μL of substrate mixture (60 nM H3K27me3 peptide KAPRKQLATKAARK(me3)SAPATGG, 100 μM 2-oxoglutarate, 10 μM ammonium ferric sulphate, 100 μM ascorbic acid) in AlphaScreen buffer. The reaction was stopped by adding 5 μL of 30 mM EDTA after 3 minutes. 5 μL of antibody-alpha beads mixture was added to the reaction and incubated for an hour. The plate was analysed with a microplate reader (BMG PHERAstar FS). The sample was excited with 600 nm light and emission light was measured at 520-620 nm.

9.8 Immunofluorescence (IF) assay

2 μg of plasmid containing Flag-JmjD3 in pcDNA5/FRT/TO vector was diluted in 100 μL pure water and mixed with 5 μL of FuGENE HD Transfection Reagent. The mixture was incubated for 15 min in room temperature to form the transfection complex. 5 μL of transfection complex solution was added to 96 well plates with 8000 HeLa cells per well in 90 μL medium (Dulbecco's Modified Eagle Medium, 10% fetal calf serum (FCS) without antibiotics).

After 4 hours of incubation (37°C, 5 % CO_2), 5 μL of JmjD3 inhibitors were added to the medium at these concentrations of 100 μM, 50 μM, 25 μM, 12.5 μM, 6.3 μM and 3.2 μM. Medium was removed 24 hours after transfection. Cells were fixed with 4% paraformaldehyde for 20 min at room temperature followed by theree phosphate buffered saline (PBS) washes. Cells were then permeabilized with 0.5% Triton X-100 and the wash steps were repeated. Cells were blocked with 3% fetal calf serum in PBS for 1 hour. Blocking solution was removed and cells were stained with anti-Flag antibody (Sigma 1:500) and anti-H3K27me3 antibody (Millipore 1:500) for at least 16 hours

overnight. After removal of primary antibodies, cells were washed and secondary antibodies (Anti-mouse IgG alexa 594, Invitrogen, 1:500 Anti-rabbit-IgG alexa 488 Invitrogen 1:500) in PBS were added and incubated for 1 hour. The antibody solution also contained 100 ng/mL DAPI to stain the nuclei. After PBS washes, cells were examined in a fluorescence microscope (BD Pathway 855). All the above steps were performed at room temperature unless specified. Medium contains not more than 0.1% DMSO.

9.9 Macrophage experiments

9.9.1 M1 macrophage cell culture

Peripheral blood mononuclear cells (PBMCs) were extracted from human whole blood using Ficoll-paque (GE healthcare) centrifugation. CD14+ cells were selected using magnetic CD14 microbeads (Miltenyibiotec) according to the manufacturer's instructions. CD14+ cells were cultured in RPMI 1640 medium supplemented with 5% fetal calf serum (Invitrogen), 100 μg/mL penicillin-streptomycin, 1% glutamine and 5 ng/mL human GM-CSF (R&D systems) for 5 days to allow differentiation of CD14+ cells into M1 macrophage.

On day 5, cells were replaced with fresh medium. JmjD3 inhibitors were added to the medium (DMSO not exceeding more than 0.5% (v/v)) and incubated in 37°C in a CO_2 regulated incubator at 5% CO_2 level. 1 μL of lipopolysaccharide was added to a final concentration of 100 ng/mL.

9.9.2 M2 macrophage cell culture

PBMCs were extracted from human whole blood as described above. Selected CD14+ cells were cultured in medium (X-vivo, Lonza) supplemented with 10% (v/v) human serum for 3 days. IL-4 (R&D systems) was added to a final concentration of 20 ng/mL and compounds (DMSO, 20 μM GSK-J4 or 20 μM GSK-J5) were added.

9.10 Osteoclast methods

9.10.1 Osteoclast cell culture

CD14+ cells were selected as described above. Two million CD14+ cells were plated on 6 cm culture dishes in 3 mL of medium (α-MEM supplemented with 10% fetal calf serum (Invitrogen), 100 μg/mL penicillin-streptomycin, 1% GlutaMAX (Invitrogen) and 25 ng/mL human M-CSF (R&D systems)) for 6 days. 50 ng/mL human RANKL and compounds (DMSO, 20 μM GSK-J4 or 20 μM GSK-J5 were added on day 7. The medium was replaced every 3 days for up to 3 weeks.

9.10.2 Immunofluorescence microscopy

Osteoclasts grown on 6 mm glass cover slides in 6 cm culture dishes were transferred to 24 well plates and fixed in 1 mL 4% paraformaldehydes for 20 minutes. The cells were washed 3 times with 2 mL PBS, and then permeabilized in 1mL 1% Triton X-100 for 10 minutes. After washing the cells with 2 mL PBS for 3 times, the cells were incubated with PBS supplemented with 3% FCS to block non-specific antigens. Subsequently, the cells were then incubated overnight with Anti-beta actin antibody (Abcam, ab8227) and Anti-VNR antibody (Abcam, ab78289) for at least 16 hours. Both antibodies were diluted 1:500 in PBS supplemented with 3% FCS. The anti-body solutions were then removed and cells were washed 3 times with PBS. The cells were incubated with Anti-rat IgG antibody conjugated with Alexa 488 and Anti-mouse IgG conjugated with Alexa 594 for 1 hour. DAPI (1:5000, Invitrogen) for 10 minutes, washed 3 times with 2 mL PBS, and examined in fluorescence microscope (Zeiss Z-1). All steps were performed at room temperature.

9.10.3 TRAP and Bone resorption assays

For the tartrate resistant acid phosphatase (TRAP) assay, osteoclasts grown on 6 mm glass cover slides were transferred to 24 well plates and fixed in 1 mL 4% paraformaldehyde solution for 20 minutes. The cells were washed 3 times with 2 mL PBS then permeablized in 1 mL 1% Triton X-100 for 10 minutes. Cells were stained with 0.3 g/L fast violent B (Sigma F1631) and 0.17 g/L Napthol AS-Bi phosphate (Sigma N2125) dissolved in sodium acetate buffer pH 5.0 containing 0.1 mM sodium tartrate. Cells were incubated at 37°C for 2 hours. The reaction was stopped by the addition of 0.5

mL of 4 g/L NaF for 30 minutes at room temperature. Cells were washed with PBS 3 times and examined using a light microscope (Zeiss).

For the bone resorption assay, CD14+ selected cells were allowed to grow on ivory tusk dentin discs (6 mM diameter, 0.5 mM thick) for 3 weeks. The dentin discs were removed and soaked in 1 M NH_4OH overnight, sonicated in a waterbath for 30 minutes and washed with distilled water. The dentin discs were stained with 1% Toluidine Blue solution for 5 minutes, washed 10 times with distilled water and examined under a light microscope (Nikon).

9.10.4 Quantification of collagen fragments

CD14+ cells were seeded on 24 well plates at 2 x 10^5 cell density with 3 dentin discs in 0.5 mL of medium. 200 μL of medium was removed and stored at -20°C in every medium change. The collagen fragments in the medium were quantified by CrossLaps Culture ELISA (ImmunoDiagnosticSystems) according to the manufacturers manual.

9.11 RNA isolation, Reverse Transcription and Real-Time Quantitative PCR (qPCR)

Cells were lysed in 500 μL Trizol (Life technologies) at 1-week, 2-week and 3-week time points after removal of medium. Trizol cell lysates were stored at -20°C for subsequent RNA extraction. For extraction, Trizol samples were thawed and mixed with 100 μL chloroform and incubated for 5 minutes on ice. The samples were centrifuged at 16000g, 4° for 5 minutes. The supernatant was transferred to a clean tube on ice. An equal volume of 70% ethanol was added and mixed. The samples were transferred to RNeasy mini-columns (Qiagen) and subsequent extraction procedures were performed according to the manufacturer' s instructions. Pure RNA was eluted from RNeasy columns and quantified using Nanodrop spectrophotometer (Thermofisher) by monitoring absorbance at 260 nm. RNA samples were stored at -80°C.

Reverse transcription was performed using the QuantiTect Reverse Transcript Kit (Qiagen). In brief, 1 μg of RNA was incubated with 2 μL gDNA Wipeout Buffer 7x in 14 μL volume for 2 min at 42°C. 4 μL Quantiscript RT Buffer 5x, 1 μL RT Primer Mix and 1 μL Quantiscript Reverse

Transcriptase were added to the samples and incubated for 30 min at 42°C. The cDNA was then diluted 1:10 with distilled water to 200 μL.

qPCR was performed using Sybrgreen based protocol using FastSybr Green regent (Life technologies). 2 μL of diluted cDNA were mixed with 2X FastSybr Green Master Mix and 0.3 μM of forward and reverse primers in a final reaction volume of 10 μL. 18S Ribosomal RNA was used as a housekeeping gene. The thermocycler reaction was performed in a ViiA 7 System (Life Technologies) using the following program: initial denaturation at 95°C for 20s, 40 cycles of denaturation at 95°C for 1s, annealing and extension at 60°C for 20s. The relative fold change compared with control was calculated using the equation: Fold = $2^{-\Delta\Delta Ct}$ where Ct is the cycle threshold.

9.12 Chromatin Immunoprecipitation (ChIP) Assay

Two million CD14+ derived osteoclast cells were fixed in 1% paraformaldehyde solution in PBS for 10 min at room temperature. The reaction was quenched with 125 mM glycine for 5 min. Cells were scraped, collected by centrifugation (1000g for 5 min at 4°C) and stored at -80°C. Cells were suspended in 0.5 mL SDS Lysis Buffer (1% SDS, 10 mM EDTA, 50 mM Tris-Cl pH 8.1) supplemented with protease inhibitor cocktails (Roche). The lysate was sonicated to shear DNA to fragment lengths between 200-1000 basepairs with a sonicator (Sonics VCX 750). Af- ter centrifugation (12,000 g, 10 min, 4°C) to remove insoluble debris, the supernatant was diluted 10 fold in ChIP dilution buffer (0.01% SDS, 1.1% Triton X-100, 1.2 mM EDTA, 16.7 Tris-Cl pH 8.1, 167 mM NaCl). 1 μg antibodies (Anti-H3K27me3 Mill- pore 07-449; Anti-H3K4me3 Abcam 8580;, Anti-H3K27ac Abcam ab4729) were added to 1 μg of chromatin and incubated for at least 16 hours at 4°C. 20 μL protein G magnetic beads (Invitrogen) were added to the solution and incubated at 4°C for 1 hour. After retrieval by magnetic separation, the chromatin was washed with 1 mL of the following buffers in succession: 1) low salt immune complex wash buffer (0.1% SDS, 1% Triton X-100, 2 mM EDTA, 20 mM Tris-HCl, pH 8.1, 150 mM NaCl), 2) high salt immune complex wash buffer (0.1% SDS, 1% Triton X-100, 2 mM EDTA, 20 mM Tris-HCl, pH 8.1, 500 mM NaCl), 3) LiCl immune complex wash buffer (0.25M LiCl, 1% IGEPAL CA630, 1% deoxycholic acid (sodium salt), 1 mM EDTA, 10 mM Tris, pH 8.1), 4) TE buffer (10 mM Tris-Cl pH 8.0, 1 mM EDTA). The chromatin was eluted with

100 μL of elution buffer (1%SDS, 0.1M NaHCO 3) in two steps. 5 M NaCl was added to the eluate to a final concentration of 0.2 M and heated to 65°C with 1U protease K for 16 hours. The DNA was purified by Qiagen MiniElute Reaction Cleanup Kit according to the manufacturers instructions.

References

Adamopoulos, I. E. I., Xia, Z. Z., Lau, Y. S. Y., and Athanasou, N. A. N. (2006). Hepatocyte growth factor can substitute for M-CSF to support osteoclastogenesis. *Biochemical and biophysical research communications*, 350(2):6–6.

Agger, K., Cloos, P. A. C., Christensen, J., Pasini, D., Rose, S., Rappsilber, J., Issaeva, I., Canaani, E., Salcini, A. E., and Helin, K. (2007). UTX and JMJD3 are histone H3K27 demethylases involved in HOX gene regulation and development. *Nature*, 449(7163):731–734.

Agger, K., Cloos, P. A. C., Rudkjaer, L., Williams, K., Andersen, G., Christensen, J., and Helin, K. (2009). The H3K27me3 demethylase JMJD3 contributes to the activation of the INK4A-ARF locus in response to oncogene- and stress-induced senescence. *Genes & development*, 23(10):1171–1176.

Agherbi, H., Gaussmann-Wenger, A., Verthuy, C., Chasson, L., Serrano, M., and Djabali, M. (2009). Polycomb Mediated Epigenetic Silencing and Replication Timing at the INK4a/ARF Locus during Senescence. *PloS one*, 4(5):e5622.

Akira, S. and Takeda, K. (2004). Toll-like receptor signalling. *Nature Reviews Immunology*, 4(7):499–511.

Allfrey, V. G., Faulkner, G., and Mirsky, A. E. (1964). Acetylation and Methylation of Histones and their possible role in the regulation of RNA Synthesis. . *PNAS*, 51:786–794.

Allis, C. D. (2007). *Epigenetics*. CSHL Press.

Anderton, J. A., Bose, S., Vockerodt, M., Vrzalikova, K., Wei, W., Kuo, M., Helin, K., Christensen, J., Rowe, M., Murray, P. G., and Woodman, C. B. (2011). The H3K27me3 demethylase,

KDM6B, is induced by Epstein-Barr virus and over-expressed in Hodgkin's Lymphoma. *Oncogene*, 30(17):2037–2043.

Awe, J. P. and Byrne, J. A. (2013). Identifying Candidate Oocyte Reprogramming Factors Using Cross-Species Global Transcriptional Analysis. *Cellular Reprogramming*, pages –.

Bannister, A. J. A. and Kouzarides, T. T. (2011). Regulation of chromatin by histone modifications. *Cell research*, 21(3):381–395.

Barradas, M., Anderton, E., Acosta, J. C., Li, S., Banito, A., Rodriguez-Niedenführ, M., Maertens, G., Banck, M., Zhou, M.-M., Walsh, M. J., Peters, G., and Gil, J. (2009). Histone demethylase JMJD3 contributes to epigenetic control of INK4a/ARF by oncogenic RAS. *Genes & development*, 23(10):1177–1182.

Berger, S. L., Kouzarides, T., Shiekhattar, R., and Shilatifard, A. (2009). An operational definition of epigenetics. *Genes & development*, 23(7):781–783.

Bernstein, B. E., Mikkelsen, T. S., Xie, X., Kamal, M., Huebert, D. J., Cuff, J., Fry, B., Meissner, A., Wernig, M., Plath, K., Jaenisch, R., Wagschal, A., Feil, R., Schreiber, S. L., and Lander, E. S. (2006). A bivalent chromatin structure marks key developmental genes in embryonic stem cells. *Cell*, 125(2):315–326.

Bernstein, B. E., Stamatoyannopoulos, J. A., Costello, J. F., Ren, B., Milosavljevic, A., Meissner, A., Kellis, M., Marra, M. A., Beaudet, A. L., Ecker, J. R., Farnham, P. J., Hirst, M., Lander, E. S., Mikkelsen, T. S., and Thomson, J. A. (2010). The NIH Roadmap Epigenomics Mapping Consortium. *Nature Biotechnology*, 28(10):1045–1048.

Bilezikian, J. P., Raisz, L. G., and Martin, T. J. (2008). *Principles of Bone Biology, Two-Volume Set*. Academic Press.

Binda, C. C., Valente, S. S., Romanenghi, M. M., Pilotto, S. S., Cirilli, R. R., Karytinos, A. A., Ciossani, G. G., Botrugno, O. A. O., Forneris, F. F., Tardugno, M. M., Edmondson, D. E. D., Minucci, S. S., Mattevi, A. A., and Mai, A. A. (2010). Biochemical, structural, and biological

evaluation of tranylcypromine derivatives as inhibitors of histone demethylases LSD1 and LSD2. *Audio, Transactions of the IRE Professional Group on*, 132(19):6827–6833.

Biswas, S. K. and Mantovani, A. (2010). Macrophage plasticity and interaction with lymphocyte subsets: cancer as a paradigm. *Nature immunology*, 11(10):889–896.

Blystone, S. D., Graham, I. L., Lindberg, F. P., and Brown, E. J. (1994). Integrin alpha v beta 3 differentially regulates adhesive and phagocytic functions of the fibronectin receptor alpha 5 beta 1. *The Journal of cell biology*, 127(4):1129–1137.

Bonewald, L. F. and Johnson, M. L. (2008). Osteocytes, mechanosensing and Wnt signaling. *Bone*, 42(4):606–615.

Bozec, A., Bakiri, L., Hoebertz, A., Eferl, R., Schilling, A. F., Komnenovic, V., Scheuch, H., Priemel, M., Stewart, C. L., Amling, M., and Wagner, E. F. (2008). Osteoclast size is controlled by Fra-2 through LIF/LIF-receptor signalling and hypoxia. *Nature*, 454(7201):221–225.

Bunt, J., Hasselt, N. A., Zwijnenburg, D. A., Koster, J., Versteeg, R., and Kool, M. (2012). OTX2 sustains a bivalent-like state of OTX2-bound promoters in medulloblastoma by maintaining their H3K27me3 levels. *Acta Neuropathologica*, 125:385–394.

Burgold, T., Spreafico, F., De Santa, F., Totaro, M. G., Prosperini, E., Natoli, G., and Testa, G. (2008). The Histone H3 Lysine 27-Specific Demethylase Jmjd3 Is Required for Neural Commitment. *PloS one*, 3(8):e3034.

Burgold, T., Voituron, N., Caganova, M., Tripathi, P. P., Menuet, C., Tusi, B. K., Spreafico, F., Bévengut, M., Gestreau, C., Buontempo, S., Simeone, A., Kruidenier, L., Natoli, G., Casola, S., Hilaire, G., and Testa, G. (2012). The H3K27 Demethylase JMJD3 Is Required for Maintenance of the Embryonic Respiratory Neuronal Network, Neonatal Breathing, and Survival. *Cell reports*.

Canovas, S., Cibelli, J. B., and Ross, P. J. (2012). Jumonji domain-containing protein 3 regulates histone 3 lysine 27 methylation during bovine preimplantation development. *Proceedings of the National Academy of Sciences of the United States of America*, 109(7):2400–2405.

Carpenter, A. E., Jones, T. R., Lamprecht, M. R., Clarke, C., Kang, I., Friman, O., Guertin, D. A., Chang, J., Lindquist, R. A., Moffat, J., Golland, P., and Sabatini, D. M. (2006). CellProfiler: image analysis software for identifying and quantifying cell phenotypes. *Genome Biology*, 7(10):R100.

Chang, K.-H., King, O. N. F., Tumber, A., Woon, E. C. Y., Heightman, T. D., Mcdonough, M. A., Schofield, C. J., and Rose, N. R. (2011). Inhibition of Histone Demethylases by 4-Carboxy-2,2-Bipyridyl Compounds. *ChemMedChem*, 6(5):759–764.

Chen, C., Bartenhagen, C., Gombert, M., Okpanyi, V., Binder, V., Röttgers, S., Bradtke, J., Teigler-Schlegel, A., Harbott, J., Ginzel, S., Thiele, R., Fischer, U., Dugas, M., Hu, J., and Borkhardt, A. (2013). Next-generation-sequencing-based risk stratification and identification of new genes involved in structural and sequence variations in near haploid lymphoblastic leukemia. *Genes, chromosomes & cancer*, pages –.

Chen, H., Giri, N. C., Zhang, R., Yamane, K., Zhang, Y., Maroney, M., and Costa, M. (2010). Nickel Ions Inhibit Histone Demethylase JMJD1A and DNA Repair Enzyme ABH2 by Replacing the Ferrous Iron in the Catalytic Centers. *The Journal of biological chemistry*, 285(10):7374–7383.

Chen, S., Ma, J., Wu, F., Xiong, L.-J., Ma, H., Xu, W., Lv, R., Li, X., Villen, J., Gygi, S. P., Liu, X. S., and Shi, Y. (2012). The histone H3 Lys 27 demethylase JMJD3 regulates gene expression by impacting transcriptional elongation. *Genes & development*, 26(12):1364–1375.

Cheng, S., Zhao, S. L., Nelson, B., Kesavan, C., Qin, X., Wergedal, J., Mohan, S., and Xing, W. (2012). Targeted Disruption of Ephrin B1 in Cells of Myeloid Lineage Increases Osteoclast Differentiation and Bone Resorption in Mice. *PloS one*, 7(3):e32887.

Clissold, P. M. and Ponting, C. P. (2001). JmjC: cupin metalloenzyme-like domains in jumonji, hairless and phospholipase A2beta. *Trends in biochemical sciences*, 26(1):7–9.

Core, L. J. and Lis, J. T. (2008). Transcription Regulation Through Promoter-Proximal Pausing of RNA Polymerase II. *Science*, 319(5871):1791–1792.

Cory, A. H. A., Owen, T. C. T., Barltrop, J. A. J., and Cory, J. G. J. (1991). Use of an aqueous soluble tetrazolium/formazan assay for cell growth assays in culture. *Cancer communications*, 3(7):207–212.

Crockett, J. C., Rogers, M. J., Coxon, F. P., Hocking, L. J., and Helfrich, M. H. (2011). Bone remodelling at a glance. *Journal of cell science*, 124(Pt 7):991–998.

Cuthbert, G. L., Daujat, S., Snowden, A. W., Erdjument-Bromage, H., Hagiwara, T., Yamada, M., Schneider, R., Gregory, P. D., Tempst, P., Bannister, A. J., and Kouzarides, T. (2004). Histone deimination antagonizes arginine methylation. *Cell*, 118(5):545–553.

Dai, J.-p., Lu, J.-y., Zhang, Y., and Shen, Y.-f. (2010). Jmjd3 activates Mash1 gene in RA-induced neuronal differentiation of P19 cells. *Journal of cellular biochemistry*, 110(6):1457–1463.

Das, N. D., Jung, K. H., and Chai, Y. G. (2010). The role of NF-kappaB and H3K27me3 demethylase, Jmjd3, on the anthrax lethal toxin tolerance of RAW 264.7 cells. *PloS one*, 5(3):e9913.

Das, N. D., Jung, K. H., Choi, M. R., Yoon, H. S., Kim, S. H., and Chai, Y. G. (2012). Gene networking and inflammatory pathway analysis in a JMJD3 knockdown human monocytic cell line. *Cell biochemistry and function*, 30(3):224–232.

David, J.-P., Sabapathy, K., Hoffmann, O., Idarraga, M. H., and Wagner, E. F. (2002). JNK1 modulates osteoclastogenesis through both c-Jun phosphorylation-dependent and -independent mechanisms. *Journal of cell science*, 115(Pt 22):4317–4325.

Dawson, M. A., Prinjha, R. K., Dittmann, A., Giotopoulos, G., Bantscheff, M., Chan, W.-I., Robson, S. C., Chung, C.-w., Hopf, C., Savitski, M. M., Huthmacher, C., Gudgin, E., Lugo, D., Beinke, S., Chapman, T. D., Roberts, E. J., Soden, P. E., Auger, K. R., Mirguet, O., Doehner, K., Delwel, R., Burnett, A. K., Jeffrey, P., Drewes, G., Lee, K., Huntly, B. J. P., and Kouzarides, T. (2011). Inhibition of BET recruitment to chromatin as an effective treatment for MLL-fusion leukaemia. *Nature*, 478(7370):529–533.

Day, C. J., Kim, M. S., Stephens, S. R. J., Simcock, W. E., Aitken, C. J., Nicholson, G. C., and Morrison, N. A. (2004). Gene array identification of osteoclast genes: differential inhibition of

osteoclastogenesis by cyclosporin A and granulocyte macrophage colony stimulating factor. *Journal of cellular biochemistry*, 91(2):303–315.

de Camargo Pereira, G., Guimarães, G. N., Planello, A. C., Santamaria, M. P., de Souza, A. P., Line, S. R., and Marques, M. R. (2012). Porphyromonas gingivalis LPS stimulation downregulates DNMT1, DNMT3a, and JMJD3 gene expression levels in human HaCaT keratinocytes. *Clinical oral investigations*.

De Santa, F., Narang, V., Yap, Z. H., Tusi, B. K., Burgold, T., Austenaa, L., Bucci, G., Caganova, M., Notarbartolo, S., Casola, S., Testa, G., Sung, W.-K., Wei, C.-L., and Natoli, G. (2009). Jmjd3 contributes to the control of gene expression in LPS-activated macrophages. *The EMBO journal*, 28(21):3341–3352.

De Santa, F., Totaro, M. G., Prosperini, E., Notarbartolo, S., Testa, G., and Natoli, G. (2007). The histone H3 lysine-27 demethylase Jmjd3 links inflammation to inhibition of polycomb-mediated gene silencing. *Cell*, 130(6):1083–1094.

de Vries, T. J., Schoenmaker, T., Beertsen, W., van der Neut, R., and Everts, V. (2005). Effect of CD44 deficiency on in vitro and in vivo osteoclast formation. *Journal of cellular biochemistry*, 94(5):954–966.

Del Rizzo, P. A., Krishnan, S., and Trievel, R. C. (2012). Crystal structure and functional analysis of JMJD5 indicate an alternate specificity and function. *Molecular and cellular biology*, 32(19):4044–4052.

Dubuc, A. M., Remke, M., Korshunov, A., Northcott, P. A., Zhan, S. H., Mendez-Lago, M., Kool, M., Jones, D. T. W., Unterberger, A., Morrissy, A. S., Shih, D., Peacock, J., Ramaswamy, V., Rolider, A., Wang, X., Witt, H., Hielscher, T., Hawkins, C., Vibhakar, R., Croul, S., Rutka, J. T., Weiss, W. A., Jones, S. J. M., Eberhart, C. G., Marra, M. A., Pfister, S. M., and Taylor, M. D. (2012). Aberrant patterns of H3K4 and H3K27 histone lysine methylation occur across subgroups in medulloblastoma. *Acta Neuropathologica*, 125:373–384.

Dumon, S., Walton, D. S., Volpe, G., Wilson, N., Dassé, E., Del Pozzo, W., Landry, J.-R., Turner, B., O'Neill, L. P., Göttgens, B., and Frampton, J. (2012). Itga2b regulation at the onset of definitive hematopoiesis and commitment to differentiation. *PloS one*, 7(8):e43300.

Emsley, P. and Cowtan, K. (2004). Coot: model-building tools for molecular graphics. *Acta Crystallographica Section D Biological Crystallography*, 60(12):2126–2132.

Estarás, C., Akizu, N., García, A., Beltrán, S., de la Cruz, X., and Martínez-Balbás, M. A. (2012). Genome-wide analysis reveals that Smad3 and JMJD3 HDM co-activate the neural developmental program. *Development (Cambridge, England)*, 139(15):2681–2691.

Estarás, C., Fueyo, R., Akizu, N., Beltrán, S., and Martínez-Balbás, M. A. (2013). RNA polymerase II progression through H3K27me3-enriched gene bodies requires JMJD3 histone demethylase. *Molecular biology of the cell*, 24(3):351–360.

Esteller, M. (2007). Cancer epigenomics: DNA methylomes and histone-modification maps. *Nature Reviews Genetics*, 8(4):286–298.

Fang, R. R., Barbera, A. J. A., Xu, Y. Y., Rutenberg, M. M., Leonor, T. T., Bi, Q. Q., Lan, F. F., Mei, P. P., Yuan, G.-C. G., Lian, C. C., Peng, J. J., Cheng, D. D., Sui, G. G., Kaiser, U. B. U., Shi, Y. Y., and Shi, Y. G. Y. (2010). Human LSD2/KDM1b/AOF1 regulates gene transcription by modulating intragenic H3K4me2 methylation. *Molecular Cell*, 39(2):222–233.

Faulkner, G. (2000). FATZ, a Filamin-, Actinin-, and Telethonin-binding Protein of the Z-disc of Skeletal Muscle. *Journal of Biological Chemistry*, 275(52):41234–41242.

Fei, T., Xia, K., Li, Z., Zhou, B., Zhu, S., Chen, H., Zhang, J., Chen, Z., Xiao, H., Han, J.-D. J., and Chen, Y.-G. (2010). Genome-wide mapping of SMAD target genes reveals the role of BMP signaling in embryonic stem cell fate determination. *Genome research*, 20(1):36–44.

Filippakopoulos, P., Qi, J., Picaud, S., Shen, Y., Smith, W. B., Fedorov, O., Morse, E. M., Keates, T., Hickman, T. T., Felletar, I., Philpott, M., Munro, S., McKeown, M. R., Wang, Y., Christie, A. L., West, N., Cameron, M. J., Schwartz, B., Heightman, T. D., La Thangue, N., French, C. A., Wiest,

O., Kung, A. L., Knapp, S., and Bradner, J. E. (2010). Selective inhibition of BET bromodomains. *Nature*, 468(7327):1067–1073.

Fleetwood, A. J., Dinh, H., Cook, A. D., Hertzog, P. J., and Hamilton, J. A. (2009). GM-CSF- and M-CSF-dependent macrophage phenotypes display differential dependence on type I interferon signaling. *Journal of leukocyte biology*, 86(2):411–421.

Francis, D. M. and Page, R. (2001). *Strategies to Optimize Protein Expression in E. coli*. Current Protocols in Protein Science. John Wiley & Sons, Inc., Hoboken, NJ, USA.

Franzoso, G., Carlson, L., Xing, L., Poljak, L., Shores, E. W., Brown, K. D., Leonardi, A., Tran, T., Boyce, B. F., and Siebenlist, U. (1997). Requirement for NF-kappa B in osteoclast and B-cell development. *Genes & development*, 11(24):3482–3496.

Fujikawa, Y., Quinn, J. M., Sabokbar, A., McGee, J. O., and Athanasou, N. A. (1996). The human osteoclast precursor circulates in the monocyte fraction. *Endocrinology*, 137(9):4058–4060.

Fuller, K., Ross, J. L., Szewczyk, K. A., Moss, R., and Chambers, T. J. (2010). Bone Is Not Essential for Osteoclast Activation. *PloS one*, 5(9):e12837.

Gaasch, J. A., Bolwahnn, A. B., and Suzanne Lindsey, J. (2006). Hepatocyte growth factor-regulated genes in differentiated RAW 264.7 osteoclast and undifferentiated cells. *Gene*, 369:142–152.

Gao, Y., Hyttel, P., and Hall, V. J. (2010). Regulation of H3K27me3 and H3K4me3 during early porcine embryonic development. *Molecular reproduction and development*, 77(6):540–549.

Garnero, P. (1998). The Collagenolytic Activity of Cathepsin K Is Unique among Mammalian Proteinases. *Journal of Biological Chemistry*, 273(48):32347–32352.

Gelb, B. D., Shi, G. P., Chapman, H. A., and Desnick, R. J. (1996). Pycnodysostosis, a Lysosomal Disease Caused by Cathepsin K Deficiency. *Science*, 273(5279):1236–1238.

Ghisletti, S., Barozzi, I., Mietton, F., Polletti, S., De Santa, F., Venturini, E., Gregory, L., Lonie, L., Chew, A., Wei, C.-L., Ragoussis, J., and Natoli, G. (2010). Identification and characterization of enhancers controlling the inflammatory gene expression program in macrophages. *Immunity*, 32(3):317–328.

Giovarelli, M., Bucci, G., Pasero, M., Gherzi, R., and Briata, P. (2013). KSRP silencing favors neural differentiation of P19 teratocarcinoma cells. *Biochimica et biophysica acta*, 1829(5):469–479.

Gohda, J., Akiyama, T., Koga, T., Takayanagi, H., Tanaka, S., and Inoue, J.-i. (2005). RANK-mediated amplification of TRAF6 signaling leads to NFATc1 induction during osteoclastogenesis. *The EMBO journal*, 24(4):790–799.

Gordon, S. and Martinez, F. O. (2010). Alternative activation of macrophages: mechanism and functions. *Immunity*, 32(5):593–604.

Ha, B. G., Hong, J. M., Park, J.-Y., Ha, M.-H., Kim, T.-H., Cho, J.-Y., Ryoo, H.-M., Choi, J.-Y., Shin, H.-I., Chun, S. Y., Kim, S.-Y., and Park, E. K. (2008a). Proteomic profile of osteoclast membrane proteins: Identification of Na +/H +exchanger domain containing 2 and its role in osteoclast fusion. *PROTEOMICS*, 8(13):2625–2639.

Ha, B. G., Hong, J. M., Park, J.-Y., Ha, M.-H., Kim, T.-H., Cho, J.-Y., Ryoo, H.-M., Choi, J.-Y., Shin, H.-I., Chun, S. Y., Kim, S.-Y., and Park, E. K. (2008b). Proteomic profile of osteoclast membrane proteins: Identification of Na +/H +exchanger domain containing 2 and its role in osteoclast fusion. *PROTEOMICS*, 8(13):2625–2639.

Hamada, S., Suzuki, T., Mino, K., Koseki, K., Oehme, F., Flamme, I., Ozasa, H., Itoh, Y., Ogasawara, D., Komaarashi, H., Kato, A., Tsumoto, H., Nakagawa, H., Hasegawa, M., Sasaki, R., Mizukami, T., and Miyata, N. (2010). Design, synthesis, enzyme-inhibitory activity, and effect on human cancer cells of a novel series of jumonji domain-containing protein 2 histone demethylase inhibitors. *Journal of Medicinal Chemistry*, 53(15):5629–5638.

Hargreaves, D. C., Horng, T., and Medzhitov, R. (2009). Control of inducible gene expression by signal-dependent transcriptional elongation. *Cell*, 138(1):129–145.

Harp, J. M., Hanson, B. L., Timm, D. E., and Bunick, G. J. (2000). Asymmetries in the nucleosome core particle at 2.5Å resolution. *Acta Crystallographica Section D Biological Crystallography*, 56(12):1513–1534.

Hayden, M. S. and Ghosh, S. (2004). Signaling to NF-kappaB. *Genes & development*, 18(18):2195–2224.

Heino, T. J., Hentunen, T. A., and V n nen, H. K. (2002). Osteocytes inhibit osteoclastic bone resorption through transforming growth factor: Enhancement by estrogen. *Journal of cellular biochemistry*, 85(1):185–197.

Heinz, S., Benner, C., Spann, N., Bertolino, E., Lin, Y. C., Laslo, P., Cheng, J. X., Murre, C., Singh, H., and Glass, C. K. (2010). Simple combinations of lineage-determining transcription factors prime cis-regulatory elements required for macrophage and B cell identities. *Molecular Cell*, 38(4):576–589.

Hong, X., Zang, J., White, J., Wang, C., Pan, C.-H., Zhao, R., Murphy, R. C., Dai, S., Henson, P., Kappler, J. W., Hagman, J., and Zhang, G. (2010). Interaction of JMJD6 with single-stranded RNA. *Proceedings of the National Academy of Sciences of the United States of America*, 107(33):14568–14572.

Huang, H. H., Chang, E.-J. E., Ryu, J. J., Lee, Z. H. Z., Lee, Y. Y., and Kim, H.-H. H. (2006). Induction of c-Fos and NFATc1 during RANKL-stimulated osteoclast differentiation is mediated by the p38 signaling pathway. *Biochemical and biophysical research communications*, 351(1):7–7.

Huang, J., Sengupta, R., Espejo, A. B., Lee, M. G., Dorsey, J. A., Richter, M., Opravil, S., Shiekhattar, R., Bedford, M. T., Jenuwein, T., and Berger, S. L. (2007). p53 is regulated by the lysine demethylase LSD1. *Nature*, 449(7158):105–108.

Hughes, A., Kleine-Albers, J., Helfrich, M. H., Ralston, S. H., and Rogers, M. J. (2012). A Class III Semaphorin (Sema3e) Inhibits Mouse Osteoblast Migration and Decreases Osteoclast Formation In Vitro. *Calcified Tissue International*, 90(2):151–162.

Ikeda, F., Nishimura, R., Matsubara, T., Tanaka, S., Inoue, J.-i., Reddy, S. V., Hata, K., Yamashita, K., Hiraga, T., Watanabe, T., Kukita, T., Yoshioka, K., Rao, A., and Yoneda, T. (2004a). Critical roles of c-Jun signaling in regulation of NFAT family and RANKL-regulated osteoclast differentiation. *The Journal of clinical investigation*, 114(4):475–484.

Ikeda, F., Nishimura, R., Matsubara, T., Tanaka, S., Inoue, J.-i., Reddy, S. V., Hata, K., Yamashita, K., Hiraga, T., Watanabe, T., Kukita, T., Yoshioka, K., Rao, A., and Yoneda, T. (2004b). Critical roles of c-Jun signaling in regulation of NFAT family and RANKL-regulated osteoclast differentiation. *Journal of Clinical Investigation*, 114(4):475–484.

Ishida, N. (2002). Large Scale Gene Expression Analysis of Osteoclastogenesis in Vitro and Elucidation of NFAT2 as a Key Regulator. *Journal of Biological Chemistry*, 277(43):41147–41156.

Ishii, K.-a., Fumoto, T., Iwai, K., Takeshita, S., Ito, M., Shimohata, N., Aburatani, H., Taketani, S., Lelliott, C. J., Vidal-Puig, A., and Ikeda, K. (2009a). Coordination of PGC-1 and iron uptake in mitochondrial biogenesis and osteoclast activation. *Nature Medicine*, 15(3):259–266.

Ishii, M., Wen, H., Corsa, C. A. S., Liu, T., Coelho, A. L., Allen, R. M., Carson, W. F., Cavassani, K. A., Li, X., Lukacs, N. W., Hogaboam, C. M., Dou, Y., and Kunkel, S. L. (2009b). Epigenetic regulation of the alternatively activated macrophage phenotype. *Blood*, 114(15):3244–3254.

Iwai, K., Ishii, M., Ohshima, S., Miyatake, K., and Saeki, Y. (2007). Expression and function of transmembrane-4 superfamily (tetraspanin) proteins in osteoclasts: reciprocal roles of Tspan-5 and NET-6 during osteoclastogenesis. *Allergology international : official journal of the Japanese Society of Allergology*, 56(4):457–463.

Jepsen, K., Solum, D., Zhou, T., McEvilly, R. J., Kim, H.-J., Glass, C. K., Hermanson, O., and Rosenfeld, M. G. (2007). SMRT-mediated repression of an H3K27 demethylase in progression from neural stem cell to neuron. *Nature*, 450(7168):415–419.

Jiang, W., Wang, J., and Zhang, Y. (2013). Histone H3K27me3 demethylases KDM6A and KDM6B modulate definitive endoderm differentiation from human ESCs by regulating WNT signaling pathway. *Cell research*, 23(1):122–130.

John W Edmunds, L. C. M. A. L. C. (2008). Dynamic histone H3 methylation during gene induction: HYPB/Setd2 mediates all H3K36 trimethylation. *The EMBO journal*, 27(2):406–420.

Kania, J. R., Kehat-Stadler, T., and Kupfer, S. R. (1997). CD44 Antibodies Inhibit Osteoclast Formation. *Journal of Bone and Mineral Research*, 12(8):1155–1164.

Kim, H., Kim, T., Jeong, B.-C., Cho, I.-T., Han, D., Takegahara, N., Negishi-Koga, T., Takayanagi, H., Lee, J. H., Sul, J.-Y., Prasad, V., Lee, S. H., and Choi, Y. (2013). Tmem64 Modulates Calcium Signaling during RANKL-Mediated Osteoclast Differentiation. *Cell metabolism*, 17(2):249–260.

Kim, H.-J., Zou, W., Ito, Y., Kim, S.-Y., Chappel, J., Ross, F. P., and Teitelbaum, S. L. (2010). Src-like adaptor protein regulates osteoclast generation and survival. *Journal of cellular biochemistry*, pages n/a–n/a.

Kim, K., Lee, S. H., Ha Kim, J., Choi, Y., and Kim, N. (2007). NFATc1 Induces Osteoclast Fusion Via Up-Regulation of Atp6v0d2 and the Dendritic Cell-Specific Transmembrane Protein (DC-STAMP). *Molecular Endocrinology*, 22(1):176–185.

Kim, S. W., Yoon, S.-J., Chuong, E., Oyolu, C., Wills, A. E., Gupta, R., and Baker, J. (2011). Chromatin and transcriptional signatures for Nodal signaling during endoderm formation in hESCs. *Developmental biology*, 357(2):492–504.

Kim, T. and Buratowski, S. (2009). Dimethylation of H3K4 by Set1 Recruits the Set3 Histone Deacetylase Complex to 5 Transcribed Regions. *Cell*, 137(2):259–272.

King, O. N. F., Li, X. S., Sakurai, M., Kawamura, A., Rose, N. R., Ng, S. S., Quinn, A. M., Rai, G., Mott, B. T., Beswick, P., Klose, R. J., Oppermann, U., Jadhav, A., Heightman, T. D., Maloney, D. J., Schofield, C. J., and Simeonov, A. (2010). Quantitative high-throughput screening identifies 8-hydroxyquinolines as cell-active histone demethylase inhibitors. *PloS one*, 5(11):e15535–e15535.

Klose, R. J., Kallin, E. M., and Zhang, Y. (2006a). JmjC-domain-containing proteins and histone demethylation. *Nature Reviews Genetics*, 7(9):715–727.

Klose, R. J., Yamane, K., Bae, Y., Zhang, D., Erdjument-Bromage, H., Tempst, P., Wong, J., and Zhang, Y. (2006b). The transcriptional repressor JHDM3A demethylates trimethyl histone H3 lysine 9 and lysine 36. *Nature*, 442(7100):312–316.

Koga, T., Matsui, Y., Asagiri, M., Kodama, T., de Crombrugghe, B., Nakashima, K., and Takayanagi, H. (2005). NFAT and Osterix cooperatively regulate bone formation. *Nature Medicine*, 11(8):880–885.

Kontaki, H. and Talianidis, I. (2010). Lysine methylation regulates E2F1-induced cell death. *Molecular Cell*, 39(1):152–160.

Kristensen, J., Nielsen, A. L., and Jørgensen, L. (2011a). Erratum to "Enzyme kinetic studies of histone demethylases KDM4C and KDM6A: Towards understanding selectivity of inhibitors targeting oncogenic .... *FEBS* ....

Kristensen, J. B. L., Nielsen, A. L., Jorgensen, L., Kristensen, L. H., Helgstrand, C., Juknaite, L., Kristensen, J. L., Kastrup, J. S., Clausen, R. P., Olsen, L., and Gajhede, M. (2011b). Enzyme kinetic studies of histone demethylases KDM4C and KDM6A: Towards understanding selectivity of inhibitors targeting oncogenic histone demethylases. *Febs Letters*, 585(12):1951–1956.

Kristensen, L. H. L., Nielsen, A. L. A., Helgstrand, C. C., Lees, M. M., Cloos, P. P., Kastrup, J. S. J., Helin, K. K., Olsen, L. L., and Gajhede, M. M. (2012). Studies of H3K4me3 demethylation by KDM5B/Jarid1B/PLU1 reveals strong substrate recognition invitro and identifies 2,4-pyridinedicarboxylic acid as an invitro and incell inhibitor. *FEBS Journal*, 279(11):1905–1914.

Kruidenier, L., Chung, C.-w., Cheng, Z., Liddle, J., Che, K., Joberty, G., Bantscheff, M., Bountra, C., Bridges, A., Diallo, H., Eberhard, D., Hutchinson, S., Jones, E., Katso, R., Leveridge, M., Mander, P. K., Mosley, J., Ramirez-Molina, C., Rowland, P., Schofield, C. J., Sheppard, R. J., Smith, J. E., Swales, C., Tanner, R., Thomas, P., Tumber, A., Drewes, G., Oppermann, U., Patel, D. J., Lee, K., and Wilson, D. M. (2012). A selective jumonji H3K27 demethylase inhibitor modulates the proinflammatory macrophage response. *Nature*, 488(7411):404–408.

Lacey, D. L., Timms, E., Tan, H. L., Kelley, M. J., Dunstan, C. R., Burgess, T., Elliott, R., Colombero, A., Elliott, G., Scully, S., Hsu, H., Sullivan, J., Hawkins, N., Davy, E., Capparelli, C., Eli, A., Qian, Y. X., Kaufman, S., Sarosi, I., Shalhoub, V., Senaldi, G., Guo, J., Delaney, J., and Boyle, W. J. (1998). Osteoprotegerin Ligand Is a Cytokine that Regulates Osteoclast Differentiation and Activation. *Cell*, 93(2):165–176.

Lan, F., Bayliss, P. E., Rinn, J. L., Whetstine, J. R., Wang, J. K., Chen, S., Iwase, S., Alpatov, R., Issaeva, I., Canaani, E., Roberts, T. M., Chang, H. Y., and Shi, Y. (2007). A histone H3 lysine 27 demethylase regulates animal posterior development. *Nature*, 449(7163):689–694.

Lawrence, T. and Natoli, G. (2011). Transcriptional regulation of macrophage polarization: enabling diversity with identity. *Nature Reviews Immunology*, 11(11):750–761.

Lee, K., Na, W., Lee, J. Y., Na, J., Cho, H., Wu, H., Yune, T. Y., Kim, W.-S., and Ju, B.-G. (2012). Molecular mechanism of Jmjd3-mediated interleukin-6 gene regulation in endothelial cells underlying spinal cord injury. *Journal of neurochemistry*, pages no–no.

Lee, M. G. M., Wynder, C. C., Schmidt, D. M. D., McCafferty, D. G. D., and Shiekhattar, R. R. (2006). Histone H3 lysine 4 demethylation is a target of nonselective antidepressive medications. *Chemistry & Biology*, 13(6):563–567.

Liu, C. L., Schreiber, S. L., and Bernstein, B. E. (2003). BMC Genomics — Full text — Development and validation of a T7 based linear amplification for genomic DNA. *BMC Genomics*, 4(1):19.

Lohse, B., Kristensen, J. L., Kristensen, L. H., Agger, K., Helin, K., Gajhede, M., and Clausen, R. P. (2011). Inhibitors of histone demethylases. *Bioorganic & medicinal chemistry*, 19(12):12–12.

Luikart, S., Wahl, D., Hinkel, T., Masri, M., and Oegema, T. (1999). A fragment of -actinin promotes monocyte/macrophage maturation in vitro. *Experimental Hematology*, 27(2):337–344.

Luo, X., Liu, Y., Kubicek, S., Myllyharju, J., Tumber, A., Ng, S., Che, K. H., Podoll, J., Heightman, T. D., Oppermann, U., Schreiber, S. L., and Wang, X. (2011). A selective inhibitor and probe of the cellular functions of Jumonji C domain-containing histone demethylases. *Journal of the American Chemical Society*, 133(24):9451–9456.

Margueron, R., Li, G., Sarma, K., Blais, A., Zavadil, J., Woodcock, C. L., Dynlacht, B. D., and Reinberg, D. (2008). Ezh1 and Ezh2 Maintain Repressive Chromatin through Different Mechanisms. *Molecular Cell*, 32(4):503–518.

Martinez, F. O., Gordon, S., Locati, M., and Mantovani, A. (2006). Transcriptional profiling of the human monocyte-to-macrophage differentiation and polarization: new molecules and patterns of gene expression. *Journal of immunology (Baltimore, Md. : 1950)*, 177(10):7303–7311.

Martinez, F. O., Helming, L., Milde, R., Varin, A., Melgert, B. N., Draijer, C., Thomas, B., Fabbri, M., Crawshaw, A., Ho, L. P., Ten Hacken, N. H., Cobos Jiménez, V., Kootstra, N. A., Hamann,

J., Greaves, D. R., Locati, M., Mantovani, A., and Gordon, S. (2013). Genetic programs expressed in resting and IL-4 alternatively activated mouse and human macrophages: similarities and differences. *Blood*, 121(9):e57–69.

Matsumoto, M., Kogawa, M., Wada, S., Takayanagi, H., Tsujimoto, M., Katayama, S., Hisatake, K., and Nogi, Y. (2004). Essential Role of p38 Mitogen-activated Protein Kinase in Cathepsin K Gene Expression during Osteoclastogenesis through Association of NFATc1 and PU.1. *Journal of Biological Chemistry*, 279(44):45969–45979.

Matsuo, K. (2004). Nuclear Factor of Activated T-cells (NFAT) Rescues Osteoclastogenesis in Precursors Lacking c-Fos. *Journal of Biological Chemistry*, 279(25):26475–26480.

McLaughlin-Drubin, M. E. M., Crum, C. P. C., and Münger, K. K. (2011). Human papillomavirus E7 oncoprotein induces KDM6A and KDM6B histone demethylase expression and causes epigenetic reprogramming. *PNAS*, 108(5):2130–2135.

Metzger, E., Wissmann, M., Yin, N., Müller, J. M., Schneider, R., Peters, A. H. F. M., Günther, T., Buettner, R., and Schüle, R. (2005). LSD1 demethylates repressive histone marks to promote androgen-receptor-dependent transcription. *Nature*.

Miller, S. A., Mohn, S. E., and Weinmann, A. S. (2010). Jmjd3 and UTX Play a Demethylase-Independent Role in Chromatin Remodeling to Regulate T-Box Family Member-Dependent Gene Expression. *Molecular Cell*, 40(4):594–605.

Miller, S. A. and Weinmann, A. S. (2009). An essential interaction between T-box proteins and histone-modifying enzymes. *Epigenetics : official journal of the DNA Methylation Society*, 4(2):85–88.

Miller, S. A. and Weinmann, A. S. (2010). Molecular mechanisms by which T-bet regulates T-helper cell commitment. *Immunological reviews*, 238(1):233–246.

Mimasu, S., Umezawa, N., Sato, S., Higuchi, T., Umehara, T., and Yokoyama, S. (2010). Structurally designed trans-2-phenylcyclopropylamine derivatives potently inhibit histone demethylase LSD1/KDM1 . *Biochemistry (Washington)*, 49(30):6494–6503.

Ng, S. S., Kavanagh, K. L., Mcdonough, M. A., Butler, D., Pilka, E. S., Lienard, B. M. R., Bray, J. E., Savitsky, P., Gileadi, O., Von Delft, F., Rose, N. R., Offer, J., Scheinost, J. C., Borowski, T., Sundstrom, M., Schofield, C. J., and Oppermann, U. (2007). Crystal structures of histone demethylase JMJD2A reveal basis for substrate specificity. *Nature*, 448(7149):87–91.

Niesen, F. H., Berglund, H., and Vedadi, M. (2007). The use of differential scanning fluorimetry to detect ligand interactions that promote protein stability. *Nature protocols*, 2(9):2212–2221.

Pavri, R., Zhu, B., Li, G., Trojer, P., Mandal, S., Shilatifard, A., and Reinberg, D. (2006). Histone H2B Monoubiquitination Functions Cooperatively with FACT to Regulate Elongation by RNA Polymerase II. *Cell*, 125(4):703–717.

Pereira, F., Barbáchano, A., Silva, J., Bonilla, F., Campbell, M. J., Muñoz, A., and Larriba, M. J. (2011). KDM6B/JMJD3 histone demethylase is induced by vitamin D and modulates its effects in colon cancer cells. *Human molecular genetics*, 20(23):4655–4665.

Pereira, F., Barbáchano, A., Singh, P. K., Campbell, M. J., Muñoz, A., and Larriba, M. J. (2012). Vitamin D has wide regulatory effects on histone demethylase genes. *Cell cycle (Georgetown, Tex)*, 11(6):1081–1089.

Purev, E., Neff, L., Horne, W. C., and Baron, R. (2009). c-Cbl and Cbl-b act redundantly to protect osteoclasts from apoptosis and to displace HDAC6 from beta-tubulin, stabilizing microtubules and podosomes. *Molecular biology of the cell*, 20(18):4021–4030.

Ramadoss, S., Chen, X., and Wang, C.-Y. (2012). Histone demethylase KDM6B promotes epithelial-mesenchymal transition. *Journal of Biological Chemistry*, 287(53):44508–44517.

Ramirez-Carrozzi, V. R., Braas, D., Bhatt, D. M., Cheng, C. S., Hong, C., Doty, K. R., Black, J. C., Hoffmann, A., Carey, M., and Smale, S. T. (2009). A unifying model for the selective regulation of inducible transcription by CpG islands and nucleosome remodeling. *Cell*, 138(1):114–128.

Reigh, G., McMahon, H., Ishizaki, M., Ohara, T., Shimane, K., Esumi, Y., Green, C., Tyson, C., and Ninomiya, S. (1996). Cytochrome P450 species involved in the metabolism of quinoline. *Carcinogenesis*, 17(9):1989–1996.

Richards, C. D., Langdon, C., Deschamps, P., Pennica, D., and Shaughnessy, S. G. (2000). Stimulation of osteoclast differentiation in vitro by mouse oncostatin M, leukaemia inhibitory factor, cardiotrophin-1 and interleukin 6: synergy with dexamethasone. *Cytokine*, 12(6):613–621.

Riihonen, R., Supuran, C. T., Parkkila, S., Pastorekova, S., Väänänen, H. K., and Laitala-Leinonen, T. (2007). Membrane-bound carbonic anhydrases in osteoclasts. *Bone*, 40(4):1021–1031.

Rose, N. R., Mcdonough, M. A., King, O. N. F., Kawamura, A., and Schofield, C. J. (2011). Inhibition of 2-oxoglutarate dependent oxygenases. *Chemical Society Reviews*, 40(8):4364–4397.

Rose, N. R., Ng, S. S., Mecinović, J., Lienard, B. M. R., Bello, S. H., Sun, Z., Mcdonough, M. A., Oppermann, U., and Schofield, C. J. (2008). Inhibitor scaffolds for 2-oxoglutarate-dependent histone lysine demethylases. *Journal of Medicinal Chemistry*, 51(22):7053–7056.

Rose, N. R., Woon, E. C. Y., Kingham, G. L., King, O. N. F., Mecinović, J., Clifton, I. J., Ng, S. S., Talib-Hardy, J., Oppermann, U., Mcdonough, M. A., and Schofield, C. J. (2010a). Selective Inhibitors of the JMJD2 Histone Demethylases: Combined Nondenaturing Mass Spectrometric Screening and Crystallographic Approaches. *Journal of Medicinal Chemistry*, 53(4):1810–1818.

Rose, N. R., Woon, E. C. Y., Kingham, G. L., King, O. N. F., Mecinović, J., Clifton, I. J., Ng, S. S., Talib-Hardy, J., Oppermann, U., Mcdonough, M. A., and Schofield, C. J. (2010b). Selective Inhibitors of the JMJD2 Histone Demethylases: Combined Nondenaturing Mass Spectrometric Screening and Crystallographic Approaches. *Journal of Medicinal Chemistry*, 53(4):1810–1818.

Rose, N. R., Woon, E. C. Y., Tumber, A., Walport, L. J., Chowdhury, R., Li, X. S., King, O. N. F., Lejeune, C., Ng, S. S., Krojer, T., Chan, M. C., Rydzik, A. M., Hopkinson, R. J., Che, K. H., Daniel, M., Strain-Damerell, C., Gileadi, C., Kochan, G., Leung, I. K. H., Dunford, J., Yeoh, K. K., Ratcliffe, P. J., Burgess-Brown, N., Von Delft, F., Müller, S., Marsden, B., Brennan, P. E., Mcdonough, M. A., Oppermann, U., Klose, R. J., Schofield, C. J., and Kawamura, A. (2012). Plant Growth Regulator Daminozide Is a Selective Inhibitor of Human KDM2/7 Histone Demethylases. *Journal of Medicinal Chemistry*, 55(14):6639–6643.

Russell, R. G. G., Watts, N. B., Ebetino, F. H., and Rogers, M. J. (2008). Mechanisms of action of bisphosphonates: similarities and differences and their potential influence on clinical efficacy.

Osteoporosis international : a journal established as result of cooperation between the European Foundation for Osteoporosis and the National Osteoporosis Foundation of the USA, 19(6):733–759.

Russo, V. E. A. (1996). *Epigenetic mechanisms of gene regulation*. Cold Spring Harbor Laboratory Pr.

Sabokbar, A. A. and Athanasou, N. S. N. (2003). Generating human osteoclasts from peripheral blood. *Methods in Molecular Medicine*, 80:101–111.

Satoh, T., Takeuchi, O., Vandenbon, A., Yasuda, K., Tanaka, Y., Kumagai, Y., Miyake, T., Matsushita, K., Okazaki, T., Saitoh, T., Honma, K., Matsuyama, T., Yui, K., Tsujimura, T., Standley, D. M., Nakanishi, K., Nakai, K., and Akira, S. (2010). The Jmjd3-Irf4 axis regulates M2 macrophage polarization and host responses against helminth infection. *Nature immunology*, 11(10):936–944.

Schuettengruber, B., Chourrout, D., Vervoort, M., Leblanc, B., and Cavalli, G. (2007). Genome regulation by polycomb and trithorax proteins. *Cell*, 128(4):735–745.

Seales, E. C., Micoli, K. J., and McDonald, J. M. (2005). Calmodulin is a critical regulator of osteoclastic differentiation, function, and survival. *Journal of cellular biochemistry*, 97(1):45–55.

Sen, G. L., Webster, D. E., Barragan, D. I., Chang, H. Y., and Khavari, P. A. (2008). Control of differentiation in a self-renewing mammalian tissue by the histone demethylase JMJD3. *Genes & development*, 22(14):1865–1870.

Sengoku, T. T. and Yokoyama, S. S. (2011). Structural basis for histone H3 Lys 27 demethylation by UTX/KDM6A. *Genes & development*, 25(21):2266–2277.

Shahhoseini, M., Taghizadeh, Z., Hatami, M., and Baharvand, H. (2013). Retinoic acid dependent histone 3 demethylation of the clustered HOX genes during neural differentiation of human embryonic stem cells. *Biochemistry and cell biology = Biochimie et biologie cellulaire*, 91(2):116–122.

Shankaranarayanan, P., Mendoza-Parra, M.-A., Walia, M., Wang, L., Li, N., Trindade, L. M., and Gronemeyer, H. (2011). Single-tube linear DNA amplification (LinDA) for robust ChIP-seq. *Nature Methods*, 8(7):565–567.

Shaw, T. and Martin, P. (2009). Epigenetic reprogramming during wound healing: loss of polycomb-mediated silencing may enable upregulation of repair genes. *EMBO reports*, 10(8):881–886.

Shen, Y., Guo, X., Wang, Y., Qiu, W., Chang, Y., Zhang, A., and Duan, X. (2012). Expression and significance of histone H3K27 demethylases in renal cell carcinoma. *BMC cancer*, 12(1):470.

Shi, Y., Lan, F., Matson, C., Mulligan, P., Whetstine, J. R., Cole, P. A., Casero, R. A., and Shi, Y. (2004). Histone demethylation mediated by the nuclear amine oxidase homolog LSD1. *Cell*, 119(7):941–953.

Sica, A. and Mantovani, A. (2012). Macrophage plasticity and polarization: in vivo veritas. *The Journal of clinical investigation*, 122(3):787–795.

Skelton, L., Cooper, M., Murphy, M., and Platt, A. (2003). Human immature monocyte-derived dendritic cells express the G protein-coupled receptor GPR105 (KIAA0001, P2Y14) and increase intracellular calcium in response to its agonist, uridine diphosphoglucose. *Journal of immunology (Baltimore, Md. : 1950)*, 171(4):1941–1949.

Solá, S., Xavier, J. M., Santos, D. M., Aranha, M. M., Morgado, A. L., Jepsen, K., and Rodrigues, C. M. P. (2011). p53 Interaction with JMJD3 Results in Its Nuclear Distribution during Mouse Neural Stem Cell Differentiation. *PloS one*, 6(3):e18421.

Sun, D., Layer, R., Mueller, A. C., Cichewicz, M. A., Negishi, M., Paschal, B. M., and Dutta, A. (2013). Regulation of several androgen-induced genes through the repression of the miR-99a/let-7c/miR-125b-2 miRNA cluster in prostate cancer cells. *Oncogene*, pages –.

Sundaram, K., Nishimura, R., Senn, J., Youssef, R. F., London, S. D., and Reddy, S. V. (2007). RANK ligand signaling modulates the matrix metalloproteinase-9 gene expression during osteoclast differentiation. *Experimental Cell Research*, 313(1):11–11.

Svotelis, A., Bianco, S. e. p., Madore, J., eacute, G. H., Nordell-Markovits, A., Mes-Masson, A.-M., and vry, N. G. e. (2011). H3K27 demethylation by JMJD3 at a poised enhancer of anti-apoptotic gene BCL2 determines ERα ligand dependency. *The EMBO journal*, pages 1–15.

Swigut, T. and Wysocka, J. (2007). H3K27 demethylases, at long last. *Cell*, 131(1):29–32.

Takayanagi, H., Kim, S., Koga, T., Nishina, H., Isshiki, M., Yoshida, H., Saiura, A., Isobe, M., Yokochi, T., Inoue, J.-i., Wagner, E. F., Mak, T. W., Kodama, T., and Taniguchi, T. (2002). Induction and Activation of the Transcription Factor NFATc1 (NFAT2) Integrate RANKL Signaling in Terminal Differentiation of Osteoclasts. *Developmental Cell*, 3(6):13–13.

Thirunavukkarasu, K. (2001). Stimulation of Osteoprotegerin (OPG) Gene Expression by Transforming Growth Factor-beta (TGF-beta). MAPPING OF THE OPG PROMOTER REGION THAT MEDIATES TGF-beta EFFECTS. *Journal of Biological Chemistry*, 276(39):36241–36250.

Thirunavukkarasu, K. K., Miles, R. R. R., Halladay, D. L. D., Yang, X. X., Galvin, R. J. R., Chandrasekhar, S. S., Martin, T. J. T., and Onyia, J. E. J. (2001). Stimulation of osteoprotegerin (OPG) gene expression by transforming growth factor-beta (TGF-beta). Mapping of the OPG promoter region that mediates TGF-beta effects. *The Journal of biological chemistry*, 276(39):36241–36250.

Tian, C., Deng, H., Tang, X., Hu, H., Liu, X., and Luo, F. (2012). [Effect of Jumonji domain-containing protein-3 on the proliferation and migration of lung cancer cell line]. *Sheng wu yi xue gong cheng xue za zhi = Journal of biomedical engineering = Shengwu yixue gongchengxue zazhi*, 29(3):514–518.

Tsukada, Y.-i., Fang, J., Erdjument-Bromage, H., Warren, M. E., Borchers, C. H., Tempst, P., and Zhang, Y. (2005). Histone demethylation by a family of JmjC domain-containing proteins. *Nature*, 439(7078):811–816.

Ueda, R., Suzuki, T., Mino, K., Tsumoto, H., Nakagawa, H., Hasegawa, M., Sasaki, R., Mizukami, T., and Miyata, N. (2009). Identification of cell-active lysine specific demethylase 1-selective inhibitors. *Journal of the American Chemical Society*, 131(48):17536–17537.

Upadhyay, A. K., Rotili, D., Han, J. W., Hu, R., Chang, Y., Labella, D., Zhang, X., Yoon, Y.-s., Mai, A., and Cheng, X. (2012). An Analog of BIX-01294 Selectively Inhibits a Family of Histone H3 Lysine 9 Jumonji Demethylases. *Journal of molecular biology*, 416(3):9–9.

Vaananen, H. K., Zhao, H., Mulari, M., and Halleen, J. M. (2000). The cell biology of osteoclast function. *Journal of cell science*, 113 (Pt 3):377–381.

Vasanthi, P., Nalini, G., and RajASEKHAR, G. (2007). Role of tumor necrosis factor-alpha in rheumatoid arthritis: a review. *APLAR Journal of Rheumatology*, 10(4):270–274.

Waddington, C. H. (1957). The strategy of the genes. A discussion of some aspects of theoretical biology. With an appendix by H. Kacser. *cabdirect.org*, pages ix +–262 .

Wang, J., Hevi, S., Kurash, J. K., Lei, H., Gay, F., Bajko, J., Su, H., Sun, W., Chang, H., Xu, G., Gaudet, F., Li, E., and Chen, T. (2008). The lysine demethylase LSD1 (KDM1) is required for maintenance of global DNA methylation. *Nature genetics*, 41(1):125–129.

Wang, J., Lu, F., Ren, Q., Sun, H., Xu, Z., Lan, R., Liu, Y., Ward, D., Quan, J., Ye, T., and Zhang, H. (2011). Novel histone demethylase LSD1 inhibitors selectively target cancer cells with pluripotent stem cell properties. *Cancer Research*, 71(23):7238–7249.

Wang, Y., Wysocka, J., Sayegh, J., Lee, Y.-H., Perlin, J. R., Leonelli, L., Sonbuchner, L. S., McDonald, C. H., Cook, R. G., Dou, Y., Roeder, R. G., Clarke, S., Stallcup, M. R., Allis, C. D., and Coonrod, S. A. (2004). Human PAD4 regulates histone arginine methylation levels via demethylimination. *Science*, 306(5694):279–283.

Wei, W., Wang, X., Yang, M., Smith, L. C., Dechow, P. C., and Wan, Y. (2010). PGC1 Mediates PPAR Activation of Osteoclastogenesis and Rosiglitazone-Induced Bone Loss. *Cell metabolism*, 11(6):503–516.

Wei, Y., Chen, R., Bueso-Ramos, C. E., Wang, H., Song, X., Wang, J., Yao, H., Nguyen, M., Fernandez, M., Yang, H., and Garcia-Manero, G. (2009). Genome-Wide Chip-Seq Analysis of Histone Methylation Reveals Modulators of NF-kappaB Signaling and the Histone Demethylase JMJD3 as Implicated in Disease Progression in Myelodysplastic Syndrome (MDS). *ASH Annual Meeting Abstracts*, 114(22):291.

Wei, Y., Chen, R., Dimicoli, S., Bueso-Ramos, C., Neuberg, D., Pierce, S., Wang, H., Yang, H., Jia, Y., Zheng, H., Fang, Z., Nguyen, M., Ganan-Gomez, I., Ebert, B., Levine, R., Kantarjian, H., and Garcia-Manero, G. (2013). Global H3K4me3 genome mapping reveals alterations of innate immunity signaling and overexpression of JMJD3 in human myelodysplastic syndrome CD34+

cells. *Leukemia : official journal of the Leukemia Society of America, Leukemia Research Fund, UK*.

Weilbaecher, K. N., Guise, T. A., and McCauley, L. K. (2011). Cancer to bone: a fatal attraction. *Nature Publishing Group*, 11(6):411–425.

Wickramasinghe, S. N. (1987). Evidence of drug metabolism by macrophages: possible role of macrophages in the pathogenesis of drug-induced tissue damage and in the activation of environmental procarcinogens. *Clinical and laboratory haematology*, 9(3):271–280.

Williams, J. A. and Shacter, E. (1997). Regulation of macrophage cytokine production by prostaglandin E2. Distinct roles of cyclooxygenase-1 and -2. *The Journal of biological chemistry*, 272(41):25693–25699.

Wingender, E., Chen, X., Hehl, R., Karas, H., Liebich, I., Matys, V., Meinhardt, T., Prüß, M., Reuter, I., and Schacherer, F. (2000). TRANSFAC: an integrated system for gene expression regulation. *Nucleic acids research*, 28(1):316–319.

Winn, M. D., Ballard, C. C., Cowtan, K. D., Dodson, E. J., Emsley, P., Evans, P. R., Keegan, R. M., Krissinel, E. B., Leslie, A. G. W., McCoy, A., McNicholas, S. J., Murshudov, G. N., Pannu, N. S., Potterton, E. A., Powell, H. R., Read, R. J., Vagin, A., and Wilson, K. S. (2011). Overview of the CCP4 suite and current developments. *Acta Crystallographica Section D Biological Crystallography*, 67(Pt 4):235–242.

Wu, H., Xu, G., and Li, Y.-P. (2009). Atp6v0d2 Is an Essential Component of the Osteoclast-Specific Proton Pump That Mediates Extracellular Acidification in Bone Resorption. *Journal of Bone and Mineral Research*, 24(5):871–885.

Xiang, Y., Zhu, Z., Han, G., Lin, H., Xu, L., and Chen, C. D. (2007). JMJD3 is a histone H3K27 demethylase. *Cell research*, 17(10):850–857.

Xing, L., Bushnell, T. P., Carlson, L., Tai, Z., Tondravi, M., Siebenlist, U., Young, F., and Boyce, B. F. (2002). NF-B p50 and p52 Expression Is Not Required for RANK-Expressing Osteoclast Pro-

genitor Formation but Is Essential for RANK- and Cytokine-Mediated Osteoclastogenesis. *Journal of Bone and Mineral Research*, 17(7):1200–1210.

Xu, W., Podoll, J. D., Dong, X., Tumber, A., Oppermann, U. C. T., and Wang, X. (2013). Quantitative Analysis of Histone Demethylase Probes Using Fluorescence Polarization. *Journal of Medicinal Chemistry*, page 130530204016007.

Yagi, M., Miyamoto, T., Toyama, Y., and Suda, T. (2006). Role of DC-STAMP in cellular fusion of osteoclasts and macrophage giant cells. *Journal of Bone and Mineral Metabolism*, 24(5):355–358.

Yasuda, H., Shima, N., Nakagawa, N., Yamaguchi, K., Kinosaki, M., Mochizuki, S.-i., Tomoyasu, A., Yano, K., Goto, M., Murakami, A., Tsuda, E., Morinaga, T., Higashio, K., Udagawa, N., TAKAHASHI, N., and SUDA, T. (1998). Osteoclast differentiation factor is a ligand for osteoprotegerin/osteoclastogenesis-inhibitory factor and is identical to TRANCE/RANKL. *pnasorg*, 95(7):3597.

Yasui, T., Hirose, J., Tsutsumi, S., Nakamura, K., Aburatani, H., and Tanaka, S. (2011). Epigenetic regulation of osteoclast differentiation: Possible involvement of Jmjd3 in the histone demethylation of Nfatc1. *Journal of Bone and Mineral Research*, 26(11):2665–2671.

Ye, L. L., Fan, Z. Z., Yu, B. B., Chang, J. J., Al Hezaimi, K. K., Zhou, X. X., Park, N.-H. N., and Wang, C.-Y. C. (2012). Histone demethylases KDM4B and KDM6B promotes osteogenic differentiation of human MSCs. *Cell Stem Cell*, 11(1):50–61.

Zaidi, S. K., Young, D. W., Montecino, M., Lian, J. B., Stein, J. L., van Wijnen, A. J., and Stein, G. S. (2010). Architectural Epigenetics: Mitotic Retention of Mammalian Transcriptional Regulatory Information. *Molecular and cellular biology*, 30(20):4758–4766.

Zhang, Q., Long, H., Liao, J., Zhao, M., Liang, G., Wu, X., Zhang, P., Ding, S., Luo, S., and Lu, Q. (2011). Inhibited expression of hematopoietic progenitor kinase 1 associated with loss of jumonji domain containing 3 promoter binding contributes to autoimmunity in systemic lupus erythematosus. *Journal of autoimmunity*, 37(3):180–189.

Zhao, B., Takami, M., Yamada, A., Wang, X., Koga, T., Hu, X., Tamura, T., Ozato, K., Choi, Y., Ivashkiv, L. B., Takayanagi, H., and Kamijo, R. (2009). Interferon regulatory factor-8 regulates bone metabolism by suppressing osteoclastogenesis. *Nature Medicine*, 15(9):1066–1071.

Zhao, W., Li, Q., Ayers, S., Gu, Y., Shi, Z., Zhu, Q., Chen, Y., Wang, H. Y., and Wang, R.-F. (2013). Jmjd3 Inhibits Reprogramming by Upregulating Expression of INK4a/Arf and Targeting PHF20 for Ubiquitination. *Cell*, 152(5):1037–1050.

Zock, J. M. (2009). Applications of high content screening in life science research. *Combinatorial chemistry & high throughput screening*, 12(9):870–876.

Appendices

Appendix I

Effect of Temperature and different constructs to the solubility of JmjD3.

Appendix II

List of genes induced by IL-4 in macrophage.

Appendix III

List of genes induced by IL-4 counter regulated by GSK-J4 in macrophage

Appendix IV

List of genes induced by RANKL at day 8 in differentiating osteoclast.

Appendix V

List of genes induced by RANKL counter-regulated by GSK-J4 at day 8 in differentiating osteoclast.

Appendix VI

List of osteoclast genes induced by RANKL at day 14 in differentiating osteoclast.

Appendix VII

List of genes induced by RANKL counter-regulated by GSK-J4 at day 14 in differentiating osteoclast.

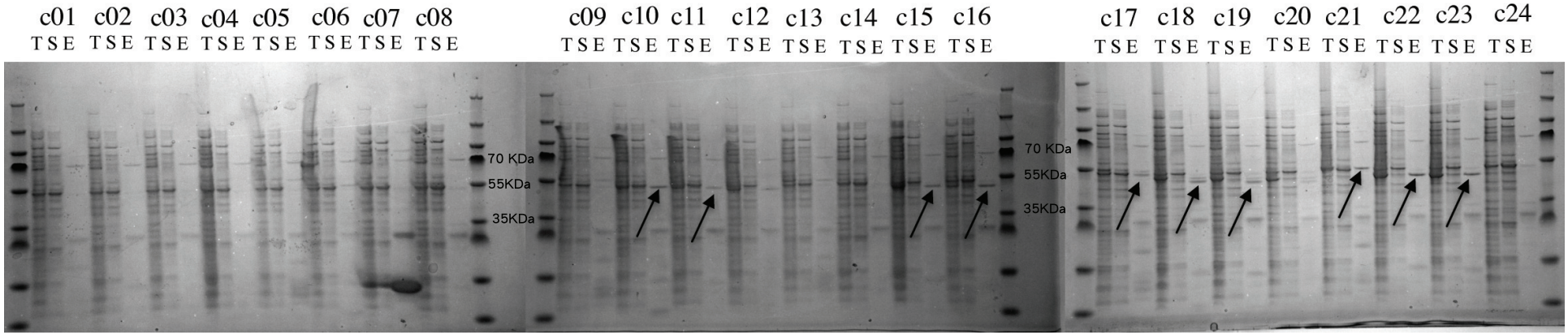
Appendix VIII

List of osteoclast genes induced by RANKL in mature osteoclast.

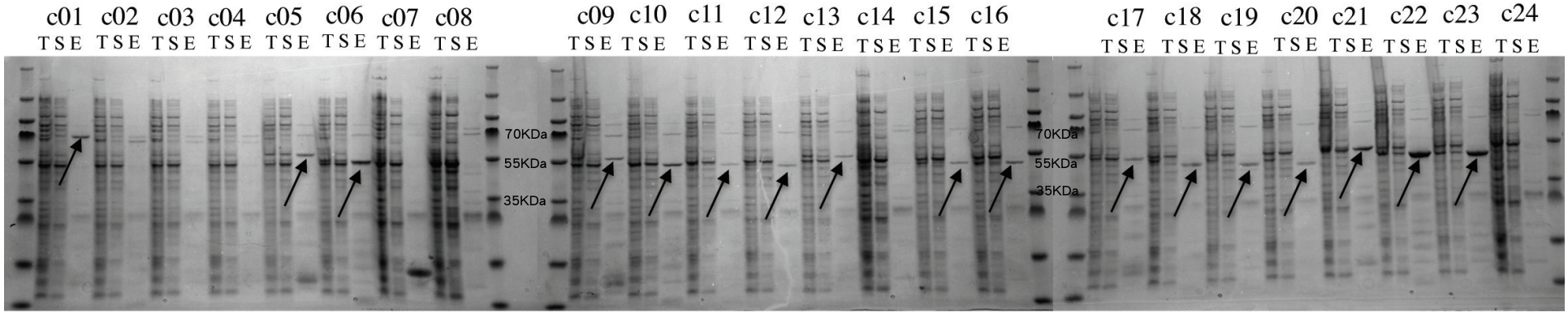
Appendix IX

List of osteoclast genes induced by counter-regulated by GSK-J4 in mature osteoclast.

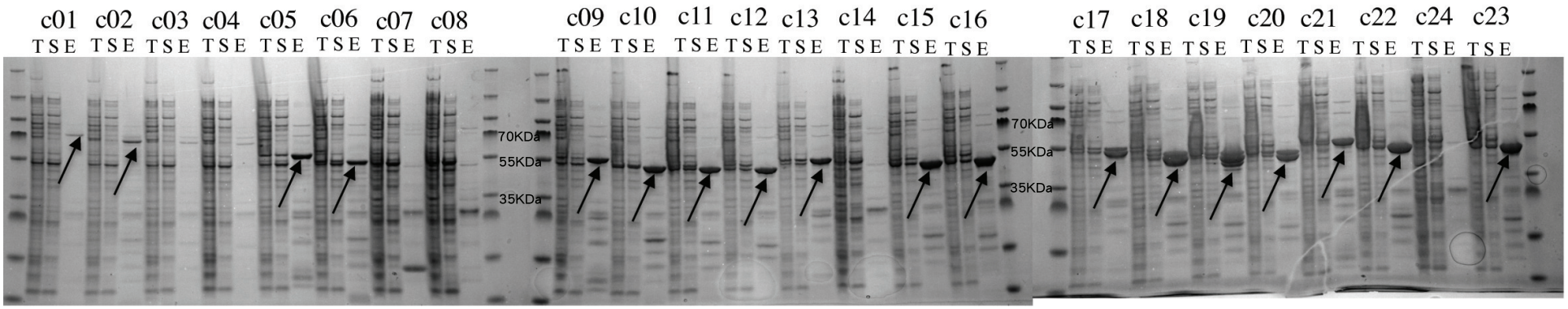
Appendix I



(a) 37°C growth temperature.



(b) 25°C growth temperature.



(c) 18°C growth temperature.

Figure 9.1: Effect of Temperature and different constructs to the solubility of JmjD3. Arrows represent the position of JmjD3 protein. Total Cell lysate (T), Clarified supernatant (S) and IMAC elution (E) were shown in each JmjD3 construct. Clarified supernatant and IMAC elution fraction do not contain inclusion bodies.

Appendix II

List of genes induced by IL-4 in macrophage

Probe ID	Gene symbol	Gene Name	-IL4	+IL4	j4	j5	Fold IL-4
8123744	F13A1	coagulation factor XIII, A1 polypeptide	5.548	10.057	7.497	9.785	4.509
8163063	CTNNAL1	catenin (cadherin-associated protein), alpha-like 1	5.796	9.466	8.802	9.510	3.671
8043602	NCAPH	non-SMC condensin I complex, subunit H	6.560	9.950	9.101	10.110	3.390
8033420	FCER2	Fc fragment of IgE, low affinity II, receptor for (CD23)	7.343	10.399	9.121	10.274	3.056
8006594	CCL18	chemokine (C-C motif) ligand 18 (pulmonary and activation-regulated)	8.415	11.299	10.476	10.862	2.883
8155898	PCSK5	proprotein convertase subtilisin/kexin type 5	6.797	9.619	8.970	9.513	2.821
7981708	IGHE	immunoglobulin heavy constant epsilon	6.278	8.957	8.290	9.682	2.679
8066214	TGM2	transglutaminase 2 (C polypeptide, protein-glutamine-gamma-glutamyltransferase)	10.282	12.846	12.695	12.733	2.565
8140463	FGL2	fibrinogen-like 2	8.306	10.846	9.729	11.055	2.540
8033445	CD209	CD209 molecule	7.924	10.442	9.141	10.404	2.518
7926410	MRC1	mannose receptor, C type 1	9.794	12.301	11.715	12.218	2.507
7926451	MRC1	mannose receptor, C type 1	9.794	12.301	11.715	12.218	2.507
8028311	SPINT2	serine peptidase inhibitor, Kunitz type, 2	7.461	9.832	9.442	9.997	2.372
7996022	CCL22	chemokine (C-C motif) ligand 22	8.633	10.860	9.999	10.834	2.227
8087739	CISH	cytokine inducible SH2-containing protein	7.268	9.492	8.669	9.194	2.224
8080562	IL17RB	interleukin 17 receptor B	4.806	6.808	6.569	7.284	2.002
8166925	MAOA	monoamine oxidase A	6.035	8.030	8.043	8.329	1.995
7974689	DACT1	dapper, antagonist of beta-catenin, homolog 1 (Xenopus laevis)	6.163	8.083	6.794	8.105	1.920
8157650	PTGS1	prostaglandin-endoperoxide synthase 1 (prostaglandin G/H synthase and cyclooxygenase)	7.800	9.625	8.363	9.618	1.825
7961546	EPS8	epidermal growth factor receptor pathway substrate 8	6.917	8.670	8.354	8.267	1.753
7991335	ANPEP	alanyl (membrane) aminopeptidase	10.382	12.111	12.365	12.372	1.729
8091511	P2RY14	purinergic receptor P2Y, G-protein coupled, 14	4.961	6.675	5.202	6.089	1.714
8003344	SNAI3	snail homolog 3 (Drosophila)	8.965	10.531	10.378	10.535	1.565
7986350	ARRDC4	arrestin domain containing 4	8.311	9.871	10.568	9.919	1.559
8006655	DHRS11	dehydrogenase/reductase (SDR family) member 11	8.075	9.632	9.403	9.601	1.557
7999423	SOCS1	suppressor of cytokine signaling 1	6.827	8.378	7.761	8.155	1.551
7904293	PTGFRN	prostaglandin F2 receptor negative regulator	7.076	8.610	7.926	8.795	1.534
8006459	CCL13	chemokine (C-C motif) ligand 13	5.167	6.662	6.035	6.466	1.495
8165752	IL3RA	interleukin 3 receptor, alpha (low affinity)	6.111	7.590	7.870	7.409	1.478
8176323	IL3RA	interleukin 3 receptor, alpha (low affinity)	6.111	7.590	7.870	7.409	1.478
8088371	DNASE1L3	deoxyribonuclease I-like 3	5.294	6.769	6.128	6.703	1.475
8122660	UST	uronyl-2-sulfotransferase	6.282	7.724	7.824	7.552	1.441
7954631	FAR2	fatty acyl CoA reductase 2	10.268	11.709	10.671	11.761	1.441
8012013	CLEC10A	C-type lectin domain family 10, member A	7.085	8.523	6.637	8.852	1.438
8088142	CHDH	choline dehydrogenase	6.299	7.728	7.521	7.939	1.429
8025301	CD209	CD209 molecule	7.214	8.639	8.123	9.382	1.425
8152988	SLA	Src-like-adaptor	9.385	10.805	9.913	10.764	1.419
7906777	FCGR2B	Fc fragment of IgG, low affinity IIb, receptor (CD32)	10.264	11.669	11.518	11.828	1.405
8005557	EPN2	epsin 2	6.788	8.185	7.694	8.009	1.396
8089568	CD200R1	CD200 receptor 1	5.438	6.827	6.195	6.785	1.388
7903719	AMPD2	adenosine monophosphate deaminase 2	7.904	9.286	8.755	9.270	1.382
7932132	FRMD4A	FERM domain containing 4A	7.592	8.966	8.947	9.099	1.375
8070173	KCNE1	potassium voltage-gated channel, Isk-related family, member 1	8.314	9.653	9.535	9.763	1.339
8058765	FN1	fibronectin 1	6.196	7.525	6.542	7.227	1.329
7928046	TSPAN15	tetraspanin 15	8.082	9.407	8.971	9.662	1.325
8163908	GGTA1	glycoprotein, alpha-galactosyltransferase 1 pseudogene	8.326	9.639	8.393	9.781	1.313
7932407	ST8SIA6	ST8 alpha-N-acetyl-neuraminide alpha-2,8-sialyltransferase 6	4.849	6.157	6.182	6.784	1.309
8091523	P2RY13	purinergic receptor P2Y, G-protein coupled, 13	8.513	9.802	7.819	9.753	1.289
7953723	CLEC4A	C-type lectin domain family 4, member A	8.603	9.882	9.157	9.904	1.279
7956759	SRGAP1	SLIT-ROBO Rho GTPase activating protein 1	6.880	8.155	8.317	8.629	1.275
8049722	GPR35	G protein-coupled receptor 35	6.847	8.120	7.407	7.904	1.273
7976726	EVL	Enah/Vasp-like	9.084	10.316	9.649	10.218	1.232
8140358	CCL26	chemokine (C-C motif) ligand 26	5.363	6.592	5.835	6.143	1.229
7907830	QSOX1	quiescin Q6 sulfhydryl oxidase 1	9.435	10.646	10.594	10.766	1.211
7924166	BATF3	basic leucine zipper transcription factor, ATF-like 3	6.583	7.788	7.712	7.292	1.205
8069142	KRTAP10-4	keratin associated protein 10-4	7.493	8.687	7.998	7.931	1.195
7906797	FCRLB	Fc receptor-like B	7.337	8.508	7.969	8.367	1.171
7994609	QPRT	quinolinate phosphoribosyltransferase	7.454	8.602	7.803	9.007	1.149
8094938	NIPAL1	NIPA-like domain containing 1	6.120	7.256	6.966	7.346	1.136
7933872	EGR2	early growth response 2	10.335	11.466	11.095	11.553	1.131
7937700	KRTAP5-5	keratin associated protein 5-5	5.736	6.862	5.891	6.272	1.127
8075005	C22orf45	chromosome 22 open reading frame 45	6.302	7.427	6.764	6.610	1.125
8144516	ERI1	exoribonuclease 1	8.222	9.346	9.377	9.603	1.124
8129937	CITED2	Cbp/p300-interacting transactivator, with Glu/Asp-rich carboxy-terminal domain, 2	10.789	11.910	11.965	11.848	1.121
8136067	TSPAN33	tetraspanin 33	7.932	9.048	8.626	9.207	1.116
7906775	HSPA7	heat shock 70kDa protein 7 (HSP70B)	8.568	9.678	9.120	9.441	1.110
7991034	HOMER2	homer homolog 2 (Drosophila)	6.137	7.242	6.902	7.535	1.104
8093906	WFS1	Wolfram syndrome 1 (wolframin)	7.397	8.478	8.600	8.510	1.082
8101675	ABCG2	ATP-binding cassette, sub-family G (WHITE), member 2	7.556	8.627	9.681	8.969	1.072
8123760	LY86-AS	LY86 antisense RNA (non-protein coding)	6.587	7.655	6.902	6.795	1.068
7993624	SYT17	synaptotagmin XVII	6.777	7.844	7.245	7.591	1.066
8000028	DCUN1D3	DCN1, defective in cullin neddylation 1, domain containing 3 (S. cerevisiae)	8.328	9.394	9.642	9.729	1.066
7989985	ITGA11	integrin, alpha 11	6.037	7.102	6.426	7.291	1.066
7898256	TMEM82	transmembrane protein 82	6.206	7.270	6.563	6.806	1.063
8009096	ACE	angiotensin I converting enzyme (peptidyl-dipeptidase A) 1	7.820	8.882	8.523	8.694	1.062
8131067	GPR146	G protein-coupled receptor 146	7.669	8.730	8.553	8.795	1.061
7928944	PAPSS2	3'-phosphoadenosine 5'-phosphosulfate synthase 2	9.076	10.131	10.022	10.148	1.055
8123101	C6orf99	chromosome 6 open reading frame 99	5.137	6.178	5.552	5.231	1.040
8160521	MOBKL2B	MOB1, Mps One Binder kinase activator-like 2B (yeast)	7.013	8.014	7.760	7.952	1.000
8119898	VEGFA	vascular endothelial growth factor A	8.077	7.076	8.355	7.005	-1.001
7966259	GLTP	glycolipid transfer protein	10.911	9.909	10.129	9.901	-1.002

8061114	DSTN	destrin (actin depolymerizing factor)	8.911	7.907	8.595	8.584	-1.003
7963970	SILV	silver homolog (mouse)	9.675	8.666	9.433	9.037	-1.009
8131927	MPP6	membrane protein, palmitoylated 6 (MAGUK p55 subfamily member 6)	6.887	5.877	6.360	6.146	-1.010
8130556	SOD2	superoxide dismutase 2, mitochondrial	12.141	11.130	11.605	11.495	-1.010
8114612	CD14	CD14 molecule	12.381	11.370	10.753	11.342	-1.011
7994769	CORO1A	coronin, actin binding protein, 1A	11.361	10.350	9.552	10.294	-1.011
8121510	RPF2	ribosome production factor 2 homolog (S. cerevisiae)	8.562	7.550	8.404	8.264	-1.012
8096160	ARHGAP24	Rho GTPase activating protein 24	7.508	6.496	6.875	6.564	-1.012
8107474	DMXL1	Dmx-like 1	10.393	9.379	10.142	9.863	-1.014
8117034	GMPR	guanosine monophosphate reductase	8.791	7.776	7.805	7.887	-1.015
8030978	ZNF845	zinc finger protein 845	8.773	7.757	8.579	8.737	-1.017
7981958	SNORD116-5	small nucleolar RNA, C/D box 116-5	6.096	5.079	5.132	5.471	-1.017
7981962	SNORD116-5	small nucleolar RNA, C/D box 116-5	6.096	5.079	5.132	5.471	-1.017
7923547	CHI3L1	chitinase 3-like 1 (cartilage glycoprotein-39)	12.103	11.085	11.512	11.300	-1.018
7938951	ANO5	anoctamin 5	5.822	4.804	5.321	5.044	-1.018
7971590	CAB39L	calcium binding protein 39-like	8.224	7.205	7.752	7.665	-1.018
7933139	ZNF33B	zinc finger protein 33B	7.128	6.109	6.326	6.370	-1.018
7998722	SNORD60	small nucleolar RNA, C/D box 60	6.645	5.624	5.854	5.975	-1.021
7942594	SNORD15B	small nucleolar RNA, C/D box 15B	8.994	7.973	7.797	8.310	-1.021
8054722	IL1B	interleukin 1, beta	7.090	6.069	7.736	7.294	-1.021
8006237	LOC400590	hypothetical LOC400590	8.303	7.278	8.056	8.085	-1.025
7938396	AMPD3	adenosine monophosphate deaminase 3	8.645	7.619	8.138	8.085	-1.026
7988644	ATP8B4	ATPase, class I, type 8B, member 4	6.953	5.926	5.679	6.159	-1.026
8020702	TAF4B	TAF4b RNA polymerase II, TATA box binding protein (TBP)-associated factor, 105kDa	5.755	4.728	5.458	5.354	-1.026
8159006	SNORD36B	small nucleolar RNA, C/D box 36B	7.542	6.515	6.603	6.831	-1.027
7970844	KATNAL1	katanin p60 subunit A-like 1	7.090	6.063	6.621	6.453	-1.027
7933619	SGMS1	sphingomyelin synthase 1	9.157	8.130	8.514	8.560	-1.027
7908351	PLA2G4A	phospholipase A2, group IVA (cytosolic, calcium-dependent)	7.316	6.289	6.775	6.987	-1.028
8174361	TSC22D3	TSC22 domain family, member 3	9.637	8.608	8.453	8.782	-1.029
8029914	GPR77	G protein-coupled receptor 77	8.232	7.202	7.309	7.408	-1.030
7929065	IFIT1	interferon-induced protein with tetratricopeptide repeats 1	6.673	5.643	5.742	5.724	-1.031
8163618	TNFSF15	tumor necrosis factor (ligand) superfamily, member 15	7.104	6.072	5.728	5.974	-1.032
8048717	SGPP2	sphingosine-1-phosphate phosphatase 2	7.476	6.442	7.130	7.373	-1.034
8171248	KAL1	Kallmann syndrome 1 sequence	7.475	6.438	6.443	6.612	-1.037
8005134	ADORA2B	adenosine A2b receptor	10.222	9.184	10.592	9.169	-1.038
8129728	AHI1	Abelson helper integration site 1	8.604	7.564	8.649	7.862	-1.040
7948364	MPEG1	macrophage expressed 1	10.961	9.920	9.607	10.031	-1.041
8047596	NBEAL1	neurobeachin-like 1	7.759	6.710	7.348	7.313	-1.049
8023259	SNORD58A	small nucleolar RNA, C/D box 58A	6.019	4.966	5.769	5.657	-1.053
8044295	SH3RF3	SH3 domain containing ring finger 3	9.105	8.051	7.786	7.890	-1.054
8001410	AKTIP	AKT interacting protein	8.148	7.087	7.449	7.544	-1.061
8039692	ZNF814	zinc finger protein 814	8.080	7.018	7.700	7.687	-1.062
7973084	ANG	angiogenin, ribonuclease, RNase A family, 5	7.607	6.545	6.883	6.738	-1.062
8063115	MMP9	matrix metallopeptidase 9 (gelatinase B, 92kDa gelatinase, 92kDa type IV collagenase)	10.763	9.700	9.479	9.933	-1.063
7983940	FAM63B	family with sequence similarity 63, member B	8.032	6.968	7.393	7.709	-1.064
7971388	SLC25A30	solute carrier family 25, member 30	8.373	7.309	8.145	8.244	-1.065
8051993	PIGF	phosphatidylinositol glycan anchor biosynthesis, class F	7.069	6.003	6.286	6.593	-1.066
8106743	VCAN	versican	6.865	5.799	5.771	5.763	-1.067
7948904	SNORD28	small nucleolar RNA, C/D box 28	9.020	7.946	8.757	8.782	-1.074
7951038	SNORA40	small nucleolar RNA, H/ACA box 40	6.776	5.702	6.597	6.783	-1.074
8089771	CD80	CD80 molecule	7.808	6.734	7.227	6.846	-1.074
8171418	PIGA	phosphatidylinositol glycan anchor biosynthesis, class A	8.602	7.527	7.876	7.918	-1.075
7918157	VAV3	vav 3 guanine nucleotide exchange factor	8.701	7.625	7.934	8.110	-1.076
7912157	ERRFI1	ERBB receptor feedback inhibitor 1	7.344	6.267	7.026	6.446	-1.077
8080847	C3orf14	chromosome 3 open reading frame 14	8.535	7.458	7.894	7.891	-1.077
8056829	CIR1	corepressor interacting with RBPJ, 1	9.609	8.525	9.345	8.746	-1.084
7966089	CMKLR1	chemokine-like receptor 1	10.073	8.987	7.758	9.256	-1.086
8137250	GIMAP2	GTPase, IMAP family member 2	8.832	7.739	8.153	8.365	-1.093
8143555	OR9A2	olfactory receptor, family 9, subfamily A, member 2	7.584	6.490	6.920	6.801	-1.094
8064451	SIRPB2	signal-regulatory protein beta 2	8.965	7.862	7.254	7.866	-1.103
8063345	SNORD12C	small nucleolar RNA, C/D box 12C	6.669	5.565	6.335	6.280	-1.104
7928695	C10orf58	chromosome 10 open reading frame 58	7.623	6.518	7.062	6.901	-1.105
8114572	HBEGF	heparin-binding EGF-like growth factor	8.729	7.623	7.362	7.966	-1.106
7961829	BCAT1	branched chain amino-acid transaminase 1, cytosolic	10.475	9.369	9.992	9.353	-1.106
8079733	KLHDC8B	kelch domain containing 8B	10.121	9.010	9.707	9.124	-1.112
7928308	DDIT4	DNA-damage-inducible transcript 4	7.772	6.660	7.013	6.600	-1.112
8047606	NBEAL1	neurobeachin-like 1	7.875	6.762	7.665	7.610	-1.113
8137240	GIMAP7	GTPase, IMAP family member 7	7.339	6.225	5.954	5.916	-1.114
7953218	RAD51AP1	RAD51 associated protein 1	8.760	7.644	8.001	8.341	-1.116
8129649	C6orf192	chromosome 6 open reading frame 192	9.493	8.372	7.777	8.247	-1.121
8168873	ARMCX6	armadillo repeat containing, X-linked 6	9.510	8.387	9.016	8.889	-1.122
8002303	NQO1	NAD(P)H dehydrogenase, quinone 1	10.916	9.791	11.141	10.317	-1.125
8103563	DDX60	DEAD (Asp-Glu-Ala-Asp) box polypeptide 60	7.350	6.223	6.643	6.932	-1.126
8091354	HLTF	helicase-like transcription factor	8.656	7.529	7.983	8.088	-1.127
8169022	WBP5	WW domain binding protein 5	7.168	6.041	6.653	6.199	-1.127
8005202	SNORD49A	small nucleolar RNA, C/D box 49A	6.569	5.436	6.408	6.246	-1.133
7905060	FCGR1A	Fc fragment of IgG, high affinity Ia, receptor (CD64)	10.131	8.995	8.989	8.726	-1.136
8148280	SQLE	squalene epoxidase	9.566	8.425	8.659	8.684	-1.141
8091656	METT5D1	methyltransferase 5 domain containing 1	8.050	6.904	7.734	7.703	-1.146
7970441	GJB2	gap junction protein, beta 2, 26kDa	9.333	8.187	8.245	8.191	-1.146
7935776	SCD	stearoyl-CoA desaturase (delta-9-desaturase)	7.728	6.580	8.132	7.414	-1.148
8126303	TREM1	triggering receptor expressed on myeloid cells 1	7.852	6.703	7.099	6.632	-1.149
7965510	TMCC3	transmembrane and coiled-coil domain family 3	10.115	8.964	9.320	8.946	-1.151
7897522	RBP7	retinol binding protein 7, cellular	7.502	6.349	6.931	6.493	-1.153
8113130	MCTP1	multiple C2 domains, transmembrane 1	9.746	8.589	8.631	8.767	-1.157
7928999	LIPN	lipase, family member N	6.014	4.857	6.238	5.558	-1.157
8077376	ITPR1	inositol 1,4,5-triphosphate receptor, type 1	9.292	8.130	9.070	8.359	-1.162

7915718	TESK2	testis-specific kinase 2	9.555	8.391	8.906	8.514	-1.164
8052956	EXOC6B	exocyst complex component 6B	8.795	7.629	8.226	8.219	-1.166
8153021	ST3GAL1	ST3 beta-galactoside alpha-2,3-sialyltransferase 1	10.848	9.680	10.333	9.793	-1.168
8102800	SLC7A11	solute carrier family 7, (cationic amino acid transporter, y+ system) member 11	11.040	9.866	11.994	10.705	-1.175
7960874	C3AR1	complement component 3a receptor 1	11.705	10.528	9.807	10.321	-1.177
7969933	BIVM	basic, immunoglobulin-like variable motif containing	6.982	5.799	6.250	6.321	-1.183
7919133	FCGR1B	Fc fragment of IgG, high affinity Ib, receptor (CD64)	10.442	9.253	9.282	9.053	-1.189
8091715	LXN	latexin	7.938	6.747	6.581	6.989	-1.191
7989023	RAB27A	RAB27A, member RAS oncogene family	9.850	8.653	9.108	8.728	-1.196
7995681	MMP2	matrix metallopeptidase 2 (gelatinase A, 72kDa gelatinase, 72kDa type IV collagenase)	8.614	7.415	7.645	7.285	-1.199
8014115	MYO1D	myosin ID	7.486	6.281	6.411	6.435	-1.205
8027862	FFAR2	free fatty acid receptor 2	6.791	5.583	5.727	5.906	-1.208
8044391	MERTK	c-mer proto-oncogene tyrosine kinase	9.210	8.000	8.086	8.115	-1.210
8123080	SYTL3	synaptotagmin-like 3	7.745	6.535	6.381	6.597	-1.210
7995729	CES1P1	carboxylesterase 1 pseudogene 1	10.844	9.627	10.707	10.278	-1.217
8151587	C8orf59	chromosome 8 open reading frame 59	8.230	7.010	7.825	7.773	-1.220
8137257	GIMAP5	GTPase, IMAP family member 5	8.651	7.430	6.782	7.176	-1.221
8123951	C6orf105	chromosome 6 open reading frame 105	8.837	7.610	8.460	8.036	-1.227
7982377	GREM1	gremlin 1	8.851	7.623	8.407	7.803	-1.228
8147145	ATP6V0D2	ATPase, H+ transporting, lysosomal 38kDa, V0 subunit d2	11.210	9.981	10.615	10.268	-1.229
8031374	FCAR	Fc fragment of IgA, receptor for	7.763	6.521	7.720	7.508	-1.242
8101322	MOP-1	MOP-1	8.216	6.972	7.726	7.379	-1.244
8054712	IL1A	interleukin 1, alpha	6.692	5.442	8.153	6.535	-1.250
8053797	LOC400986	ankyrin repeat domain-containing protein 36C	7.225	5.963	6.486	7.051	-1.262
7987145	FMN1	formin 1	8.429	7.162	7.477	7.354	-1.267
7948906	SNORD27	small nucleolar RNA, C/D box 27	6.793	5.525	6.247	6.361	-1.268
7912224	SLC2A5	solute carrier family 2 (facilitated glucose/fructose transporter), member 5	8.434	7.166	7.050	7.037	-1.269
8039236	LILRA5	leukocyte immunoglobulin-like receptor, subfamily A (with TM domain), member 5	10.024	8.749	8.467	8.973	-1.275
8065089	KIF16B	kinesin family member 16B	8.871	7.593	8.448	7.891	-1.278
7922410	SNORD44	small nucleolar RNA, C/D box 44	7.648	6.363	7.203	7.300	-1.285
8173745	CYSLTR1	cysteinyl leukotriene receptor 1	7.769	6.474	5.629	7.782	-1.295
8127854	ME1	malic enzyme 1, NADP(+)-dependent, cytosolic	9.883	8.577	10.147	9.159	-1.306
7981949	SNORD116-1	small nucleolar RNA, C/D box 116-1	6.397	5.081	5.349	6.037	-1.316
8119161	PIM1	pim-1 oncogene	11.536	10.219	11.418	10.421	-1.317
7932765	MPP7	membrane protein, palmitoylated 7 (MAGUK p55 subfamily member 7)	8.872	7.553	8.086	7.981	-1.318
8035847	ZNF675	zinc finger protein 675	8.478	7.156	7.724	8.172	-1.322
8130578	SNORA20	small nucleolar RNA, H/ACA box 20	9.626	8.298	7.719	8.624	-1.328
7922408	SNORD78	small nucleolar RNA, C/D box 78	6.998	5.663	6.728	6.591	-1.336
8085628	ANKRD28	ankyrin repeat domain 28	8.994	7.659	8.478	8.019	-1.336
7926037	PFKFB3	6-phosphofructo-2-kinase/fructose-2,6-biphosphatase 3	10.726	9.388	9.721	9.524	-1.338
8113358	ST8SIA4	ST8 alpha-N-acetyl-neuraminide alpha-2,8-sialyltransferase 4	8.198	6.857	6.718	7.094	-1.341
8068713	MX1	myxovirus (influenza virus) resistance 1, interferon-inducible protein p78 (mouse)	8.526	7.184	6.830	7.307	-1.342
7959834	GLT1D1	glycosyltransferase 1 domain containing 1	8.069	6.726	6.923	6.726	-1.343
7912145	TNFRSF9	tumor necrosis factor receptor superfamily, member 9	7.762	6.418	6.833	6.874	-1.345
7991602	PCSK6	proprotein convertase subtilisin/kexin type 6	9.454	8.108	9.904	8.174	-1.346
8059712	SNORD82	small nucleolar RNA, C/D box 82	7.107	5.722	5.858	6.039	-1.385
7935270	BLNK	B-cell linker	8.756	7.370	7.374	7.569	-1.386
8121257	PRDM1	PR domain containing 1, with ZNF domain	8.227	6.819	8.152	7.570	-1.408
7925929	AKR1C3	aldo-keto reductase family 1, member C3 (3-alpha hydroxysteroid dehydrogenase, type II)	7.042	5.629	8.184	5.721	-1.413
7974341	GNG2	guanine nucleotide binding protein (G protein), gamma 2	8.226	6.807	6.255	6.527	-1.419
8140556	HGF	hepatocyte growth factor (hepapoietin A; scatter factor)	7.021	5.599	5.072	5.635	-1.422
7905047	FCGR1A	Fc fragment of IgG, high affinity Ia, receptor (CD64)	10.491	9.066	9.341	9.082	-1.425
8068100	NCRNA00189	non-protein coding RNA 189	7.908	6.478	7.493	7.014	-1.430
7980744	RPS6KA5	ribosomal protein S6 kinase, 90kDa, polypeptide 5	7.213	5.777	5.968	6.117	-1.436
8041995	SPTBN1	spectrin, beta, non-erythrocytic 1	10.916	9.475	9.844	9.286	-1.440
7899480	SNORA73A	small nucleolar RNA, H/ACA box 73A	10.936	9.494	10.039	10.565	-1.442
7951408	CARD16	caspase recruitment domain family, member 16	7.060	5.617	6.201	6.111	-1.443
7983478	C15orf48	chromosome 15 open reading frame 48	8.732	7.273	8.374	8.075	-1.460
8175217	GPC4	glypican 4	7.496	6.021	6.346	6.269	-1.475
7951397	CASP1	caspase 1, apoptosis-related cysteine peptidase (interleukin 1, beta, convertase)	10.215	8.729	9.653	9.273	-1.486
8132843	HAUS6	HAUS augmin-like complex, subunit 6	7.389	5.902	7.259	6.776	-1.487
8165672	RFC1	replication factor C (activator 1) 1, 145kDa	5.904	4.401	5.589	5.963	-1.503
8039096	NLRP12	NLR family, pyrin domain containing 12	8.110	6.606	7.131	6.817	-1.504
8162059	SLC28A3	solute carrier family 28 (sodium-coupled nucleoside transporter), member 3	8.191	6.677	7.514	6.757	-1.515
7902400	SNORD45B	small nucleolar RNA, C/D box 45B	7.773	6.232	6.719	6.812	-1.542
7999909	GPRC5B	G protein-coupled receptor, family C, group 5, member B	9.366	7.821	6.787	7.384	-1.545
8101429	PLAC8	placenta-specific 8	6.635	5.087	5.325	5.617	-1.548
8111136	FAM134B	family with sequence similarity 134, member B	8.908	7.359	7.813	7.282	-1.549
8045688	TNFAIP6	tumor necrosis factor, alpha-induced protein 6	6.986	5.435	6.101	6.114	-1.552
7951686	IL18	interleukin 18 (interferon-gamma-inducing factor)	8.311	6.758	7.227	7.339	-1.553
7932227	NMT2	N-myristoyltransferase 2	9.220	7.652	8.954	8.109	-1.568
7965979	ALDH1L2	aldehyde dehydrogenase 1 family, member L2	7.183	5.613	6.555	6.049	-1.570
7943160	SCARNA9	small Cajal body-specific RNA 9	8.232	6.658	7.529	7.627	-1.575
8145293	ADAM28	ADAM metallopeptidase domain 28	7.687	6.103	6.231	6.288	-1.584
8000574	NUPR1	nuclear protein, transcriptional regulator, 1	11.964	10.380	10.964	10.443	-1.584
8095680	IL8	interleukin 8	12.448	10.853	12.440	11.352	-1.596
7974835	PRKCH	protein kinase C, eta	9.353	7.744	8.288	7.903	-1.609
8145317	ADAMDEC1	ADAM-like, decysin 1	8.624	7.007	7.215	7.652	-1.617
8075838	PVALB	parvalbumin	8.504	6.886	7.162	7.274	-1.617
7920244	S100A8	S100 calcium binding protein A8	10.619	8.993	8.194	9.312	-1.627
8162940	ABCA1	ATP-binding cassette, sub-family A (ABC1), member 1	9.217	7.557	8.245	8.081	-1.660
7965335	DUSP6	dual specificity phosphatase 6	8.363	6.684	7.712	7.061	-1.678
8046380	ITGA6	integrin, alpha 6	9.271	7.590	8.216	7.893	-1.681
8157446	ORM1	orosomucoid 1	7.386	5.678	5.873	6.331	-1.708
7927215	ALOX5	arachidonate 5-lipoxygenase	9.568	7.845	7.816	8.396	-1.723
8143471	CLEC5A	C-type lectin domain family 5, member A	6.781	5.035	5.497	5.087	-1.746
7987163	FMN1	formin 1	7.982	6.220	6.815	6.692	-1.762

7922402	SNORD47	small nucleolar RNA, C/D box 47	7.979	6.216	7.102	7.485	-1.763
8021635	SERPINB2	serpin peptidase inhibitor, clade B (ovalbumin), member 2	8.141	6.368	6.920	6.974	-1.773
7940643	ASRGL1	asparaginase like 1	8.966	7.178	7.190	7.297	-1.788
7960900	CLEC4E	C-type lectin domain family 4, member E	6.745	4.910	4.830	5.208	-1.835
7966621	SDS	serine dehydratase	11.306	9.424	9.380	9.127	-1.882
8003667	SERPINF1	serpin peptidase inhibitor, clade F (alpha-2 antiplasmin, pigment epithelium derived factor), member 1	9.115	7.229	7.078	7.525	-1.887
8166906	GPR34	G protein-coupled receptor 34	7.147	5.248	5.306	5.868	-1.899
7912937	PADI2	peptidyl arginine deiminase, type II	9.338	7.435	7.269	7.846	-1.903
7929511	ENTPD1	ectonucleoside triphosphate diphosphohydrolase 1	9.393	7.401	6.750	7.785	-1.992
8055350	TMEM163	transmembrane protein 163	9.502	7.456	9.073	7.877	-2.045
8101449	HPSE	heparanase	10.208	8.149	8.780	8.139	-2.060
7980828	CCDC88C	coiled-coil domain containing 88C	9.231	7.139	7.728	7.723	-2.092
8129637	VNN2	vanin 2	7.722	5.614	6.138	5.940	-2.108
8091260	SLC9A9	solute carrier family 9 (sodium/hydrogen exchanger), member 9	8.494	6.368	6.507	7.213	-2.126
8166059	TLR7	toll-like receptor 7	8.202	6.007	5.752	6.051	-2.195
8129618	VNN1	vanin 1	9.102	6.846	7.542	6.985	-2.256

Appendix III

List of genes induced by IL-4 counter-regulated by GSK-J4 in macrophage

Probe ID	Gene symbol	Gene Name	-IL4	+IL4	j4	j5	Fold IL-4	Fold J4
8160521	MOBKL2B	MOB1, Mps One Binder kinase activator-like 2B (yeast)	7.013	8.014	7.760	7.952	1.000	0.746
8009096	ACE	angiotensin I converting enzyme (peptidyl-dipeptidase A) 1	7.820	8.882	8.523	8.694	1.062	0.703
8136067	TSPAN33	tetraspanin 33	7.932	9.048	8.626	9.207	1.116	0.694
8054722	IL1B	interleukin 1, beta	7.090	6.069	7.736	7.294	-1.021	0.646
7906797	FCRLB	Fc receptor-like B	7.337	8.508	7.969	8.367	1.171	0.632
7974689	DACT1	dapper, antagonist of beta-catenin, homolog 1 (Xenopus laevis)	6.163	8.083	6.794	8.105	1.920	0.630
7976726	EVL	Enah/Vasp-like	9.084	10.316	9.649	10.218	1.232	0.564
8157650	PTGS1	prostaglandin-endoperoxide synthase 1 (prostaglandin G/H synthase and cyclooxygenase)	7.800	9.625	8.363	9.618	1.825	0.563
8049722	GPR35	G protein-coupled receptor 35	6.847	8.120	7.407	7.904	1.273	0.560
7953723	CLEC4A	C-type lectin domain family 4, member A	8.603	9.882	9.157	9.904	1.279	0.554
7906775	HSPA7	heat shock 70kDa protein 7 (HSP70B)	8.568	9.678	9.120	9.441	1.110	0.552
8152988	SLA	Src-like-adaptor	9.385	10.805	9.913	10.764	1.419	0.528
8069142	KRTAP10-4	keratin associated protein 10-4	7.493	8.687	7.998	7.931	1.195	0.505
8140358	CCL26	chemokine (C-C motif) ligand 26	5.363	6.592	5.835	6.143	1.229	0.472
7993624	SYT17	synaptotagmin XVII	6.777	7.844	7.245	7.591	1.066	0.467
8075005	C22orf45	chromosome 22 open reading frame 45	6.302	7.427	6.764	6.610	1.125	0.462
7991602	PCSK6	proprotein convertase subtilisin/kexin type 6	9.454	8.108	9.904	8.174	-1.346	0.450
8123101	C6orf99	chromosome 6 open reading frame 99	5.137	6.178	5.552	5.231	1.040	0.414
7935776	SCD	stearoyl-CoA desaturase (delta-9-desaturase)	7.728	6.580	8.132	7.414	-1.148	0.403
7954631	FAR2	fatty acyl CoA reductase 2	10.268	11.709	10.671	11.761	1.441	0.402
7989985	ITGA11	integrin, alpha 11	6.037	7.102	6.426	7.291	1.066	0.390
8005134	ADORA2B	adenosine A2b receptor	10.222	9.184	10.592	9.169	-1.038	0.370
7898256	TMEM82	transmembrane protein 82	6.206	7.270	6.563	6.806	1.063	0.357
7994609	QPRT	quinolinate phosphoribosyltransferase	7.454	8.602	7.803	9.007	1.149	0.350
8058765	FN1	fibronectin 1	6.196	7.525	6.542	7.227	1.329	0.346
8123760	LY86-AS	LY86 antisense RNA (non-protein coding)	6.587	7.655	6.902	6.795	1.068	0.315
8119898	VEGFA	vascular endothelial growth factor A	8.077	7.076	8.355	7.005	-1.001	0.278
8127854	ME1	malic enzyme 1, NADP(+)-dependent, cytosolic	9.883	8.577	10.147	9.159	-1.306	0.263
8091511	P2RY14	purinergic receptor P2Y, G-protein coupled, 14	4.961	6.675	5.202	6.089	1.714	0.241
8002303	NQO1	NAD(P)H dehydrogenase, quinone 1	10.916	9.791	11.141	10.317	-1.125	0.225
7928999	LIPN	lipase, family member N	6.014	4.857	6.238	5.558	-1.157	0.224
7937700	KRTAP5-5	keratin associated protein 5-5	5.736	6.862	5.891	6.272	1.127	0.156
8163908	GGTA1	glycoprotein, alpha-galactosyltransferase 1 pseudogene	8.326	9.639	8.393	9.781	1.313	0.067
8129728	AHI1	Abelson helper integration site 1	8.604	7.564	8.649	7.862	-1.040	0.044
8095680	IL8	interleukin 8	12.448	10.853	12.440	11.352	-1.596	-0.008
8031374	FCAR	Fc fragment of IgA, receptor for	7.763	6.521	7.720	7.508	-1.242	-0.043
8121257	PRDM1	PR domain containing 1, with ZNF domain	8.227	6.819	8.152	7.570	-1.408	-0.076
8119161	PIM1	pim-1 oncogene	11.536	10.219	11.418	10.421	-1.317	-0.118
8132843	HAUS6	HAUS augmin-like complex, subunit 6	7.389	5.902	7.259	6.776	-1.487	-0.130
7995729	CES1P1	carboxylesterase 1 pseudogene 1	10.844	9.627	10.707	10.278	-1.217	-0.137
8121510	RPF2	ribosome production factor 2 homolog (S. cerevisiae)	8.562	7.550	8.404	8.264	-1.012	-0.158
8005202	SNORD49A	small nucleolar RNA, C/D box 49A	6.569	5.436	6.408	6.246	-1.133	-0.161
7951038	SNORA40	small nucleolar RNA, H/ACA box 40	6.776	5.702	6.597	6.783	-1.074	-0.179
8030978	ZNF845	zinc finger protein 845	8.773	7.757	8.579	8.737	-1.017	-0.194
8047606	NBEAL1	neurobeachin-like 1	7.875	6.762	7.665	7.610	-1.113	-0.210
8077376	ITPR1	inositol 1,4,5-triphosphate receptor, type 1	9.292	8.130	9.070	8.359	-1.162	-0.222
7971388	SLC25A30	solute carrier family 25, member 30	8.373	7.309	8.145	8.244	-1.065	-0.229
7963970	SILV	silver homolog (mouse)	9.675	8.666	9.433	9.037	-1.009	-0.242
8006237	LOC400590	hypothetical LOC400590	8.303	7.278	8.056	8.085	-1.025	-0.247
8023259	SNORD58A	small nucleolar RNA, C/D box 58A	6.019	4.966	5.769	5.657	-1.053	-0.250
8107474	DMXL1	Dmx-like 1	10.393	9.379	10.142	9.863	-1.014	-0.251
7948904	SNORD28	small nucleolar RNA, C/D box 28	9.020	7.946	8.757	8.782	-1.074	-0.263
8056829	CIR1	corepressor interacting with RBPJ, 1	9.609	8.525	9.345	8.746	-1.084	-0.264
7932227	NMT2	N-myristoyltransferase 2	9.220	7.652	8.954	8.109	-1.568	-0.265
7922408	SNORD78	small nucleolar RNA, C/D box 78	6.998	5.663	6.728	6.591	-1.336	-0.270
8020702	TAF4B	TAF4b RNA polymerase II, TATA box binding protein (TBP)-associated factor, 105kDa	5.755	4.728	5.458	5.354	-1.026	-0.297
8165672	RFC1	replication factor C (activator 1) 1, 145kDa	5.904	4.401	5.589	5.963	-1.503	-0.315
8061114	DSTN	destrin (actin depolymerizing factor)	8.911	7.907	8.595	8.584	-1.003	-0.315
8091656	METT5D1	methyltransferase 5 domain containing 1	8.050	6.904	7.734	7.703	-1.146	-0.316
7912157	ERRFI1	ERBB receptor feedback inhibitor 1	7.344	6.267	7.026	6.446	-1.077	-0.318
8063345	SNORD12C	small nucleolar RNA, C/D box 12C	6.669	5.565	6.335	6.280	-1.104	-0.334
8048717	SGPP2	sphingosine-1-phosphate phosphatase 2	7.476	6.442	7.130	7.373	-1.034	-0.346
7983478	C15orf48	chromosome 15 open reading frame 48	8.732	7.273	8.374	8.075	-1.460	-0.358
8123951	C6orf105	chromosome 6 open reading frame 105	8.837	7.610	8.460	8.036	-1.227	-0.377
8039692	ZNF814	zinc finger protein 814	8.080	7.018	7.700	7.687	-1.062	-0.380
8151587	C8orf59	chromosome 8 open reading frame 59	8.230	7.010	7.825	7.773	-1.220	-0.405
8047596	NBEAL1	neurobeachin-like 1	7.759	6.710	7.348	7.313	-1.049	-0.410
8068100	NCRNA00189	non-protein coding RNA 189	7.908	6.478	7.493	7.014	-1.430	-0.415
8079733	KLHDC8B	kelch domain containing 8B	10.121	9.010	9.707	9.124	-1.112	-0.415
8065089	KIF16B	kinesin family member 16B	8.871	7.593	8.448	7.891	-1.278	-0.422
8055350	TMEM163	transmembrane protein 163	9.502	7.456	9.073	7.877	-2.045	-0.429
7982377	GREM1	gremlin 1	8.851	7.623	8.407	7.803	-1.228	-0.444
7922410	SNORD44	small nucleolar RNA, C/D box 44	7.648	6.363	7.203	7.300	-1.285	-0.445
8012013	CLEC10A	C-type lectin domain family 10, member A	7.085	8.523	6.637	8.852	1.438	-0.448
7970844	KATNAL1	katanin p60 subunit A-like 1	7.090	6.063	6.621	6.453	-1.027	-0.469
7971590	CAB39L	calcium binding protein 39-like	8.224	7.205	7.752	7.665	-1.018	-0.472
7961829	BCAT1	branched chain amino-acid transaminase 1, cytosolic	10.475	9.369	9.992	9.353	-1.106	-0.483

8101322	MOP-1	MOP-1	8.216	6.972	7.726	7.379	-1.244	-0.489
8168873	ARMCX6	armadillo repeat containing, X-linked 6	9.510	8.387	9.016	8.889	-1.122	-0.494
7938951	ANO5	anoctamin 5	5.822	4.804	5.321	5.044	-1.018	-0.500
7938396	AMPD3	adenosine monophosphate deaminase 3	8.645	7.619	8.138	8.085	-1.026	-0.507
8169022	WBP5	WW domain binding protein 5	7.168	6.041	6.653	6.199	-1.127	-0.516
8153021	ST3GAL1	ST3 beta-galactoside alpha-2,3-sialyltransferase 1	10.848	9.680	10.333	9.793	-1.168	-0.516
8085628	ANKRD28	ankyrin repeat domain 28	8.994	7.659	8.478	8.019	-1.336	-0.517
8131927	MPP6	membrane protein, palmitoylated 6 (MAGUK p55 subfamily member 6)	6.887	5.877	6.360	6.146	-1.010	-0.526
8130556	SOD2	superoxide dismutase 2, mitochondrial	12.141	11.130	11.605	11.495	-1.010	-0.535
7908351	PLA2G4A	phospholipase A2, group IVA (cytosolic, calcium-dependent)	7.316	6.289	6.775	6.987	-1.028	-0.541
7948906	SNORD27	small nucleolar RNA, C/D box 27	6.793	5.525	6.247	6.361	-1.268	-0.546
7928695	C10orf58	chromosome 10 open reading frame 58	7.623	6.518	7.062	6.901	-1.105	-0.561
7951397	CASP1	caspase 1, apoptosis-related cysteine peptidase (interleukin 1, beta, convertase)	10.215	8.729	9.653	9.273	-1.486	-0.561
8052956	EXOC6B	exocyst complex component 6B	8.795	7.629	8.226	8.219	-1.166	-0.569
7897522	RBP7	retinol binding protein 7, cellular	7.502	6.349	6.931	6.493	-1.153	-0.571
8089771	CD80	CD80 molecule	7.808	6.734	7.227	6.846	-1.074	-0.581
7923547	CHI3L1	chitinase 3-like 1 (cartilage glycoprotein-39)	12.103	11.085	11.512	11.300	-1.018	-0.591
8147145	ATP6V0D2	ATPase, H+ transporting, lysosomal 38kDa, V0 subunit d2	11.210	9.981	10.615	10.268	-1.229	-0.596
7965979	ALDH1L2	aldehyde dehydrogenase 1 family, member L2	7.183	5.613	6.555	6.049	-1.570	-0.627
8096160	ARHGAP24	Rho GTPase activating protein 24	7.508	6.496	6.875	6.564	-1.012	-0.633
7983940	FAM63B	family with sequence similarity 63, member B	8.032	6.968	7.393	7.709	-1.064	-0.639
8080847	C3orf14	chromosome 3 open reading frame 14	8.535	7.458	7.894	7.891	-1.077	-0.641
7933619	SGMS1	sphingomyelin synthase 1	9.157	8.130	8.514	8.560	-1.027	-0.644
7915718	TESK2	testis-specific kinase 2	9.555	8.391	8.906	8.514	-1.164	-0.649
7965335	DUSP6	dual specificity phosphatase 6	8.363	6.684	7.712	7.061	-1.678	-0.650
8143555	OR9A2	olfactory receptor, family 9, subfamily A, member 2	7.584	6.490	6.920	6.801	-1.094	-0.664
8091354	HLTF	helicase-like transcription factor	8.656	7.529	7.983	8.088	-1.127	-0.673
8162059	SLC28A3	solute carrier family 28 (sodium-coupled nucleoside transporter), member 3	8.191	6.677	7.514	6.757	-1.515	-0.678
8137250	GIMAP2	GTPase, IMAP family member 2	8.832	7.739	8.153	8.365	-1.093	-0.679
8091523	P2RY13	purinergic receptor P2Y, G-protein coupled, 13	8.513	9.802	7.819	9.753	1.289	-0.694
8001410	AKTIP	AKT interacting protein	8.148	7.087	7.449	7.544	-1.061	-0.699
7943160	SCARNA9	small Cajal body-specific RNA 9	8.232	6.658	7.529	7.627	-1.575	-0.703
8103563	DDX60	DEAD (Asp-Glu-Ala-Asp) box polypeptide 60	7.350	6.223	6.643	6.932	-1.126	-0.706
7973084	ANG	angiogenin, ribonuclease, RNase A family, 5	7.607	6.545	6.883	6.738	-1.062	-0.724
8171418	PIGA	phosphatidylinositol glycan anchor biosynthesis, class A	8.602	7.527	7.876	7.918	-1.075	-0.727
7969933	BIVM	basic, immunoglobulin-like variable motif containing	6.982	5.799	6.250	6.321	-1.183	-0.732
8053797	LOC400986	ankyrin repeat domain-containing protein 36C	7.225	5.963	6.486	7.051	-1.262	-0.738
7989023	RAB27A	RAB27A, member RAS oncogene family	9.850	8.653	9.108	8.728	-1.196	-0.742

Appendix IV

List of genes induced by RANKL at day 8 in differentiating osteoclast

Probe ID	Gene symbol	Gene Name	m	mR	J4	J5	folds (mr-m)
8100798	SULT1B1	sulfotransferase family, cytosolic, 1B, member 1	6.590	11.257	9.801	10.366	4.667
8092707	LEPREL1	leprecan-like 1	6.731	10.785	9.883	10.233	4.054
7943413	BIRC3	baculoviral IAP repeat-containing 3	8.005	11.573	11.001	11.167	3.568
8100977	CXCL5	chemokine (C-X-C motif) ligand 5	8.176	11.702	11.443	11.676	3.527
8021635	SERPINB2	serpin peptidase inhibitor, clade B (ovalbumin), member 2	7.905	11.304	11.887	12.085	3.399
8091411	TM4SF1	transmembrane 4 L six family member 1	5.607	8.971	7.634	8.224	3.364
8128565	POPDC3	popeye domain containing 3	5.612	8.884	8.034	9.237	3.272
8116418	GFPT2	glutamine-fructose-6-phosphate transaminase 2	5.573	8.838	8.271	8.716	3.265
7980316	TGFB3	transforming growth factor, beta 3	6.061	9.217	8.243	8.408	3.156
8095680	IL8	interleukin 8	8.278	11.209	11.311	11.990	2.931
8058063	RFTN2	raftlin family member 2	6.022	8.943	7.203	8.067	2.920
8104901	IL7R	interleukin 7 receptor	7.998	10.903	10.900	10.966	2.905
7979133	NID2	nidogen 2 (osteonidogen)	6.283	8.975	7.959	8.735	2.691
8121749	GJA1	gap junction protein, alpha 1, 43kDa	5.652	8.270	7.540	8.101	2.619
7982377	GREM1	gremlin 1	9.153	11.738	11.166	11.345	2.585
8089544	CCDC80	coiled-coil domain containing 80	5.696	8.090	6.811	7.306	2.394
8122660	UST	uronyl-2-sulfotransferase	6.124	8.511	7.499	7.648	2.386
8131600	TSPAN13	tetraspanin 13	6.693	9.068	7.817	8.357	2.376
8103812	ASB5	ankyrin repeat and SOCS box-containing 5	5.350	7.675	5.841	7.232	2.325
7921652	SLAMF1	signaling lymphocytic activation molecule family member 1	5.303	7.612	7.364	7.506	2.310
8150550	CHRNA6	cholinergic receptor, nicotinic, alpha 6	4.909	7.214	6.060	6.371	2.305
8172220	NDP	Norrie disease (pseudoglioma)	6.156	8.452	7.445	7.805	2.296
8142270	NRCAM	neuronal cell adhesion molecule	5.622	7.854	7.246	7.979	2.232
8152491	EXT1	exostosin 1	8.020	10.155	9.521	9.685	2.134
8047243	MARS2	methionyl-tRNA synthetase 2, mitochondrial	8.205	10.333	9.930	9.962	2.128
8157105	ZNF462	zinc finger protein 462	7.468	9.555	8.905	9.007	2.087
7920278	S100A3	S100 calcium binding protein A3	7.123	9.184	8.555	8.517	2.061
7922174	F5	coagulation factor V (proaccelerin, labile factor)	6.967	9.016	8.445	8.614	2.049
8166925	MAOA	monoamine oxidase A	7.368	9.390	9.228	9.231	2.022
8147012	PKIA	protein kinase (cAMP-dependent, catalytic) inhibitor alpha	7.291	9.247	7.976	8.401	1.956
8087611	HYAL1	hyaluronoglucosaminidase 1	8.276	10.220	9.900	9.850	1.944
8128956	FYN	FYN oncogene related to SRC, FGR, YES	7.707	9.637	9.065	9.181	1.930
8082974	ESYT3	extended synaptotagmin-like protein 3	6.242	8.159	7.227	7.701	1.917
7926875	BAMBI	BMP and activin membrane-bound inhibitor homolog (Xenopus laevis)	7.598	9.509	9.055	9.361	1.912
8123176	MAS1	MAS1 oncogene	5.114	7.019	6.232	6.485	1.905
7997139	CALB2	calbindin 2	6.284	8.148	7.089	7.272	1.864
8135601	MET	met proto-oncogene (hepatocyte growth factor receptor)	4.407	6.265	4.945	5.619	1.858
8102594	TNIP3	TNFAIP3 interacting protein 3	5.001	6.842	6.656	6.989	1.841
7957298	NAV3	neuron navigator 3	5.237	7.069	6.532	6.573	1.832
8163825	TRAF1	TNF receptor-associated factor 1	6.763	8.593	8.121	8.279	1.830
7960900	CLEC4E	C-type lectin domain family 4, member E	5.408	7.235	7.159	7.924	1.827
8109773	WWC1	WW and C2 domain containing 1	6.854	8.676	7.893	8.193	1.822
8115210	TNIP1	TNFAIP3 interacting protein 1	8.454	10.260	10.214	10.066	1.806
8105267	ITGA2	integrin, alpha 2 (CD49B, alpha 2 subunit of VLA-2 receptor)	7.691	9.473	8.530	9.020	1.783
8041048	FOSL2	FOS-like antigen 2	9.064	10.830	10.481	10.515	1.766
8075310	LIF	leukemia inhibitory factor (cholinergic differentiation factor)	5.723	7.472	7.467	7.613	1.749
8135594	CAV1	caveolin 1, caveolae protein, 22kDa	5.188	6.932	5.194	5.734	1.744
8105741	MAST4	microtubule associated serine/threonine kinase family member 4	6.692	8.434	7.669	8.081	1.742
8138527	MGC87042	STEAP family protein MGC87042	6.174	7.888	6.781	7.479	1.714
7981427	CKB	creatine kinase, brain	10.112	11.813	11.411	11.410	1.701
7964759	GRIP1	glutamate receptor interacting protein 1	5.143	6.831	5.754	6.265	1.688
7912145	TNFRSF9	tumor necrosis factor receptor superfamily, member 9	10.296	11.965	11.776	11.804	1.669
7910727	ACTN2	actinin, alpha 2	5.657	7.318	6.480	6.658	1.661
8140668	SEMA3A	sema domain, immunoglobulin domain (Ig), short basic domain, secreted, (semaphorin) 3A	6.582	8.238	8.148	8.483	1.656
8097991	TDO2	tryptophan 2,3-dioxygenase	5.741	7.391	7.171	8.071	1.650
8080964	GXYLT2	glucoside xylosyltransferase 2	6.353	7.985	7.726	7.889	1.632
7939365	FJX1	four jointed box 1 (Drosophila)	7.236	8.837	8.075	8.102	1.601
8080714	FLNB	filamin B, beta	8.210	9.808	9.706	9.620	1.597
8106820	POLR3G	polymerase (RNA) III (DNA directed) polypeptide G (32kD)	7.553	9.143	8.253	8.378	1.589
7987405	RASGRP1	RAS guanyl releasing protein 1 (calcium and DAG-regulated)	6.607	8.178	7.744	7.966	1.571
8095751	PARM1	prostate androgen-regulated mucin-like protein 1	7.655	9.225	8.199	8.571	1.570
8112980	EDIL3	EGF-like repeats and discoidin I-like domains 3	5.426	6.991	5.630	6.419	1.565
8063923	SLCO4A1	solute carrier organic anion transporter family, member 4A1	8.780	10.293	9.448	9.586	1.513
7971150	LHFP	lipoma HMGIC fusion partner	8.769	10.268	9.647	9.758	1.500
7901993	CACHD1	cache domain containing 1	5.088	6.582	6.714	6.915	1.495
8059854	ARL4C	ADP-ribosylation factor-like 4C	8.782	10.269	9.768	9.880	1.487
8066754	C20orf123	chromosome 20 open reading frame 123	8.142	9.627	9.344	9.471	1.485
7972682	KDELC1	KDEL (Lys-Asp-Glu-Leu) containing 1	5.323	6.804	5.560	5.979	1.480
8140367	CCL24	chemokine (C-C motif) ligand 24	6.257	7.728	7.239	8.233	1.472
8111153	MYO10	myosin X	8.181	9.647	9.237	9.187	1.466
7946446	NRIP3	nuclear receptor interacting protein 3	10.101	11.566	10.988	11.081	1.466
7969171	DLEU1	deleted in lymphocytic leukemia 1 (non-protein coding)	7.382	8.829	7.792	7.903	1.447
8111136	FAM134B	family with sequence similarity 134, member B	7.758	9.194	8.463	8.848	1.435
7963946	MMP19	matrix metallopeptidase 19	10.383	11.805	11.587	11.679	1.423
8086538	LOC644714	hypothetical LOC644714	6.422	7.833	6.976	7.384	1.411
8100971	PPBP	pro-platelet basic protein (chemokine (C-X-C motif) ligand 7)	8.795	10.205	10.247	10.939	1.410
8154233	CD274	CD274 molecule	7.257	8.666	8.685	8.954	1.409
8166202	GRPR	gastrin-releasing peptide receptor	5.608	6.988	6.671	6.637	1.380
8134030	STEAP1	six transmembrane epithelial antigen of the prostate 1	8.038	9.415	8.591	9.060	1.377
7917283	MCOLN2	mucolipin 2	6.700	8.077	8.139	8.004	1.377
8166784	TSPAN7	tetraspanin 7	7.053	8.425	8.327	8.458	1.372
7995829	MT1H	metallothionein 1H	8.889	10.248	10.237	11.900	1.359
7975787	JDP2	Jun dimerization protein 2	10.179	11.534	11.068	10.997	1.354
7932160	FAM107B	family with sequence similarity 107, member B	9.205	10.552	10.429	10.486	1.347
7922474	KIAA0040	KIAA0040	10.121	11.465	10.802	11.007	1.344
8156897	C9orf30	chromosome 9 open reading frame 30	10.309	11.647	11.484	11.630	1.338
8095728	EREG	epiregulin	7.994	9.321	10.264	11.027	1.327
7983650	SLC27A2	solute carrier family 27 (fatty acid transporter), member 2	6.180	7.496	5.553	5.956	1.316
8128553	BVES	blood vessel epicardial substance	5.510	6.819	5.821	6.501	1.309
8071147	TUBA8	tubulin, alpha 8	7.935	9.240	8.817	8.896	1.304

7903092	FNBP1L	formin binding protein 1-like	8.640	9.945	9.092	9.351	1.304
8014700	C17orf96	chromosome 17 open reading frame 96	6.781	8.084	8.184	8.233	1.303
8162850	TEX10	testis expressed 10	8.944	10.240	9.843	9.990	1.297
7949264	EHD1	EH-domain containing 1	8.575	9.856	9.901	9.884	1.281
8172425	SLC38A5	solute carrier family 38, member 5	6.029	7.304	6.933	6.645	1.275
7962183	AK4	adenylate kinase 4	8.159	9.423	9.018	9.153	1.265
8101126	CXCL10	chemokine (C-X-C motif) ligand 10	8.066	9.324	9.126	10.257	1.259
8006440	CCL7	chemokine (C-C motif) ligand 7	7.527	8.781	8.234	9.333	1.254
7982366	SCG5	secretogranin V (7B2 protein)	6.376	7.629	7.625	7.793	1.253
8151334	MSC	musculin	9.181	10.433	10.659	10.904	1.253
8069269	COL6A1	collagen, type VI, alpha 1	8.977	10.222	10.288	10.322	1.245
8017843	SLC16A6	solute carrier family 16, member 6 (monocarboxylic acid transporter 7)	9.505	10.749	11.289	11.308	1.244
8089261	CBLB	Cas-Br-M (murine) ecotropic retroviral transforming sequence b	10.686	11.909	11.636	11.653	1.223
8098263	PALLD	palladin, cytoskeletal associated protein	6.892	8.114	7.250	7.665	1.222
7977621	NDRG2	NDRG family member 2	9.343	10.561	10.689	10.944	1.218
8102050	NHEDC2	Na+/H+ exchanger domain containing 2	10.983	12.201	11.572	11.819	1.218
8023727	DSEL	dermatan sulfate epimerase-like	4.837	6.042	5.265	5.454	1.205
7956878	IRAK3	interleukin-1 receptor-associated kinase 3	8.914	10.115	10.087	10.279	1.201
8091715	LXN	latexin	8.506	9.706	9.340	9.513	1.200
7927280	PPYR1	pancreatic polypeptide receptor 1	5.160	6.358	4.756	5.736	1.199
8135218	LRRC17	leucine rich repeat containing 17	5.347	6.535	5.197	5.802	1.188
8117079	LOC644714	hypothetical LOC644714	6.116	7.302	6.098	6.914	1.186
7983478	C15orf48	chromosome 15 open reading frame 48	8.107	9.285	9.086	9.498	1.178
7974835	PRKCH	protein kinase C, eta	9.233	10.411	9.913	10.115	1.177
8145122	SLC39A14	solute carrier family 39 (zinc transporter), member 14	7.826	8.994	8.575	8.679	1.168
8001531	MT1G	metallothionein 1G	11.624	12.765	12.702	13.511	1.142
8051298	GALNT14	UDP-N-acetyl-alpha-D-galactosamine:polypeptide N-acetylgalactosaminyltransferase 14 (GalNAc-T14)	7.735	8.860	8.470	8.336	1.124
7972674	C13orf27	chromosome 13 open reading frame 27	7.930	9.047	8.141	8.303	1.117
8121257	PRDM1	PR domain containing 1, with ZNF domain	9.841	10.948	10.731	10.765	1.108
7961111	CLEC1A	C-type lectin domain family 1, member A	6.067	7.174	7.231	7.983	1.107
8166797	MID1IP1	MID1 interacting protein 1 (gastrulation specific G12 homolog (zebrafish))	9.765	10.868	10.498	10.547	1.103
8147132	CA2	carbonic anhydrase II	11.197	12.296	12.084	12.098	1.099
8092726	CLDN1	claudin 1	8.748	9.846	8.509	9.159	1.098
8099850	TMEM156	transmembrane protein 156	5.120	6.216	5.458	5.886	1.097
8089112	FILIP1L	filamin A interacting protein 1-like	8.305	9.398	9.154	9.228	1.093
8101131	CXCL11	chemokine (C-X-C motif) ligand 11	4.786	5.878	5.373	6.051	1.092
8105411	IL31RA	interleukin 31 receptor A	5.173	6.260	5.430	5.815	1.087
7902861	LRRC8B	leucine rich repeat containing 8 family, member B	9.262	10.346	9.654	10.020	1.084
8089082	DCBLD2	discoidin, CUB and LCCL domain containing 2	8.910	9.990	9.355	9.444	1.080
7914603	RNF19B	ring finger protein 19B	9.167	10.246	10.029	10.006	1.079
8148029	COLEC10	collectin sub-family member 10 (C-type lectin)	4.900	5.978	5.460	5.668	1.078
7924996	C1orf198	chromosome 1 open reading frame 198	8.765	9.839	9.504	9.672	1.074
8064904	FERMT1	fermitin family member 1	5.187	6.261	5.579	5.763	1.074
7977270	LOC388022	hypothetical LOC388022	8.939	10.011	10.116	9.903	1.072
8136115	FAM40B	family with sequence similarity 40, member B	7.752	8.822	7.778	8.119	1.069
7930074	NFKB2	nuclear factor of kappa light polypeptide gene enhancer in B-cells 2 (p49/p100)	8.476	9.541	9.394	9.548	1.065
8135069	SERPINE1	serpin peptidase inhibitor, clade E (nexin, plasminogen activator inhibitor type 1), member 1	9.137	10.201	10.738	10.752	1.064
8129953	HIVEP2	human immunodeficiency virus type I enhancer binding protein 2	6.477	7.538	7.251	7.369	1.061
7948910	SNORD25	small nucleolar RNA, C/D box 25	4.754	5.811	5.070	5.128	1.058
8102800	SLC7A11	solute carrier family 7, (cationic amino acid transporter, y+ system) member 11	9.591	10.641	11.578	11.885	1.050
8141016	TFPI2	tissue factor pathway inhibitor 2	4.704	5.747	5.035	5.199	1.043
8161442	FAM27D1	family with sequence similarity 27, member D1	6.891	7.932	7.939	7.472	1.041
7918657	PTPN22	protein tyrosine phosphatase, non-receptor type 22 (lymphoid)	10.777	11.805	11.144	11.404	1.027
8022338	GPR125	G protein-coupled receptor 125	6.964	7.991	7.005	6.934	1.027
8006736	DUSP14	dual specificity phosphatase 14	8.041	9.066	8.524	8.695	1.025
8131927	MPP6	membrane protein, palmitoylated 6 (MAGUK p55 subfamily member 6)	6.536	7.558	6.776	7.006	1.022
8135587	CAV2	caveolin 2	5.550	6.566	5.515	5.818	1.016
8086880	CDC25A	cell division cycle 25 homolog A (S. pombe)	7.415	8.431	7.287	7.303	1.016
7938834	NAV2	neuron navigator 2	5.947	6.960	6.519	6.787	1.013
7992789	TNFRSF12A	tumor necrosis factor receptor superfamily, member 12A	9.586	10.599	10.346	10.266	1.013
8014316	CCL5	chemokine (C-C motif) ligand 5	10.666	11.678	11.402	11.500	1.013
8071044	MAFIP	MAFF interacting protein	7.905	8.912	8.773	8.767	1.007
8112274	ELOVL7	ELOVL family member 7, elongation of long chain fatty acids (yeast)	6.248	7.251	7.138	7.321	1.003
8147848	OXR1	oxidation resistance 1	9.561	10.563	9.773	10.054	1.002
8008819	YPEL2	yippee-like 2 (Drosophila)	9.241	8.239	8.571	8.697	-1.002
8152988	SLA	Src-like-adaptor	10.466	9.464	9.521	9.480	-1.002
8093858	STK32B	serine/threonine kinase 32B	6.902	5.899	5.806	5.525	-1.003
7940237	MS4A4A	membrane-spanning 4-domains, subfamily A, member 4	10.754	9.744	9.211	9.639	-1.010
8091523	P2RY13	purinergic receptor P2Y, G-protein coupled, 13	6.350	5.337	5.326	5.535	-1.013
8140556	HGF	hepatocyte growth factor (hepapoietin A; scatter factor)	7.510	6.492	6.234	6.300	-1.018
8033445	CD209	CD209 molecule	9.732	8.708	8.611	8.851	-1.024
8163839	C5	complement component 5	7.615	6.590	6.105	6.428	-1.025
7971486	C13orf18	chromosome 13 open reading frame 18	7.794	6.768	6.539	6.746	-1.026
8128698	SESN1	sestrin 1	9.378	8.350	8.303	8.472	-1.028
8044813	TMEM37	transmembrane protein 37	10.617	9.585	9.631	9.735	-1.032
7984932	SCAMP5	secretory carrier membrane protein 5	7.715	6.648	6.733	6.689	-1.068
7981960	SNORD116-6	small nucleolar RNA, C/D box 116-6	6.881	5.812	5.702	5.727	-1.069
8137244	GIMAP4	GTPase, IMAP family member 4	8.209	7.137	7.018	7.212	-1.072
8063785	C20orf197	chromosome 20 open reading frame 197	6.336	5.262	5.289	5.056	-1.074
7978272	CIDEB	cell death-inducing DFFA-like effector b	8.181	7.102	7.015	7.001	-1.078
8122637	SASH1	SAM and SH3 domain containing 1	9.258	8.178	8.473	8.547	-1.080
8009653	CD300A	CD300a molecule	9.418	8.328	8.464	8.548	-1.090
8059680	HTR2B	5-hydroxytryptamine (serotonin) receptor 2B	8.597	7.504	7.897	8.182	-1.093
7906377	MNDA	myeloid cell nuclear differentiation antigen	10.482	9.372	9.181	9.570	-1.110
7965873	IGF1	insulin-like growth factor 1 (somatomedin C)	10.331	9.204	9.645	9.919	-1.126
8114536	TMEM173	transmembrane protein 173	9.559	8.420	8.143	7.877	-1.140
8078619	ITGA9	integrin, alpha 9	8.817	7.674	7.761	7.630	-1.143
8089568	CD200R1	CD200 receptor 1	9.781	8.637	8.253	8.203	-1.144
7908376	RGS18	regulator of G-protein signaling 18	8.684	7.535	7.148	7.568	-1.149
7954436	LRMP	lymphoid-restricted membrane protein	8.919	7.769	7.678	7.977	-1.149
8098611	TLR3	toll-like receptor 3	8.758	7.601	7.323	7.538	-1.156
8115397	C5orf4	chromosome 5 open reading frame 4	8.109	6.951	7.021	6.820	-1.158
8060997	SPTLC3	serine palmitoyltransferase, long chain base subunit 3	7.144	5.973	5.719	5.903	-1.171
8002969	MAF	v-maf musculoaponeurotic fibrosarcoma oncogene homolog (avian)	9.360	8.189	8.341	8.341	-1.171
8122827	C6orf97	chromosome 6 open reading frame 97	8.532	7.354	7.178	7.139	-1.178
7968344	ALOX5AP	arachidonate 5-lipoxygenase-activating protein	12.155	10.967	10.853	10.973	-1.188

8101449	HPSE	heparanase	9.426	8.234	7.707	7.961	-1.192
8082673	ACPP	acid phosphatase, prostate	9.140	7.938	7.953	8.014	-1.202
7929344	GPR120	G protein-coupled receptor 120	8.680	7.469	7.303	7.361	-1.211
7939383	PRR5L	proline rich 5 like	7.713	6.502	6.415	6.362	-1.211
8065359	CD93	CD93 molecule	10.806	9.584	9.532	9.590	-1.221
8143781	GIMAP6	GTPase, IMAP family member 6	9.325	8.100	7.856	7.935	-1.225
8067040	NFATC2	nuclear factor of activated T-cells, cytoplasmic, calcineurin-dependent 2	7.032	5.793	5.945	5.765	-1.240
7919133	FCGR1B	Fc fragment of IgG, high affinity Ib, receptor (CD64)	10.571	9.327	8.957	9.343	-1.244
7905047	FCGR1A	Fc fragment of IgG, high affinity Ia, receptor (CD64)	10.851	9.602	9.186	9.636	-1.249
7905060	FCGR1A	Fc fragment of IgG, high affinity Ia, receptor (CD64)	10.525	9.273	8.901	9.274	-1.252
8092169	TNFSF10	tumor necrosis factor (ligand) superfamily, member 10	9.412	8.157	7.860	8.509	-1.256
8163908	GGTA1	glycoprotein, alpha-galactosyltransferase 1 pseudogene	10.273	9.015	8.626	9.057	-1.258
8064451	SIRPB2	signal-regulatory protein beta 2	7.803	6.514	6.611	6.594	-1.289
7948455	MS4A6A	membrane-spanning 4-domains, subfamily A, member 6A	10.212	8.877	8.726	8.963	-1.335
8084717	ST6GAL1	ST6 beta-galactosamide alpha-2,6-sialyltranferase 1	10.883	9.534	8.980	9.116	-1.349
8166059	TLR7	toll-like receptor 7	9.108	7.740	7.519	7.540	-1.367
7906777	FCGR2B	Fc fragment of IgG, low affinity IIb, receptor (CD32)	8.765	7.373	7.278	7.434	-1.393
7904158	OLFML3	olfactomedin-like 3	9.021	7.597	7.285	7.271	-1.424
7986195	SV2B	synaptic vesicle glycoprotein 2B	7.960	6.491	6.270	6.376	-1.470
8057677	SLC40A1	solute carrier family 40 (iron-regulated transporter), member 1	9.534	8.028	7.765	8.135	-1.506
8141094	PDK4	pyruvate dehydrogenase kinase, isozyme 4	9.310	7.784	8.502	8.998	-1.526
7940441	PGA5	pepsinogen 5, group I (pepsinogen A)	11.175	9.645	9.269	9.087	-1.531
7940431	PGA4	pepsinogen 4, group I (pepsinogen A)	11.337	9.786	9.443	9.256	-1.551
8036787	FCGBP	Fc fragment of IgG binding protein	9.676	8.120	8.082	7.927	-1.556
8007100	IGFBP4	insulin-like growth factor binding protein 4	11.538	9.967	9.752	9.715	-1.571
8101780	HPGDS	hematopoietic prostaglandin D synthase	10.633	9.059	8.458	8.841	-1.574
7940421	PGA3	pepsinogen 3, group I (pepsinogen A)	11.433	9.837	9.500	9.331	-1.595
8155754	MAMDC2	MAM domain containing 2	6.550	4.905	5.038	4.984	-1.645
8130408	IPCEF1	interaction protein for cytohesin exchange factors 1	8.769	7.116	6.642	7.207	-1.654
8123744	F13A1	coagulation factor XIII, A1 polypeptide	12.574	10.742	11.122	11.306	-1.832
7961151	KLRK1	killer cell lectin-like receptor subfamily K, member 1	6.016	4.089	3.803	3.985	-1.927
8152976	TMEM71	transmembrane protein 71	8.040	5.833	5.692	5.820	-2.208
7946579	LYVE1	lymphatic vessel endothelial hyaluronan receptor 1	8.430	5.603	5.138	5.253	-2.827

Appendix V

List of genes induced by RANKL counter-regulated by GSK-J4 at day 8 in differentiating osteoclast

Probe ID	Gene symbol	Gene Name	m	mr	j4	j5	folds(mr-m)	folds (J4-m)
8145122	SLC39A14	solute carrier family 39 (zinc transporter), member 14	7.826	8.994	8.575	8.679	1.168	0.750
7924996	C1orf198	chromosome 1 open reading frame 198	8.765	9.839	9.504	9.672	1.074	0.739
8014316	CCL5	chemokine (C-C motif) ligand 5	10.666	11.678	11.402	11.500	1.013	0.736
8051298	GALNT14	UDP-N-acetyl-alpha-D-galactosamine:polypeptide N-acetylgalactosaminyltransferase 14 (GalNAc-T14)	7.735	8.860	8.470	8.336	1.124	0.735
8166797	MID1IP1	MID1 interacting protein 1 (gastrulation specific G12 homolog (zebrafish))	9.765	10.868	10.498	10.547	1.103	0.733
8006440	CCL7	chemokine (C-C motif) ligand 7	7.527	8.781	8.234	9.333	1.254	0.708
8111136	FAM134B	family with sequence similarity 134, member B	7.758	9.194	8.463	8.848	1.435	0.704
8106820	POLR3G	polymerase (RNA) III (DNA directed) polypeptide G (32kD)	7.553	9.143	8.253	8.378	1.589	0.699
8147012	PKIA	protein kinase (cAMP-dependent, catalytic) inhibitor alpha	7.291	9.247	7.976	8.401	1.956	0.685
7922474	KIAA0040	KIAA0040	10.121	11.465	10.802	11.007	1.344	0.682
7974835	PRKCH	protein kinase C, eta	9.233	10.411	9.913	10.115	1.177	0.680
8063923	SLCO4A1	solute carrier organic anion transporter family, member 4A1	8.780	10.293	9.448	9.586	1.513	0.668
7964759	GRIP1	glutamate receptor interacting protein 1	5.143	6.831	5.754	6.265	1.688	0.611
8138527	MGC87042	STEAP family protein MGC87042	6.174	7.888	6.781	7.479	1.714	0.607
8102050	NHEDC2	Na+/H+ exchanger domain containing 2	10.983	12.201	11.572	11.819	1.218	0.589
8101131	CXCL11	chemokine (C-X-C motif) ligand 11	4.786	5.878	5.373	6.051	1.092	0.587
7938834	NAV2	neuron navigator 2	5.947	6.960	6.519	6.787	1.013	0.573
8148029	COLEC10	collectin sub-family member 10 (C-type lectin)	4.900	5.978	5.460	5.668	1.078	0.561
8086538	LOC644714	hypothetical LOC644714	6.422	7.833	6.976	7.384	1.411	0.554
8134030	STEAP1	six transmembrane epithelial antigen of the prostate 1	8.038	9.415	8.591	9.060	1.377	0.553
8095751	PARM1	prostate androgen-regulated mucin-like protein 1	7.655	9.225	8.199	8.571	1.570	0.543
8135601	MET	met proto-oncogene (hepatocyte growth factor receptor)	4.407	6.265	4.945	5.619	1.858	0.538
8103812	ASB5	ankyrin repeat and SOCS box-containing 5	5.350	7.675	5.841	7.232	2.325	0.491
8006736	DUSP14	dual specificity phosphatase 14	8.041	9.066	8.524	8.695	1.025	0.483
7903092	FNBP1L	formin binding protein 1-like	8.640	9.945	9.092	9.351	1.304	0.452
8089082	DCBLD2	discoidin, CUB and LCCL domain containing 2	8.910	9.990	9.355	9.444	1.080	0.445
8023727	DSEL	dermatan sulfate epimerase-like	4.837	6.042	5.265	5.454	1.205	0.428
7969171	DLEU1	deleted in lymphocytic leukemia 1 (non-protein coding)	7.382	8.829	7.792	7.903	1.447	0.409
7902861	LRRC8B	leucine rich repeat containing 8 family, member B	9.262	10.346	9.654	10.020	1.084	0.392
8064904	FERMT1	fermitin family member 1	5.187	6.261	5.579	5.763	1.074	0.392
7918657	PTPN22	protein tyrosine phosphatase, non-receptor type 22 (lymphoid)	10.777	11.805	11.144	11.404	1.027	0.366
8098263	PALLD	palladin, cytoskeletal associated protein	6.892	8.114	7.250	7.665	1.222	0.358
8099850	TMEM156	transmembrane protein 156	5.120	6.216	5.458	5.886	1.097	0.338
8141016	TFPI2	tissue factor pathway inhibitor 2	4.704	5.747	5.035	5.199	1.043	0.331
7948910	SNORD25	small nucleolar RNA, C/D box 25	4.754	5.811	5.070	5.128	1.058	0.316
8128553	BVES	blood vessel epicardial substance	5.510	6.819	5.821	6.501	1.309	0.311
8105411	IL31RA	interleukin 31 receptor A	5.173	6.260	5.430	5.815	1.087	0.257
8131927	MPP6	membrane protein, palmitoylated 6 (MAGUK p55 subfamily member 6)	6.536	7.558	6.776	7.006	1.022	0.240
7972682	KDELC1	KDEL (Lys-Asp-Glu-Leu) containing 1	5.323	6.804	5.560	5.979	1.480	0.236
8147848	OXR1	oxidation resistance 1	9.561	10.563	9.773	10.054	1.002	0.212
7972674	C13orf27	chromosome 13 open reading frame 27	7.930	9.047	8.141	8.303	1.117	0.211
8112980	EDIL3	EGF-like repeats and discoidin I-like domains 3	5.426	6.991	5.630	6.419	1.565	0.204
8022338	GPR125	G protein-coupled receptor 125	6.964	7.991	7.005	6.934	1.027	0.041
8136115	FAM40B	family with sequence similarity 40, member B	7.752	8.822	7.778	8.119	1.069	0.025
8135594	CAV1	caveolin 1, caveolae protein, 22kDa	5.188	6.932	5.194	5.734	1.744	0.006
8117079	LOC644714	hypothetical LOC644714	6.116	7.302	6.098	6.914	1.186	-0.018
8135587	CAV2	caveolin 2	5.550	6.566	5.515	5.818	1.016	-0.036
8086880	CDC25A	cell division cycle 25 homolog A (S. pombe)	7.415	8.431	7.287	7.303	1.016	-0.128
8135218	LRRC17	leucine rich repeat containing 17	5.347	6.535	5.197	5.802	1.188	-0.151
8092726	CLDN1	claudin 1	8.748	9.846	8.509	9.159	1.098	-0.239
7927280	PPYR1	pancreatic polypeptide receptor 1	5.160	6.358	4.756	5.736	1.199	-0.403
7983650	SLC27A2	solute carrier family 27 (fatty acid transporter), member 2	6.180	7.496	5.553	5.956	1.316	-0.627
8008819	YPEL2	yippee-like 2 (Drosophila)	9.241	8.239	8.571	8.697	-1.002	-0.670
7965873	IGF1	insulin-like growth factor 1 (somatomedin C)	10.331	9.204	9.645	9.919	-1.126	-0.686
8059680	HTR2B	5-hydroxytryptamine (serotonin) receptor 2B	8.597	7.504	7.897	8.182	-1.093	-0.700

Appendix VI

List of osteoclast genes induced by RANKL at day 14 in differentiating osteoclast

Probe ID	Gene symbol	Gene Name	m	mR	j4	j5	folds (mr-m)
8091411	TM4SF1	transmembrane 4 L six family member 1	5.855	11.569	10.109	10.956	5.714
8021635	SERPINB2	serpin peptidase inhibitor, clade B (ovalbumin), member 2	4.829	9.885	11.214	9.611	5.056
8135601	MET	met proto-oncogene (hepatocyte growth factor receptor)	5.266	9.996	7.987	9.127	4.730
8103812	ASB5	ankyrin repeat and SOCS box-containing 5	6.374	10.502	9.340	7.772	4.128
8150550	CHRNA6	cholinergic receptor, nicotinic, alpha 6	5.231	9.261	8.008	8.262	4.030
8140650	SEMA3E	sema domain, immunoglobulin domain (Ig), short basic domain, secreted, (semaphorin) 3E	4.981	8.677	5.836	6.758	3.697
8128565	POPDC3	popeye domain containing 3	5.888	9.310	8.406	9.180	3.422
8075310	LIF	leukemia inhibitory factor (cholinergic differentiation factor)	6.530	9.873	8.518	9.349	3.343
8105741	MAST4	microtubule associated serine/threonine kinase family member 4	6.502	9.631	8.096	8.924	3.130
7910727	ACTN2	actinin, alpha 2	6.701	9.819	8.011	8.688	3.118
8048763	KIAA1486	KIAA1486	5.773	8.871	7.403	7.898	3.098
8100798	SULT1B1	sulfotransferase family, cytosolic, 1B, member 1	7.241	10.335	6.994	9.597	3.095
8102342	ELOVL6	ELOVL family member 6, elongation of long chain fatty acids (FEN1/Elo2, SUR4/Elo3-like, yeast)	7.288	10.382	9.293	9.735	3.094
8169249	MID2	midline 2	6.723	9.812	7.943	8.465	3.088
8111136	FAM134B	family with sequence similarity 134, member B	8.427	11.494	9.868	10.884	3.067
8058063	RFTN2	raftlin family member 2	7.454	10.510	8.493	10.074	3.057
8100362	LNX1	ligand of numb-protein X 1	6.790	9.805	8.319	8.336	3.014
7990080	LARP6	La ribonucleoprotein domain family, member 6	6.756	9.749	8.192	9.466	2.994
8099633	PPARGC1A	peroxisome proliferator-activated receptor gamma, coactivator 1 alpha	5.712	8.669	6.454	7.224	2.957
8162254	DIRAS2	DIRAS family, GTP-binding RAS-like 2	6.981	9.854	7.501	9.142	2.873
8109563	NIPAL4	NIPA-like domain containing 4	7.397	10.198	8.764	8.451	2.801
8082974	ESYT3	extended synaptotagmin-like protein 3	6.692	9.484	7.793	8.770	2.791
8000574	NUPR1	nuclear protein, transcriptional regulator, 1	8.452	11.209	10.646	10.063	2.757
8100298	OCIAD2	OCIA domain containing 2	6.786	9.509	7.990	9.037	2.724
8143154	DGKI	diacylglycerol kinase, iota	7.141	9.852	8.509	9.063	2.711
7953532	ENO2	enolase 2 (gamma, neuronal)	7.693	10.372	8.820	9.656	2.679
8023757	CD226	CD226 molecule	5.848	8.506	9.406	8.661	2.658
8164343	FAM102A	family with sequence similarity 102, member A	8.193	10.826	10.045	10.588	2.633
7984001	GCNT3	glucosaminyl (N-acetyl) transferase 3, mucin type	6.333	8.947	7.647	7.968	2.614
8120011	SPATS1	spermatogenesis associated, serine-rich 1	6.348	8.947	7.802	8.278	2.598
7926916	ZEB1	zinc finger E-box binding homeobox 1	7.775	10.341	8.640	9.637	2.567
8021376	NEDD4L	neural precursor cell expressed, developmentally down-regulated 4-like	7.477	10.027	8.727	9.144	2.550
8097282	SPRY1	sprouty homolog 1, antagonist of FGF signaling (Drosophila)	7.303	9.852	8.140	8.441	2.549
8087611	HYAL1	hyaluronoglucosaminidase 1	8.218	10.754	9.814	10.710	2.536
7909789	TGFB2	transforming growth factor, beta 2	6.748	9.284	7.626	6.943	2.536
8063923	SLCO4A1	solute carrier organic anion transporter family, member 4A1	8.803	11.322	9.536	10.754	2.519
8151816	GEM	GTP binding protein overexpressed in skeletal muscle	7.131	9.643	8.202	8.428	2.512
8092541	LIPH	lipase, member H	5.608	8.033	6.544	7.412	2.425
7943413	BIRC3	baculoviral IAP repeat-containing 3	8.200	10.578	9.839	10.301	2.378
8065084	LOC613266	hypothetical LOC613266	6.741	9.063	8.380	8.545	2.322
8134091	CLDN12	claudin 12	8.924	11.231	10.329	10.657	2.308
7920278	S100A3	S100 calcium binding protein A3	6.596	8.887	7.432	8.138	2.290
7909225	DYRK3	dual-specificity tyrosine-(Y)-phosphorylation regulated kinase 3	7.789	10.077	8.727	9.203	2.288
7926875	BAMBI	BMP and activin membrane-bound inhibitor homolog (Xenopus laevis)	8.645	10.931	10.028	10.705	2.286
8092707	LEPREL1	leprecan-like 1	7.466	9.748	7.657	9.411	2.283
8131600	TSPAN13	tetraspanin 13	7.190	9.455	8.341	9.199	2.265
7985147	DNAJA4	DnaJ (Hsp40) homolog, subfamily A, member 4	8.694	10.943	9.586	10.519	2.248
7996219	NDRG4	NDRG family member 4	6.973	9.213	8.172	8.914	2.240
8041225	EHD3	EH-domain containing 3	7.847	10.076	8.962	9.443	2.229
8171205	NLGN4X	neuroligin 4, X-linked	5.684	7.909	6.475	7.468	2.225
7938834	NAV2	neuron navigator 2	6.422	8.646	7.409	8.475	2.224
7919699	OTUD7B	OTU domain containing 7B	5.403	7.625	6.221	6.649	2.222
7917875	F3	coagulation factor III (thromboplastin, tissue factor)	8.399	10.612	9.208	8.860	2.213
8022747	B4GALT6	UDP-Gal:betaGlcNAc beta 1,4- galactosyltransferase, polypeptide 6	6.910	9.113	7.257	7.930	2.203
8136115	FAM40B	family with sequence similarity 40, member B	8.555	10.743	9.248	10.375	2.188
8095680	IL8	interleukin 8	10.632	12.817	13.417	12.273	2.185
8006736	DUSP14	dual specificity phosphatase 14	8.472	10.603	9.381	9.597	2.131
7902810	LMO4	LIM domain only 4	6.907	9.032	7.867	8.220	2.125
7922174	F5	coagulation factor V (proaccelerin, labile factor)	7.702	9.826	8.708	9.554	2.124
8100971	PPBP	pro-platelet basic protein (chemokine (C-X-C motif) ligand 7)	9.069	11.179	10.341	10.203	2.110
7979204	FERMT2	fermitin family member 2	6.140	8.246	7.196	6.678	2.106
8147012	PKIA	protein kinase (cAMP-dependent, catalytic) inhibitor alpha	7.669	9.763	8.159	9.462	2.094
8111892	OXCT1	3-oxoacid CoA transferase 1	9.344	11.436	10.599	11.189	2.092
7915472	SLC2A1	solute carrier family 2 (facilitated glucose transporter), member 1	9.142	11.229	9.873	10.605	2.087
7981427	CKB	creatine kinase, brain	10.710	12.782	12.163	12.821	2.073
7951271	MMP1	matrix metallopeptidase 1 (interstitial collagenase)	4.773	6.845	5.958	5.275	2.072
8006440	CCL7	chemokine (C-C motif) ligand 7	7.873	9.924	10.720	9.573	2.050
8109773	WWC1	WW and C2 domain containing 1	7.239	9.284	7.887	8.916	2.045
8109629	FABP6	fatty acid binding protein 6, ileal	6.020	8.063	6.489	8.498	2.043
7942328	FOLR3	folate receptor 3 (gamma)	6.843	8.870	8.183	8.071	2.027
8098263	PALLD	palladin, cytoskeletal associated protein	7.774	9.795	8.463	8.742	2.021
8032789	STAP2	signal transducing adaptor family member 2	5.920	7.928	6.836	7.410	2.008
8059376	SERPINE2	serpin peptidase inhibitor, clade E (nexin, plasminogen activator inhibitor type 1), member 2	5.537	7.529	6.714	7.050	1.993
8095728	EREG	epiregulin	8.310	10.296	11.999	10.440	1.986
8044212	SULT1C2	sulfotransferase family, cytosolic, 1C, member 2	8.117	10.099	9.560	9.984	1.983
8142270	NRCAM	neuronal cell adhesion molecule	6.330	8.306	7.847	7.668	1.977
8068361	SLC5A3	solute carrier family 5 (sodium/myo-inositol cotransporter), member 3	10.495	12.471	11.532	12.122	1.977
8100977	CXCL5	chemokine (C-X-C motif) ligand 5	10.584	12.559	12.663	12.423	1.975
8146660	DNAJC5B	DnaJ (Hsp40) homolog, subfamily C, member 5 beta	6.577	8.546	8.621	8.033	1.969
8046124	DHRS9	dehydrogenase/reductase (SDR family) member 9	8.687	10.649	9.326	10.025	1.962
8150076	DUSP4	dual specificity phosphatase 4	7.439	9.399	7.857	8.391	1.960
8091550	KIAA1328	KIAA1328	7.923	9.871	8.303	9.002	1.948
7964759	GRIP1	glutamate receptor interacting protein 1	5.265	7.206	6.206	5.802	1.941
8123176	MAS1	MAS1 oncogene	5.488	7.421	6.873	6.251	1.933
8072170	KREMEN1	kringle containing transmembrane protein 1	6.619	8.550	7.157	7.813	1.931
8173551	PHKA1	phosphorylase kinase, alpha 1 (muscle)	7.370	9.290	7.962	8.772	1.920
7934411	USP54	ubiquitin specific peptidase 54	6.897	8.813	7.375	8.028	1.915
7969861	ITGBL1	integrin, beta-like 1 (with EGF-like repeat domains)	6.542	8.447	7.077	8.186	1.905
7946446	NRIP3	nuclear receptor interacting protein 3	10.601	12.503	11.755	12.214	1.902
8103226	TMEM154	transmembrane protein 154	5.485	7.386	5.604	6.485	1.902
8021001	KIAA1328	KIAA1328	6.634	8.515	7.073	7.542	1.881
7902189	IL23R	interleukin 23 receptor	4.180	6.042	5.433	4.710	1.862
7916024	TTC39A	tetratricopeptide repeat domain 39A	6.305	8.162	7.369	7.690	1.857
8106743	VCAN	versican	4.934	6.779	5.552	7.885	1.845
8155673	PIP5K1B	phosphatidylinositol-4-phosphate 5-kinase, type I, beta	6.183	8.026	6.814	7.019	1.843
8145122	SLC39A14	solute carrier family 39 (zinc transporter), member 14	7.682	9.507	8.646	8.784	1.825
8147848	OXR1	oxidation resistance 1	10.015	11.838	10.650	11.100	1.823
8129880	PERP	PERP, TP53 apoptosis effector	6.891	8.708	8.002	8.309	1.817
8068353	SLC5A3	solute carrier family 5 (sodium/myo-inositol cotransporter), member 3	10.225	12.038	11.111	11.723	1.813
7983228	MAP1A	microtubule-associated protein 1A	6.941	8.753	7.863	8.893	1.812
8042283	HSPC159	galectin-related protein	9.017	10.825	9.906	10.201	1.808
7913787	C1orf201	chromosome 1 open reading frame 201	6.441	8.237	7.094	7.797	1.796
7995292	SLC6A8	solute carrier family 6 (neurotransmitter transporter, creatine), member 8	9.143	10.923	10.156	10.677	1.780
7980316	TGFB3	transforming growth factor, beta 3	5.997	7.763	6.165	7.282	1.766
8174985	SMARCA1	SWI/SNF related, matrix associated, actin dependent regulator of chromatin, subfamily a, member 1	4.819	6.582	5.601	5.824	1.763
8080911	KBTBD8	kelch repeat and BTB (POZ) domain containing 8	7.763	9.515	8.548	8.329	1.752
8089820	GPR156	G protein-coupled receptor 156	5.288	7.037	5.992	6.081	1.749
8105267	ITGA2	integrin, alpha 2 (CD49B, alpha 2 subunit of VLA-2 receptor)	9.046	10.777	9.477	10.373	1.731
8081288	TMEM45A	transmembrane protein 45A	5.949	7.677	6.695	7.126	1.728
8158183	DNM1	dynamin 1	7.803	9.529	8.378	9.217	1.726
8115455	HAVCR1	hepatitis A virus cellular receptor 1	6.045	7.754	7.008	6.614	1.709
7974870	SNAPC1	small nuclear RNA activating complex, polypeptide 1, 43kDa	8.694	10.398	9.190	8.607	1.704
8058221	TRAK2	trafficking protein, kinesin binding 2	10.146	11.848	10.829	11.293	1.702
8041048	FOSL2	FOS-like antigen 2	9.488	11.186	10.551	11.084	1.697
7982366	SCG5	secretogranin V (7B2 protein)	6.829	8.526	7.901	8.078	1.697
8062844	TTPAL	tocopherol (alpha) transfer protein-like	7.279	8.966	7.987	8.753	1.687
8169473	PLS3	plastin 3	8.698	10.383	8.767	9.591	1.685
7922474	KIAA0040	KIAA0040	10.591	12.275	11.176	12.029	1.684
8070665	SIK1	salt-inducible kinase 1	7.425	9.107	8.264	8.692	1.682
7968029	PCOTH	prostate collagen triple helix	6.223	7.904	7.017	7.247	1.681
7981514	AHNAK2	AHNAK nucleoprotein 2	7.655	9.334	8.528	9.181	1.678
8080714	FLNB	filamin B, beta	8.336	10.001	9.006	9.869	1.665
7962183	AK4	adenylate kinase 4	8.460	10.121	8.974	9.663	1.661
8029728	GIPR	gastric inhibitory polypeptide receptor	7.443	9.098	8.353	9.154	1.655
7902452	AK5	adenylate kinase 5	9.545	11.200	9.680	10.782	1.654
8050894	KIF3C	kinesin family member 3C	7.669	9.323	8.163	9.121	1.653

8094393	ZCCHC4	zinc finger, CCHC domain containing 4	8.093	9.747	8.431	8.763	1.653
8139680	COBL	cordon-bleu homolog (mouse)	6.661	8.307	7.238	7.872	1.646
8162236	SEMA4D	sema domain, immunoglobulin domain (Ig), transmembrane domain (TM) and short cytoplasmic domain, (semaphorin) 4D	8.544	10.187	9.137	9.741	1.644
8001082	SLC6A8	solute carrier family 6 (neurotransmitter transporter, creatine), member 8	9.169	10.813	10.072	10.568	1.644
8093096	TCTEX1D2	Tctex1 domain containing 2	7.626	9.271	8.153	8.499	1.644
7930413	DUSP5	dual specificity phosphatase 5	8.240	9.879	9.065	9.008	1.639
8138527	MGC87042	STEAP family protein MGC87042	6.623	8.261	6.796	7.812	1.639
8008682	MSI2	musashi homolog 2 (Drosophila)	6.372	8.006	6.702	7.516	1.634
7908993	SOX13	SRY (sex determining region Y)-box 13	7.018	8.648	7.932	8.452	1.630
8112668	GCNT4	glucosaminyl (N-acetyl) transferase 4, core 2	4.508	6.135	4.906	5.246	1.627
8058203	ALS2CR12	amyotrophic lateral sclerosis 2 (juvenile) chromosome region, candidate 12	5.485	7.109	5.948	5.992	1.624
8152491	EXT1	exostosin 1	8.783	10.406	9.090	10.089	1.623
7952927	B4GALNT3	beta-1,4-N-acetyl-galactosaminyl transferase 3	7.108	8.728	7.805	8.480	1.620
7952341	ASAM	adipocyte-specific adhesion molecule	7.346	8.961	7.149	8.227	1.616
8083000	FAIM	Fas apoptotic inhibitory molecule	8.509	10.125	9.455	9.507	1.616
7919872	FAM63A	family with sequence similarity 63, member A	8.048	9.660	8.601	9.114	1.611
8174598	IL13RA2	interleukin 13 receptor, alpha 2	4.071	5.671	4.744	4.397	1.600
7942674	TSKU	tsukushi small leucine rich proteoglycan homolog (Xenopus laevis)	8.352	9.950	9.764	9.437	1.598
8029950	EHD2	EH-domain containing 2	8.272	9.868	9.193	9.686	1.597
8147145	ATP6V0D2	ATPase, H+ transporting, lysosomal 38kDa, V0 subunit d2	10.848	12.443	11.537	12.118	1.595
7922976	PTGS2	prostaglandin-endoperoxide synthase 2 (prostaglandin G/H synthase and cyclooxygenase)	8.003	9.597	9.671	8.111	1.594
7989069	PYGO1	pygopus homolog 1 (Drosophila)	5.265	6.856	5.714	5.871	1.592
8119898	VEGFA	vascular endothelial growth factor A	7.417	9.006	8.384	8.788	1.589
8054722	IL1B	interleukin 1, beta	9.983	11.556	13.002	11.823	1.573
7904830	RNF115	ring finger protein 115	9.999	11.563	10.633	10.884	1.564
7961371	DUSP16	dual specificity phosphatase 16	7.494	9.057	8.237	8.498	1.563
7933933	DNAJC12	DnaJ (Hsp40) homolog, subfamily C, member 12	6.959	8.520	7.633	8.111	1.561
7963946	MMP19	matrix metallopeptidase 19	10.331	11.888	11.343	11.895	1.558
7944803	VWA5A	von Willebrand factor A domain containing 5A	9.183	10.738	9.613	10.531	1.555
8089261	CBLB	Cas-Br-M (murine) ecotropic retroviral transforming sequence b	10.897	12.451	11.628	12.068	1.554
8056222	DPP4	dipeptidyl-peptidase 4	11.567	13.121	12.600	12.828	1.554
8046408	PDK1	pyruvate dehydrogenase kinase, isozyme 1	9.308	10.858	9.912	10.339	1.550
8118734	ITPR3	inositol 1,4,5-triphosphate receptor, type 3	6.380	7.927	7.548	7.800	1.548
7954065	GPRC5A	G protein-coupled receptor, family C, group 5, member A	5.531	7.078	6.239	6.273	1.547
8022711	DSC2	desmocollin 2	8.591	10.131	9.237	9.488	1.540
7907861	XPR1	xenotropic and polytropic retrovirus receptor 1	10.449	11.981	11.233	11.527	1.532
7990545	CSPG4	chondroitin sulfate proteoglycan 4	6.683	8.209	7.124	7.480	1.526
7994541	LAT	linker for activation of T cells	8.835	10.360	9.712	10.022	1.525
7951752	USP28	ubiquitin specific peptidase 28	8.772	10.295	9.335	9.752	1.523
7917754	BCAR3	breast cancer anti-estrogen resistance 3	7.063	8.583	7.677	7.893	1.520
7950899	RAB38	RAB38, member RAS oncogene family	10.446	11.966	11.041	11.625	1.520
8055465	CXCR4	chemokine (C-X-C motif) receptor 4	7.909	9.427	8.768	8.901	1.518
8075673	RBFOX2	RNA binding protein, fox-1 homolog (C. elegans) 2	7.025	8.538	7.632	7.910	1.513
8051298	GALNT14	UDP-N-acetyl-alpha-D-galactosamine:polypeptide N-acetylgalactosaminyltransferase 14 (GalNAc-T14)	8.071	9.581	8.661	9.335	1.509
7971590	CAB39L	calcium binding protein 39-like	8.791	10.299	9.161	9.559	1.508
8089082	DCBLD2	discoidin, CUB and LCCL domain containing 2	8.411	9.916	9.012	9.289	1.505
8162216	SHC3	SHC (Src homology 2 domain containing) transforming protein 3	8.092	9.593	8.225	8.988	1.501
8096160	ARHGAP24	Rho GTPase activating protein 24	6.679	8.180	6.837	7.173	1.500
8073015	KDELR3	KDEL (Lys-Asp-Glu-Leu) endoplasmic reticulum protein retention receptor 3	5.981	7.474	6.905	6.873	1.493
8112980	EDIL3	EGF-like repeats and discoidin I-like domains 3	7.902	9.392	6.256	7.629	1.490
7921652	SLAMF1	signaling lymphocytic activation molecule family member 1	5.292	6.782	6.624	6.452	1.490
8129649	C6orf192	chromosome 6 open reading frame 192	9.068	10.557	9.088	10.303	1.489
8166950	DUSP21	dual specificity phosphatase 21	4.850	6.337	5.449	5.473	1.487
8121749	GJA1	gap junction protein, alpha 1, 43kDa	5.551	7.025	5.818	6.823	1.474
7989365	RORA	RAR-related orphan receptor A	5.759	7.223	6.334	6.102	1.465
8089647	KIAA2018	KIAA2018	9.739	11.199	10.791	10.534	1.460
8156897	C9orf30	chromosome 9 open reading frame 30	10.391	11.850	11.577	11.533	1.459
7969544	NDFIP2	Nedd4 family interacting protein 2	8.607	10.066	9.043	9.464	1.459
7982377	GREM1	gremlin 1	10.931	12.389	11.927	11.754	1.458
8169898	RAB33A	RAB33A, member RAS oncogene family	7.486	8.942	8.144	8.252	1.456
7967202	RHOF	ras homolog gene family, member F (in filopodia)	9.384	10.838	10.145	10.822	1.454
8000932	C16orf93	chromosome 16 open reading frame 93	7.471	8.921	8.425	9.065	1.449
8138824	SCRN1	secernin 1	8.297	9.741	8.958	9.604	1.444
8061416	CST7	cystatin F (leukocystatin)	7.587	9.025	8.810	8.531	1.438
8021091	SIGLEC15	sialic acid binding Ig-like lectin 15	9.967	11.403	10.456	11.097	1.436
8089544	CCDC80	coiled-coil domain containing 80	5.199	6.634	5.334	5.814	1.435
8173086	FGD1	FYVE, RhoGEF and PH domain containing 1	6.695	8.130	7.170	7.847	1.435
7966738	C12orf49	chromosome 12 open reading frame 49	10.230	11.664	10.928	11.196	1.433
8055688	RND3	Rho family GTPase 3	9.073	10.502	9.838	9.543	1.429
8054872	TFCP2L1	transcription factor CP2-like 1	7.481	8.907	8.387	9.041	1.425
7959638	TCTN2	tectonic family member 2	7.614	9.029	8.275	8.351	1.416
7915718	TESK2	testis-specific kinase 2	7.419	8.825	7.957	7.795	1.406
8088958	GBE1	glucan (1,4-alpha-), branching enzyme 1	10.456	11.855	11.039	11.183	1.400
8014115	MYO1D	myosin ID	10.169	11.570	10.439	11.386	1.400
7940530	C11orf9	chromosome 11 open reading frame 9	6.292	7.691	6.771	7.485	1.399
7945663	LOC402778	CD225 family protein FLJ76511	8.976	10.374	10.307	10.058	1.398
8016239	PLEKHM1	pleckstrin homology domain containing, family M (with RUN domain) member 1	9.228	10.623	9.906	10.491	1.395
7922610	ABL2	v-abl Abelson murine leukemia viral oncogene homolog 2	9.199	10.593	10.025	9.903	1.394
8044605	LOC654433	hypothetical LOC654433	6.908	8.297	7.476	6.935	1.389
7934979	ANKRD1	ankyrin repeat domain 1 (cardiac muscle)	6.083	7.472	6.925	6.434	1.388
8135594	CAV1	caveolin 1, caveolae protein, 22kDa	5.741	7.127	5.178	5.971	1.387
8057517	NCKAP1	NCK-associated protein 1	9.274	10.661	9.810	10.008	1.387
8045860	PKP4	plakophilin 4	7.443	8.827	7.421	8.130	1.384
8157105	ZNF462	zinc finger protein 462	8.538	9.921	8.678	9.579	1.383
8120719	CD109	CD109 molecule	10.492	11.873	11.113	11.442	1.381
8166797	MID1IP1	MID1 interacting protein 1 (gastrulation specific G12 homolog (zebrafish))	9.837	11.218	10.292	11.227	1.381
8069301	COL6A2	collagen, type VI, alpha 2	9.001	10.377	10.080	10.370	1.375
7898957	RCAN3	RCAN family member 3	8.734	10.109	9.224	9.850	1.375
7903092	FNBP1L	formin binding protein 1-like	9.151	10.522	9.079	9.630	1.370
8105411	IL31RA	interleukin 31 receptor A	5.079	6.446	5.550	6.032	1.367
7937878	TRPC2	transient receptor potential cation channel, subfamily C, member 2, pseudogene	7.042	8.406	7.588	7.816	1.364
8114733	ARAP3	ArfGAP with RhoGAP domain, ankyrin repeat and PH domain 3	7.173	8.535	7.808	8.120	1.363
8085797	THRB	thyroid hormone receptor, beta (erythroblastic leukemia viral (v-erb-a) oncogene homolog 2, avian)	7.257	8.620	7.383	7.842	1.363
8082869	PPP2R3A	protein phosphatase 2, regulatory subunit B'', alpha	7.047	8.395	7.218	7.664	1.348
7942204	CTTN	cortactin	8.880	10.217	9.288	10.019	1.337
7951977	FXYD6	FXYD domain containing ion transport regulator 6	8.816	10.151	8.869	10.077	1.335
8010061	SPHK1	sphingosine kinase 1	8.632	9.962	9.617	9.751	1.330
7956759	SRGAP1	SLIT-ROBO Rho GTPase activating protein 1	7.645	8.969	7.816	8.341	1.324
8093878	EVC	Ellis van Creveld syndrome	7.423	8.745	8.080	8.334	1.321
8071147	TUBA8	tubulin, alpha 8	8.176	9.488	8.726	9.748	1.312
8127346	RAB23	RAB23, member RAS oncogene family	7.560	8.867	7.598	7.539	1.307
8007931	ITGB3	integrin, beta 3 (platelet glycoprotein IIIa, antigen CD61)	11.529	12.831	12.075	12.668	1.303
7992594	CCNF	cyclin F	7.149	8.452	7.377	7.466	1.302
7913357	ECE1	endothelin converting enzyme 1	8.323	9.623	8.958	9.480	1.301
8145989	HTRA4	HtrA serine peptidase 4	8.917	10.217	9.557	9.783	1.300
8162850	TEX10	testis expressed 10	9.078	10.376	9.667	9.927	1.299
8002421	VAC14	Vac14 homolog (S. cerevisiae)	10.379	11.675	11.154	11.452	1.297
8152280	LRP12	low density lipoprotein receptor-related protein 12	9.005	10.302	10.046	9.645	1.296
7965040	PHLDA1	pleckstrin homology-like domain, family A, member 1	8.235	9.528	9.652	9.797	1.293
7959002	SDSL	serine dehydratase-like	8.398	9.690	8.552	9.641	1.292
7909104	CDK18	cyclin-dependent kinase 18	7.949	9.237	8.578	8.949	1.288
8098103	FNIP2	folliculin interacting protein 2	10.789	12.077	11.425	11.812	1.288
8043945	MAP4K4	mitogen-activated protein kinase kinase kinase kinase 4	9.390	10.670	9.819	10.181	1.280
7931832	AKR1C2	aldo-keto reductase family 1, member C2 (dihydrodiol dehydrogenase 2; bile acid binding protein; 3-alpha hydroxysteroid dehydrogenase, type III)	7.697	8.974	8.545	8.420	1.277
8147132	CA2	carbonic anhydrase II	11.856	13.129	12.582	13.040	1.273
7932765	MPP7	membrane protein, palmitoylated 7 (MAGUK p55 subfamily member 7)	6.860	8.132	7.194	7.624	1.272
8005305	C17orf39	chromosome 17 open reading frame 39	7.912	9.183	8.459	8.625	1.271
7943803	DIXDC1	DIX domain containing 1	7.022	8.292	7.397	8.030	1.271
7977161	TDRD9	tudor domain containing 9	5.569	6.838	5.763	6.413	1.269
7997139	CALB2	calbindin 2	6.385	7.650	6.842	7.209	1.265
8122279	KIAA1244	KIAA1244	7.353	8.612	7.444	8.243	1.260
8022941	C18orf10	chromosome 18 open reading frame 10	11.434	12.692	12.080	12.352	1.258
8093219	BDH1	3-hydroxybutyrate dehydrogenase, type 1	7.749	9.006	8.231	8.595	1.257
8113796	FLJ44606	glutaredoxin-like protein YDR286C homolog	6.109	7.365	5.745	6.416	1.256
7906613	SLAMF7	SLAM family member 7	10.719	11.975	11.677	11.385	1.256
7955217	SPATS2	spermatogenesis associated, serine-rich 2	8.006	9.262	8.503	8.716	1.256
8132710	C7orf69	chromosome 7 open reading frame 69	4.703	5.958	5.835	5.128	1.255
7991602	PCSK6	proprotein convertase subtilisin/kexin type 6	8.964	10.215	9.368	9.742	1.250
8030128	PPP1R15A	protein phosphatase 1, regulatory (inhibitor) subunit 15A	9.314	10.562	10.379	10.158	1.248
8164013	STRBP	spermatid perinuclear RNA binding protein	6.514	7.763	6.912	7.541	1.248

7992789	TNFRSF12A	tumor necrosis factor receptor superfamily, member 12A	9.954	11.200	10.453	11.045	1.246
7936928	MMP21	matrix metallopeptidase 21	6.121	7.366	6.649	6.809	1.245
7925876	PFKP	phosphofructokinase, platelet	9.754	10.999	10.253	10.790	1.245
7909967	CAPN2	calpain 2, (m/II) large subunit	10.871	12.112	11.378	11.849	1.241
8134098	CDK14	cyclin-dependent kinase 14	8.123	9.363	9.498	8.771	1.240
7930760	PNLIPRP3	pancreatic lipase-related protein 3	4.157	5.397	4.513	4.293	1.239
7932826	KIAA1462	KIAA1462	6.321	7.556	7.295	7.479	1.236
7941714	C11orf80	chromosome 11 open reading frame 80	6.857	8.089	7.224	7.824	1.232
8109528	CYFIP2	cytoplasmic FMR1 interacting protein 2	7.548	8.780	7.459	7.954	1.232
7900129	C1orf113	chromosome 1 open reading frame 113	6.779	8.009	7.646	7.841	1.231
8131631	HDAC9	histone deacetylase 9	6.853	8.085	7.135	7.621	1.231
8122365	GPR126	G protein-coupled receptor 126	7.269	8.497	7.147	7.798	1.228
7957298	NAV3	neuron navigator 3	5.347	6.575	5.477	6.358	1.228
7936463	ABLIM1	actin binding LIM protein 1	5.800	7.027	6.250	6.391	1.227
7978586	CFL2	cofilin 2 (muscle)	9.304	10.529	9.553	9.962	1.226
8135587	CAV2	caveolin 2	5.469	6.694	5.552	6.028	1.225
7901175	TSPAN1	tetraspanin 1	4.804	6.020	5.113	5.574	1.216
7965431	CLLU1OS	chronic lymphocytic leukemia up-regulated 1 opposite strand	5.374	6.589	5.972	6.589	1.215
7929958	BTRC	beta-transducin repeat containing	8.420	9.634	9.013	9.297	1.214
7960865	SLC2A3	solute carrier family 2 (facilitated glucose transporter), member 3	10.066	11.278	10.774	10.652	1.212
8076195	PDGFB	platelet-derived growth factor beta polypeptide (simian sarcoma viral (v-sis) oncogene homolog)	7.108	8.318	8.010	8.052	1.210
8091009	PIK3CB	phosphoinositide-3-kinase, catalytic, beta polypeptide	10.449	11.657	10.984	11.406	1.208
8104788	RAI14	retinoic acid induced 14	9.201	10.407	9.777	9.923	1.206
8059350	AP1S3	adaptor-related protein complex 1, sigma 3 subunit	6.703	7.906	6.832	7.341	1.203
8059361	WDFY1	WD repeat and FYVE domain containing 1	10.174	11.377	10.714	11.035	1.203
8161919	TLE1	transducin-like enhancer of split 1 (E(sp1) homolog, Drosophila)	7.133	8.335	7.644	7.555	1.202
7962058	TMTC1	transmembrane and tetratricopeptide repeat containing 1	7.112	8.311	8.104	7.527	1.199
8099982	APBB2	amyloid beta (A4) precursor protein-binding, family B, member 2	9.027	10.225	9.407	9.672	1.198
7934898	ANKRD22	ankyrin repeat domain 22	5.114	6.308	5.278	5.273	1.194
7958398	WSCD2	WSC domain containing 2	6.291	7.481	6.691	7.192	1.190
8092552	IGF2BP2	insulin-like growth factor 2 mRNA binding protein 2	7.040	8.229	7.502	7.696	1.189
8040587	EFR3B	EFR3 homolog B (S. cerevisiae)	7.370	8.551	7.788	8.052	1.182
8164810	RALGDS	ral guanine nucleotide dissociation stimulator	8.886	10.068	9.281	9.710	1.182
7917996	LRRC39	leucine rich repeat containing 39	6.223	7.403	6.278	6.012	1.180
8048211	RUFY4	RUN and FYVE domain containing 4	8.096	9.273	8.152	9.126	1.177
8090988	CEP70	centrosomal protein 70kDa	5.955	7.126	6.110	6.583	1.171
8108478	C5orf32	chromosome 5 open reading frame 32	10.417	11.584	11.158	11.438	1.167
8094719	N4BP2	NEDD4 binding protein 2	7.984	9.149	8.243	8.105	1.165
7986675	NIPA1	non imprinted in Prader-Willi/Angelman syndrome 1	8.025	9.188	8.636	8.646	1.163
7902512	DNAJB4	DnaJ (Hsp40) homolog, subfamily B, member 4	8.369	9.530	8.873	9.043	1.162
7955469	SLC4A8	solute carrier family 4, sodium bicarbonate cotransporter, member 8	7.521	8.683	7.999	8.250	1.162
8155048	RUSC2	RUN and SH3 domain containing 2	7.799	8.960	8.187	8.728	1.161
8050176	ITGB1BP1	integrin beta 1 binding protein 1	10.366	11.524	10.568	11.371	1.158
8032839	SEMA6B	sema domain, transmembrane domain (TM), and cytoplasmic domain, (semaphorin) 6B	7.422	8.580	9.756	8.882	1.158
8013159	TOM1L2	target of myb1-like 2 (chicken)	8.754	9.912	9.511	9.751	1.158
7964736	HMGA2	high mobility group AT-hook 2	6.411	7.565	6.119	6.807	1.155
8065089	KIF16B	kinesin family member 16B	8.322	9.477	8.683	8.696	1.155
8005707	MAP2K3	mitogen-activated protein kinase kinase 3	9.815	10.970	10.309	10.782	1.155
8050766	ADCY3	adenylate cyclase 3	10.129	11.283	10.714	11.143	1.154
8156761	NANS	N-acetylneuraminic acid synthase	9.496	10.651	9.912	10.238	1.154
8077441	BHLHE40	basic helix-loop-helix family, member e40	10.245	11.397	10.856	11.363	1.152
7958253	C12orf75	chromosome 12 open reading frame 75	7.643	8.794	8.084	8.485	1.150
8078227	KAT2B	K(lysine) acetyltransferase 2B	10.253	11.404	10.666	10.915	1.150
8128939	TRAF3IP2	TRAF3 interacting protein 2	7.843	8.989	8.787	9.008	1.146
8162059	SLC28A3	solute carrier family 28 (sodium-coupled nucleoside transporter), member 3	9.927	11.072	10.363	10.520	1.145
8013660	ALDOC	aldolase C, fructose-bisphosphate	8.472	9.615	8.499	9.310	1.143
8088680	C3orf64	chromosome 3 open reading frame 64	10.176	11.317	10.586	11.011	1.141
7991070	HDGFRP3	hepatoma-derived growth factor, related protein 3	8.010	9.151	8.391	8.723	1.141
7924526	TP53BP2	tumor protein p53 binding protein, 2	9.703	10.843	10.377	10.288	1.140
8134036	STEAP2	six transmembrane epithelial antigen of the prostate 2	5.477	6.612	5.726	6.169	1.135
8113790	40971	membrane-associated ring finger (C3HC4) 3	9.745	10.879	10.089	10.417	1.134
8056343	COBLL1	COBL-like 1	6.952	8.086	7.132	7.829	1.134
8110055	CPEB4	cytoplasmic polyadenylation element binding protein 4	9.603	10.736	10.163	10.009	1.133
7952249	USP2	ubiquitin specific peptidase 2	8.817	9.948	9.254	9.777	1.132
8146092	IDO1	indoleamine 2,3-dioxygenase 1	4.896	6.027	6.120	5.469	1.131
8114964	SPINK1	serine peptidase inhibitor, Kazal type 1	5.143	6.270	6.153	5.372	1.127
8066513	SDC4	syndecan 4	9.359	10.484	10.346	10.571	1.125
7962151	DENND5B	DENN/MADD domain containing 5B	7.078	8.202	7.451	7.349	1.124
8128956	FYN	FYN oncogene related to SRC, FGR, YES	7.343	8.466	7.712	8.099	1.123
8038213	HSD17B14	hydroxysteroid (17-beta) dehydrogenase 14	7.139	8.261	8.025	8.146	1.123
8148448	KHDRBS3	KH domain containing, RNA binding, signal transduction associated 3	7.232	8.355	7.920	7.671	1.123
7972297	ABCC4	ATP-binding cassette, sub-family C (CFTR/MRP), member 4	8.552	9.672	8.377	8.931	1.120
8162610	CDC14B	CDC14 cell division cycle 14 homolog B (S. cerevisiae)	6.047	7.164	6.126	6.255	1.117
8137526	INSIG1	insulin induced gene 1	10.156	11.273	11.028	11.479	1.117
7904433	PHGDH	phosphoglycerate dehydrogenase	6.288	7.404	7.007	7.072	1.116
7965541	FGD6	FYVE, RhoGEF and PH domain containing 6	9.277	10.392	9.765	9.635	1.115
7951554	RDX	radixin	10.806	11.921	11.760	11.586	1.115
8066822	SULF2	sulfatase 2	6.345	7.460	7.459	7.194	1.115
8161004	CD72	CD72 molecule	8.156	9.269	8.698	9.175	1.114
7924119	INTS7	integrator complex subunit 7	9.398	10.512	9.552	9.887	1.114
8139207	INHBA	inhibin, beta A	6.227	7.341	6.929	6.639	1.113
8172220	NDP	Norrie disease (pseudoglioma)	7.595	8.707	7.777	7.981	1.112
8046861	ITGAV	integrin, alpha V (vitronectin receptor, alpha polypeptide, antigen CD51)	11.516	12.626	12.243	12.317	1.111
8128553	BVES	blood vessel epicardial substance	5.069	6.172	5.448	5.664	1.103
7927599	ASAH2	N-acylsphingosine amidohydrolase (non-lysosomal ceramidase) 2	6.259	7.361	6.437	6.523	1.102
7902861	LRRC8B	leucine rich repeat containing 8 family, member B	9.021	10.123	9.628	9.564	1.102
8143850	CDK5	cyclin-dependent kinase 5	10.169	11.269	10.713	11.377	1.101
8050557	SDC1	syndecan 1	8.305	9.406	8.581	9.425	1.101
8162117	GOLM1	golgi membrane protein 1	9.143	10.241	9.084	10.010	1.098
7917304	MCOLN3	mucolipin 3	8.396	9.494	8.947	9.131	1.098
8156905	TMEFF1	transmembrane protein with EGF-like and two follistatin-like domains 1	6.912	8.010	7.528	7.608	1.098
8141150	ASNS	asparagine synthetase (glutamine-hydrolyzing)	5.786	6.884	7.113	7.343	1.097
8126710	SUPT3H	suppressor of Ty 3 homolog (S. cerevisiae)	6.851	7.944	7.050	7.466	1.094
7979698	ATP6V1D	ATPase, H+ transporting, lysosomal 34kDa, V1 subunit D	10.548	11.636	10.866	11.419	1.088
8063394	PTPN1	protein tyrosine phosphatase, non-receptor type 1	10.288	11.375	10.916	11.485	1.087
8065280	RALGAPA2	Ral GTPase activating protein, alpha subunit 2 (catalytic)	7.819	8.905	8.423	8.301	1.086
7910014	CNIH4	cornichon homolog 4 (Drosophila)	10.491	11.576	11.027	11.359	1.085
8054712	IL1A	interleukin 1, alpha	5.430	6.515	9.531	6.917	1.085
8054377	FHL2	four and a half LIM domains 2	6.475	7.559	6.928	7.433	1.084
7901460	GPX7	glutathione peroxidase 7	5.805	6.886	6.841	7.164	1.082
8091283	PLOD2	procollagen-lysine, 2-oxoglutarate 5-dioxygenase 2	5.333	6.414	5.705	5.976	1.081
8040503	UBXN2A	UBX domain protein 2A	7.199	8.280	7.701	7.530	1.080
7965964	SLC41A2	solute carrier family 41, member 2	9.610	10.688	10.221	10.274	1.078
8089112	FILIP1L	filamin A interacting protein 1-like	8.421	9.497	9.002	9.242	1.076
8137352	SLC4A2	solute carrier family 4, anion exchanger, member 2 (erythrocyte membrane protein band 3-like 1)	9.431	10.507	10.026	10.405	1.076
8106962	ARSK	arylsulfatase family, member K	7.479	8.553	7.690	7.789	1.075
7901054	PLK3	polo-like kinase 3	8.368	9.443	9.402	9.213	1.075
8094169	CPEB2	cytoplasmic polyadenylation element binding protein 2	8.832	9.906	9.317	9.240	1.074
8066939	B4GALT5	UDP-Gal:betaGlcNAc beta 1,4- galactosyltransferase, polypeptide 5	10.922	11.993	11.627	11.899	1.071
8160531	C9orf72	chromosome 9 open reading frame 72	9.608	10.679	10.115	10.196	1.071
8120239	TMEM14A	transmembrane protein 14A	7.620	8.690	8.165	8.060	1.070
8005557	EPN2	epsin 2	7.232	8.298	7.467	8.110	1.066
7942118	MYEOV	myeloma overexpressed (in a subset of t(11;14) positive multiple myelomas)	6.544	7.609	7.128	7.454	1.065
8115210	TNIP1	TNFAIP3 interacting protein 1	8.764	9.827	10.046	9.834	1.062
8149749	TNFRSF10D	tumor necrosis factor receptor superfamily, member 10d, decoy with truncated death domain	9.278	10.339	9.941	9.966	1.061
8015884	PPY	pancreatic polypeptide	4.706	5.765	5.516	5.637	1.059
7901140	MAST2	microtubule associated serine/threonine kinase 2	8.487	9.543	9.065	9.141	1.056
7952036	MPZL3	myelin protein zero-like 3	7.712	8.767	8.289	8.261	1.055
8115814	SH3PXD2B	SH3 and PX domains 2B	9.781	10.835	11.014	10.393	1.054
8128123	RRAGD	Ras-related GTP binding D	10.670	11.723	11.095	11.382	1.053
8098549	STOX2	storkhead box 2	6.261	7.314	6.726	6.845	1.053
8091385	CP	ceruloplasmin (ferroxidase)	4.246	5.297	4.780	4.553	1.051
7977270	LOC388022	hypothetical LOC388022	8.413	9.464	9.117	9.211	1.050
7912102	KLHL21	kelch-like 21 (Drosophila)	6.872	7.920	7.436	7.854	1.048
8133176	RABGEF1	RAB guanine nucleotide exchange factor (GEF) 1	9.098	10.146	9.519	9.586	1.047
7898939	NIPAL3	NIPA-like domain containing 3	7.878	8.924	7.983	8.501	1.046
8085556	SH3BP5	SH3-domain binding protein 5 (BTK-associated)	9.116	10.161	9.748	9.780	1.045
8060339	NRSN2	neurensin 2	6.735	7.777	7.520	7.348	1.043
7902660	WDR63	WD repeat domain 63	7.088	8.131	7.125	7.235	1.043
7999419	DEXI	Dexi homolog (mouse)	9.707	10.748	9.769	10.394	1.042
8109201	HMGXB3	HMG box domain containing 3	9.159	10.197	9.857	10.046	1.038

8152962	LRRC6	leucine rich repeat containing 6	7.330	8.367	7.415	7.612	1.038
7923967	YOD1	YOD1 OTU deubiquinating enzyme 1 homolog (S. cerevisiae)	8.193	9.231	8.559	8.780	1.038
7986977	TJP1	tight junction protein 1 (zona occludens 1)	6.893	7.927	7.417	7.497	1.034
8119088	CDKN1A	cyclin-dependent kinase inhibitor 1A (p21, Cip1)	10.683	11.717	11.473	11.245	1.033
8032009	MIER2	mesoderm induction early response 1, family member 2	7.824	8.857	8.239	8.295	1.033
7902425	ST6GALNAC3	ST6 (alpha-N-acetyl-neuraminyl-2,3-beta-galactosyl-1,3)-N-acetylgalactosaminide alpha-2,6-sialyltransferase 3	4.925	5.957	5.542	5.525	1.032
8133818	PHTF2	putative homeodomain transcription factor 2	10.003	11.033	10.109	10.526	1.030
8095688	CXCL6	chemokine (C-X-C motif) ligand 6 (granulocyte chemotactic protein 2)	5.618	6.646	6.859	6.354	1.028
8010092	MFSD11	major facilitator superfamily domain containing 11	9.690	10.718	10.274	10.470	1.028
8163599	DFNB31	deafness, autosomal recessive 31	6.703	7.730	7.422	7.726	1.027
8080964	GXYLT2	glucoside xylosyltransferase 2	6.870	7.896	7.247	7.666	1.026
7962884	RND1	Rho family GTPase 1	6.336	7.362	6.740	6.980	1.026
8035120	EPS15L1	epidermal growth factor receptor pathway substrate 15-like 1	9.211	10.235	9.643	9.929	1.024
7963631	RARG	retinoic acid receptor, gamma	6.312	7.336	6.807	7.009	1.024
8130739	RPS6KA2	ribosomal protein S6 kinase, 90kDa, polypeptide 2	9.194	10.216	9.276	9.690	1.022
7929882	SEMA4G	sema domain, immunoglobulin domain (Ig), transmembrane domain (TM) and short cytoplasmic domain, (semaphorin) 4G	6.246	7.266	7.053	7.156	1.020
7925062	SIPA1L2	signal-induced proliferation-associated 1 like 2	8.297	9.317	8.772	8.920	1.020
7932512	DNAJC1	DnaJ (Hsp40) homolog, subfamily C, member 1	9.755	10.773	10.089	10.494	1.019
7917103	ZZZ3	zinc finger, ZZ-type containing 3	9.751	10.770	10.051	10.339	1.019
7987163	FMN1	formin 1	6.581	7.599	8.098	6.879	1.018
8068024	JAM2	junctional adhesion molecule 2	5.807	6.825	6.042	5.913	1.018
8126303	TREM1	triggering receptor expressed on myeloid cells 1	7.794	8.808	9.360	9.108	1.015
8072314	LIF	leukemia inhibitory factor (cholinergic differentiation factor)	6.332	7.345	6.687	6.821	1.012
8069269	COL6A1	collagen, type VI, alpha 1	9.468	10.480	10.462	10.593	1.011
7975787	JDP2	Jun dimerization protein 2	10.512	11.523	10.551	11.345	1.011
8032682	MATK	megakaryocyte-associated tyrosine kinase	8.416	9.427	8.778	9.344	1.011
7899821	KIAA1522	KIAA1522	6.962	7.970	7.707	7.863	1.009
8017675	PLEKHM1P	pleckstrin homology domain containing, family M (with RUN domain) member 1 pseudogene	10.294	11.302	10.743	11.289	1.009
7909603	NENF	neuron derived neurotrophic factor	10.334	11.342	10.947	10.684	1.008
8102050	NHEDC2	Na+/H+ exchanger domain containing 2	12.003	13.011	12.218	12.841	1.008
7974835	PRKCH	protein kinase C, eta	9.637	10.644	9.636	10.483	1.008
8021565	PHLPP1	PH domain and leucine rich repeat protein phosphatase 1	7.767	8.773	8.296	8.179	1.006
7933204	C10orf10	chromosome 10 open reading frame 10	5.952	6.957	6.273	6.453	1.005
7982185	DEXI	Dexi homolog (mouse)	10.281	11.285	10.536	11.160	1.004
7986685	DEXI	Dexi homolog (mouse)	10.281	11.285	10.536	11.160	1.004
7980720	TTC7B	tetratricopeptide repeat domain 7B	9.149	10.152	9.800	9.814	1.004
7897119	C1orf93	chromosome 1 open reading frame 93	8.855	9.857	9.538	9.480	1.002
7982204	HMGN2	high-mobility group nucleosomal binding domain 2	11.316	10.315	10.608	10.632	-1.000
8157761	NEK6	NIMA (never in mitosis gene a)-related kinase 6	10.413	9.413	10.183	9.683	-1.000
7971661	MIR15A	microRNA 15a	6.980	5.978	6.266	6.075	-1.001
8149673	REEP4	receptor accessory protein 4	8.664	7.663	8.037	7.615	-1.001
8046003	GCA	grancalcin, EF-hand calcium binding protein	9.968	8.965	9.290	8.703	-1.002
8036304	ZFP14	zinc finger protein 14 homolog (mouse)	6.007	5.004	5.180	4.906	-1.003
8068593	ETS2	v-ets erythroblastosis virus E26 oncogene homolog 2 (avian)	9.587	8.582	9.168	8.272	-1.005
8000582	SULT1A2	sulfotransferase family, cytosolic, 1A, phenol-preferring, member 2	8.430	7.425	8.021	7.551	-1.005
8118594	HLA-DPB1	major histocompatibility complex, class II, DP beta 1	12.849	11.843	12.473	12.234	-1.006
8138613	OSBPL3	oxysterol binding protein-like 3	8.879	7.874	7.887	7.533	-1.006
8179228	TCF19	transcription factor 19	8.040	7.033	6.551	7.276	-1.007
8099685	LGI2	leucine-rich repeat LGI family, member 2	10.789	9.781	10.392	8.729	-1.008
7965359	ATP2B1	ATPase, Ca++ transporting, plasma membrane 1	10.079	9.069	9.545	9.161	-1.009
7901010	KIF2C	kinesin family member 2C	7.301	6.291	6.090	6.437	-1.010
8024900	UHRF1	ubiquitin-like with PHD and ring finger domains 1	8.476	7.466	7.095	7.552	-1.010
7910198	ZNF678	zinc finger protein 678	6.775	5.765	6.225	6.059	-1.010
7989132	RFX7	regulatory factor X, 7	8.917	7.904	8.180	8.007	-1.013
7994109	PLK1	polo-like kinase 1	9.461	8.445	7.519	8.665	-1.016
8027260	ZNF486	zinc finger protein 486	8.187	7.170	7.531	6.956	-1.016
8135211	FAM185A	family with sequence similarity 185, member A	7.816	6.799	6.900	6.771	-1.018
8145418	CDCA2	cell division cycle associated 2	6.902	5.882	5.433	5.718	-1.020
8092726	CLDN1	claudin 1	7.236	6.214	5.939	6.465	-1.022
8059650	SP110	SP110 nuclear body protein	8.616	7.593	8.374	7.605	-1.022
7908125	RGL1	ral guanine nucleotide dissociation stimulator-like 1	11.579	10.556	11.420	10.363	-1.023
8021707	SOCS6	suppressor of cytokine signaling 6	9.098	8.076	8.533	7.811	-1.023
8021286	C18orf54	chromosome 18 open reading frame 54	5.646	4.622	4.616	4.498	-1.024
8179519	HLA-DPB1	major histocompatibility complex, class II, DP beta 1	13.024	11.998	12.603	12.485	-1.026
8151447	IL7	interleukin 7	6.878	5.852	5.505	5.559	-1.026
8091723	RARRES1	retinoic acid receptor responder (tazarotene induced) 1	8.272	7.246	7.906	7.349	-1.026
7958031	C12orf48	chromosome 12 open reading frame 48	6.828	5.801	5.718	5.547	-1.027
8033332	EMR4P	egf-like module containing, mucin-like, hormone receptor-like 4 pseudogene	8.687	7.660	7.819	7.489	-1.028
8113602	CCDC112	coiled-coil domain containing 112	7.302	6.273	6.392	5.762	-1.029
8006634	PIGW	phosphatidylinositol glycan anchor biosynthesis, class W	8.939	7.910	8.081	7.617	-1.029
8072687	MCM5	minichromosome maintenance complex component 5	9.284	8.254	7.772	8.278	-1.030
8003844	GSG2	germ cell associated 2 (haspin)	6.793	5.761	6.287	6.235	-1.032
8125545	HLA-DOA	major histocompatibility complex, class II, DO alpha	8.246	7.214	7.584	7.672	-1.032
8009476	MAP2K6	mitogen-activated protein kinase kinase 6	6.502	5.468	5.467	5.588	-1.034
7944152	IL10RA	interleukin 10 receptor, alpha	11.445	10.410	11.553	10.722	-1.035
7922121	ANKRD36BP1	ankyrin repeat domain 36B pseudogene 1	7.166	6.131	6.672	5.932	-1.036
8117330	HIST1H3A	histone cluster 1, H3a	8.315	7.279	7.239	7.151	-1.036
8144153	NCAPG2	non-SMC condensin II complex, subunit G2	7.832	6.795	6.436	6.262	-1.037
8084100	USP13	ubiquitin specific peptidase 13 (isopeptidase T-3)	7.635	6.596	7.432	6.676	-1.039
8178199	HLA-DQA1	major histocompatibility complex, class II, DQ alpha 1	13.171	12.131	12.847	12.615	-1.040
8179489	HLA-DQA1	major histocompatibility complex, class II, DQ alpha 1	13.171	12.131	12.847	12.615	-1.040
8095043	RASL11B	RAS-like, family 11, member B	7.525	6.485	6.842	6.862	-1.040
8002969	MAF	v-maf musculoaponeurotic fibrosarcoma oncogene homolog (avian)	8.583	7.542	7.554	7.445	-1.041
7983650	SLC27A2	solute carrier family 27 (fatty acid transporter), member 2	6.009	4.968	4.760	4.990	-1.041
8039212	LILRB2	leukocyte immunoglobulin-like receptor, subfamily B (with TM and ITIM domains), member 2	10.894	9.852	10.613	9.865	-1.042
8144036	XRCC2	X-ray repair complementing defective repair in Chinese hamster cells 2	7.867	6.825	6.238	6.306	-1.042
7954729	FGD4	FYVE, RhoGEF and PH domain containing 4	9.510	8.467	8.568	8.233	-1.043
8055702	NMI	N-myc (and STAT) interactor	9.709	8.666	9.119	8.223	-1.044
8156982	SMC2	structural maintenance of chromosomes 2	8.898	7.854	7.910	7.220	-1.044
7905067	HIST2H4A	histone cluster 2, H4a	6.934	5.889	6.827	6.691	-1.045
7919627	HIST2H4A	histone cluster 2, H4a	6.934	5.889	6.827	6.691	-1.045
7969243	CKAP2	cytoskeleton associated protein 2	9.881	8.835	8.797	8.579	-1.046
8125556	HLA-DPA1	major histocompatibility complex, class II, DP alpha 1	12.970	11.924	12.427	12.308	-1.046
8178891	HLA-DPA1	major histocompatibility complex, class II, DP alpha 1	12.970	11.924	12.427	12.308	-1.046
7972055	KCTD12	potassium channel tetramerisation domain containing 12	11.600	10.553	11.233	10.486	-1.047
8061247	RIN2	Ras and Rab interactor 2	10.526	9.476	10.111	9.444	-1.050
8000409	HMGN2	high-mobility group nucleosomal binding domain 2	11.291	10.239	10.607	10.598	-1.051
7940259	MS4A7	membrane-spanning 4-domains, subfamily A, member 7	10.273	9.222	9.783	9.627	-1.052
8006602	CCL4	chemokine (C-C motif) ligand 4	9.107	8.054	10.484	7.338	-1.053
8138805	CPVL	carboxypeptidase, vitellogenic-like	10.127	9.075	9.632	9.383	-1.053
8125530	HLA-DMB	major histocompatibility complex, class II, DM beta	12.007	10.944	11.265	11.169	-1.062
8025076	VAV1	vav 1 guanine nucleotide exchange factor	10.677	9.615	10.307	9.581	-1.062
8027241	ZNF253	zinc finger protein 253	7.610	6.547	6.681	6.206	-1.063
7991777	C4orf46	chromosome 4 open reading frame 46	8.347	7.283	6.967	7.057	-1.064
8117589	HIST1H3H	histone cluster 1, H3h	7.128	6.065	6.241	6.240	-1.064
8169859	SASH3	SAM and SH3 domain containing 3	9.875	8.811	9.338	8.747	-1.064
8099841	TLR6	toll-like receptor 6	10.064	8.999	9.392	8.869	-1.065
8027247	ZNF93	zinc finger protein 93	7.964	6.900	7.052	6.637	-1.065
8180078	HLA-DMB	major histocompatibility complex, class II, DM beta	11.918	10.852	11.177	11.068	-1.066
8117580	HIST1H2AI	histone cluster 1, H2ai	8.004	6.937	6.489	7.054	-1.067
7945014	CHEK1	CHK1 checkpoint homolog (S. pombe)	8.625	7.555	7.404	7.499	-1.069
8105111	FBXO4	F-box protein 4	7.882	6.811	7.034	6.815	-1.071
8124521	HIST1H4K	histone cluster 1, H4k	9.598	8.526	8.347	8.348	-1.072
7924096	NEK2	NIMA (never in mitosis gene a)-related kinase 2	6.637	5.565	5.503	6.203	-1.072
7906757	FCGR2A	Fc fragment of IgG, low affinity IIa, receptor (CD32)	11.974	10.902	11.606	10.811	-1.073
8043791	INPP4A	inositol polyphosphate-4-phosphatase, type I, 107kDa	9.781	8.708	9.407	8.635	-1.073
7984540	KIF23	kinesin family member 23	8.169	7.095	6.668	6.831	-1.073
7961069	CLECL1	C-type lectin-like 1	5.839	4.765	5.057	4.882	-1.074
8168691	DIAPH2	diaphanous homolog 2 (Drosophila)	9.190	8.115	8.888	7.477	-1.075
8168794	CENPI	centromere protein I	7.572	6.495	6.241	6.192	-1.076
8054064	ANKRD36B	ankyrin repeat domain 36B	8.011	6.934	7.191	6.500	-1.077
8011826	C17orf87	chromosome 17 open reading frame 87	10.425	9.347	10.554	10.361	-1.078
7930148	SFXN2	sideroflexin 2	7.990	6.911	7.217	6.730	-1.078
8083223	C3orf58	chromosome 3 open reading frame 58	8.938	7.860	8.352	7.674	-1.079
8075118	CRYBB1	crystallin, beta B1	8.670	7.591	7.718	7.554	-1.079
8022338	GPR125	G protein-coupled receptor 125	7.335	6.256	6.083	6.105	-1.079
7924499	TLR5	toll-like receptor 5	8.252	7.173	7.707	7.083	-1.079
7933707	ZWINT	ZW10 interactor	8.487	7.407	7.363	7.469	-1.080
8117395	HIST1H2BF	histone cluster 1, H2bf	10.311	9.230	8.810	8.800	-1.081
8107632	SNX24	sorting nexin 24	10.018	8.937	9.035	8.822	-1.081
8168146	KIF4A	kinesin family member 4A	6.540	5.458	5.530	5.618	-1.082

7930454	PDCD4	programmed cell death 4 (neoplastic transformation inhibitor)	9.091	8.008	7.996	8.086	-1.083
8065359	CD93	CD93 molecule	9.095	8.010	7.338	7.524	-1.085
8156770	GALNT12	UDP-N-acetyl-alpha-D-galactosamine:polypeptide N-acetylgalactosaminyltransferase 12 (GalNAc-T12)	7.960	6.875	7.464	8.095	-1.085
8078619	ITGA9	integrin, alpha 9	7.808	6.723	6.741	6.845	-1.085
8035847	ZNF675	zinc finger protein 675	8.653	7.568	7.728	7.202	-1.085
7923917	FAIM3	Fas apoptotic inhibitory molecule 3	8.596	7.508	8.000	9.484	-1.089
7923562	CHIT1	chitinase 1 (chitotriosidase)	11.843	10.753	11.184	11.963	-1.090
8127031	MCM3	minichromosome maintenance complex component 3	9.282	8.193	7.562	8.037	-1.090
7981990	snoRD116-21	small nucleolar RNA, C/D box 116-21	6.167	5.075	4.994	4.870	-1.092
8150002	FBXO16	F-box protein 16	6.153	5.060	4.878	5.060	-1.093
8151890	TP53INP1	tumor protein p53 inducible nuclear protein 1	10.109	9.015	9.369	9.231	-1.094
8035896	TSHZ3	teashirt zinc finger homeobox 3	9.408	8.314	8.600	8.206	-1.094
8059387	FAM124B	family with sequence similarity 124B	7.436	6.340	6.295	6.592	-1.096
8052010	CALM2	calmodulin 2 (phosphorylase kinase, delta)	10.826	9.729	10.340	9.826	-1.097
7947248	KIF18A	kinesin family member 18A	6.676	5.578	5.112	5.105	-1.099
8070083	TMEM50B	transmembrane protein 50B	9.089	7.988	8.510	8.041	-1.101
8139820	ZNF680	zinc finger protein 680	7.334	6.233	6.482	5.958	-1.101
8073062	APOBEC3B	apolipoprotein B mRNA editing enzyme, catalytic polypeptide-like 3B	9.676	8.574	7.583	8.548	-1.102
8137232	GIMAP8	GTPase, IMAP family member 8	8.204	7.101	7.242	6.935	-1.102
7968563	RFC3	replication factor C (activator 1) 3, 38kDa	9.215	8.111	7.900	7.738	-1.104
8051396	NLRC4	NLR family, CARD domain containing 4	8.668	7.563	8.575	8.104	-1.105
8027862	FFAR2	free fatty acid receptor 2	7.475	6.368	6.716	5.542	-1.106
8003171	COTL1	coactosin-like 1 (Dictyostelium)	11.139	10.032	10.678	10.283	-1.107
8101728	FAM13A	family with sequence similarity 13, member A	7.892	6.784	7.040	7.122	-1.107
8107706	LMNB1	lamin B1	7.777	6.669	6.110	6.422	-1.108
8102862	MAML3	mastermind-like 3 (Drosophila)	7.956	6.842	6.850	7.061	-1.114
8115756	KCNMB1	potassium large conductance calcium-activated channel, subfamily M, beta member 1	7.900	6.784	6.971	6.930	-1.116
8131550	SCIN	scinderin	7.475	6.356	6.622	6.672	-1.119
7960518	TNFRSF1A	tumor necrosis factor receptor superfamily, member 1A	10.370	9.251	10.159	9.526	-1.119
8104234	TRIP13	thyroid hormone receptor interactor 13	7.997	6.878	6.466	6.584	-1.119
8049246	INPP5D	inositol polyphosphate-5-phosphatase, 145kDa	10.914	9.794	10.422	9.943	-1.120
7971573	RCBTB2	regulator of chromosome condensation (RCC1) and BTB (POZ) domain containing protein 2	10.637	9.517	10.569	9.331	-1.120
8131339	FSCN1	fascin homolog 1, actin-bundling protein (Strongylocentrotus purpuratus)	11.035	9.913	9.555	9.712	-1.121
8163002	KLF4	Kruppel-like factor 4 (gut)	7.166	6.039	6.201	6.128	-1.128
7906061	SYT11	synaptotagmin XI	9.142	8.012	9.038	8.103	-1.130
7959251	P2RX7	purinergic receptor P2X, ligand-gated ion channel, 7	9.459	8.327	9.023	8.524	-1.132
8135378	PRKAR2B	protein kinase, cAMP-dependent, regulatory, type II, beta	7.853	6.719	6.990	6.867	-1.133
7954436	LRMP	lymphoid-restricted membrane protein	9.139	8.003	7.796	8.035	-1.136
8075483	PIK3IP1	phosphoinositide-3-kinase interacting protein 1	8.103	6.968	7.373	7.268	-1.136
8135734	C7orf58	chromosome 7 open reading frame 58	8.176	7.040	8.899	7.032	-1.137
8117476	BTN3A3	butyrophilin, subfamily 3, member A3	7.769	6.632	6.930	6.689	-1.138
8104570	FAM105A	family with sequence similarity 105, member A	10.726	9.588	9.688	9.110	-1.138
7898521	IGSF21	immunoglobin superfamily, member 21	9.029	7.891	7.179	7.522	-1.139
7951397	CASP1	caspase 1, apoptosis-related cysteine peptidase (interleukin 1, beta, convertase)	9.656	8.516	9.037	7.932	-1.140
8129924	TXLNB	taxilin beta	10.328	9.186	8.874	8.685	-1.141
8175393	ARHGEF6	Rac/Cdc42 guanine nucleotide exchange factor (GEF) 6	9.978	8.835	8.822	8.669	-1.142
8137264	TMEM176A	transmembrane protein 176A	10.116	8.974	10.744	9.548	-1.142
8178086	HSPA1B	heat shock 70kDa protein 1B	9.527	8.383	9.400	8.681	-1.143
8179324	HSPA1B	heat shock 70kDa protein 1B	9.527	8.383	9.400	8.681	-1.143
7971866	DIAPH3	diaphanous homolog 3 (Drosophila)	6.501	5.357	4.802	5.214	-1.144
8054135	MGAT4A	mannosyl (alpha-1,3-)-glycoprotein beta-1,4-N-acetylglucosaminyltransferase, isozyme A	11.137	9.993	10.983	9.787	-1.144
8099834	TLR1	toll-like receptor 1	10.512	9.368	10.284	9.198	-1.144
8038824	SIGLEC10	sialic acid binding Ig-like lectin 10	10.572	9.427	10.733	9.530	-1.145
7942409	P2RY6	pyrimidinergic receptor P2Y, G-protein coupled, 6	8.500	7.350	8.501	7.715	-1.150
8035813	ZNF43	zinc finger protein 43	7.839	6.688	6.912	6.390	-1.150
8074237	CECR1	cat eye syndrome chromosome region, candidate 1	11.600	10.449	11.583	10.886	-1.152
7914851	CLSPN	claspin	6.990	5.838	5.467	5.876	-1.152
8046380	ITGA6	integrin, alpha 6	9.938	8.786	9.263	8.872	-1.152
8041867	MSH2	mutS homolog 2, colon cancer, nonpolyposis type 1 (E. coli)	7.587	6.432	6.275	6.139	-1.155
7929438	HELLS	helicase, lymphoid-specific	6.428	5.270	4.492	5.172	-1.158
8138466	MACC1	metastasis associated in colon cancer 1	8.267	7.108	8.493	7.599	-1.158
8096808	CCDC109B	coiled-coil domain containing 109B	10.289	9.130	9.053	8.943	-1.159
8157534	CEP110	centrosomal protein 110kDa	7.720	6.560	6.815	6.121	-1.159
8125447	HLA-DQB1	major histocompatibility complex, class II, DQ beta 1	9.055	7.895	8.325	7.971	-1.160
7995354	ORC6	origin recognition complex, subunit 6	7.151	5.991	6.012	6.038	-1.160
8035779	ZNF253	zinc finger protein 253	10.158	8.998	9.555	9.070	-1.160
8150592	CEBPD	CCAAT/enhancer binding protein (C/EBP), delta	9.781	8.619	9.183	9.133	-1.162
7939173	DEPDC7	DEP domain containing 7	7.598	6.434	6.119	6.167	-1.164
8141395	MCM7	minichromosome maintenance complex component 7	9.275	8.112	7.295	7.993	-1.164
8124534	HIST1H4L	histone cluster 1, H4l	10.218	9.053	8.524	9.261	-1.165
8118314	HSPA1B	heat shock 70kDa protein 1B	9.464	8.293	9.324	8.596	-1.170
8097857	MND1	meiotic nuclear divisions 1 homolog (S. cerevisiae)	6.002	4.832	4.433	4.855	-1.170
8124537	HIST1H3J	histone cluster 1, H3j	7.728	6.558	6.472	6.682	-1.171
8063785	C20orf197	chromosome 20 open reading frame 197	6.117	4.942	4.951	5.058	-1.175
7911178	NLRP3	NLR family, pyrin domain containing 3	8.878	7.701	9.230	7.851	-1.177
7920238	S100A12	S100 calcium binding protein A12	7.037	5.860	7.577	5.887	-1.177
7899187	HMGN2	high-mobility group nucleosomal binding domain 2	11.901	10.723	11.222	10.932	-1.178
8124531	HIST1H3I	histone cluster 1, H3i	12.211	11.032	10.654	11.164	-1.179
7933194	CXCL12	chemokine (C-X-C motif) ligand 12	7.586	6.406	6.956	6.490	-1.180
8149448	MSR1	macrophage scavenger receptor 1	12.531	11.348	12.142	11.582	-1.182
8174767	FAM70A	family with sequence similarity 70, member A	8.596	7.413	9.105	7.816	-1.183
8014233	SLFN11	schlafen family member 11	9.775	8.592	8.642	8.949	-1.183
8113073	ARRDC3	arrestin domain containing 3	11.474	10.290	11.240	10.466	-1.184
7975779	FOS	FBJ murine osteosarcoma viral oncogene homolog	10.520	9.336	10.028	9.746	-1.184
8152988	SLA	Src-like-adaptor	10.400	9.213	9.886	9.714	-1.187
7909455	TRAF3IP3	TRAF3 interacting protein 3	7.276	6.088	6.557	6.072	-1.187
7981142	CLMN	calmin (calponin-like, transmembrane)	9.083	7.893	8.936	8.164	-1.191
7938012	RIM6-TRIM3	TRIM6-TRIM34 readthrough	7.772	6.581	7.155	6.702	-1.191
8012257	TP53	tumor protein p53	9.711	8.516	9.186	8.462	-1.195
8098423	NEIL3	nei endonuclease VIII-like 3 (E. coli)	7.465	6.266	5.517	5.880	-1.199
7983828	TEX9	testis expressed 9	5.940	4.741	4.498	4.528	-1.199
7951297	MMP12	matrix metallopeptidase 12 (macrophage elastase)	7.623	6.422	7.111	6.896	-1.200
8056113	LY75	lymphocyte antigen 75	8.854	7.652	8.113	8.078	-1.202
8118564	HLA-DQA2	major histocompatibility complex, class II, DQ alpha 2	10.137	8.934	9.580	9.260	-1.203
8129637	VNN2	vanin 2	11.017	9.815	11.454	9.655	-1.203
7926223	CAMK1D	calcium/calmodulin-dependent protein kinase ID	8.249	7.041	7.845	6.991	-1.207
8137252	GIMAP1	GTPase, IMAP family member 1	8.497	7.290	7.242	7.290	-1.207
8132347	GPR141	G protein-coupled receptor 141	9.749	8.539	10.285	8.454	-1.210
8155214	MELK	maternal embryonic leucine zipper kinase	8.330	7.119	6.364	6.572	-1.210
7914282	SDC3	syndecan 3	9.192	7.982	7.680	8.454	-1.210
8152522	ENPP2	ectonucleotide pyrophosphatase/phosphodiesterase 2	7.237	6.027	6.116	5.740	-1.211
8006187	ATAD5	ATPase family, AAA domain containing 5	7.338	6.123	5.797	5.949	-1.216
8013616	SLC46A1	solute carrier family 46 (folate transporter), member 1	8.853	7.635	8.071	7.849	-1.218
8008185	ABI3	ABI family, member 3	9.260	8.040	8.891	7.788	-1.220
7987636	OIP5	Opa interacting protein 5	7.176	5.950	5.990	6.106	-1.226
8118556	HLA-DQA1	major histocompatibility complex, class II, DQ alpha 1	11.395	10.168	10.932	10.600	-1.227
7980438	SPTLC2	serine palmitoyltransferase, long chain base subunit 2	9.355	8.128	8.526	8.142	-1.227
8117583	HIST1H2AI	histone cluster 1, H2ai	8.642	7.413	7.018	7.494	-1.229
8064844	PCNA	proliferating cell nuclear antigen	9.721	8.488	8.515	8.443	-1.233
7994769	CORO1A	coronin, actin binding protein, 1A	11.747	10.513	10.879	10.437	-1.234
7938629	PDE3B	phosphodiesterase 3B, cGMP-inhibited	7.220	5.985	6.824	7.358	-1.234
7951408	CARD16	caspase recruitment domain family, member 16	7.698	6.460	6.882	6.085	-1.237
8117426	HIST1H2BH	histone cluster 1, H2bh	11.013	9.775	9.085	9.833	-1.238
8143781	GIMAP6	GTPase, IMAP family member 6	8.059	6.818	6.671	6.711	-1.240
8157524	TLR4	toll-like receptor 4	11.811	10.571	11.282	11.086	-1.240
8080320	NISCH	nischarin	9.570	8.329	9.342	8.570	-1.241
8066431	ADA	adenosine deaminase	10.412	9.169	9.737	9.056	-1.242
8178205	HLA-DQA2	major histocompatibility complex, class II, DQ alpha 2	10.054	8.811	9.457	9.138	-1.243
8103932	MLF1IP	MLF1 interacting protein	7.832	6.589	5.678	6.025	-1.243
8104912	SKP2	S-phase kinase-associated protein 2 (p45)	9.700	8.451	8.358	8.580	-1.249
8036787	FCGBP	Fc fragment of IgG binding protein	7.644	6.394	6.647	6.925	-1.250
8056837	GPR155	G protein-coupled receptor 155	9.778	8.527	8.631	8.176	-1.250
8124437	HIST1H3F	histone cluster 1, H3f	9.286	8.035	8.265	8.371	-1.252
8105436	MAP3K1	mitogen-activated protein kinase kinase kinase 1	10.780	9.526	9.877	9.375	-1.254
8021470	PMAIP1	phorbol-12-myristate-13-acetate-induced protein 1	7.540	6.286	6.738	5.705	-1.254
7964271	PRIM1	primase, DNA, polypeptide 1 (49kDa)	9.482	8.227	7.367	8.110	-1.255
8126839	TNFRSF21	tumor necrosis factor receptor superfamily, member 21	9.678	8.423	8.454	9.211	-1.255
8106516	JMY	junction mediating and regulatory protein, p53 cofactor	7.501	6.245	7.033	6.081	-1.256
7934459	NDST2	N-deacetylase/N-sulfotransferase (heparan glucosaminyl) 2	10.482	9.226	9.586	9.106	-1.256
8036136	TMEM149	transmembrane protein 149	10.081	8.821	10.161	8.689	-1.259
8151101	MYBL1	v-myb myeloblastosis viral oncogene homolog (avian)-like 1	5.618	4.358	4.435	4.373	-1.260

7915926	STIL	SCL/TAL1 interrupting locus	8.195	6.935	6.558	6.722	-1.260
7926259	MCM10	minichromosome maintenance complex component 10	7.794	6.531	5.734	6.819	-1.263
8122637	SASH1	SAM and SH3 domain containing 1	9.170	7.904	8.736	7.202	-1.266
8071212	CDC45	cell division cycle 45 homolog (S. cerevisiae)	8.309	7.040	6.592	7.051	-1.269
7969986	TNFSF13B	tumor necrosis factor (ligand) superfamily, member 13b	10.635	9.366	10.384	9.461	-1.269
7943160	SCARNA9	small Cajal body-specific RNA 9	7.833	6.560	7.295	6.192	-1.272
7938035	TRIM22	tripartite motif-containing 22	10.422	9.151	10.118	9.366	-1.272
8008784	PRR11	proline rich 11	9.092	7.818	8.323	7.864	-1.274
8124391	HIST1H2AB	histone cluster 1, H2ab	7.602	6.327	6.066	6.393	-1.276
8019486	SECTM1	secreted and transmembrane 1	9.588	8.309	9.236	8.509	-1.279
8014241	SLFN12	schlafen family member 12	7.873	6.592	7.311	6.574	-1.281
7976080	GPR65	G protein-coupled receptor 65	10.695	9.413	10.194	9.888	-1.282
7919612	HIST2H3D	histone cluster 2, H3d	10.581	9.299	8.807	9.277	-1.282
8179322	HSPA1A	heat shock 70kDa protein 1A	11.375	10.092	11.248	10.475	-1.283
8102389	C4orf21	chromosome 4 open reading frame 21	6.726	5.441	5.511	5.113	-1.285
7902874	LRRC8C	leucine rich repeat containing 8 family, member C	9.351	8.064	8.545	7.791	-1.287
7940441	PGA5	pepsinogen 5, group I (pepsinogen A)	8.354	7.067	6.591	6.214	-1.287
7943577	RAB39	RAB39, member RAS oncogene family	9.223	7.934	8.793	7.763	-1.289
8079237	KIF15	kinesin family member 15	6.684	5.390	4.629	4.795	-1.294
8123609	SERPINB9	serpin peptidase inhibitor, clade B (ovalbumin), member 9	10.193	8.898	9.617	8.687	-1.295
8058695	BARD1	BRCA1 associated RING domain 1	8.240	6.942	7.129	6.774	-1.298
8111739	FYB	FYN binding protein	11.400	10.099	10.882	10.159	-1.301
7971565	LPAR6	lysophosphatidic acid receptor 6	10.859	9.556	10.277	9.656	-1.303
8119132	FGD2	FYVE, RhoGEF and PH domain containing 2	7.890	6.584	7.209	7.240	-1.306
7948364	MPEG1	macrophage expressed 1	11.830	10.523	11.562	10.666	-1.306
8118310	HSPA1A	heat shock 70kDa protein 1A	11.434	10.125	11.284	10.504	-1.309
8041447	CRIM1	cysteine rich transmembrane BMP regulator 1 (chordin-like)	10.249	8.937	11.409	9.283	-1.312
8103728	HMGB2	high-mobility group box 2	7.196	5.884	6.018	5.645	-1.312
8129804	MAP3K5	mitogen-activated protein kinase kinase kinase 5	8.803	7.491	8.069	7.564	-1.312
7910997	EXO1	exonuclease 1	7.514	6.200	5.922	6.175	-1.313
8112376	CENPK	centromere protein K	8.340	7.026	5.717	6.198	-1.314
7951217	MMP7	matrix metallopeptidase 7 (matrilysin, uterine)	10.339	9.023	9.140	8.484	-1.316
7970513	SKA3	spindle and kinetochore associated complex subunit 3	8.333	7.015	6.250	6.542	-1.318
8015769	BRCA1	breast cancer 1, early onset	7.984	6.664	6.171	6.343	-1.319
8155192	GLIPR2	GLI pathogenesis-related 2	10.615	9.294	10.068	9.941	-1.321
8062766	MYBL2	v-myb myeloblastosis viral oncogene homolog (avian)-like 2	8.632	7.311	6.590	7.457	-1.321
7986068	BLM	Bloom syndrome, RecQ helicase-like	7.624	6.301	5.718	5.817	-1.323
8096602	DAPP1	dual adaptor of phosphotyrosine and 3-phosphoinositides	8.438	7.113	8.393	7.371	-1.325
8101762	SNCA	synuclein, alpha (non A4 component of amyloid precursor)	10.028	8.701	8.808	9.095	-1.327
7898809	EPHB2	EPH receptor B2	9.764	8.433	9.799	8.491	-1.331
7948910	SNORD25	small nucleolar RNA, C/D box 25	6.242	4.910	4.193	4.567	-1.332
7985873	C15orf42	chromosome 15 open reading frame 42	7.440	6.104	5.783	6.170	-1.336
8102560	MAD2L1	MAD2 mitotic arrest deficient-like 1 (yeast)	7.906	6.569	6.221	6.271	-1.337
8035456	LRRC25	leucine rich repeat containing 25	10.353	9.016	9.750	9.239	-1.338
7917503	GBP3	guanylate binding protein 3	7.885	6.545	7.520	6.645	-1.341
8137257	GIMAP5	GTPase, IMAP family member 5	8.839	7.498	7.622	7.175	-1.341
8140463	FGL2	fibrinogen-like 2	9.204	7.862	8.517	7.722	-1.342
8128698	SESN1	sestrin 1	9.122	7.778	8.221	7.675	-1.344
8101757	GPRIN3	GPRIN family member 3	10.321	8.975	9.614	9.716	-1.346
7908351	PLA2G4A	phospholipase A2, group IVA (cytosolic, calcium-dependent)	8.902	7.555	8.349	6.979	-1.347
8103508	40969	membrane-associated ring finger (C3HC4) 1	10.915	9.567	10.765	9.889	-1.348
7940431	PGA4	pepsinogen 4, group I (pepsinogen A)	8.457	7.108	6.721	6.350	-1.349
8148059	DEPDC6	DEP domain containing 6	8.566	7.215	7.022	6.897	-1.350
8166065	TLR8	toll-like receptor 8	9.438	8.085	9.245	8.244	-1.352
7898793	C1QA	complement component 1, q subcomponent, A chain	10.644	9.291	10.176	9.500	-1.353
7971486	C13orf18	chromosome 13 open reading frame 18	7.288	5.931	5.954	6.154	-1.357
8064716	SIGLEC1	sialic acid binding Ig-like lectin 1, sialoadhesin	10.107	8.742	10.000	9.139	-1.365
8152668	ATAD2	ATPase family, AAA domain containing 2	8.408	7.043	6.412	6.867	-1.366
8103399	PDGFC	platelet derived growth factor C	8.178	6.801	8.380	6.591	-1.377
7940421	PGA3	pepsinogen 3, group I (pepsinogen A)	8.475	7.097	6.907	6.373	-1.378
7923189	KIF14	kinesin family member 14	6.944	5.564	5.160	5.039	-1.379
7898799	C1QC	complement component 1, q subcomponent, C chain	12.392	11.009	12.032	11.323	-1.383
7937335	IFITM1	interferon induced transmembrane protein 1 (9-27)	7.432	6.049	7.204	6.293	-1.383
7929145	HECTD2	HECT domain containing 2	8.035	6.651	7.022	6.222	-1.385
8091757	TRIM59	tripartite motif-containing 59	7.061	5.676	5.402	5.498	-1.385
8047288	SGOL2	shugoshin-like 2 (S. pombe)	7.469	6.083	6.516	5.740	-1.387
7919642	HIST2H2AB	histone cluster 2, H2ab	10.143	8.752	9.087	8.838	-1.391
8068478	CHAF1B	chromatin assembly factor 1, subunit B (p60)	7.648	6.254	5.913	6.451	-1.393
8033257	C3	complement component 3	10.910	9.516	11.391	10.019	-1.394
7966089	CMKLR1	chemokine-like receptor 1	10.719	9.323	11.005	9.189	-1.396
8139033	AOAH	acyloxyacyl hydrolase (neutrophil)	11.526	10.127	11.171	10.357	-1.400
8112615	ENC1	ectodermal-neural cortex 1 (with BTB-like domain)	8.303	6.902	6.558	6.962	-1.401
8136067	TSPAN33	tetraspanin 33	10.648	9.244	10.218	8.726	-1.404
8146357	MCM4	minichromosome maintenance complex component 4	9.049	7.641	6.911	7.832	-1.408
8113356	PAM // GPAM	glycerol-3-phosphate acyltransferase, mitochondrial // glycerol-3-phosphate acyltransferase, mitochondrial	5.498	4.089	4.818	3.782	-1.409
8092169	TNFSF10	tumor necrosis factor (ligand) superfamily, member 10	9.246	7.835	8.388	7.787	-1.411
7960340	FOXM1	forkhead box M1	7.967	6.549	5.916	6.589	-1.418
7942569	SLCO2B1	solute carrier organic anion transporter family, member 2B1	12.061	10.642	11.512	10.592	-1.419
7901788	NFIA	nuclear factor I/A	8.152	6.731	6.271	6.208	-1.420
7947110	E2F8	E2F transcription factor 8	7.650	6.228	5.698	6.491	-1.421
7982792	RAD51	RAD51 homolog (RecA homolog, E. coli) (S. cerevisiae)	7.815	6.388	5.983	6.167	-1.427
8171136	P2RY8	purinergic receptor P2Y, G-protein coupled, 8	8.073	6.640	6.632	6.859	-1.433
8177926	P2RY8	purinergic receptor P2Y, G-protein coupled, 8	8.073	6.640	6.632	6.859	-1.433
8069541	SAMSN1	SAM domain, SH3 domain and nuclear localization signals 1	10.089	8.653	9.276	8.247	-1.436
8056102	CD302	CD302 molecule	12.355	10.917	11.325	11.028	-1.438
8054580	BUB1	budding uninhibited by benzimidazoles 1 homolog (yeast)	8.193	6.754	6.820	6.636	-1.439
7929282	HHEX	hematopoietically expressed homeobox	8.258	6.816	6.929	6.975	-1.442
8138489	CDCA7L	cell division cycle associated 7-like	8.451	6.993	5.736	6.821	-1.458
8092578	ETV5	ets variant 5	10.952	9.490	9.841	9.288	-1.462
8043602	NCAPH	non-SMC condensin I complex, subunit H	10.524	9.060	9.048	10.320	-1.464
7935270	BLNK	B-cell linker	9.202	7.735	8.268	7.193	-1.467
8130374	FBXO5	F-box protein 5	9.478	8.011	7.640	7.684	-1.467
8110971	CMBL	carboxymethylenebutenolidase homolog (Pseudomonas)	8.992	7.523	7.489	7.455	-1.469
7909708	CENPF	centromere protein F, 350/400kDa (mitosin)	7.700	6.229	5.734	5.984	-1.471
7913869	STMN1	stathmin 1	8.912	7.441	6.072	7.631	-1.471
8080344	STAB1	stabilin 1	11.490	10.017	11.179	10.185	-1.473
8020630	TTC39C	tetratricopeptide repeat domain 39C	8.511	7.038	7.992	7.198	-1.473
7988644	ATP8B4	ATPase, class I, type 8B, member 4	10.200	8.717	9.338	8.405	-1.483
7997712	IRF8	interferon regulatory factor 8	10.521	9.036	10.409	9.883	-1.485
7994826	ITGAL	integrin, alpha L (antigen CD11A (p180), lymphocyte function-associated antigen 1; alpha polypeptide)	9.342	7.837	9.535	7.826	-1.505
8111915	SEPP1	selenoprotein P, plasma, 1	13.224	11.717	11.873	11.053	-1.507
8035793	ZNF737	zinc finger protein 737	9.603	8.096	8.149	7.687	-1.507
8061471	GINS1	GINS complex subunit 1 (Psf1 homolog)	8.636	7.126	6.684	6.988	-1.509
8171248	KAL1	Kallmann syndrome 1 sequence	7.580	6.070	7.201	6.457	-1.510
8145570	ESCO2	establishment of cohesion 1 homolog 2 (S. cerevisiae)	9.531	8.015	6.650	7.465	-1.516
8171896	CXorf21	chromosome X open reading frame 21	8.700	7.179	8.200	7.749	-1.521
7989647	KIAA0101	KIAA0101	8.458	6.935	4.837	6.428	-1.523
8039692	ZNF814	zinc finger protein 814	8.272	6.742	7.540	6.456	-1.530
7978846	POLE2	polymerase (DNA directed), epsilon 2 (p59 subunit)	7.760	6.227	5.489	5.516	-1.532
8132819	IKZF1	IKAROS family zinc finger 1 (Ikaros)	9.027	7.492	8.567	7.595	-1.534
8014361	CCL23	chemokine (C-C motif) ligand 23	6.935	5.400	5.384	5.071	-1.535
8143441	KIAA1147	KIAA1147	9.444	7.906	8.442	7.494	-1.538
8112478	NAIP	NLR family, apoptosis inhibitory protein	11.916	10.376	10.850	10.380	-1.540
7945132	FLI1	Friend leukemia virus integration 1	10.369	8.823	9.358	8.814	-1.546
8097867	KIAA0922	KIAA0922	7.697	6.143	6.948	6.239	-1.554
8057677	SLC40A1	solute carrier family 40 (iron-regulated transporter), member 1	8.098	6.541	6.265	6.327	-1.557
8137250	GIMAP2	GTPase, IMAP family member 2	9.254	7.690	8.124	7.315	-1.564
8112521	NAIP	NLR family, apoptosis inhibitory protein	11.330	9.761	10.211	9.753	-1.569
8177527	NAIP	NLR family, apoptosis inhibitory protein	11.330	9.761	10.211	9.753	-1.569
7923086	ASPM	asp (abnormal spindle) homolog, microcephaly associated (Drosophila)	6.792	5.221	4.545	4.746	-1.572
7918533	ADORA3	adenosine A3 receptor	10.074	8.495	9.279	7.555	-1.579
8023497	ATP8B1	ATPase, aminophospholipid transporter, class I, type 8B, member 1	9.649	8.061	9.212	7.364	-1.587
7929078	KIF20B	kinesin family member 20B	7.189	5.594	5.493	5.093	-1.594
8091260	SLC9A9	solute carrier family 9 (sodium/hydrogen exchanger), member 9	11.278	9.685	11.010	9.514	-1.594
8124527	HIST1H1B	histone cluster 1, H1b	8.866	7.269	6.542	7.262	-1.598
7900699	CDC20	cell division cycle 20 homolog (S. cerevisiae)	8.545	6.934	6.517	7.313	-1.611
8017262	BRIP1	BRCA1 interacting protein C-terminal helicase 1	7.172	5.556	4.645	5.252	-1.616
8003204	GINS2	GINS complex subunit 2 (Psf2 homolog)	9.801	8.183	7.126	8.382	-1.619
8039928	FAM72D	family with sequence similarity 72, member D	8.606	6.986	7.092	6.645	-1.620
8137244	GIMAP4	GTPase, IMAP family member 4	7.459	5.839	5.853	5.867	-1.620
8116734	LY86	lymphocyte antigen 86	11.127	9.504	10.541	9.663	-1.623

8166919	GPR82	G protein-coupled receptor 82	9.200	7.573	8.061	7.740	-1.627
7989146	MNS1	meiosis-specific nuclear structural 1	7.275	5.647	5.013	5.060	-1.628
8115397	C5orf4	chromosome 5 open reading frame 4	8.308	6.678	6.589	6.579	-1.630
8137240	GIMAP7	GTPase, IMAP family member 7	8.311	6.675	6.729	5.973	-1.635
8046333	CYBRD1	cytochrome b reductase 1	10.292	8.652	8.915	8.894	-1.641
7919591	FAM72D	family with sequence similarity 72, member D	8.157	6.514	6.458	6.219	-1.643
8163629	TNFSF8	tumor necrosis factor (ligand) superfamily, member 8	10.765	9.121	9.758	8.984	-1.644
7942832	C11orf82	chromosome 11 open reading frame 82	8.106	6.454	6.042	5.958	-1.651
7974404	CDKN3	cyclin-dependent kinase inhibitor 3	7.975	6.323	6.727	6.019	-1.652
7982358	ARHGAP11A	Rho GTPase activating protein 11A	7.886	6.230	6.349	5.763	-1.657
8149955	PBK	PDZ binding kinase	6.129	4.471	4.308	4.580	-1.658
8112007	EMB	embigin	10.135	8.475	8.233	8.216	-1.660
7957338	SYT1	synaptotagmin I	9.373	7.704	8.627	7.350	-1.669
8112940	SSBP2	single-stranded DNA binding protein 2	10.059	8.389	8.986	7.824	-1.670
8109712	HMMR	hyaluronan-mediated motility receptor (RHAMM)	7.074	5.403	4.985	4.980	-1.671
7991406	PRC1	protein regulator of cytokinesis 1	8.712	7.039	6.081	6.977	-1.674
8085754	SGOL1	shugoshin-like 1 (S. pombe)	7.684	6.003	5.590	5.674	-1.681
7904452	FAM72D	family with sequence similarity 72, member D	8.645	6.962	7.111	6.642	-1.683
7909146	FAM72D	family with sequence similarity 72, member D	8.657	6.970	7.109	6.650	-1.687
8094278	NCAPG	non-SMC condensin I complex, subunit G	8.491	6.804	5.428	6.533	-1.687
7914878	CLSPN	claspin	7.445	5.756	4.695	5.368	-1.689
7983969	CCNB2	cyclin B2	8.623	6.932	6.537	6.825	-1.691
8054702	CKAP2L	cytoskeleton associated protein 2-like	7.481	5.787	5.545	5.741	-1.693
8056572	SPC25	SPC25, NDC80 kinetochore complex component, homolog (S. cerevisiae)	6.635	4.935	4.447	5.038	-1.700
7929334	CEP55	centrosomal protein 55kDa	8.873	7.172	6.574	6.984	-1.701
8001133	SHCBP1	SHC SH2-domain binding protein 1	8.400	6.694	5.927	6.448	-1.706
8102076	CENPE	centromere protein E, 312kDa	6.704	4.985	5.242	4.845	-1.718
7951077	SESN3	sestrin 3	10.589	8.868	10.056	8.605	-1.720
8040223	RRM2	ribonucleotide reductase M2	9.336	7.615	5.866	7.749	-1.721
8124394	HIST1H2BB	histone cluster 1, H2bb	7.854	6.132	5.298	5.995	-1.722
8097356	PLK4	polo-like kinase 4	8.241	6.519	5.898	6.068	-1.722
8098611	TLR3	toll-like receptor 3	8.377	6.651	7.115	6.526	-1.726
8047677	CD28	CD28 molecule	7.490	5.753	5.603	5.706	-1.737
7904158	OLFML3	olfactomedin-like 3	8.755	7.014	7.055	6.479	-1.741
8166906	GPR34	G protein-coupled receptor 34	11.309	9.567	9.379	9.021	-1.742
7982757	CASC5	cancer susceptibility candidate 5	7.918	6.174	5.785	5.790	-1.745
8122827	C6orf97	chromosome 6 open reading frame 97	7.793	6.046	6.272	5.924	-1.747
8124388	HIST1H3B	histone cluster 1, H3b	10.599	8.851	6.720	8.962	-1.748
7957570	PLXNC1	plexin C1	11.326	9.576	10.848	9.783	-1.750
7982663	BUB1B	budding uninhibited by benzimidazoles 1 homolog beta (yeast)	7.890	6.129	5.346	5.838	-1.761
8117594	HIST1H2BM	histone cluster 1, H2bm	11.589	9.827	8.002	10.277	-1.762
7908376	RGS18	regulator of G-protein signaling 18	8.049	6.286	5.379	5.780	-1.763
8024792	EBI3	Epstein-Barr virus induced 3	9.002	7.237	7.753	7.180	-1.765
8023361	MRO	maestro	9.084	7.318	7.139	6.989	-1.765
7943892	NCAM1	neural cell adhesion molecule 1	7.813	6.045	7.471	6.589	-1.768
7909568	DTL	denticleless homolog (Drosophila)	9.310	7.540	5.623	7.283	-1.770
8007100	IGFBP4	insulin-like growth factor binding protein 4	10.684	8.909	9.083	8.881	-1.775
8113039	MEF2C	myocyte enhancer factor 2C	11.527	9.749	9.276	9.496	-1.779
7982889	NUSAP1	nucleolar and spindle associated protein 1	9.422	7.641	7.312	7.341	-1.781
8120838	TTK	TTK protein kinase	7.119	5.335	5.451	4.978	-1.784
7908409	RGS2	regulator of G-protein signaling 2, 24kDa	9.074	7.281	7.239	7.204	-1.794
8019857	NDC80	NDC80 homolog, kinetochore complex component (S. cerevisiae)	7.191	5.396	4.799	5.218	-1.795
8061579	TPX2	TPX2, microtubule-associated, homolog (Xenopus laevis)	8.353	6.558	6.138	6.632	-1.795
8160260	BNC2	basonuclin 2	8.194	6.398	6.715	6.193	-1.796
7937020	MKI67	antigen identified by monoclonal antibody Ki-67	8.818	7.017	5.555	7.181	-1.801
8178826	HLA-DQB1	major histocompatibility complex, class II, DQ beta 1	10.502	8.700	9.534	9.251	-1.803
8180022	HLA-DQB1	major histocompatibility complex, class II, DQ beta 1	10.502	8.700	9.534	9.251	-1.803
7916898	DEPDC1	DEP domain containing 1	6.854	5.026	4.792	5.016	-1.828
7906377	MNDA	myeloid cell nuclear differentiation antigen	9.730	7.900	8.643	8.332	-1.830
7929511	ENTPD1	ectonucleoside triphosphate diphosphohydrolase 1	10.802	8.955	9.168	8.838	-1.847
8034772	ASF1B	ASF1 anti-silencing function 1 homolog B (S. cerevisiae)	9.475	7.624	7.651	7.678	-1.851
8048717	SGPP2	sphingosine-1-phosphate phosphatase 2	8.584	6.731	9.499	5.692	-1.853
8122334	CCRL1	chemokine (C-C motif) receptor-like 1	7.998	6.137	6.021	6.192	-1.860
8035838	ZNF724P	zinc finger protein 724, pseudogene	8.085	6.220	6.676	6.116	-1.866
7929344	GPR120	G protein-coupled receptor 120	8.529	6.653	7.226	6.932	-1.876
8007071	CDC6	cell division cycle 6 homolog (S. cerevisiae)	8.870	6.990	5.495	6.665	-1.880
8021187	SKA1	spindle and kinetochore associated complex subunit 1	6.942	5.055	4.921	4.866	-1.887
7905060	FCGR1A	Fc fragment of IgG, high affinity Ia, receptor (CD64)	10.881	8.991	9.370	8.379	-1.889
7919133	FCGR1B	Fc fragment of IgG, high affinity Ib, receptor (CD64)	10.935	9.046	9.457	8.487	-1.889
7906930	NUF2	NUF2, NDC80 kinetochore complex component, homolog (S. cerevisiae)	7.186	5.276	4.606	5.164	-1.910
7905047	FCGR1A	Fc fragment of IgG, high affinity Ia, receptor (CD64)	11.215	9.297	9.740	8.699	-1.918
8089568	CD200R1	CD200 receptor 1	8.627	6.676	6.082	5.650	-1.951
8019842	TYMS	thymidylate synthetase	10.209	8.258	5.868	8.145	-1.951
8140556	HGF	hepatocyte growth factor (hepapoietin A; scatter factor)	7.116	5.156	5.050	5.083	-1.960
8108301	KIF20A	kinesin family member 20A	7.768	5.807	5.069	5.552	-1.961
8124166	MBOAT1	membrane bound O-acyltransferase domain containing 1	10.011	8.046	8.093	8.027	-1.965
8020806	RNF125	ring finger protein 125	9.199	7.233	7.913	7.139	-1.966
8084717	ST6GAL1	ST6 beta-galactosamide alpha-2,6-sialyltranferase 1	10.549	8.578	8.197	8.133	-1.970
7922337	TNFSF18	tumor necrosis factor (ligand) superfamily, member 18	6.315	4.340	4.406	4.432	-1.975
8141459	GAL3ST4	galactose-3-O-sulfotransferase 4	9.524	7.534	8.397	7.572	-1.990
8044813	TMEM37	transmembrane protein 37	9.986	7.978	8.418	8.481	-2.008
7927710	CDK1	cyclin-dependent kinase 1	8.419	6.408	4.529	5.548	-2.011
8102643	CCNA2	cyclin A2	9.740	7.709	6.770	7.884	-2.030
8014974	TOP2A	topoisomerase (DNA) II alpha 170kDa	9.304	7.265	5.956	7.007	-2.039
8155930	GCNT1	glucosaminyl (N-acetyl) transferase 1, core 2	9.618	7.575	8.355	7.504	-2.043
8132318	ANLN	anillin, actin binding protein	9.135	7.087	5.815	6.936	-2.049
7979307	DLGAP5	discs, large (Drosophila) homolog-associated protein 5	7.701	5.640	4.934	5.218	-2.061
7953218	RAD51AP1	RAD51 associated protein 1	8.272	6.175	5.910	5.706	-2.097
8021946	COLEC12	collectin sub-family member 12	10.399	8.279	9.761	7.545	-2.119
8006968	GSDMA	gasdermin A	9.316	7.188	7.584	6.656	-2.128
7940147	FAM111B	family with sequence similarity 111, member B	9.406	7.256	5.308	6.630	-2.150
8123744	F13A1	coagulation factor XIII, A1 polypeptide	10.823	8.669	8.487	7.259	-2.154
8046695	ITGA4	integrin, alpha 4 (antigen CD49D, alpha 4 subunit of VLA-4 receptor)	9.414	7.259	7.631	6.839	-2.155
7972157	EDNRB	endothelin receptor type B	8.667	6.511	7.344	6.191	-2.156
8012605	GAS7	growth arrest-specific 7	10.209	8.050	9.845	8.265	-2.159
7988414	GATM	glycine amidinotransferase (L-arginine:glycine amidinotransferase)	10.337	8.146	8.117	8.167	-2.191
7929258	KIF11	kinesin family member 11	8.524	6.314	5.472	5.990	-2.210
8025103	EMR1	egf-like module containing, mucin-like, hormone receptor-like 1	8.916	6.703	7.569	6.570	-2.213
8166059	TLR7	toll-like receptor 7	8.386	6.154	6.545	5.756	-2.232
8151871	CCNE2	cyclin E2	9.397	7.122	5.412	6.750	-2.274
7948455	MS4A6A	membrane-spanning 4-domains, subfamily A, member 6A	9.693	7.387	6.773	7.016	-2.306
7898805	C1QB	complement component 1, q subcomponent, B chain	11.390	9.067	9.580	9.331	-2.323
7965873	IGF1	insulin-like growth factor 1 (somatomedin C)	9.387	6.903	7.148	5.789	-2.484
8151532	FABP4	fatty acid binding protein 4, adipocyte	8.460	5.945	8.346	10.895	-2.515
8059680	HTR2B	5-hydroxytryptamine (serotonin) receptor 2B	9.318	6.701	7.693	5.584	-2.617
7957962	SPIC	Spi-C transcription factor (Spi-1/PU.1 related)	9.337	6.560	5.553	5.253	-2.777
8112428	CD180	CD180 molecule	10.141	7.284	8.532	6.945	-2.857
8105481	GAPT	GRB2-binding adaptor protein, transmembrane	9.497	6.536	9.274	6.469	-2.961
8163908	GGTA1	glycoprotein, alpha-galactosyltransferase 1 pseudogene	10.175	6.916	7.263	6.877	-3.259

Appendix VII

List of genes induced by RANKL counter-regulated by GSK-J4 at day 14 in differentiating osteoclast.

Probe ID	Gene symbol	Gene Name	m	mr	j4	j5	mr-m	folds (J4-m)
7899821	KIAA1522	KIAA1522	6.962	7.970	7.707	7.863	1.009	0.746
8081288	TMEM45A	transmembrane protein 45A	5.949	7.677	6.695	7.126	1.728	0.746
7961371	DUSP16	dual specificity phosphatase 16	7.494	9.057	8.237	8.498	1.563	0.743
8099633	PPARGC1A	peroxisome proliferator-activated receptor gamma, coactivator 1 alpha	5.712	8.669	6.454	7.224	2.957	0.742
8108478	C5orf32	chromosome 5 open reading frame 32	10.417	11.584	11.158	11.438	1.167	0.741
8063923	SLCO4A1	solute carrier organic anion transporter family, member 4A1	8.803	11.322	9.536	10.754	2.519	0.733
8089261	CBLB	Cas-Br-M (murine) ecotropic retroviral transforming sequence b	10.897	12.451	11.628	12.068	1.554	0.731
7915472	SLC2A1	solute carrier family 2 (facilitated glucose transporter), member 1	9.142	11.229	9.873	10.605	2.087	0.731
8046861	ITGAV	integrin, alpha V (vitronectin receptor, alpha polypeptide, antigen CD51)	11.516	12.626	12.243	12.317	1.111	0.727
8147132	CA2	carbonic anhydrase II	11.856	13.129	12.582	13.040	1.273	0.726
8135734	C7orf58	chromosome 7 open reading frame 58	8.176	7.040	8.899	7.032	-1.137	0.722
8163599	DFNB31	deafness, autosomal recessive 31	6.703	7.730	7.422	7.726	1.027	0.719
7904433	PHGDH	phosphoglycerate dehydrogenase	6.288	7.404	7.007	7.072	1.116	0.719
7960865	SLC2A3	solute carrier family 2 (facilitated glucose transporter), member 3	10.066	11.278	10.774	10.652	1.212	0.709
7954065	GPRC5A	G protein-coupled receptor, family C, group 5, member A	5.531	7.078	6.239	6.273	1.547	0.708
8062844	TTPAL	tocopherol (alpha) transfer protein-like	7.279	8.966	7.987	8.753	1.687	0.708
8066939	B4GALT5	UDP-Gal:betaGlcNAc beta 1,4- galactosyltransferase, polypeptide 5	10.922	11.993	11.627	11.899	1.071	0.705
8089820	GPR156	G protein-coupled receptor 156	5.288	7.037	5.992	6.081	1.749	0.704
7977270	LOC388022	hypothetical LOC388022	8.413	9.464	9.117	9.211	1.050	0.704
8139207	INHBA	inhibin, beta A	6.227	7.341	6.929	6.639	1.113	0.702
7966738	C12orf49	chromosome 12 open reading frame 49	10.230	11.664	10.928	11.196	1.433	0.698
8109201	HMGXB3	HMG box domain containing 3	9.159	10.197	9.857	10.046	1.038	0.698
7952927	B4GALNT3	beta-1,4-N-acetyl-galactosaminyl transferase 3	7.108	8.728	7.805	8.480	1.620	0.696
8136115	FAM40B	family with sequence similarity 40, member B	8.555	10.743	9.248	10.375	2.188	0.693
8147145	ATP6V0D2	ATPase, H+ transporting, lysosomal 38kDa, V0 subunit d2	10.848	12.443	11.537	12.118	1.595	0.689
8098263	PALLD	palladin, cytoskeletal associated protein	7.774	9.795	8.463	8.742	2.021	0.689
8148448	KHDRBS3	KH domain containing, RNA binding, signal transduction associated 3	7.232	8.355	7.920	7.671	1.123	0.688
8058221	TRAK2	trafficking protein, kinesin binding 2	10.146	11.848	10.829	11.293	1.702	0.684
7897119	C1orf93	chromosome 1 open reading frame 93	8.855	9.857	9.538	9.480	1.002	0.682
8016239	PLEKHM1	pleckstrin homology domain containing, family M (with RUN domain) member 1	9.228	10.623	9.906	10.491	1.395	0.678
7933933	DNAJC12	DnaJ (Hsp40) homolog, subfamily C, member 12	6.959	8.520	7.633	8.111	1.561	0.674
7924526	TP53BP2	tumor protein p53 binding protein, 2	9.703	10.843	10.377	10.288	1.140	0.674
8174598	IL13RA2	interleukin 13 receptor, alpha 2	4.071	5.671	4.744	4.397	1.600	0.673
8080714	FLNB	filamin B, beta	8.336	10.001	9.006	9.869	1.665	0.670
8149749	TNFRSF10D	tumor necrosis factor receptor superfamily, member 10d, decoy with truncated death domain	9.278	10.339	9.941	9.966	1.061	0.663
8138824	SCRN1	secernin 1	8.297	9.741	8.958	9.604	1.444	0.661
7959638	TCTN2	tectonic family member 2	7.614	9.029	8.275	8.351	1.416	0.661
8169898	RAB33A	RAB33A, member RAS oncogene family	7.486	8.942	8.144	8.252	1.456	0.658
8093878	EVC	Ellis van Creveld syndrome	7.423	8.745	8.080	8.334	1.321	0.657
7913787	C1orf201	chromosome 1 open reading frame 201	6.441	8.237	7.094	7.797	1.796	0.653
7980720	TTC7B	tetratricopeptide repeat domain 7B	9.149	10.152	9.800	9.814	1.004	0.651
8109773	WWC1	WW and C2 domain containing 1	7.239	9.284	7.887	8.916	2.045	0.648
8022941	C18orf10	chromosome 18 open reading frame 10	11.434	12.692	12.080	12.352	1.258	0.647
8022711	DSC2	desmocollin 2	8.591	10.131	9.237	9.488	1.540	0.646
8145989	HTRA4	HtrA serine peptidase 4	8.917	10.217	9.557	9.783	1.300	0.640
8046124	DHRS9	dehydrogenase/reductase (SDR family) member 9	8.687	10.649	9.326	10.025	1.962	0.639
7913357	ECE1	endothelin converting enzyme 1	8.323	9.623	8.958	9.480	1.301	0.636
8098103	FNIP2	folliculin interacting protein 2	10.789	12.077	11.425	11.812	1.288	0.636
8114733	ARAP3	ArfGAP with RhoGAP domain, ankyrin repeat and PH domain 3	7.173	8.535	7.808	8.120	1.363	0.635
8147848	OXR1	oxidation resistance 1	10.015	11.838	10.650	11.100	1.823	0.634
7904830	RNF115	ring finger protein 115	9.999	11.563	10.633	10.884	1.564	0.634
8155673	PIP5K1B	phosphatidylinositol-4-phosphate 5-kinase, type I, beta	6.183	8.026	6.814	7.019	1.843	0.632
8085556	SH3BP5	SH3-domain binding protein 5 (BTK-associated)	9.116	10.161	9.748	9.780	1.045	0.632
7909104	CDK18	cyclin-dependent kinase 18	7.949	9.237	8.578	8.949	1.288	0.629
8063394	PTPN1	protein tyrosine phosphatase, non-receptor type 1	10.288	11.375	10.916	11.485	1.087	0.628
8137264	TMEM176A	transmembrane protein 176A	10.116	8.974	10.744	9.548	-1.142	0.627
8120719	CD109	CD109 molecule	10.492	11.873	11.113	11.442	1.381	0.621
8106743	VCAN	versican	4.934	6.779	5.552	7.885	1.845	0.618
7902425	ST6GALNAC3	ST6 (alpha-N-acetyl-neuraminyl-2,3-beta-galactosyl-1,3)-N-acetylgalactosaminide alpha-2,6-sialyltransfe	4.925	5.957	5.542	5.525	1.032	0.617
8156905	TMEFF1	transmembrane protein with EGF-like and two follistatin-like domains 1	6.912	8.010	7.528	7.608	1.098	0.616
7917754	BCAR3	breast cancer anti-estrogen resistance 3	7.063	8.583	7.677	7.893	1.520	0.613
7909603	NENF	neuron derived neurotrophic factor	10.334	11.342	10.947	10.684	1.008	0.613
7965964	SLC41A2	solute carrier family 41, member 2	9.610	10.688	10.221	10.274	1.078	0.612
8077441	BHLHE40	basic helix-loop-helix family, member e40	10.245	11.397	10.856	11.363	1.152	0.611
7986675	NIPA1	non imprinted in Prader-Willi/Angelman syndrome 1	8.025	9.188	8.636	8.646	1.163	0.610
7902861	LRRC8B	leucine rich repeat containing 8 family, member B	9.021	10.123	9.628	9.564	1.102	0.607
8075673	RBFOX2	RNA binding protein, fox-1 homolog (C. elegans) 2	7.025	8.538	7.632	7.910	1.513	0.607
8046408	PDK1	pyruvate dehydrogenase kinase, isozyme 1	9.308	10.858	9.912	10.339	1.550	0.604
8065280	RALGAPA2	Ral GTPase activating protein, alpha subunit 2 (catalytic)	7.819	8.905	8.423	8.301	1.086	0.604
8089082	DCBLD2	discoidin, CUB and LCCL domain containing 2	8.411	9.916	9.012	9.289	1.505	0.601
7965431	CLLU1OS	chronic lymphocytic leukemia up-regulated 1 opposite strand	5.374	6.589	5.972	6.589	1.215	0.598
8166950	DUSP21	dual specificity phosphatase 21	4.850	6.337	5.449	5.473	1.487	0.598
7950899	RAB38	RAB38, member RAS oncogene family	10.446	11.966	11.041	11.625	1.520	0.595
8137352	SLC4A2	solute carrier family 4, anion exchanger, member 2 (erythrocyte membrane protein band 3-like 1)	9.431	10.507	10.026	10.405	1.076	0.595
7929958	BTRC	beta-transducin repeat containing	8.420	9.634	9.013	9.297	1.214	0.593
8162236	SEMA4D	sema domain, immunoglobulin domain (Ig), transmembrane domain (TM) and short cytoplasmic domai	8.544	10.187	9.137	9.741	1.644	0.593
8173551	PHKA1	phosphorylase kinase, alpha 1 (muscle)	7.370	9.290	7.962	8.772	1.920	0.592
8051298	GALNT14	UDP-N-acetyl-alpha-D-galactosamine:polypeptide N-acetylgalactosaminyltransferase 14 (GalNAc-T14)	8.071	9.581	8.661	9.335	1.509	0.590
8162850	TEX10	testis expressed 10	9.078	10.376	9.667	9.927	1.299	0.589
8050766	ADCY3	adenylate cyclase 3	10.129	11.283	10.714	11.143	1.154	0.585
7922474	KIAA0040	KIAA0040	10.591	12.275	11.176	12.029	1.684	0.585
8088958	GBE1	glucan (1,4-alpha-), branching enzyme 1	10.456	11.855	11.039	11.183	1.400	0.584
7942118	MYEOV	myeloma overexpressed (in a subset of t(11;14) positive multiple myelomas)	6.544	7.609	7.128	7.454	1.065	0.584
8010092	MFSD11	major facilitator superfamily domain containing 11	9.690	10.718	10.274	10.470	1.028	0.583
8089112	FILIP1L	filamin A interacting protein 1-like	8.421	9.497	9.002	9.242	1.076	0.581
7901140	MAST2	microtubule associated serine/threonine kinase 2	8.487	9.543	9.065	9.141	1.056	0.578
7952036	MPZL3	myelin protein zero-like 3	7.712	8.767	8.289	8.261	1.055	0.578
8139680	COBL	cordon-bleu homolog (mouse)	6.661	8.307	7.238	7.872	1.646	0.577
8104788	RAI14	retinoic acid induced 14	9.201	10.407	9.777	9.923	1.206	0.576
8158183	DNM1	dynamin 1	7.803	9.529	8.378	9.217	1.726	0.575
7989365	RORA	RAR-related orphan receptor A	5.759	7.223	6.334	6.102	1.465	0.575
8044605	LOC654433	hypothetical LOC654433	6.908	8.297	7.476	6.935	1.389	0.568
7912102	KLHL21	kelch-like 21 (Drosophila)	6.872	7.920	7.436	7.854	1.048	0.564
7951752	USP28	ubiquitin specific peptidase 28	8.772	10.295	9.335	9.752	1.523	0.562
8110055	CPEB4	cytoplasmic polyadenylation element binding protein 4	9.603	10.736	10.163	10.009	1.133	0.560
7919872	FAM63A	family with sequence similarity 63, member A	8.048	9.660	8.601	9.114	1.611	0.553
7917304	MCOLN3	mucolipin 3	8.396	9.494	8.947	9.131	1.098	0.551
8071147	TUBA8	tubulin, alpha 8	8.176	9.488	8.726	9.748	1.312	0.550
8005305	C17orf39	chromosome 17 open reading frame 39	7.912	9.183	8.459	8.625	1.271	0.547
8007931	ITGB3	integrin, beta 3 (platelet glycoprotein IIIa, antigen CD61)	11.529	12.831	12.075	12.668	1.303	0.547
7937878	TRPC2	transient receptor potential cation channel, subfamily C, member 2, pseudogene	7.042	8.406	7.588	7.816	1.364	0.547
8120239	TMEM14A	transmembrane protein 14A	7.620	8.690	8.165	8.060	1.070	0.545
8143850	CDK5	cyclin-dependent kinase 5	10.169	11.269	10.713	11.377	1.101	0.544
8161004	CD72	CD72 molecule	8.156	9.269	8.698	9.175	1.114	0.543
7920238	S100A12	S100 calcium binding protein A12	7.037	5.860	7.577	5.887	-1.177	0.540
8059361	WDFY1	WD repeat and FYVE domain containing 1	10.174	11.377	10.714	11.035	1.203	0.540
8072170	KREMEN1	kringle containing transmembrane protein 1	6.619	8.550	7.157	7.813	1.931	0.538
7915718	TESK2	testis-specific kinase 2	7.419	8.825	7.957	7.795	1.406	0.538
7910014	CNIH4	cornichon homolog 4 (Drosophila)	10.491	11.576	11.027	11.359	1.085	0.536
8132347	GPR141	G protein-coupled receptor 141	9.749	8.539	10.285	8.454	-1.210	0.536

8057517	NCKAP1	NCK-associated protein 1	9.274	10.661	9.810	10.008	1.387	0.536
7969861	ITGBL1	integrin, beta-like 1 (with EGF-like repeat domains)	6.542	8.447	7.077	8.186	1.905	0.535
8091009	PIK3CB	phosphoinositide-3-kinase, catalytic, beta polypeptide	10.449	11.657	10.984	11.406	1.208	0.535
8091385	CP	ceruloplasmin (ferroxidase)	4.246	5.297	4.780	4.553	1.051	0.533
8021565	PHLPP1	PH domain and leucine rich repeat protein phosphatase 1	7.767	8.773	8.296	8.179	1.006	0.529
7936928	MMP21	matrix metallopeptidase 21	6.121	7.366	6.649	6.809	1.245	0.528
8093096	TCTEX1D2	Tctex1 domain containing 2	7.626	9.271	8.153	8.499	1.644	0.527
7986977	TJP1	tight junction protein 1 (zona occludens 1)	6.893	7.927	7.417	7.497	1.034	0.525
8162254	DIRAS2	DIRAS family, GTP-binding RAS-like 2	6.981	9.854	7.501	9.142	2.873	0.519
7962183	AK4	adenylate kinase 4	8.460	10.121	8.974	9.663	1.661	0.514
8161919	TLE1	transducin-like enhancer of split 1 (E(sp1) homolog, Drosophila)	7.133	8.335	7.644	7.555	1.202	0.511
8174767	FAM70A	family with sequence similarity 70, member A	8.596	7.413	9.105	7.816	-1.183	0.509
7909967	CAPN2	calpain 2, (m/II) large subunit	10.871	12.112	11.378	11.849	1.241	0.507
8160531	C9orf72	chromosome 9 open reading frame 72	9.608	10.679	10.115	10.196	1.071	0.506
7902512	DNAJB4	DnaJ (Hsp40) homolog, subfamily B, member 4	8.369	9.530	8.873	9.043	1.162	0.504
8040503	UBXN2A	UBX domain protein 2A	7.199	8.280	7.701	7.530	1.080	0.502
7925876	PFKP	phosphofructokinase, platelet	9.754	10.999	10.253	10.790	1.245	0.499
7992789	TNFRSF12A	tumor necrosis factor receptor superfamily, member 12A	9.954	11.200	10.453	11.045	1.246	0.499
7955217	SPATS2	spermatogenesis associated, serine-rich 2	8.006	9.262	8.503	8.716	1.256	0.498
7974870	SNAPC1	small nuclear RNA activating complex, polypeptide 1, 43kDa	8.694	10.398	9.190	8.607	1.704	0.496
7963631	RARG	retinoic acid receptor, gamma	6.312	7.336	6.807	7.009	1.024	0.495
8005707	MAP2K3	mitogen-activated protein kinase kinase 3	9.815	10.970	10.309	10.782	1.155	0.494
8050894	KIF3C	kinesin family member 3C	7.669	9.323	8.163	9.121	1.653	0.493
8147012	PKIA	protein kinase (cAMP-dependent, catalytic) inhibitor alpha	7.669	9.763	8.159	9.462	2.094	0.490
7898957	RCAN3	RCAN family member 3	8.734	10.109	9.224	9.850	1.375	0.489
8021091	SIGLEC15	sialic acid binding Ig-like lectin 15	9.967	11.403	10.456	11.097	1.436	0.489
7965541	FGD6	FYVE, RhoGEF and PH domain containing 6	9.277	10.392	9.765	9.635	1.115	0.488
8094169	CPEB2	cytoplasmic polyadenylation element binding protein 2	8.832	9.906	9.317	9.240	1.074	0.485
8093219	BDH1	3-hydroxybutyrate dehydrogenase, type 1	7.749	9.006	8.231	8.595	1.257	0.482
8033257	C3	complement component 3	10.910	9.516	11.391	10.019	-1.394	0.481
7940530	C11orf9	chromosome 11 open reading frame 9	6.292	7.691	6.771	7.485	1.399	0.479
7955469	SLC4A8	solute carrier family 4, sodium bicarbonate cotransporter, member 8	7.521	8.683	7.999	8.250	1.162	0.479
7934411	USP54	ubiquitin specific peptidase 54	6.897	8.813	7.375	8.028	1.915	0.478
8173086	FGD1	FYVE, RhoGEF and PH domain containing 1	6.695	8.130	7.170	7.847	1.435	0.475
7925062	SIPA1L2	signal-induced proliferation-associated 1 like 2	8.297	9.317	8.772	8.920	1.020	0.475
8105411	IL31RA	interleukin 31 receptor A	5.079	6.446	5.550	6.032	1.367	0.472
8109629	FABP6	fatty acid binding protein 6, ileal	6.020	8.063	6.489	8.498	2.043	0.468
8098549	STOX2	storkhead box 2	6.261	7.314	6.726	6.845	1.053	0.465
8058203	ALS2CR12	amyotrophic lateral sclerosis 2 (juvenile) chromosome region, candidate 12	5.485	7.109	5.948	5.992	1.624	0.463
8092552	IGF2BP2	insulin-like growth factor 2 mRNA binding protein 2	7.040	8.229	7.502	7.696	1.189	0.462
7997139	CALB2	calbindin 2	6.385	7.650	6.842	7.209	1.265	0.457
8054377	FHL2	four and a half LIM domains 2	6.475	7.559	6.928	7.433	1.084	0.454
8166797	MID1IP1	MID1 interacting protein 1 (gastrulation specific G12 homolog (zebrafish))	9.837	11.218	10.292	11.227	1.381	0.454
7936463	ABLIM1	actin binding LIM protein 1	5.800	7.027	6.250	6.391	1.227	0.450
8017675	PLEKHM1P	pleckstrin homology domain containing, family M (with RUN domain) member 1 pseudogene	10.294	11.302	10.743	11.289	1.009	0.449
7989069	PYGO1	pygopus homolog 1 (Drosophila)	5.265	6.856	5.714	5.871	1.592	0.449
7990545	CSPG4	chondroitin sulfate proteoglycan 4	6.683	8.209	7.124	7.480	1.526	0.442
7958253	C12orf75	chromosome 12 open reading frame 75	7.643	8.794	8.084	8.485	1.150	0.441
8021001	KIAA1328	KIAA1328	6.634	8.515	7.073	7.542	1.881	0.439
7952249	USP2	ubiquitin specific peptidase 2	8.817	9.948	9.254	9.777	1.132	0.438
8129637	VNN2	vanin 2	11.017	9.815	11.454	9.655	-1.203	0.437
7969544	NDFIP2	Nedd4 family interacting protein 2	8.607	10.066	9.043	9.464	1.459	0.436
8162059	SLC28A3	solute carrier family 28 (sodium-coupled nucleoside transporter), member 3	9.927	11.072	10.363	10.520	1.145	0.436
8035120	EPS15L1	epidermal growth factor receptor pathway substrate 15-like 1	9.211	10.235	9.643	9.929	1.024	0.432
8105267	ITGA2	integrin, alpha 2 (CD49B, alpha 2 subunit of VLA-2 receptor)	9.046	10.777	9.477	10.373	1.731	0.431
8043945	MAP4K4	mitogen-activated protein kinase kinase kinase kinase 4	9.390	10.670	9.819	10.181	1.280	0.430
7944803	VWA5A	von Willebrand factor A domain containing 5A	9.183	10.738	9.613	10.531	1.555	0.430
8128123	RRAGD	Ras-related GTP binding D	10.670	11.723	11.095	11.382	1.053	0.425
8133176	RABGEF1	RAB guanine nucleotide exchange factor (GEF) 1	9.098	10.146	9.519	9.586	1.047	0.420
8040587	EFR3B	EFR3 homolog B (S. cerevisiae)	7.370	8.551	7.788	8.052	1.182	0.418
8150076	DUSP4	dual specificity phosphatase 4	7.439	9.399	7.857	8.391	1.960	0.417
8156761	NANS	N-acetylneuraminic acid synthase	9.496	10.651	9.912	10.238	1.154	0.416
8032009	MIER2	mesoderm induction early response 1, family member 2	7.824	8.857	8.239	8.295	1.033	0.415
8078227	KAT2B	K(lysine) acetyltransferase 2B	10.253	11.404	10.666	10.915	1.150	0.413
8088680	C3orf64	chromosome 3 open reading frame 64	10.176	11.317	10.586	11.011	1.141	0.410
7942204	CTTN	cortactin	8.880	10.217	9.288	10.019	1.337	0.408
7962884	RND1	Rho family GTPase 1	6.336	7.362	6.740	6.980	1.026	0.404
7991602	PCSK6	proprotein convertase subtilisin/kexin type 6	8.964	10.215	9.368	9.742	1.250	0.403
7958398	WSCD2	WSC domain containing 2	6.291	7.481	6.691	7.192	1.190	0.400
8112668	GCNT4	glucosaminyl (N-acetyl) transferase 4, core 2	4.508	6.135	4.906	5.246	1.627	0.398
8164013	STRBP	spermatid perinuclear RNA binding protein	6.514	7.763	6.912	7.541	1.248	0.398
8164810	RALGDS	ral guanine nucleotide dissociation stimulator	8.886	10.068	9.281	9.710	1.182	0.395
8155048	RUSC2	RUN and SH3 domain containing 2	7.799	8.960	8.187	8.728	1.161	0.388
8091550	KIAA1328	KIAA1328	7.923	9.871	8.303	9.002	1.948	0.381
8099982	APBB2	amyloid beta (A4) precursor protein-binding, family B, member 2	9.027	10.225	9.407	9.672	1.198	0.380
8128553	BVES	blood vessel epicardial substance	5.069	6.172	5.448	5.664	1.103	0.380
7991070	HDGFRP3	hepatoma-derived growth factor, related protein 3	8.010	9.151	8.391	8.723	1.141	0.380
8080964	GXYLT2	glucoside xylosyltransferase 2	6.870	7.896	7.247	7.666	1.026	0.377
7943803	DIXDC1	DIX domain containing 1	7.022	8.292	7.397	8.030	1.271	0.376
7962151	DENND5B	DENN/MADD domain containing 5B	7.078	8.202	7.451	7.349	1.124	0.373
8091283	PLOD2	procollagen-lysine, 2-oxoglutarate 5-dioxygenase 2	5.333	6.414	5.705	5.976	1.081	0.372
7971590	CAB39L	calcium binding protein 39-like	8.791	10.299	9.161	9.559	1.508	0.370
8128956	FYN	FYN oncogene related to SRC, FGR, YES	7.343	8.466	7.712	8.099	1.123	0.369
7941714	C11orf80	chromosome 11 open reading frame 80	6.857	8.089	7.224	7.824	1.232	0.367
7923967	YOD1	YOD1 OTU deubiquinating enzyme 1 homolog (S. cerevisiae)	8.193	9.231	8.559	8.780	1.038	0.366
8032682	MATK	megakaryocyte-associated tyrosine kinase	8.416	9.427	8.778	9.344	1.011	0.362
8065089	KIF16B	kinesin family member 16B	8.322	9.477	8.683	8.696	1.155	0.361
7930760	PNLIPRP3	pancreatic lipase-related protein 3	4.157	5.397	4.513	4.293	1.239	0.355
8072314	LIF	leukemia inhibitory factor (cholinergic differentiation factor)	6.332	7.345	6.687	6.821	1.012	0.354
7911178	NLRP3	NLR family, pyrin domain containing 3	8.878	7.701	9.230	7.851	-1.177	0.353
8022747	B4GALT6	UDP-Gal:betaGlcNAc beta 1,4- galactosyltransferase, polypeptide 6	6.910	9.113	7.257	7.930	2.203	0.347
8113790	40971	membrane-associated ring finger (C3HC4) 3	9.745	10.879	10.089	10.417	1.134	0.343
8094393	ZCCHC4	zinc finger, CCHC domain containing 4	8.093	9.747	8.431	8.763	1.653	0.337
7932512	DNAJC1	DnaJ (Hsp40) homolog, subfamily C, member 1	9.755	10.773	10.089	10.494	1.019	0.335
7932765	MPP7	membrane protein, palmitoylated 7 (MAGUK p55 subfamily member 7)	6.860	8.132	7.194	7.624	1.272	0.333
8008682	MSI2	musashi homolog 2 (Drosophila)	6.372	8.006	6.702	7.516	1.634	0.330
7933204	C10orf10	chromosome 10 open reading frame 10	5.952	6.957	6.273	6.453	1.005	0.321
7979698	ATP6V1D	ATPase, H+ transporting, lysosomal 34kDa, V1 subunit D	10.548	11.636	10.866	11.419	1.088	0.318
7901175	TSPAN1	tetraspanin 1	4.804	6.020	5.113	5.574	1.216	0.309
8152491	EXT1	exostosin 1	8.783	10.406	9.090	10.089	1.623	0.307
7917103	ZZZ3	zinc finger, ZZ-type containing 3	9.751	10.770	10.051	10.339	1.019	0.300
7966089	CMKLR1	chemokine-like receptor 1	10.719	9.323	11.005	9.189	-1.396	0.286
8131631	HDAC9	histone deacetylase 9	6.853	8.085	7.135	7.621	1.231	0.281
8050557	SDC1	syndecan 1	8.305	9.406	8.581	9.425	1.101	0.275
8014115	MYO1D	myosin ID	10.169	11.570	10.439	11.386	1.400	0.270
8121749	GJA1	gap junction protein, alpha 1, 43kDa	5.551	7.025	5.818	6.823	1.474	0.267
8094719	N4BP2	NEDD4 binding protein 2	7.984	9.149	8.243	8.105	1.165	0.259
7982185	DEXI	Dexi homolog (mouse)	10.281	11.285	10.536	11.160	1.004	0.255
7986685	DEXI	Dexi homolog (mouse)	10.281	11.285	10.536	11.160	1.004	0.255
7978586	CFL2	cofilin 2 (muscle)	9.304	10.529	9.553	9.962	1.226	0.250
8134036	STEAP2	six transmembrane epithelial antigen of the prostate 2	5.477	6.612	5.726	6.169	1.135	0.249
8068024	JAM2	junctional adhesion molecule 2	5.807	6.825	6.042	5.913	1.018	0.235
8005557	EPN2	epsin 2	7.232	8.298	7.467	8.110	1.066	0.234
7992594	CCNF	cyclin F	7.149	8.452	7.377	7.466	1.302	0.228
8138466	MACC1	metastasis associated in colon cancer 1	8.267	7.108	8.493	7.599	-1.158	0.226

8102050	NHEDC2	Na+/H+ exchanger domain containing 2	12.003	13.011	12.218	12.841	1.008	0.215
8106962	ARSK	arylsulfatase family, member K	7.479	8.553	7.690	7.789	1.075	0.211
8050176	ITGB1BP1	integrin beta 1 binding protein 1	10.366	11.524	10.568	11.371	1.158	0.202
8103399	PDGFC	platelet derived growth factor C	8.178	6.801	8.380	6.591	-1.377	0.202
8126710	SUPT3H	suppressor of Ty 3 homolog (S. cerevisiae)	6.851	7.944	7.050	7.466	1.094	0.199
7994826	ITGAL	integrin, alpha L (antigen CD11A (p180), lymphocyte function-associated antigen 1; alpha polypeptide)	9.342	7.837	9.535	7.826	-1.505	0.193
7977161	TDRD9	tudor domain containing 9	5.569	6.838	5.763	6.413	1.269	0.193
8092707	LEPREL1	leprecan-like 1	7.466	9.748	7.657	9.411	2.283	0.191
8172220	NDP	Norrie disease (pseudoglioma)	7.595	8.707	7.777	7.981	1.112	0.182
8056343	COBLL1	COBL-like 1	6.952	8.086	7.132	7.829	1.134	0.180
7927599	ASAH2	N-acylsphingosine amidohydrolase (non-lysosomal ceramidase) 2	6.259	7.361	6.437	6.523	1.102	0.178
8138527	MGC87042	STEAP family protein MGC87042	6.623	8.261	6.796	7.812	1.639	0.173
8082869	PPP2R3A	protein phosphatase 2, regulatory subunit B'', alpha	7.047	8.395	7.218	7.664	1.348	0.171
7956759	SRGAP1	SLIT-ROBO Rho GTPase activating protein 1	7.645	8.969	7.816	8.341	1.324	0.171
7980316	TGFB3	transforming growth factor, beta 3	5.997	7.763	6.165	7.282	1.766	0.168
7934898	ANKRD22	ankyrin repeat domain 22	5.114	6.308	5.278	5.273	1.194	0.164
8038824	SIGLEC10	sialic acid binding Ig-like lectin 10	10.572	9.427	10.733	9.530	-1.145	0.161
8096160	ARHGAP24	Rho GTPase activating protein 24	6.679	8.180	6.837	7.173	1.500	0.158
8090988	CEP70	centrosomal protein 70kDa	5.955	7.126	6.110	6.583	1.171	0.155
7924119	INTS7	integrator complex subunit 7	9.398	10.512	9.552	9.887	1.114	0.154
7959002	SDSL	serine dehydratase-like	8.398	9.690	8.552	9.641	1.292	0.154
8157105	ZNF462	zinc finger protein 462	8.538	9.921	8.678	9.579	1.383	0.140
7902452	AK5	adenylate kinase 5	9.545	11.200	9.680	10.782	1.654	0.135
8089544	CCDC80	coiled-coil domain containing 80	5.199	6.634	5.334	5.814	1.435	0.134
8162216	SHC3	SHC (Src homology 2 domain containing) transforming protein 3	8.092	9.593	8.225	8.988	1.501	0.133
8059350	AP1S3	adaptor-related protein complex 1, sigma 3 subunit	6.703	7.906	6.832	7.341	1.203	0.130
8011826	C17orf87	chromosome 17 open reading frame 87	10.425	9.347	10.554	10.361	-1.078	0.129
7957298	NAV3	neuron navigator 3	5.347	6.575	5.477	6.358	1.228	0.129
8085797	THRB	thyroid hormone receptor, beta (erythroblastic leukemia viral (v-erb-a) oncogene homolog 2, avian)	7.257	8.620	7.383	7.842	1.363	0.126
8103226	TMEM154	transmembrane protein 154	5.485	7.386	5.604	6.485	1.902	0.120
7944152	IL10RA	interleukin 10 receptor, alpha	11.445	10.410	11.553	10.722	-1.035	0.108
8133818	PHTF2	putative homeodomain transcription factor 2	10.003	11.033	10.109	10.526	1.030	0.106
7898939	NIPAL3	NIPA-like domain containing 3	7.878	8.924	7.983	8.501	1.046	0.105
8122279	KIAA1244	KIAA1244	7.353	8.612	7.444	8.243	1.260	0.092
8152962	LRRC6	leucine rich repeat containing 6	7.330	8.367	7.415	7.612	1.038	0.086
8135587	CAV2	caveolin 2	5.469	6.694	5.552	6.028	1.225	0.083
8130739	RPS6KA2	ribosomal protein S6 kinase, 90kDa, polypeptide 2	9.194	10.216	9.276	9.690	1.022	0.082
8036136	TMEM149	transmembrane protein 149	10.081	8.821	10.161	8.689	-1.259	0.080
8162610	CDC14B	CDC14 cell division cycle 14 homolog B (S. cerevisiae)	6.047	7.164	6.126	6.255	1.117	0.079
8169473	PLS3	plastin 3	8.698	10.383	8.767	9.591	1.685	0.069
7999419	DEXI	Dexi homolog (mouse)	9.707	10.748	9.769	10.394	1.042	0.063
8048211	RUFY4	RUN and FYVE domain containing 4	8.096	9.273	8.152	9.126	1.177	0.056
7917996	LRRC39	leucine rich repeat containing 39	6.223	7.403	6.278	6.012	1.180	0.055
7951977	FXYD6	FXYD domain containing ion transport regulator 6	8.816	10.151	8.869	10.077	1.335	0.053
7975787	JDP2	Jun dimerization protein 2	10.512	11.523	10.551	11.345	1.011	0.039
8127346	RAB23	RAB23, member RAS oncogene family	7.560	8.867	7.598	7.539	1.307	0.038
7902660	WDR63	WD repeat domain 63	7.088	8.131	7.125	7.235	1.043	0.037
7898809	EPHB2	EPH receptor B2	9.764	8.433	9.799	8.491	-1.331	0.035
8013660	ALDOC	aldolase C, fructose-bisphosphate	8.472	9.615	8.499	9.310	1.143	0.027
8129649	C6orf192	chromosome 6 open reading frame 192	9.068	10.557	9.088	10.303	1.489	0.021
7942409	P2RY6	pyrimidinergic receptor P2Y, G-protein coupled, 6	8.500	7.350	8.501	7.715	-1.150	0.001
7974835	PRKCH	protein kinase C, eta	9.637	10.644	9.636	10.483	1.008	-0.001
8074237	CECR1	cat eye syndrome chromosome region, candidate 1	11.600	10.449	11.583	10.886	-1.152	-0.017
8045860	PKP4	plakophilin 4	7.443	8.827	7.421	8.130	1.384	-0.022
8096602	DAPP1	dual adaptor of phosphotyrosine and 3-phosphoinositides	8.438	7.113	8.393	7.371	-1.325	-0.045
8162117	GOLM1	golgi membrane protein 1	9.143	10.241	9.084	10.010	1.098	-0.059
7971573	RCBTB2	regulator of chromosome condensation (RCC1) and BTB (POZ) domain containing protein 2	10.637	9.517	10.569	9.331	-1.120	-0.068
7903092	FNBP1L	formin binding protein 1-like	9.151	10.522	9.079	9.630	1.370	-0.072
8109528	CYFIP2	cytoplasmic FMR1 interacting protein 2	7.548	8.780	7.459	7.954	1.232	-0.089
8051396	NLRC4	NLR family, CARD domain containing 4	8.668	7.563	8.575	8.104	-1.105	-0.093
7906061	SYT11	synaptotagmin XI	9.142	8.012	9.038	8.103	-1.130	-0.104
7905067	HIST2H4A	histone cluster 2, H4a	6.934	5.889	6.827	6.691	-1.045	-0.107
7919627	HIST2H4A	histone cluster 2, H4a	6.934	5.889	6.827	6.691	-1.045	-0.107
8064716	SIGLEC1	sialic acid binding Ig-like lectin 1, sialoadhesin	10.107	8.742	10.000	9.139	-1.365	-0.107
7997712	IRF8	interferon regulatory factor 8	10.521	9.036	10.409	9.883	-1.485	-0.113
8151532	FABP4	fatty acid binding protein 4, adipocyte	8.460	5.945	8.346	10.895	-2.515	-0.114
8122365	GPR126	G protein-coupled receptor 126	7.269	8.497	7.147	7.798	1.228	-0.122
8179322	HSPA1A	heat shock 70kDa protein 1A	11.375	10.092	11.248	10.475	-1.283	-0.127
8178086	HSPA1B	heat shock 70kDa protein 1B	9.527	8.383	9.400	8.681	-1.143	-0.127
8179324	HSPA1B	heat shock 70kDa protein 1B	9.527	8.383	9.400	8.681	-1.143	-0.127
8118314	HSPA1B	heat shock 70kDa protein 1B	9.464	8.293	9.324	8.596	-1.170	-0.140
7981142	CLMN	calmin (calponin-like, transmembrane)	9.083	7.893	8.936	8.164	-1.191	-0.147
8103508	40969	membrane-associated ring finger (C3HC4) 1	10.915	9.567	10.765	9.889	-1.348	-0.150
8118310	HSPA1A	heat shock 70kDa protein 1A	11.434	10.125	11.284	10.504	-1.309	-0.150
8054135	MGAT4A	mannosyl (alpha-1,3-)-glycoprotein beta-1,4-N-acetylglucosaminyltransferase, isozyme A	11.137	9.993	10.983	9.787	-1.144	-0.155
7908125	RGL1	ral guanine nucleotide dissociation stimulator-like 1	11.579	10.556	11.420	10.363	-1.023	-0.159
7972297	ABCC4	ATP-binding cassette, sub-family C (CFTR/MRP), member 4	8.552	9.672	8.377	8.931	1.120	-0.175
8166065	TLR8	toll-like receptor 8	9.438	8.085	9.245	8.244	-1.352	-0.193
7952341	ASAM	adipocyte-specific adhesion molecule	7.346	8.961	7.149	8.227	1.616	-0.197
8084100	USP13	ubiquitin specific peptidase 13 (isopeptidase T-3)	7.635	6.596	7.432	6.676	-1.039	-0.203
7960518	TNFRSF1A	tumor necrosis factor receptor superfamily, member 1A	10.370	9.251	10.159	9.526	-1.119	-0.211
8105481	GAPT	GRB2-binding adaptor protein, transmembrane	9.497	6.536	9.274	6.469	-2.961	-0.222
7937335	IFITM1	interferon induced transmembrane protein 1 (9-27)	7.432	6.049	7.204	6.293	-1.383	-0.227
8099834	TLR1	toll-like receptor 1	10.512	9.368	10.284	9.198	-1.144	-0.227
8080320	NISCH	nischarin	9.570	8.329	9.342	8.570	-1.241	-0.228
8157761	NEK6	NIMA (never in mitosis gene a)-related kinase 6	10.413	9.413	10.183	9.683	-1.000	-0.230
8113073	ARRDC3	arrestin domain containing 3	11.474	10.290	11.240	10.466	-1.184	-0.234
8059650	SP110	SP110 nuclear body protein	8.616	7.593	8.374	7.605	-1.022	-0.242
8100798	SULT1B1	sulfotransferase family, cytosolic, 1B, member 1	7.241	10.335	6.994	9.597	3.095	-0.247
7969986	TNFSF13B	tumor necrosis factor (ligand) superfamily, member 13b	10.635	9.366	10.384	9.461	-1.269	-0.251
7948364	MPEG1	macrophage expressed 1	11.830	10.523	11.562	10.666	-1.306	-0.268
8091260	SLC9A9	solute carrier family 9 (sodium/hydrogen exchanger), member 9	11.278	9.685	11.010	9.514	-1.594	-0.269
8039212	LILRB2	leukocyte immunoglobulin-like receptor, subfamily B (with TM and ITIM domains), member 2	10.894	9.852	10.613	9.865	-1.042	-0.281
7964736	HMGA2	high mobility group AT-hook 2	6.411	7.565	6.119	6.807	1.155	-0.291
8168691	DIAPH2	diaphanous homolog 2 (Drosophila)	9.190	8.115	8.888	7.477	-1.075	-0.303
7938035	TRIM22	tripartite motif-containing 22	10.422	9.151	10.118	9.366	-1.272	-0.305
8080344	STAB1	stabilin 1	11.490	10.017	11.179	10.185	-1.473	-0.311
8178199	HLA-DQA1	major histocompatibility complex, class II, DQ alpha 1	13.171	12.131	12.847	12.615	-1.040	-0.325
8179489	HLA-DQA1	major histocompatibility complex, class II, DQ alpha 1	13.171	12.131	12.847	12.615	-1.040	-0.325
7943892	NCAM1	neural cell adhesion molecule 1	7.813	6.045	7.471	6.589	-1.768	-0.342
8019486	SECTM1	secreted and transmembrane 1	9.588	8.309	9.236	8.509	-1.279	-0.352
8139033	AOAH	acyloxyacyl hydrolase (neutrophil)	11.526	10.127	11.171	10.357	-1.400	-0.355
7898799	C1QC	complement component 1, q subcomponent, C chain	12.392	11.009	12.032	11.323	-1.383	-0.360
8113796	FLJ44606	glutaredoxin-like protein YDR286C homolog	6.109	7.365	5.745	6.416	1.256	-0.364
8012605	GAS7	growth arrest-specific 7	10.209	8.050	9.845	8.265	-2.159	-0.364
7917503	GBP3	guanylate binding protein 3	7.885	6.545	7.520	6.645	-1.341	-0.365
8091723	RARRES1	retinoic acid receptor responder (tazarotene induced) 1	8.272	7.246	7.906	7.349	-1.026	-0.366
7972055	KCTD12	potassium channel tetramerisation domain containing 12	11.600	10.553	11.233	10.486	-1.047	-0.367
7906757	FCGR2A	Fc fragment of IgG, low affinity IIa, receptor (CD32)	11.974	10.902	11.606	10.811	-1.073	-0.368
8008185	ABI3	ABI family, member 3	9.260	8.040	8.891	7.788	-1.220	-0.369
8025076	VAV1	vav 1 guanine nucleotide exchange factor	10.677	9.615	10.307	9.581	-1.062	-0.370
8043791	INPP4A	inositol polyphosphate-4-phosphatase, type I, 107kDa	9.781	8.708	9.407	8.635	-1.073	-0.373
8118594	HLA-DPB1	major histocompatibility complex, class II, DP beta 1	12.849	11.843	12.473	12.234	-1.006	-0.376
8171248	KAL1	Kallmann syndrome 1 sequence	7.580	6.070	7.201	6.457	-1.510	-0.380
8149448	MSR1	macrophage scavenger receptor 1	12.531	11.348	12.142	11.582	-1.182	-0.389

7938629	PDE3B	phosphodiesterase 3B, cGMP-inhibited	7.220	5.985	6.824	7.358	-1.234	-0.395
8099685	LGI2	leucine-rich repeat LGI family, member 2	10.789	9.781	10.392	8.729	-1.008	-0.396
7926223	CAMK1D	calcium/calmodulin-dependent protein kinase ID	8.249	7.041	7.845	6.991	-1.207	-0.403
8000582	SULT1A2	sulfotransferase family, cytosolic, 1A, phenol-preferring, member 2	8.430	7.425	8.021	7.551	-1.005	-0.410
8061247	RIN2	Ras and Rab interactor 2	10.526	9.476	10.111	9.444	-1.050	-0.415
8068593	ETS2	v-ets erythroblastosis virus E26 oncogene homolog 2 (avian)	9.587	8.582	9.168	8.272	-1.005	-0.419
8179519	HLA-DPB1	major histocompatibility complex, class II, DP beta 1	13.024	11.998	12.603	12.485	-1.026	-0.421
8136067	TSPAN33	tetraspanin 33	10.648	9.244	10.218	8.726	-1.404	-0.429
7943577	RAB39	RAB39, member RAS oncogene family	9.223	7.934	8.793	7.763	-1.289	-0.430
8122637	SASH1	SAM and SH3 domain containing 1	9.170	7.904	8.736	7.202	-1.266	-0.434
7959251	P2RX7	purinergic receptor P2X, ligand-gated ion channel, 7	9.459	8.327	9.023	8.524	-1.132	-0.436
8023497	ATP8B1	ATPase, aminophospholipid transporter, class I, type 8B, member 1	9.649	8.061	9.212	7.364	-1.587	-0.437
8132819	IKZF1	IKAROS family zinc finger 1 (Ikaros)	9.027	7.492	8.567	7.595	-1.534	-0.460
8003171	COTL1	coactosin-like 1 (Dictyostelium)	11.139	10.032	10.678	10.283	-1.107	-0.461
8118556	HLA-DQA1	major histocompatibility complex, class II, DQ alpha 1	11.395	10.168	10.932	10.600	-1.227	-0.464
7898793	C1QA	complement component 1, q subcomponent, A chain	10.644	9.291	10.176	9.500	-1.353	-0.468
8106516	JMY	junction mediating and regulatory protein, p53 cofactor	7.501	6.245	7.033	6.081	-1.256	-0.468
7957570	PLXNC1	plexin C1	11.326	9.576	10.848	9.783	-1.750	-0.478
8052010	CALM2	calmodulin 2 (phosphorylase kinase, delta)	10.826	9.729	10.340	9.826	-1.097	-0.486
7940259	MS4A7	membrane-spanning 4-domains, subfamily A, member 7	10.273	9.222	9.783	9.627	-1.052	-0.490
8049246	INPP5D	inositol polyphosphate-5-phosphatase, 145kDa	10.914	9.794	10.422	9.943	-1.120	-0.491
7975779	FOS	FBJ murine osteosarcoma viral oncogene homolog	10.520	9.336	10.028	9.746	-1.184	-0.492
7922121	ANKRD36BP1	ankyrin repeat domain 36B pseudogene 1	7.166	6.131	6.672	5.932	-1.036	-0.495
8138805	CPVL	carboxypeptidase, vitellogenic-like	10.127	9.075	9.632	9.383	-1.053	-0.495
8156770	GALNT12	UDP-N-acetyl-alpha-D-galactosamine:polypeptide N-acetylgalactosaminyltransferase 12 (GalNAc-T12)	7.960	6.875	7.464	8.095	-1.085	-0.496
8171896	CXorf21	chromosome X open reading frame 21	8.700	7.179	8.200	7.749	-1.521	-0.499
7976080	GPR65	G protein-coupled receptor 65	10.695	9.413	10.194	9.888	-1.282	-0.501
8003844	GSG2	germ cell associated 2 (haspin)	6.793	5.761	6.287	6.235	-1.032	-0.505
7951297	MMP12	matrix metallopeptidase 12 (macrophage elastase)	7.623	6.422	7.111	6.896	-1.200	-0.511
8152988	SLA	Src-like-adaptor	10.400	9.213	9.886	9.714	-1.187	-0.513
8111739	FYB	FYN binding protein	11.400	10.099	10.882	10.159	-1.301	-0.518
8020630	TTC39C	tetratricopeptide repeat domain 39C	8.511	7.038	7.992	7.198	-1.473	-0.519
8012257	TP53	tumor protein p53	9.711	8.516	9.186	8.462	-1.195	-0.525
8157524	TLR4	toll-like receptor 4	11.811	10.571	11.282	11.086	-1.240	-0.528
7951077	SESN3	sestrin 3	10.589	8.868	10.056	8.605	-1.720	-0.533
7965359	ATP2B1	ATPase, Ca++ transporting, plasma membrane 1	10.079	9.069	9.545	9.161	-1.009	-0.534
8169859	SASH3	SAM and SH3 domain containing 3	9.875	8.811	9.338	8.747	-1.064	-0.537
7943160	SCARNA9	small Cajal body-specific RNA 9	7.833	6.560	7.295	6.192	-1.272	-0.537
8125556	HLA-DPA1	major histocompatibility complex, class II, DP alpha 1	12.970	11.924	12.427	12.308	-1.046	-0.543
8178891	HLA-DPA1	major histocompatibility complex, class II, DP alpha 1	12.970	11.924	12.427	12.308	-1.046	-0.543
7924499	TLR5	toll-like receptor 5	8.252	7.173	7.707	7.083	-1.079	-0.545
8155192	GLIPR2	GLI pathogenesis-related 2	10.615	9.294	10.068	9.941	-1.321	-0.546
7942569	SLCO2B1	solute carrier organic anion transporter family, member 2B1	12.061	10.642	11.512	10.592	-1.419	-0.549
7910198	ZNF678	zinc finger protein 678	6.775	5.765	6.225	6.059	-1.010	-0.549
7908351	PLA2G4A	phospholipase A2, group IVA (cytosolic, calcium-dependent)	8.902	7.555	8.349	6.979	-1.347	-0.553
8118564	HLA-DQA2	major histocompatibility complex, class II, DQ alpha 2	10.137	8.934	9.580	9.260	-1.203	-0.557
8135594	CAV1	caveolin 1, caveolae protein, 22kDa	5.741	7.127	5.178	5.971	1.387	-0.563
8014241	SLFN12	schlafen family member 12	7.873	6.592	7.311	6.574	-1.281	-0.563
8021707	SOCS6	suppressor of cytokine signaling 6	9.098	8.076	8.533	7.811	-1.023	-0.566
8123609	SERPINB9	serpin peptidase inhibitor, clade B (ovalbumin), member 9	10.193	8.898	9.617	8.687	-1.295	-0.576
8070083	TMEM50B	transmembrane protein 50B	9.089	7.988	8.510	8.041	-1.101	-0.580
7971565	LPAR6	lysophosphatidic acid receptor 6	10.859	9.556	10.277	9.656	-1.303	-0.582
8083223	C3orf58	chromosome 3 open reading frame 58	8.938	7.860	8.352	7.674	-1.079	-0.586
8116734	LY86	lymphocyte antigen 86	11.127	9.504	10.541	9.663	-1.623	-0.586
8055702	NMI	N-myc (and STAT) interactor	9.709	8.666	9.119	8.223	-1.044	-0.591
7923917	FAIM3	Fas apoptotic inhibitory molecule 3	8.596	7.508	8.000	9.484	-1.089	-0.596
8178205	HLA-DQA2	major histocompatibility complex, class II, DQ alpha 2	10.054	8.811	9.457	9.138	-1.243	-0.597
8150592	CEBPD	CCAAT/enhancer binding protein (C/EBP), delta	9.781	8.619	9.183	9.133	-1.162	-0.598
8035779	ZNF253	zinc finger protein 253	10.158	8.998	9.555	9.070	-1.160	-0.602
8035456	LRRC25	leucine rich repeat containing 25	10.353	9.016	9.750	9.239	-1.338	-0.604
7938012	RIM6-TRIM34	TRIM6-TRIM34 readthrough	7.772	6.581	7.155	6.702	-1.191	-0.617
7951397	CASP1	caspase 1, apoptosis-related cysteine peptidase (interleukin 1, beta, convertase)	9.656	8.516	9.037	7.932	-1.140	-0.619
8149673	REEP4	receptor accessory protein 4	8.664	7.663	8.037	7.615	-1.001	-0.627
7933194	CXCL12	chemokine (C-X-C motif) ligand 12	7.586	6.406	6.956	6.490	-1.180	-0.630
8021946	COLEC12	collectin sub-family member 12	10.399	8.279	9.761	7.545	-2.119	-0.637
8027260	ZNF486	zinc finger protein 486	8.187	7.170	7.531	6.956	-1.016	-0.656
7923562	CHIT1	chitinase 1 (chitotriosidase)	11.843	10.753	11.184	11.963	-1.090	-0.659
8125545	HLA-DOA	major histocompatibility complex, class II, DO alpha	8.246	7.214	7.584	7.672	-1.032	-0.662
8099841	TLR6	toll-like receptor 6	10.064	8.999	9.392	8.869	-1.065	-0.672
8066431	ADA	adenosine deaminase	10.412	9.169	9.737	9.056	-1.242	-0.675
8046380	ITGA6	integrin, alpha 6	9.938	8.786	9.263	8.872	-1.152	-0.675
8046003	GCA	grancalcin, EF-hand calcium binding protein	9.968	8.965	9.290	8.703	-1.002	-0.678
7899187	HMGN2	high-mobility group nucleosomal binding domain 2	11.901	10.723	11.222	10.932	-1.178	-0.679
8119132	FGD2	FYVE, RhoGEF and PH domain containing 2	7.890	6.584	7.209	7.240	-1.306	-0.681
8113356	GPAM	glycerol-3-phosphate acyltransferase, mitochondrial // glycerol-3-phosphate acyltransferase, mitochon	5.498	4.089	4.818	3.782	-1.409	-0.681
8095043	RASL11B	RAS-like, family 11, member B	7.525	6.485	6.842	6.862	-1.040	-0.683
8000409	HMGN2	high-mobility group nucleosomal binding domain 2	11.291	10.239	10.607	10.598	-1.051	-0.684
8140463	FGL2	fibrinogen-like 2	9.204	7.862	8.517	7.722	-1.342	-0.687
8101757	GPRIN3	GPRIN family member 3	10.321	8.975	9.614	9.716	-1.346	-0.707
7982204	HMGN2	high-mobility group nucleosomal binding domain 2	11.316	10.315	10.608	10.632	-1.000	-0.708
7971661	MIR15A	microRNA 15a	6.980	5.978	6.266	6.075	-1.001	-0.713
7909455	TRAF3IP3	TRAF3 interacting protein 3	7.276	6.088	6.557	6.072	-1.187	-0.718
8125447	HLA-DQB1	major histocompatibility complex, class II, DQ beta 1	9.055	7.895	8.325	7.971	-1.160	-0.730
8075483	PIK3IP1	phosphoinositide-3-kinase interacting protein 1	8.103	6.968	7.373	7.268	-1.136	-0.730
8039692	ZNF814	zinc finger protein 814	8.272	6.742	7.540	6.456	-1.530	-0.732
8129804	MAP3K5	mitogen-activated protein kinase kinase kinase 5	8.803	7.491	8.069	7.564	-1.312	-0.734
7989132	RFX7	regulatory factor X, 7	8.917	7.904	8.180	8.007	-1.013	-0.737
8151890	TP53INP1	tumor protein p53 inducible nuclear protein 1	10.109	9.015	9.369	9.231	-1.094	-0.740
8180078	HLA-DMB	major histocompatibility complex, class II, DM beta	11.918	10.852	11.177	11.068	-1.066	-0.741
8056113	LY75	lymphocyte antigen 75	8.854	7.652	8.113	8.078	-1.202	-0.741
8125530	HLA-DMB	major histocompatibility complex, class II, DM beta	12.007	10.944	11.265	11.169	-1.062	-0.742
7957338	SYT1	synaptotagmin I	9.373	7.704	8.627	7.350	-1.669	-0.745
8097867	KIAA0922	KIAA0922	7.697	6.143	6.948	6.239	-1.554	-0.750

Appendix VIII

List of osteoclast genes induced by RANKL in mature osteoclast.

Probe ID	Gene symbol	Gene Name	m	mr	j4	j5	folds (mr-m)
8021635	SERPINB2	serpin peptidase inhibitor, clade B (ovalbumin), member 2	5.364	10.688	11.437	12.044	5.324
8000574	NUPR1	nuclear protein, transcriptional regulator, 1	8.189	12.151	12.112	11.712	3.962
7981427	CKB	creatine kinase, brain	8.458	12.316	12.276	11.970	3.858
8102050	NHEDC2	Na+/H+ exchanger domain containing 2	8.964	12.719	12.534	12.464	3.755
7902452	AK5	adenylate kinase 5	7.474	11.208	10.996	10.445	3.734
7926875	BAMBI	BMP and activin membrane-bound inhibitor homolog (Xenopus laevis)	6.641	10.210	10.185	10.361	3.569
8006440	CCL7	chemokine (C-C motif) ligand 7	6.366	9.713	9.635	10.166	3.347
7922174	F5	coagulation factor V (proaccelerin, labile factor)	6.157	9.496	9.318	9.816	3.338
8100977	CXCL5	chemokine (C-X-C motif) ligand 5	7.109	10.445	10.548	10.364	3.336
7981514	AHNAK2	AHNAK nucleoprotein 2	6.592	9.924	10.003	10.378	3.331
7922474	KIAA0040	KIAA0040	8.292	11.598	11.359	10.971	3.306
8095680	IL8	interleukin 8	7.949	11.149	11.899	11.521	3.199
8128565	POPDC3	popeye domain containing 3	6.115	9.309	9.118	8.849	3.194
8143154	DGKI	diacylglycerol kinase, iota	6.162	9.340	9.316	8.390	3.178
8136115	FAM40B	family with sequence similarity 40, member B	7.370	10.522	10.476	10.386	3.152
8102342	ELOVL6	ELOVL family member 6, elongation of long chain fatty acids (FEN1/Elo2, SUR4/Elo3-like, yeast)	6.965	10.091	10.168	9.374	3.126
8058063	RFTN2	raftlin family member 2	5.059	8.146	7.984	7.401	3.086
8090988	CEP70	centrosomal protein 70kDa	5.126	8.167	8.052	7.893	3.042
7942328	FOLR3	folate receptor 3 (gamma)	6.763	9.800	9.824	8.869	3.037
8097991	TDO2	tryptophan 2,3-dioxygenase	6.018	9.031	8.857	9.214	3.013
8100798	SULT1B1	sulfotransferase family, cytosolic, 1B, member 1	5.519	8.529	7.504	8.360	3.011
8109563	NIPAL4	NIPA-like domain containing 4	6.863	9.862	9.748	8.932	3.000
8007931	ITGB3	integrin, beta 3 (platelet glycoprotein IIIa, antigen CD61)	9.753	12.736	12.705	12.782	2.983
8140650	SEMA3E	sema domain, immunoglobulin domain (Ig), short basic domain, secreted, (semaphorin) 3E	4.501	7.464	7.522	7.169	2.963
8105267	ITGA2	integrin, alpha 2 (CD49B, alpha 2 subunit of VLA-2 receptor)	6.459	9.411	9.273	9.505	2.953
8091411	TM4SF1	transmembrane 4 L six family member 1	5.488	8.399	8.581	7.676	2.911
8111136	FAM134B	family with sequence similarity 134, member B	8.438	11.316	11.421	11.294	2.878
8100097	GABRG1	gamma-aminobutyric acid (GABA) A receptor, gamma 1	5.148	7.923	7.982	7.107	2.775
8111892	OXCT1	3-oxoacid CoA transferase 1	8.085	10.860	10.735	10.199	2.775
8106393	F2R	coagulation factor II (thrombin) receptor	6.698	9.464	9.113	9.122	2.766
8087611	HYAL1	hyaluronoglucosaminidase 1	7.557	10.273	10.347	10.291	2.716
8103812	ASB5	ankyrin repeat and SOCS box-containing 5	4.810	7.505	7.285	6.643	2.695
8105741	MAST4	microtubule associated serine/threonine kinase family member 4	6.461	9.155	9.331	8.727	2.694
7951246	MMP8	matrix metallopeptidase 8 (neutrophil collagenase)	6.787	9.481	9.054	9.969	2.694
8164343	FAM102A	family with sequence similarity 102, member A	8.103	10.776	11.013	10.184	2.673
8112980	EDIL3	EGF-like repeats and discoidin I-like domains 3	5.336	7.995	7.774	7.532	2.660
8098263	PALLD	palladin, cytoskeletal associated protein	7.818	10.459	10.539	9.701	2.641
7960900	CLEC4E	C-type lectin domain family 4, member E	5.922	8.561	8.666	9.084	2.640
8075310	LIF	leukemia inhibitory factor (cholinergic differentiation factor)	6.218	8.817	9.136	8.358	2.599
7909225	DYRK3	dual-specificity tyrosine-(Y)-phosphorylation regulated kinase 3	6.995	9.593	9.190	9.096	2.598
7920278	S100A3	S100 calcium binding protein A3	5.590	8.174	8.003	7.209	2.584
8032789	STAP2	signal transducing adaptor family member 2	5.755	8.327	7.571	7.459	2.571
8043981	IL1R2	interleukin 1 receptor, type II	7.464	10.033	9.842	9.681	2.568
8162254	DIRAS2	DIRAS family, GTP-binding RAS-like 2	8.127	10.690	10.719	9.683	2.563
8100362	LNX1	ligand of numb-protein X 1	6.234	8.797	9.151	7.968	2.562
7946446	NRIP3	nuclear receptor interacting protein 3	9.170	11.726	11.659	10.998	2.556
8109773	WWC1	WW and C2 domain containing 1	6.208	8.715	8.677	8.139	2.507
8152491	EXT1	exostosin 1	7.224	9.729	9.863	9.608	2.504
8083000	FAIM	Fas apoptotic inhibitory molecule	7.550	10.030	10.131	9.785	2.480
7910727	ACTN2	actinin, alpha 2	5.916	8.357	8.769	8.689	2.441
7977621	NDRG2	NDRG family member 2	7.830	10.263	10.181	10.054	2.433
8135601	MET	met proto-oncogene (hepatocyte growth factor receptor)	4.714	7.138	7.597	6.922	2.424
8100298	OCIAD2	OCIA domain containing 2	6.190	8.613	8.359	7.725	2.423
7990080	LARP6	La ribonucleoprotein domain family, member 6	6.583	8.998	8.967	7.886	2.415
8082974	ESYT3	extended synaptotagmin-like protein 3	5.987	8.402	8.372	8.103	2.415
8056222	DPP4	dipeptidyl-peptidase 4	10.771	13.168	13.160	13.110	2.397
7950899	RAB38	RAB38, member RAS oncogene family	9.056	11.443	11.319	10.670	2.387
8123176	MAS1	MAS1 oncogene	4.561	6.946	6.801	6.450	2.385
7961111	CLEC1A	C-type lectin domain family 1, member A	5.660	7.998	7.870	7.786	2.338
7983228	MAP1A	microtubule-associated protein 1A	6.076	8.393	8.334	8.672	2.317
8041048	FOSL2	FOS-like antigen 2	8.606	10.916	11.011	10.901	2.310
8058905	CXCR1	chemokine (C-X-C motif) receptor 1	6.200	8.468	8.292	7.695	2.269
8014115	MYO1D	myosin ID	9.289	11.524	11.419	11.377	2.234
8048763	KIAA1486	KIAA1486	5.173	7.400	7.101	6.410	2.227
7938834	NAV2	neuron navigator 2	6.127	8.349	8.408	8.432	2.222
8114572	HBEGF	heparin-binding EGF-like growth factor	7.826	10.046	10.184	10.371	2.220
8021376	NEDD4L	neural precursor cell expressed, developmentally down-regulated 4-like	7.465	9.683	9.855	9.338	2.218
7984001	GCNT3	glucosaminyl (N-acetyl) transferase 3, mucin type	6.305	8.519	8.270	7.272	2.214
7943413	BIRC3	baculoviral IAP repeat-containing 3	7.446	9.658	9.691	9.789	2.213
7977161	TDRD9	tudor domain containing 9	6.262	8.454	8.436	8.368	2.191
7926916	ZEB1	zinc finger E-box binding homeobox 1	7.044	9.234	9.173	8.359	2.189
8147848	OXR1	oxidation resistance 1	9.312	11.497	11.539	10.937	2.185
8157105	ZNF462	zinc finger protein 462	7.544	9.693	9.558	9.598	2.149
8114938	JAKMIP2	janus kinase and microtubule interacting protein 2	8.207	10.339	10.406	10.422	2.132
7953737	CLEC6A	C-type lectin domain family 6, member A	4.765	6.892	6.850	7.183	2.126
8100971	PPBP	pro-platelet basic protein (chemokine (C-X-C motif) ligand 7)	6.905	9.029	9.004	9.008	2.125
8091550	KIAA1328	KIAA1328	6.939	9.057	8.899	8.046	2.119
8038655	KLK4	kallikrein-related peptidase 4	6.842	8.957	8.840	8.322	2.116
8065084	LOC613266	hypothetical LOC613266	6.234	8.324	8.444	7.384	2.089
8047127	MYO1B	myosin IB	8.570	10.653	10.549	10.349	2.083
8092707	LEPREL1	leprecan-like 1	6.815	8.898	8.468	8.879	2.083
8021091	SIGLEC15	sialic acid binding Ig-like lectin 15	9.304	11.380	11.332	11.050	2.076
7994052	HS3ST2	heparan sulfate (glucosamine) 3-O-sulfotransferase 2	8.449	10.518	10.375	10.354	2.070
7917875	F3	coagulation factor III (thromboplastin, tissue factor)	7.214	9.278	9.381	9.111	2.064
8120011	SPATS1	spermatogenesis associated, serine-rich 1	5.599	7.662	7.661	6.571	2.063
7983478	C15orf48	chromosome 15 open reading frame 48	7.477	9.533	9.517	9.441	2.056
7985147	DNAJA4	DnaJ (Hsp40) homolog, subfamily A, member 4	8.502	10.514	10.430	9.497	2.012
8154233	CD274	CD274 molecule	6.977	8.969	9.112	9.141	1.992
8145989	HTRA4	HtrA serine peptidase 4	9.149	11.141	11.341	11.408	1.991
8147012	PKIA	protein kinase (cAMP-dependent, catalytic) inhibitor alpha	7.131	9.113	8.879	8.083	1.982
8017843	SLC16A6	solute carrier family 16, member 6 (monocarboxylic acid transporter 7)	8.643	10.625	11.070	11.348	1.982
8089261	CBLB	Cas-Br-M (murine) ecotropic retroviral transforming sequence b	10.367	12.336	12.382	12.284	1.969
8161004	CD72	CD72 molecule	6.811	8.765	8.564	8.230	1.953
8134091	CLDN12	claudin 12	8.825	10.764	10.797	10.675	1.939
8080714	FLNB	filamin B, beta	7.534	9.465	9.498	9.731	1.931
8155673	PIP5K1B	phosphatidylinositol-4-phosphate 5-kinase, type I, beta	5.528	7.440	6.871	6.285	1.912
8044212	SULT1C2	sulfotransferase family, cytosolic, 1C, member 2	8.592	10.503	10.699	10.873	1.911

8147132	CA2	carbonic anhydrase II	10.900	12.803	12.614	12.586	1.903
7953532	ENO2	enolase 2 (gamma, neuronal)	7.674	9.551	9.712	8.920	1.877
8122279	KIAA1244	KIAA1244	6.963	8.811	8.911	8.530	1.848
7945663	LOC402778	CD225 family protein FLJ76511	8.898	10.746	10.872	11.239	1.848
8162502	FBP1	fructose-1,6-bisphosphatase 1	9.825	11.672	11.692	11.883	1.847
7952927	B4GALNT3	beta-1,4-N-acetyl-galactosaminyl transferase 3	6.661	8.505	8.076	8.408	1.845
8042283	HSPC159	galectin-related protein	9.205	11.040	10.859	10.438	1.835
8093096	TCTEX1D2	Tctex1 domain containing 2	7.862	9.678	10.202	10.465	1.816
7952022	AMICA1	adhesion molecule, interacts with CXADR antigen 1	9.093	10.898	10.696	11.450	1.805
8022747	B4GALT6	UDP-Gal:betaGlcNAc beta 1,4- galactosyltransferase, polypeptide 6	6.628	8.430	8.124	7.955	1.802
8142270	NRCAM	neuronal cell adhesion molecule	6.133	7.933	7.949	8.119	1.800
8129880	PERP	PERP, TP53 apoptosis effector	7.542	9.335	9.449	9.175	1.793
8150076	DUSP4	dual specificity phosphatase 4	5.927	7.711	7.790	6.901	1.784
7942204	CTTN	cortactin	8.547	10.331	10.258	9.815	1.784
7938528	PARVA	parvin, alpha	8.464	10.237	10.110	9.665	1.773
8150550	CHRNA6	cholinergic receptor, nicotinic, alpha 6	4.743	6.507	6.486	5.969	1.763
7897119	C1orf93	chromosome 1 open reading frame 93	9.016	10.768	10.910	10.384	1.751
7903092	FNBP1L	formin binding protein 1-like	8.223	9.969	9.855	9.518	1.746
7969544	NDFIP2	Nedd4 family interacting protein 2	7.663	9.405	9.061	8.928	1.742
8173551	PHKA1	phosphorylase kinase, alpha 1 (muscle)	7.356	9.097	9.074	8.574	1.741
7969341	TDRD3	tudor domain containing 3	9.709	11.450	11.474	11.021	1.741
8034851	EMR3	egf-like module containing, mucin-like, hormone receptor-like 3	6.563	8.300	8.267	9.519	1.738
8115814	SH3PXD2B	SH3 and PX domains 2B	8.448	10.186	10.392	10.270	1.737
8024676	GIPC3	GIPC PDZ domain containing family, member 3	7.695	9.430	9.722	8.702	1.736
7907861	XPR1	xenotropic and polytropic retrovirus receptor 1	10.190	11.917	11.944	11.810	1.727
8156897	C9orf30	chromosome 9 open reading frame 30	9.942	11.667	11.775	11.167	1.724
7944803	VWA5A	von Willebrand factor A domain containing 5A	9.269	10.991	10.896	10.813	1.723
8021001	KIAA1328	KIAA1328	6.058	7.778	7.918	7.070	1.719
8092541	LIPH	lipase, member H	5.394	7.110	6.915	6.551	1.717
8068383	CLIC6	chloride intracellular channel 6	7.315	9.029	9.209	8.617	1.714
8058221	TRAK2	trafficking protein, kinesin binding 2	10.167	11.877	11.839	10.957	1.711
8051298	GALNT14	UDP-N-acetyl-alpha-D-galactosamine:polypeptide N-acetylgalactosaminyltransferase 14 (GalNAc-T14)	7.822	9.526	9.332	9.284	1.704
7990545	CSPG4	chondroitin sulfate proteoglycan 4	6.422	8.124	8.431	8.056	1.701
8169249	MID2	midline 2	8.500	10.196	10.451	9.392	1.696
7942674	TSKU	tsukushi small leucine rich proteoglycan homolog (Xenopus laevis)	8.195	9.888	10.279	9.924	1.693
7951662	CRYAB	crystallin, alpha B	4.537	6.227	6.319	5.127	1.691
8146660	DNAJC5B	DnaJ (Hsp40) homolog, subfamily C, member 5 beta	6.019	7.700	7.818	7.235	1.681
8131600	TSPAN13	tetraspanin 13	7.054	8.724	8.512	8.576	1.670
7974835	PRKCH	protein kinase C, eta	8.642	10.302	10.133	9.936	1.660
8102800	SLC7A11	solute carrier family 7, (cationic amino acid transporter, y+ system) member 11	8.599	10.256	10.975	11.561	1.656
7909789	TGFB2	transforming growth factor, beta 2	7.364	9.015	9.106	8.935	1.650
8128956	FYN	FYN oncogene related to SRC, FGR, YES	6.436	8.084	7.976	7.964	1.648
7943803	DIXDC1	DIX domain containing 1	6.737	8.378	8.187	7.849	1.641
8140668	SEMA3A	sema domain, immunoglobulin domain (Ig), short basic domain, secreted, (semaphorin) 3A	6.016	7.654	7.504	7.918	1.638
8069269	COL6A1	collagen, type VI, alpha 1	9.351	10.979	11.075	11.423	1.628
8088680	C3orf64	chromosome 3 open reading frame 64	9.743	11.371	11.141	11.290	1.628
7915472	SLC2A1	solute carrier family 2 (facilitated glucose transporter), member 1	8.497	10.123	10.223	10.120	1.627
8022941	C18orf10	chromosome 18 open reading frame 10	10.953	12.576	12.501	11.779	1.623
8157216	UGCG	UDP-glucose ceramide glucosyltransferase	8.926	10.547	10.601	10.596	1.621
8029950	EHD2	EH-domain containing 2	7.958	9.576	9.663	8.986	1.619
8093878	EVC	Ellis van Creveld syndrome	7.237	8.848	9.020	9.208	1.612
7982377	GREM1	gremlin 1	9.205	10.806	11.072	10.286	1.600
7917728	FAM69A	family with sequence similarity 69, member A	8.252	9.846	9.950	9.696	1.594
7995681	MMP2	matrix metallopeptidase 2 (gelatinase A, 72kDa gelatinase, 72kDa type IV collagenase)	10.084	11.675	11.735	11.861	1.591
8083494	MME	membrane metallo-endopeptidase	8.125	9.703	9.792	10.030	1.578
8057517	NCKAP1	NCK-associated protein 1	9.438	11.014	11.046	10.724	1.576
7995292	SLC6A8	solute carrier family 6 (neurotransmitter transporter, creatine), member 8	8.899	10.475	10.613	10.164	1.576
8173086	FGD1	FYVE, RhoGEF and PH domain containing 1	6.230	7.804	8.104	7.451	1.574
8081288	TMEM45A	transmembrane protein 45A	6.635	8.208	8.087	7.959	1.573
8069301	COL6A2	collagen, type VI, alpha 2	8.912	10.479	10.724	10.904	1.567
7902810	LMO4	LIM domain only 4	7.085	8.651	8.544	7.864	1.567
7977270	LOC388022	hypothetical LOC388022	8.888	10.455	10.822	10.713	1.566
7908993	SOX13	SRY (sex determining region Y)-box 13	7.104	8.652	8.803	8.582	1.548
8130739	RPS6KA2	ribosomal protein S6 kinase, 90kDa, polypeptide 2	9.040	10.581	10.551	9.965	1.541
7991070	HDGFRP3	hepatoma-derived growth factor, related protein 3	7.983	9.519	9.345	8.448	1.536
8006736	DUSP14	dual specificity phosphatase 14	8.223	9.755	9.585	9.253	1.532
8147145	ATP6V0D2	ATPase, H+ transporting, lysosomal 38kDa, V0 subunit d2	11.214	12.746	12.622	12.490	1.531
8048211	RUFY4	RUN and FYVE domain containing 4	6.861	8.392	8.624	8.312	1.531
7923372	PHLDA3	pleckstrin homology-like domain, family A, member 3	8.414	9.940	10.040	9.505	1.527
8001082	SLC6A8	solute carrier family 6 (neurotransmitter transporter, creatine), member 8	8.853	10.374	10.554	10.105	1.521
8136987	ARHGEF5	Rho guanine nucleotide exchange factor (GEF) 5	6.440	7.956	7.754	7.653	1.516
8088958	GBE1	glucan (1,4-alpha-), branching enzyme 1	10.007	11.522	11.533	11.173	1.515
8058203	ALS2CR12	amyotrophic lateral sclerosis 2 (juvenile) chromosome region, candidate 12	5.191	6.703	6.900	6.948	1.512
8058824	MREG	melanoregulin	9.139	10.650	10.638	10.161	1.512
7944867	SIAE	sialic acid acetylesterase	8.601	10.113	9.832	10.006	1.512
7994541	LAT	linker for activation of T cells	8.804	10.315	10.321	10.105	1.512
7916024	TTC39A	tetratricopeptide repeat domain 39A	6.351	7.855	7.854	7.039	1.504
7921652	SLAMF1	signaling lymphocytic activation molecule family member 1	5.283	6.783	6.652	6.540	1.500
8143610	ARHGEF5	Rho guanine nucleotide exchange factor (GEF) 5	6.462	7.962	7.676	7.706	1.500
8059376	SERPINE2	serpin peptidase inhibitor, clade E (nexin, plasminogen activator inhibitor type 1), member 2	5.036	6.531	6.292	5.726	1.495
8151816	GEM	GTP binding protein overexpressed in skeletal muscle	7.236	8.730	9.208	7.955	1.494
8119898	VEGFA	vascular endothelial growth factor A	7.484	8.973	9.132	8.803	1.489
7919872	FAM63A	family with sequence similarity 63, member A	8.577	10.063	9.996	9.728	1.486
7990815	ST20	suppressor of tumorigenicity 20	10.371	11.854	11.837	11.297	1.483
8169473	PLS3	plastin 3	8.462	9.935	9.795	9.189	1.474
7975787	JDP2	Jun dimerization protein 2	9.520	10.988	10.705	10.483	1.468
8071147	TUBA8	tubulin, alpha 8	7.950	9.416	9.328	9.084	1.465
7986977	TJP1	tight junction protein 1 (zona occludens 1)	7.204	8.666	8.735	9.051	1.462
7964460	DDIT3	DNA-damage-inducible transcript 3	8.542	10.003	9.680	9.464	1.462
8070182	RCAN1	regulator of calcineurin 1	9.375	10.836	10.559	10.273	1.461
8120719	CD109	CD109 molecule	10.460	11.910	11.967	12.153	1.450
8156905	TMEFF1	transmembrane protein with EGF-like and two follistatin-like domains 1	6.583	8.031	8.210	7.675	1.448
8062844	TTPAL	tocopherol (alpha) transfer protein-like	6.832	8.278	8.050	7.481	1.446
7932765	MPP7	membrane protein, palmitoylated 7 (MAGUK p55 subfamily member 7)	6.259	7.703	7.648	6.979	1.444
8097282	SPRY1	sprouty homolog 1, antagonist of FGF signaling (Drosophila)	7.282	8.725	8.850	8.860	1.443
8162759	TBC1D2	TBC1 domain family, member 2	10.345	11.786	11.846	11.697	1.441
8041225	EHD3	EH-domain containing 3	7.874	9.314	9.451	8.578	1.439
8129649	C6orf192	chromosome 6 open reading frame 192	9.173	10.608	10.410	10.812	1.435
8077441	BHLHE40	basic helix-loop-helix family, member e40	9.890	11.323	11.483	11.230	1.433
8158183	DNM1	dynamin 1	7.515	8.946	9.012	8.759	1.431
7941401	OVOL1	ovo-like 1(Drosophila)	7.039	8.469	8.765	8.437	1.431
7969861	ITGBL1	integrin, beta-like 1 (with EGF-like repeat domains)	7.132	8.560	8.881	8.564	1.428

8027819	HAMP	hepcidin antimicrobial peptide	7.576	9.003	8.646	8.344	1.428
7971590	CAB39L	calcium binding protein 39-like	8.728	10.150	10.022	9.435	1.422
7932160	FAM107B	family with sequence similarity 107, member B	9.385	10.806	10.660	10.191	1.421
8075462	SELM	selenoprotein M	8.263	9.677	9.191	8.869	1.414
8119161	PIM1	pim-1 oncogene	8.352	9.762	10.389	9.920	1.411
7924996	C1orf198	chromosome 1 open reading frame 198	8.322	9.729	9.687	9.202	1.407
7996219	NDRG4	NDRG family member 4	6.979	8.378	8.569	7.723	1.399
8043945	MAP4K4	mitogen-activated protein kinase kinase kinase kinase 4	9.270	10.667	10.760	10.106	1.397
8139680	COBL	cordon-bleu homolog (mouse)	6.244	7.638	7.829	7.292	1.395
7985662	PDE8A	phosphodiesterase 8A	9.826	11.220	11.177	10.968	1.394
7987163	FMN1	formin 1	6.477	7.871	8.228	8.086	1.394
8162059	SLC28A3	solute carrier family 28 (sodium-coupled nucleoside transporter), member 3	9.285	10.675	11.005	10.732	1.390
8015635	PTRF	polymerase I and transcript release factor	6.571	7.958	7.545	7.052	1.387
8099982	APBB2	amyloid beta (A4) precursor protein-binding, family B, member 2	8.825	10.211	10.176	9.854	1.385
7913357	ECE1	endothelin converting enzyme 1	8.706	10.086	10.196	10.322	1.380
7917304	MCOLN3	mucolipin 3	8.745	10.123	10.334	10.779	1.377
8094719	N4BP2	NEDD4 binding protein 2	7.010	8.387	8.201	8.423	1.377
7965040	PHLDA1	pleckstrin homology-like domain, family A, member 1	7.817	9.188	9.537	9.691	1.372
8023757	CD226	CD226 molecule	5.583	6.954	7.478	8.448	1.371
8038213	HSD17B14	hydroxysteroid (17-beta) dehydrogenase 14	7.594	8.963	8.927	8.446	1.369
7982366	SCG5	secretogranin V (7B2 protein)	5.641	7.010	7.141	6.846	1.369
8094056	HTRA3	HtrA serine peptidase 3	7.759	9.126	9.050	8.776	1.367
8104788	RAI14	retinoic acid induced 14	9.621	10.987	11.133	10.500	1.366
8113790	40971	membrane-associated ring finger (C3HC4) 3	9.125	10.488	10.337	9.478	1.363
7906613	SLAMF7	SLAM family member 7	10.678	12.040	11.906	11.901	1.362
8104901	IL7R	interleukin 7 receptor	7.539	8.899	8.956	8.923	1.360
8098549	STOX2	storkhead box 2	5.738	7.098	7.067	7.239	1.359
7995007	HSD3B7	hydroxy-delta-5-steroid dehydrogenase, 3 beta- and steroid delta-isomerase 7	9.749	11.099	11.132	10.786	1.351
7934411	USP54	ubiquitin specific peptidase 54	6.856	8.200	8.224	8.048	1.344
8135514	IFRD1	interferon-related developmental regulator 1	7.757	9.097	9.016	8.755	1.340
7931168	ACADSB	acyl-CoA dehydrogenase, short/branched chain	8.161	9.499	9.476	9.112	1.339
8056829	CIR1	corepressor interacting with RBPJ, 1	8.753	10.091	10.161	9.826	1.338
8010405	SLC26A11	solute carrier family 26, member 11	9.622	10.959	11.140	11.854	1.338
7908940	ATP2B4	ATPase, Ca++ transporting, plasma membrane 4	8.710	10.047	10.133	10.151	1.337
8062377	SRC	v-src sarcoma (Schmidt-Ruppin A-2) viral oncogene homolog (avian)	8.243	9.580	9.768	9.707	1.337
7909104	CDK18	cyclin-dependent kinase 18	8.193	9.529	9.731	9.472	1.337
8063923	SLCO4A1	solute carrier organic anion transporter family, member 4A1	8.153	9.488	9.640	9.419	1.336
7954065	GPRC5A	G protein-coupled receptor, family C, group 5, member A	5.273	6.608	6.837	6.318	1.335
7994603	SPN	sialophorin	8.443	9.776	9.828	10.224	1.333
8143850	CDK5	cyclin-dependent kinase 5	9.692	11.024	10.826	10.538	1.332
8029728	GIPR	gastric inhibitory polypeptide receptor	7.318	8.649	9.003	8.883	1.331
7920244	S100A8	S100 calcium binding protein A8	8.412	9.739	9.589	9.801	1.327
8080911	KBTBD8	kelch repeat and BTB (POZ) domain containing 8	7.339	8.655	8.469	8.065	1.316
8075142	TTC28	tetratricopeptide repeat domain 28	6.892	8.208	8.463	8.618	1.316
8059350	AP1S3	adaptor-related protein complex 1, sigma 3 subunit	6.537	7.851	7.368	7.260	1.314
8140534	SEMA3C	sema domain, immunoglobulin domain (Ig), short basic domain, secreted, (semaphorin) 3C	6.960	8.269	8.259	9.056	1.310
8166784	TSPAN7	tetraspanin 7	6.577	7.886	7.552	7.862	1.309
8066939	B4GALT5	UDP-Gal:betaGlcNAc beta 1,4- galactosyltransferase, polypeptide 5	10.928	12.236	12.293	12.076	1.309
8047443	STRADB	STE20-related kinase adaptor beta	11.036	12.345	12.270	11.853	1.308
8009568	TTYH2	tweety homolog 2 (Drosophila)	9.608	10.916	10.993	11.022	1.307
7910014	CNIH4	cornichon homolog 4 (Drosophila)	10.089	11.392	11.266	11.326	1.303
8054872	TFCP2L1	transcription factor CP2-like 1	8.072	9.372	9.385	9.078	1.301
8109333	GPX3	glutathione peroxidase 3 (plasma)	10.590	11.885	11.772	11.609	1.295
8022711	DSC2	desmocollin 2	8.927	10.217	10.267	10.546	1.290
7957654	AMDHD1	amidohydrolase domain containing 1	7.562	8.850	8.499	8.232	1.288
8115455	HAVCR1	hepatitis A virus cellular receptor 1	6.007	7.293	7.806	8.436	1.287
7963946	MMP19	matrix metallopeptidase 19	10.011	11.298	11.353	11.538	1.286
8066513	SDC4	syndecan 4	9.427	10.713	10.672	10.389	1.286
8150797	ATP6V1H	ATPase, H+ transporting, lysosomal 50/57kDa, V1 subunit H	9.872	11.157	11.144	11.136	1.285
7952036	MPZL3	myelin protein zero-like 3	7.753	9.036	9.156	8.774	1.283
7924150	TMEM206	transmembrane protein 206	9.753	11.032	10.829	10.873	1.279
7934434	MYOZ1	myozenin 1	6.981	8.256	7.716	7.853	1.275
8079407	CCRL2	chemokine (C-C motif) receptor-like 2	8.687	9.963	9.981	10.242	1.275
7901336	STRADB	STE20-related kinase adaptor beta	11.133	12.405	12.328	11.927	1.273
7980327	ANGEL1	angel homolog 1 (Drosophila)	8.875	10.145	10.199	10.513	1.270
7990810	MTHFS	5,10-methenyltetrahydrofolate synthetase (5-formyltetrahydrofolate cyclo-ligase)	7.661	8.930	8.699	8.331	1.268
8092392	KLHL6	kelch-like 6 (Drosophila)	9.494	10.761	10.856	10.664	1.268
7903786	CSF1	colony stimulating factor 1 (macrophage)	10.266	11.533	11.605	11.501	1.267
7980720	TTC7B	tetratricopeptide repeat domain 7B	9.140	10.406	10.367	9.900	1.266
8156043	PSAT1	phosphoserine aminotransferase 1	5.943	7.209	7.214	6.290	1.266
7990818	BCL2A1	BCL2-related protein A1	9.239	10.505	10.458	10.229	1.266
8160213	TTC39B	tetratricopeptide repeat domain 39B	6.292	7.556	7.640	7.885	1.265
8108478	C5orf32	chromosome 5 open reading frame 32	10.387	11.649	11.571	11.148	1.262
7924526	TP53BP2	tumor protein p53 binding protein, 2	9.289	10.551	10.501	10.316	1.261
7962058	TMTC1	transmembrane and tetratricopeptide repeat containing 1	6.869	8.128	8.343	8.198	1.259
8013159	TOM1L2	target of myb1-like 2 (chicken)	8.980	10.239	10.384	10.273	1.258
7917103	ZZZ3	zinc finger, ZZ-type containing 3	9.476	10.730	10.630	10.464	1.255
8099721	SEL1L3	sel-1 suppressor of lin-12-like 3 (C. elegans)	8.828	10.079	10.221	10.250	1.251
8093304	CCRL2	chemokine (C-C motif) receptor-like 2	7.697	8.944	9.016	9.297	1.247
7900129	C1orf113	chromosome 1 open reading frame 113	6.851	8.098	8.224	7.878	1.247
8030128	PPP1R15A	protein phosphatase 1, regulatory (inhibitor) subunit 15A	8.949	10.193	10.290	9.931	1.244
7912145	TNFRSF9	tumor necrosis factor receptor superfamily, member 9	10.351	11.594	11.409	11.394	1.243
8002854	BCAR1	breast cancer anti-estrogen resistance 1	7.182	8.422	8.555	8.548	1.240
8113981	P4HA2	prolyl 4-hydroxylase, alpha polypeptide II	8.265	9.504	9.366	9.495	1.239
8043621	ARID5A	AT rich interactive domain 5A (MRF1-like)	8.819	10.057	9.973	9.518	1.238
8089820	GPR156	G protein-coupled receptor 156	5.414	6.647	6.911	6.219	1.233
7937878	TRPC2	transient receptor potential cation channel, subfamily C, member 2, pseudogene	7.449	8.678	8.718	8.682	1.229
7918657	PTPN22	protein tyrosine phosphatase, non-receptor type 22 (lymphoid)	10.489	11.715	11.472	11.652	1.227
8162117	GOLM1	golgi membrane protein 1	9.776	11.001	10.854	10.500	1.225
7917954	FRRS1	ferric-chelate reductase 1	9.952	11.177	11.162	11.641	1.225
7996837	CDH1	cadherin 1, type 1, E-cadherin (epithelial)	5.484	6.709	6.638	7.010	1.225
8095751	PARM1	prostate androgen-regulated mucin-like protein 1	6.083	7.306	6.988	7.196	1.224
8094393	ZCCHC4	zinc finger, CCHC domain containing 4	7.620	8.841	8.943	8.490	1.221
7898957	RCAN3	RCAN family member 3	8.569	9.786	9.693	9.264	1.217
8047248	PLCL1	phospholipase C-like 1	6.792	8.004	7.948	7.476	1.212
8093219	BDH1	3-hydroxybutyrate dehydrogenase, type 1	7.261	8.472	8.360	7.741	1.210
8113214	GLRX	glutaredoxin (thioltransferase)	11.074	12.284	12.236	12.112	1.210
7982829	SPINT1	serine peptidase inhibitor, Kunitz type 1	8.848	10.058	10.199	10.116	1.210
7962183	AK4	adenylate kinase 4	8.184	9.394	9.393	8.551	1.210
7941714	C11orf80	chromosome 11 open reading frame 80	7.415	8.616	8.203	8.194	1.201
7952350	SCN3B	sodium channel, voltage-gated, type III, beta	5.913	7.110	7.141	7.146	1.197
8174985	SMARCA1	SWI/SNF related, matrix associated, actin dependent regulator of chromatin, subfamily a, member 1	5.081	6.278	6.076	6.312	1.197

7965627	LTA4H	leukotriene A4 hydrolase	11.342	12.537	12.479	12.800	1.194
8112107	PPAP2A	phosphatidic acid phosphatase type 2A	6.131	7.325	6.882	7.094	1.194
7956759	SRGAP1	SLIT-ROBO Rho GTPase activating protein 1	8.082	9.275	9.226	9.218	1.193
7981290	WARS	tryptophanyl-tRNA synthetase	11.124	12.317	12.464	12.518	1.193
8007949	C17orf57	chromosome 17 open reading frame 57	6.816	8.006	7.962	7.707	1.190
8065089	KIF16B	kinesin family member 16B	8.611	9.801	9.878	9.315	1.190
8075838	PVALB	parvalbumin	5.822	7.009	6.963	6.751	1.187
7979698	ATP6V1D	ATPase, H+ transporting, lysosomal 34kDa, V1 subunit D	10.370	11.552	11.429	10.918	1.182
7921667	CD48	CD48 molecule	10.115	11.296	11.209	11.225	1.181
8003875	SPNS2	spinster homolog 2 (Drosophila)	7.014	8.192	8.485	7.621	1.178
8050557	SDC1	syndecan 1	7.713	8.889	8.824	8.747	1.176
8166925	MAOA	monoamine oxidase A	7.399	8.574	8.500	8.472	1.175
7980765	GPR68	G protein-coupled receptor 68	5.977	7.150	7.194	7.621	1.173
7909603	NENF	neuron derived neurotrophic factor	10.577	11.749	11.586	10.958	1.172
8055465	CXCR4	chemokine (C-X-C motif) receptor 4	8.185	9.357	9.389	9.795	1.172
8161919	TLE1	transducin-like enhancer of split 1 (E(sp1) homolog, Drosophila)	7.453	8.624	8.735	8.060	1.171
8098103	FNIP2	folliculin interacting protein 2	11.067	12.238	12.358	12.104	1.171
8001531	MT1G	metallothionein 1G	10.539	11.708	12.861	11.946	1.169
8091009	PIK3CB	phosphoinositide-3-kinase, catalytic, beta polypeptide	9.952	11.120	11.072	10.904	1.169
8075673	RBFOX2	RNA binding protein, fox-1 homolog (C. elegans) 2	7.088	8.256	8.273	7.533	1.167
8049487	MLPH	melanophilin	6.832	7.999	7.877	7.683	1.167
8119088	CDKN1A	cyclin-dependent kinase inhibitor 1A (p21, Cip1)	10.725	11.889	11.955	11.355	1.164
7906838	NOS1AP	nitric oxide synthase 1 (neuronal) adaptor protein	6.848	8.010	8.253	8.356	1.163
7925876	PFKP	phosphofructokinase, platelet	9.222	10.383	10.464	10.091	1.161
8088671	FAM19A4	family with sequence similarity 19 (chemokine (C-C motif)-like), member A4	5.927	7.084	7.111	6.796	1.158
8115871	FLJ16171	FLJ16171 protein	5.738	6.896	6.877	6.828	1.157
7962884	RND1	Rho family GTPase 1	6.020	7.177	6.742	6.294	1.157
8155048	RUSC2	RUN and SH3 domain containing 2	7.735	8.890	9.100	8.865	1.156
8089011	PROS1	protein S (alpha)	7.049	8.204	8.125	8.345	1.155
8114733	ARAP3	ArfGAP with RhoGAP domain, ankyrin repeat and PH domain 3	7.001	8.155	8.553	8.096	1.154
8074316	GGT3P	gamma-glutamyltransferase 3 pseudogene	8.265	9.418	9.500	9.583	1.153
8162850	TEX10	testis expressed 10	8.712	9.865	9.850	9.819	1.153
8048432	CYP27A1	cytochrome P450, family 27, subfamily A, polypeptide 1	10.822	11.970	12.017	12.356	1.148
8027002	GDF15	growth differentiation factor 15	10.172	11.319	11.338	11.354	1.148
8103025	ZNF827	zinc finger protein 827	6.265	7.411	7.459	7.510	1.147
8080964	GXYLT2	glucoside xylosyltransferase 2	5.557	6.704	6.559	6.656	1.146
7992789	TNFRSF12A	tumor necrosis factor receptor superfamily, member 12A	9.348	10.494	10.530	10.182	1.146
7926239	OPTN	optineurin	7.784	8.928	9.181	8.681	1.144
8123232	SLC22A1	solute carrier family 22 (organic cation transporter), member 1	6.471	7.613	7.827	7.448	1.142
8072170	KREMEN1	kringle containing transmembrane protein 1	6.384	7.520	7.505	7.098	1.136
7897728	FBXO6	F-box protein 6	7.687	8.823	8.812	8.324	1.136
8032682	MATK	megakaryocyte-associated tyrosine kinase	8.327	9.461	9.554	9.187	1.134
8156761	NANS	N-acetylneuraminic acid synthase	9.238	10.372	10.279	9.832	1.134
8139656	GRB10	growth factor receptor-bound protein 10	5.831	6.964	6.783	6.738	1.133
8124448	HIST1H4H	histone cluster 1, H4h	8.704	9.837	9.416	9.630	1.132
8150722	ST18	suppression of tumorigenicity 18 (breast carcinoma) (zinc finger protein)	6.881	8.013	8.052	8.164	1.132
7946142	PRKCDBP	protein kinase C, delta binding protein	8.128	9.259	9.133	8.955	1.131
7929958	BTRC	beta-transducin repeat containing	8.465	9.594	9.744	9.057	1.128
7939751	NR1H3	nuclear receptor subfamily 1, group H, member 3	9.289	10.416	10.653	10.823	1.127
7925062	SIPA1L2	signal-induced proliferation-associated 1 like 2	8.175	9.299	9.373	9.184	1.125
8073015	KDELR3	KDEL (Lys-Asp-Glu-Leu) endoplasmic reticulum protein retention receptor 3	6.345	7.469	6.957	6.450	1.124
7914021	SLC9A1	solute carrier family 9 (sodium/hydrogen exchanger), member 1	8.517	9.640	9.834	10.177	1.123
8170443	MTMR1	myotubularin related protein 1	9.289	10.409	10.393	10.326	1.120
7986350	ARRDC4	arrestin domain containing 4	9.602	10.719	10.610	10.268	1.117
8016239	PLEKHM1	pleckstrin homology domain containing, family M (with RUN domain) member 1	9.272	10.387	10.380	9.932	1.115
7966738	C12orf49	chromosome 12 open reading frame 49	10.259	11.374	11.380	10.610	1.115
8138527	MGC87042	STEAP family protein MGC87042	5.693	6.804	6.632	6.644	1.111
8158627	NCS1	neuronal calcium sensor 1	9.520	10.631	10.627	10.133	1.111
7917754	BCAR3	breast cancer anti-estrogen resistance 3	6.931	8.040	8.012	7.838	1.109
8028058	KIRREL2	kin of IRRE like 2 (Drosophila)	5.914	7.022	6.762	6.993	1.108
8064894	LRRN4	leucine rich repeat neuronal 4	5.843	6.950	7.202	6.736	1.107
7922610	ABL2	v-abl Abelson murine leukemia viral oncogene homolog 2	9.286	10.391	10.397	10.073	1.105
8137352	SLC4A2	solute carrier family 4, anion exchanger, member 2 (erythrocyte membrane protein band 3-like 1)	9.192	10.293	10.375	10.147	1.101
8014391	CCL3L1	chemokine (C-C motif) ligand 3-like 1	9.834	10.931	11.125	10.619	1.097
8014414	CCL3L1	chemokine (C-C motif) ligand 3-like 1	9.834	10.931	11.125	10.619	1.097
8019731	CCL3L1	chemokine (C-C motif) ligand 3-like 1	9.834	10.931	11.125	10.619	1.097
8071927	GGT1	gamma-glutamyltransferase 1	8.553	9.650	9.705	9.810	1.097
8123044	TULP4	tubby like protein 4	8.766	9.857	10.002	9.919	1.091
7946401	ST5	suppression of tumorigenicity 5	6.951	8.041	7.950	7.665	1.090
7986675	NIPA1	non imprinted in Prader-Willi/Angelman syndrome 1	7.945	9.035	8.941	8.483	1.090
8165011	FCN1	ficolin (collagen/fibrinogen domain containing) 1	7.613	8.702	8.797	9.089	1.089
8131957	SNX10	sorting nexin 10	11.460	12.549	12.511	12.265	1.089
7924701	ACBD3	acyl-CoA binding domain containing 3	10.659	11.746	11.608	11.100	1.087
8002421	VAC14	Vac14 homolog (S. cerevisiae)	10.161	11.247	11.462	11.105	1.086
8021866	NFATC1	nuclear factor of activated T-cells, cytoplasmic, calcineurin-dependent 1	8.843	9.928	9.974	9.700	1.085
7919699	OTUD7B	OTU domain containing 7B	5.641	6.725	6.954	6.183	1.084
8085556	SH3BP5	SH3-domain binding protein 5 (BTK-associated)	8.976	10.059	10.143	9.947	1.083
7975607	ACOT4	acyl-CoA thioesterase 4	6.798	7.881	7.531	7.356	1.083
8046646	OSBPL6	oxysterol binding protein-like 6	6.185	7.267	6.919	6.488	1.082
8164200	ANGPTL2	angiopoietin-like 2	6.151	7.230	7.452	6.921	1.079
8145122	SLC39A14	solute carrier family 39 (zinc transporter), member 14	7.353	8.432	8.442	8.198	1.078
8107897	PDLIM4	PDZ and LIM domain 4	7.611	8.688	8.861	8.350	1.077
8094169	CPEB2	cytoplasmic polyadenylation element binding protein 2	8.741	9.817	9.982	9.738	1.075
8050176	ITGB1BP1	integrin beta 1 binding protein 1	10.330	11.405	11.367	10.919	1.075
8151334	MSC	musculin	9.022	10.095	10.482	10.240	1.074
8096160	ARHGAP24	Rho GTPase activating protein 24	6.235	7.307	7.240	7.049	1.072
7968029	PCOTH	prostate collagen triple helix	7.374	8.444	8.559	7.972	1.070
8067055	ATP9A	ATPase, class II, type 9A	7.269	8.334	8.678	8.855	1.065
8005557	EPN2	epsin 2	7.677	8.742	8.624	8.221	1.065
8022531	NPC1	Niemann-Pick disease, type C1	10.639	11.696	11.749	12.087	1.057
7964535	CYP27B1	cytochrome P450, family 27, subfamily B, polypeptide 1	6.849	7.904	8.056	8.036	1.055
8056491	SCN9A	sodium channel, voltage-gated, type IX, alpha subunit	6.077	7.132	6.610	6.870	1.054
8074716	GGT3P	gamma-glutamyltransferase 3 pseudogene	8.210	9.264	9.386	9.479	1.054
8041149	WDR43	WD repeat domain 43	10.000	11.054	10.998	10.436	1.054
8166797	MID1IP1	MID1 interacting protein 1 (gastrulation specific G12 homolog (zebrafish))	9.562	10.613	10.620	10.413	1.051
8093053	TFRC	transferrin receptor (p90, CD71)	12.237	13.288	13.239	13.396	1.051
8083569	TIPARP	TCDD-inducible poly(ADP-ribose) polymerase	10.292	11.341	11.296	11.193	1.049
8060344	TRIB3	tribbles homolog 3 (Drosophila)	6.858	7.905	7.748	7.308	1.047
7922229	SELE	selectin E	5.064	6.110	6.214	5.930	1.046
8010061	SPHK1	sphingosine kinase 1	8.666	9.712	9.855	9.418	1.046
8063394	PTPN1	protein tyrosine phosphatase, non-receptor type 1	10.015	11.059	10.995	10.748	1.044
8048752	MRPL44	mitochondrial ribosomal protein L44	8.867	9.910	9.640	9.556	1.043

7966234	TRPV4	transient receptor potential cation channel, subfamily V, member 4	8.601	9.643	9.521	9.977	1.042
8152962	LRRC6	leucine rich repeat containing 6	7.134	8.175	7.986	8.153	1.041
8020220	TUBB6	tubulin, beta 6	10.049	11.089	11.053	10.607	1.040
8124492	HIST1H2BK	histone cluster 1, H2bk	10.838	11.877	11.619	11.635	1.039
8068361	SLC5A3	solute carrier family 5 (sodium/myo-inositol cotransporter), member 3	11.016	12.055	12.280	12.356	1.038
8039166	MBOAT7	membrane bound O-acyltransferase domain containing 7	9.952	10.990	11.074	11.141	1.038
8147206	RIPK2	receptor-interacting serine-threonine kinase 2	9.979	11.016	10.911	10.747	1.037
8041508	QPCT	glutaminyl-peptide cyclotransferase	8.922	9.959	10.068	10.238	1.036
8129848	IL22RA2	interleukin 22 receptor, alpha 2	4.970	6.005	5.642	6.225	1.035
7968972	COX17	COX17 cytochrome c oxidase assembly homolog (S. cerevisiae)	8.540	9.575	9.408	9.041	1.034
8039120	OSCAR	osteoclast associated, immunoglobulin-like receptor	7.533	8.563	8.463	8.450	1.030
8051707	MAP4K3	mitogen-activated protein kinase kinase kinase kinase 3	9.294	10.322	10.383	10.013	1.028
8173444	IL2RG	interleukin 2 receptor, gamma	10.642	11.668	11.677	11.827	1.026
8123961	TBC1D7	TBC1 domain family, member 7	6.783	7.808	7.917	7.718	1.026
8145365	DOCK5	dedicator of cytokinesis 5	8.907	9.933	10.094	10.120	1.025
8050766	ADCY3	adenylate cyclase 3	10.917	11.942	12.011	11.917	1.025
8089112	FILIP1L	filamin A interacting protein 1-like	8.008	9.032	8.953	8.854	1.025
8130628	AGPAT4	1-acylglycerol-3-phosphate O-acyltransferase 4 (lysophosphatidic acid acyltransferase, delta)	7.485	8.507	8.705	9.263	1.021
8079733	KLHDC8B	kelch domain containing 8B	8.582	9.603	9.319	9.647	1.021
7902623	DNASE2B	deoxyribonuclease II beta	7.701	8.722	8.054	8.011	1.021
7902660	WDR63	WD repeat domain 63	7.012	8.031	7.945	7.717	1.019
8068353	SLC5A3	solute carrier family 5 (sodium/myo-inositol cotransporter), member 3	10.506	11.524	11.799	11.779	1.018
7923991	PLXNA2	plexin A2	7.700	8.716	8.829	8.837	1.016
8023889	MBP	myelin basic protein	8.258	9.274	9.212	9.110	1.016
8137381	AGAP3	ArfGAP with GTPase domain, ankyrin repeat and PH domain 3	8.378	9.393	9.388	9.125	1.015
8098576	SLC25A4	solute carrier family 25 (mitochondrial carrier; adenine nucleotide translocator), member 4	8.765	9.778	9.586	9.294	1.013
8021312	WDR7	WD repeat domain 7	9.970	10.982	11.134	11.005	1.012
8010092	MFSD11	major facilitator superfamily domain containing 11	9.706	10.718	10.638	10.837	1.012
8131682	ABCB5	ATP-binding cassette, sub-family B (MDR/TAP), member 5	5.683	6.690	6.350	6.688	1.008
7956878	IRAK3	interleukin-1 receptor-associated kinase 3	8.911	9.918	10.010	9.985	1.007
8174598	IL13RA2	interleukin 13 receptor, alpha 2	4.122	5.129	4.999	4.785	1.007
7993756	ACSM3	acyl-CoA synthetase medium-chain family member 3	5.473	6.479	6.325	6.544	1.006
7965800	SYCP3	synaptonemal complex protein 3	3.908	4.913	4.792	5.182	1.004
8005707	MAP2K3	mitogen-activated protein kinase kinase 3	9.585	10.589	10.725	10.089	1.003
8132406	RALA	v-ral simian leukemia viral oncogene homolog A (ras related)	10.059	11.060	10.872	10.493	1.001
8008310	EME1	essential meiotic endonuclease 1 homolog 1 (S. pombe)	6.653	5.653	5.695	5.759	-1.000
8057736	TMEM194B	transmembrane protein 194B	6.123	5.123	5.019	5.227	-1.000
8152976	TMEM71	transmembrane protein 71	6.797	5.796	5.289	5.437	-1.001
8027719	SCN1B	sodium channel, voltage-gated, type I, beta	8.030	7.027	6.979	6.940	-1.003
7983650	SLC27A2	solute carrier family 27 (fatty acid transporter), member 2	5.926	4.921	4.956	5.059	-1.005
8061247	RIN2	Ras and Rab interactor 2	10.468	9.462	9.210	9.385	-1.005
8124144	DEK	DEK oncogene	10.975	9.969	9.848	9.657	-1.005
8055702	NMI	N-myc (and STAT) interactor	9.334	8.328	8.244	8.173	-1.006
8127854	ME1	malic enzyme 1, NADP(+)-dependent, cytosolic	12.521	11.514	11.384	11.615	-1.007
8008646	SCPEP1	serine carboxypeptidase 1	11.218	10.211	9.964	10.689	-1.007
8093539	WHSC1	Wolf-Hirschhorn syndrome candidate 1	7.758	6.750	7.021	6.717	-1.009
7948910	SNORD25	small nucleolar RNA, C/D box 25	4.696	3.686	4.631	4.361	-1.010
8022488	ABHD3	abhydrolase domain containing 3	9.980	8.970	8.906	9.213	-1.010
7995697	LPCAT2	lysophosphatidylcholine acyltransferase 2	11.926	10.915	10.777	10.818	-1.011
7905079	HIST2H2AA3	histone cluster 2, H2aa3	10.370	9.359	9.157	9.161	-1.011
7919619	HIST2H2AA3	histone cluster 2, H2aa3	10.370	9.359	9.157	9.161	-1.011
8030860	FPR2	formyl peptide receptor 2	6.237	5.224	4.881	5.225	-1.013
8040802	KHK	ketohexokinase (fructokinase)	7.609	6.595	6.555	6.858	-1.014
8109843	DOCK2	dedicator of cytokinesis 2	11.488	10.474	10.494	10.916	-1.015
8124510	HIST1H2BL	histone cluster 1, H2bl	6.824	5.808	5.785	5.624	-1.015
7905147	C1orf54	chromosome 1 open reading frame 54	9.062	8.046	7.954	8.178	-1.016
7948904	SNORD28	small nucleolar RNA, C/D box 28	8.572	7.556	7.876	9.039	-1.016
8137680	ADAP1	ArfGAP with dual PH domains 1	8.976	7.960	8.001	7.719	-1.017
8105111	FBXO4	F-box protein 4	7.749	6.730	6.350	6.497	-1.019
7954711	C12orf35	chromosome 12 open reading frame 35	10.400	9.378	9.346	9.721	-1.021
8010212	TMC8	transmembrane channel-like 8	8.933	7.911	8.074	8.047	-1.022
8114612	CD14	CD14 molecule	13.056	12.034	11.771	12.627	-1.022
8032214	GAMT	guanidinoacetate N-methyltransferase	9.337	8.314	8.502	8.493	-1.023
8112902	DHFR // DHFF	dihydrofolate reductase // dihydrofolate reductase // dihydrofolate reductase // dihydrofolate reduct	10.311	9.286	8.861	8.514	-1.025
8033912	DNMT1	DNA (cytosine-5-)-methyltransferase 1	10.614	9.589	9.650	9.978	-1.026
7948906	SNORD27	small nucleolar RNA, C/D box 27	6.514	5.488	5.770	6.744	-1.026
8007569	C17orf53	chromosome 17 open reading frame 53	7.927	6.899	6.789	6.693	-1.027
8149927	CLU	clusterin	8.923	7.895	7.868	7.862	-1.028
8151532	FABP4	fatty acid binding protein 4, adipocyte	11.034	10.006	9.928	11.398	-1.028
8037579	ERCC1	excision repair cross-complementing rodent repair deficiency, complementation group 1 (includes overl	9.214	8.184	8.131	7.756	-1.029
8144378	AGPAT5	1-acylglycerol-3-phosphate O-acyltransferase 5 (lysophosphatidic acid acyltransferase, epsilon)	9.046	8.017	7.425	7.407	-1.030
8158998	SNORD36C	small nucleolar RNA, C/D box 36C	7.928	6.898	7.178	8.062	-1.030
8141076	PON2	paraoxonase 2	11.380	10.350	10.023	10.535	-1.030
8003611	FAM57A	family with sequence similarity 57, member A	8.372	7.340	7.331	7.532	-1.032
8094789	LIMCH1	LIM and calponin homology domains 1	6.363	5.329	5.194	5.329	-1.034
7960518	TNFRSF1A	tumor necrosis factor receptor superfamily, member 1A	11.007	9.971	9.920	10.306	-1.035
8147079	LRRCC1	leucine rich repeat and coiled-coil domain containing 1	7.365	6.329	5.941	5.956	-1.035
8132013	CHN2	chimerin (chimaerin) 2	9.104	8.067	8.021	8.169	-1.036
7955943	PDE1B	phosphodiesterase 1B, calmodulin-dependent	8.548	7.510	7.528	7.868	-1.038
8059996	PER2	period homolog 2 (Drosophila)	8.285	7.245	7.441	7.428	-1.040
7954655	DDX11	DEAD/H (Asp-Glu-Ala-Asp/His) box polypeptide 11	8.275	7.234	7.241	7.230	-1.040
8010832	FN3KRP	fructosamine 3 kinase related protein	9.343	8.303	8.282	7.768	-1.041
8045587	ACVR2A	activin A receptor, type IIA	9.515	8.474	8.333	8.750	-1.041
8117646	ZNF192	zinc finger protein 192	8.781	7.739	7.811	8.171	-1.042
8075217	AP1B1	adaptor-related protein complex 1, beta 1 subunit	11.504	10.462	10.425	10.572	-1.042
7968516	PDS5B	PDS5, regulator of cohesion maintenance, homolog B (S. cerevisiae)	9.279	8.237	7.905	8.293	-1.043
8017599	PECAM1	platelet/endothelial cell adhesion molecule	11.802	10.759	10.572	11.197	-1.043
8021470	PMAIP1	phorbol-12-myristate-13-acetate-induced protein 1	7.182	6.139	5.630	5.872	-1.043
7995539	NOD2	nucleotide-binding oligomerization domain containing 2	7.463	6.419	6.569	6.529	-1.044
8117675	PGBD1	piggyBac transposable element derived 1	6.721	5.677	5.724	5.635	-1.045
8073890	GRAMD4	GRAM domain containing 4	9.668	8.621	8.592	8.871	-1.046
7967386	MPHOSPH9	M-phase phosphoprotein 9	9.052	8.005	7.635	7.889	-1.047
8020847	DTNA	dystrobrevin, alpha	7.494	6.445	6.427	6.509	-1.049
8106931	ANKRD32	ankyrin repeat domain 32	6.594	5.543	5.280	5.444	-1.051
8031768	ZIK1	zinc finger protein interacting with K protein 1 homolog (mouse)	6.866	5.812	5.814	5.735	-1.054
8085914	SLC4A7	solute carrier family 4, sodium bicarbonate cotransporter, member 7	10.742	9.687	9.489	9.934	-1.054
7903334	CDC14A	CDC14 cell division cycle 14 homolog A (S. cerevisiae)	8.052	6.996	6.788	7.029	-1.056
8116494	ZFP62	zinc finger protein 62 homolog (mouse)	6.765	5.706	5.409	5.951	-1.059
7957759	APAF1	apoptotic peptidase activating factor 1	8.600	7.540	7.549	7.623	-1.061
7984330	ZWILCH	Zwilch, kinetochore associated, homolog (Drosophila)	9.869	8.807	8.345	8.256	-1.061
8088776	FOXP1	forkhead box P1	8.491	7.429	7.346	7.293	-1.062
7948896	SNORD22	small nucleolar RNA, C/D box 22	6.800	5.737	5.978	6.801	-1.063

8039687	ZNF552	zinc finger protein 552	7.463	6.398	6.423	6.734	-1.065
8117343	HFE	hemochromatosis	9.058	7.992	7.701	7.990	-1.066
7897877	TNFRSF1B	tumor necrosis factor receptor superfamily, member 1B	10.600	9.534	9.927	9.998	-1.066
8156126	RMI1	RMI1, RecQ mediated genome instability 1, homolog (S. cerevisiae)	8.622	7.555	7.310	7.144	-1.067
7926900	MAP3K8	mitogen-activated protein kinase kinase kinase 8	9.310	8.243	8.284	8.916	-1.068
7917976	SASS6	spindle assembly 6 homolog (C. elegans)	8.460	7.391	6.918	6.860	-1.069
7939383	PRR5L	proline rich 5 like	8.218	7.149	6.476	6.722	-1.069
7954777	ALG10	asparagine-linked glycosylation 10, alpha-1,2-glucosyltransferase homolog (S. pombe)	8.730	7.660	7.511	8.052	-1.070
8094190	CC2D2A	coiled-coil and C2 domain containing 2A	6.022	4.951	4.999	5.034	-1.071
8054135	MGAT4A	mannosyl (alpha-1,3-)-glycoprotein beta-1,4-N-acetylglucosaminyltransferase, isozyme A	10.977	9.906	9.855	10.009	-1.072
7955063	TMEM106C	transmembrane protein 106C	10.212	9.139	8.660	7.920	-1.073
8107520	TNFAIP8	tumor necrosis factor, alpha-induced protein 8	9.575	8.502	8.385	8.530	-1.073
8089203	SENP7	SUMO1/sentrin specific peptidase 7	7.253	6.180	5.989	6.298	-1.073
7961031	DDX12	DEAD/H (Asp-Glu-Ala-Asp/His) box polypeptide 12	8.183	7.109	7.123	7.235	-1.074
7964089	PAN2	PAN2 poly(A) specific ribonuclease subunit homolog (S. cerevisiae)	8.428	7.352	7.499	8.042	-1.076
8173208	SPIN4	spindlin family, member 4	7.902	6.826	6.860	6.778	-1.076
7944913	CCDC15	coiled-coil domain containing 15	6.776	5.697	5.447	5.532	-1.079
8111915	SEPP1	selenoprotein P, plasma, 1	13.473	12.394	12.150	12.406	-1.079
8100154	CORIN	corin, serine peptidase	6.490	5.410	5.349	5.379	-1.080
8035456	LRRC25	leucine rich repeat containing 25	10.874	9.792	9.651	10.089	-1.082
8035236	HAUS8	HAUS augmin-like complex, subunit 8	6.815	5.733	5.497	6.089	-1.082
7933619	SGMS1	sphingomyelin synthase 1	10.569	9.487	9.442	10.054	-1.082
7971218	KBTBD7	kelch repeat and BTB (POZ) domain containing 7	8.153	7.071	6.876	6.325	-1.082
8010260	BIRC5	baculoviral IAP repeat-containing 5	7.378	6.295	6.371	6.138	-1.083
8025498	NA70 // SNOF	small nucleolar RNA, H/ACA box 70 // small nucleolar RNA, H/ACA box 70	11.054	9.971	10.347	10.990	-1.083
8085145	RAD18	RAD18 homolog (S. cerevisiae)	8.869	7.786	7.616	7.523	-1.083
8111922	LOC648987	hypothetical LOC648987	8.732	7.649	7.567	7.640	-1.083
7954436	LRMP	lymphoid-restricted membrane protein	9.124	8.040	7.971	7.878	-1.084
7957737	TMPO	thymopoietin	10.214	9.130	8.926	9.068	-1.084
8112709	POC5	POC5 centriolar protein homolog (Chlamydomonas)	8.467	7.380	7.047	7.770	-1.087
8035779	ZNF253	zinc finger protein 253	9.935	8.847	8.528	8.649	-1.088
8118863	ANKS1A	ankyrin repeat and sterile alpha motif domain containing 1A	9.962	8.872	8.768	8.889	-1.089
7923662	PIK3C2B	phosphoinositide-3-kinase, class 2, beta polypeptide	7.832	6.742	6.716	6.728	-1.090
7954789	ALG10B	asparagine-linked glycosylation 10, alpha-1,2-glucosyltransferase homolog B (yeast)	8.715	7.622	7.525	8.125	-1.094
7984932	SCAMP5	secretory carrier membrane protein 5	7.677	6.579	6.569	6.692	-1.098
8166065	TLR8	toll-like receptor 8	9.230	8.132	8.161	8.567	-1.098
8134117	FZD1	frizzled homolog 1 (Drosophila)	9.331	8.230	8.234	8.007	-1.100
8020806	RNF125	ring finger protein 125	9.832	8.731	8.295	8.286	-1.101
7908409	RGS2	regulator of G-protein signaling 2, 24kDa	8.557	7.456	7.395	7.419	-1.101
7947147	SVIP	small VCP/p97-interacting protein	8.319	7.217	7.016	6.528	-1.102
7931951	SFMBT2	Scm-like with four mbt domains 2	9.967	8.863	9.003	9.109	-1.104
8162514	FANCC	Fanconi anemia, complementation group C	7.358	6.254	6.133	6.137	-1.105
8159900	GLIS3	GLIS family zinc finger 3	7.956	6.850	6.713	6.603	-1.106
8170015	ZNF449	zinc finger protein 449	7.554	6.446	6.487	6.654	-1.108
8036913	BLVRB	biliverdin reductase B (flavin reductase (NADPH))	11.072	9.964	9.845	9.682	-1.109
8069933	C21orf45	chromosome 21 open reading frame 45	7.710	6.598	6.215	6.260	-1.112
8132515	BLVRA	biliverdin reductase A	9.859	8.747	8.562	8.435	-1.112
7904469	SRGAP2	SLIT-ROBO Rho GTPase activating protein 2	10.985	9.872	9.788	9.914	-1.113
7946089	TRIM5	tripartite motif-containing 5	8.362	7.248	7.338	7.484	-1.114
7937915	RRM1	ribonucleotide reductase M1	10.430	9.315	9.072	9.125	-1.114
8133049	ZNF107	zinc finger protein 107	6.901	5.786	5.917	6.060	-1.115
8118259	MSH5	mutS homolog 5 (E. coli)	7.128	6.012	6.310	6.337	-1.115
8160238	PSIP1	PC4 and SFRS1 interacting protein 1	8.007	6.891	6.532	6.399	-1.116
8068305	ITSN1	intersectin 1 (SH3 domain protein)	10.428	9.311	9.186	9.145	-1.117
8170863	SNORA70	small nucleolar RNA, H/ACA box 70	10.994	9.875	10.246	10.976	-1.119
8171313	ARHGAP6	Rho GTPase activating protein 6	7.657	6.537	6.295	6.710	-1.120
8018975	LGALS3BP	lectin, galactoside-binding, soluble, 3 binding protein	10.345	9.225	9.198	9.831	-1.121
8000409	HMGN2	high-mobility group nucleosomal binding domain 2	11.326	10.205	9.833	10.217	-1.121
8122013	L3MBTL3	l(3)mbt-like 3 (Drosophila)	7.620	6.498	6.360	6.361	-1.121
8125545	HLA-DOA	major histocompatibility complex, class II, DO alpha	8.063	6.941	7.089	6.887	-1.122
8049246	INPP5D	inositol polyphosphate-5-phosphatase, 145kDa	11.103	9.980	9.980	10.006	-1.123
7975779	FOS	FBJ murine osteosarcoma viral oncogene homolog	9.955	8.832	8.766	9.009	-1.123
7954511	STK38L	serine/threonine kinase 38 like	10.585	9.459	9.205	9.190	-1.126
7967736	POLE	polymerase (DNA directed), epsilon	7.937	6.810	6.639	7.093	-1.127
8146130	GINS4	GINS complex subunit 4 (Sld5 homolog)	7.523	6.396	5.907	6.185	-1.127
8103431	C4orf46	chromosome 4 open reading frame 46	8.759	7.631	7.529	7.307	-1.128
8004167	FAM64A	family with sequence similarity 64, member A	6.963	5.835	5.782	6.163	-1.129
7961142	OLR1	oxidized low density lipoprotein (lectin-like) receptor 1	8.410	7.280	7.302	8.037	-1.129
8029701	PPM1N	protein phosphatase, Mg2+/Mn2+ dependent, 1N (putative)	9.001	7.871	7.795	7.703	-1.130
7982204	HMGN2	high-mobility group nucleosomal binding domain 2	11.353	10.222	9.839	10.236	-1.131
8078386	GPD1L	glycerol-3-phosphate dehydrogenase 1-like	8.413	7.279	7.093	6.803	-1.134
8064790	RASSF2	Ras association (RalGDS/AF-6) domain family member 2	11.646	10.510	10.446	10.549	-1.135
8129458	ARHGAP18	Rho GTPase activating protein 18	11.992	10.857	10.826	10.784	-1.135
8107375	YTHDC2	YTH domain containing 2	9.564	8.428	8.280	8.807	-1.136
8152582	DSCC1	defective in sister chromatid cohesion 1 homolog (S. cerevisiae)	7.528	6.391	5.847	6.039	-1.137
8168691	DIAPH2	diaphanous homolog 2 (Drosophila)	9.547	8.410	8.444	8.662	-1.137
8007483	TMEM106A	transmembrane protein 106A	10.957	9.820	9.671	9.979	-1.137
8067113	ZNF217	zinc finger protein 217	9.732	8.594	8.542	9.175	-1.138
8087839	POC1A	POC1 centriolar protein homolog A (Chlamydomonas)	6.921	5.782	6.064	6.021	-1.139
7978776	C14orf106	chromosome 14 open reading frame 106	8.756	7.617	7.735	8.002	-1.139
8038505	SIGLEC11	sialic acid binding Ig-like lectin 11	7.592	6.452	6.018	6.031	-1.140
8052010	CALM2	calmodulin 2 (phosphorylase kinase, delta)	10.842	9.700	9.840	9.833	-1.142
8012598	RCVRN	recoverin	7.604	6.462	6.522	6.615	-1.142
7905047	FCGR1A	Fc fragment of IgG, high affinity Ia, receptor (CD64)	11.334	10.191	9.340	10.473	-1.143
7984364	SMAD3	SMAD family member 3	7.386	6.242	6.462	6.452	-1.144
7983734	TMOD2	tropomodulin 2 (neuronal)	8.779	7.634	7.498	7.573	-1.145
8151447	IL7	interleukin 7	6.787	5.641	5.390	5.419	-1.146
8136869	CASP2	caspase 2, apoptosis-related cysteine peptidase	9.929	8.783	8.777	8.623	-1.146
7960874	C3AR1	complement component 3a receptor 1	12.664	11.517	10.882	11.496	-1.147
7938687	NUCB2	nucleobindin 2	9.236	8.088	7.817	8.414	-1.147
7938364	WEE1	WEE1 homolog (S. pombe)	6.629	5.481	5.612	5.692	-1.148
7930454	PDCD4	programmed cell death 4 (neoplastic transformation inhibitor)	9.732	8.583	8.422	9.029	-1.150
7976080	GPR65	G protein-coupled receptor 65	10.716	9.565	8.975	10.047	-1.151
8129924	TXLNB	taxilin beta	9.181	8.030	7.556	7.622	-1.152
8110971	CMBL	carboxymethylenebutenolidase homolog (Pseudomonas)	9.034	7.880	7.441	7.436	-1.153
8034122	SPC24	SPC24, NDC80 kinetochore complex component, homolog (S. cerevisiae)	7.333	6.178	5.706	5.966	-1.154
8030383	RCN3	reticulocalbin 3, EF-hand calcium binding domain	8.647	7.493	7.577	7.798	-1.155
7903507	FAM102B	family with sequence similarity 102, member B	9.634	8.479	8.360	8.330	-1.155
7953200	CCND2	cyclin D2	8.783	7.628	7.911	7.294	-1.155
8023259	SNORD58A	small nucleolar RNA, C/D box 58A	6.679	5.522	5.577	6.673	-1.157
7953981	ETV6	ets variant 6	10.673	9.516	9.632	10.014	-1.157
8150592	CEBPD	CCAAT/enhancer binding protein (C/EBP), delta	9.880	8.722	8.770	8.639	-1.158

7988537	CEP152	centrosomal protein 152kDa	6.692	5.533	5.534	6.037	-1.159
8019622	TMEM106A	transmembrane protein 106A	11.300	10.139	10.012	10.319	-1.160
8031213	LILRA1	leukocyte immunoglobulin-like receptor, subfamily A (with TM domain), member 1	8.208	7.047	6.749	7.431	-1.161
8058837	PECR	peroxisomal trans-2-enoyl-CoA reductase	8.116	6.954	6.620	6.677	-1.161
7903049	CCDC18	coiled-coil domain containing 18	6.590	5.427	5.078	5.292	-1.162
7902553	IFI44	interferon-induced protein 44	9.065	7.901	7.525	8.317	-1.164
8013243	SHMT1	serine hydroxymethyltransferase 1 (soluble)	8.500	7.334	6.961	7.142	-1.166
8114425	CDC25C	cell division cycle 25 homolog C (S. pombe)	6.508	5.341	5.345	5.138	-1.167
8012403	AURKB	aurora kinase B	8.526	7.359	7.077	7.291	-1.167
8105067	PTGER4	prostaglandin E receptor 4 (subtype EP4)	9.537	8.370	8.331	8.574	-1.167
7985213	CHRNA5	cholinergic receptor, nicotinic, alpha 5	6.204	5.037	4.800	4.835	-1.168
8025076	VAV1	vav 1 guanine nucleotide exchange factor	10.948	9.780	9.716	9.927	-1.168
8060627	ATRN	attractin	10.807	9.638	9.585	10.008	-1.169
7926410	MRC1	mannose receptor, C type 1	12.421	11.250	11.092	11.669	-1.171
7926451	MRC1	mannose receptor, C type 1	12.421	11.250	11.092	11.669	-1.171
7905349	TNFAIP8L2	tumor necrosis factor, alpha-induced protein 8-like 2	8.279	7.108	6.930	7.075	-1.171
7953844	DDX12	DEAD/H (Asp-Glu-Ala-Asp/His) box polypeptide 12	8.239	7.066	6.947	7.060	-1.173
8023766	RTTN	rotatin	7.072	5.896	5.780	5.932	-1.175
7901192	RAD54L	RAD54-like (S. cerevisiae)	6.607	5.432	5.579	5.193	-1.175
7904482	SRGAP2P2	SLIT-ROBO Rho GTPase activating protein 2 pseudogene 2	10.992	9.817	9.916	10.085	-1.176
8054945	BIN1	bridging integrator 1	9.893	8.713	8.749	8.519	-1.180
7963157	RACGAP1	Rac GTPase activating protein 1	9.483	8.302	8.066	8.216	-1.180
7917576	GBP5	guanylate binding protein 5	6.997	5.816	5.610	5.811	-1.181
7983335	CTDSPL2	CTD (carboxy-terminal domain, RNA polymerase II, polypeptide A) small phosphatase like 2	10.711	9.528	9.289	9.412	-1.183
8066136	RBL1	retinoblastoma-like 1 (p107)	9.477	8.294	8.090	8.278	-1.183
7904293	PTGFRN	prostaglandin F2 receptor negative regulator	9.818	8.635	8.677	9.009	-1.184
8124553	ZKSCAN4	zinc finger with KRAB and SCAN domains 4	7.915	6.730	6.714	6.957	-1.186
7960794	CD163	CD163 molecule	12.283	11.097	10.857	11.465	-1.186
7935011	CPEB3	cytoplasmic polyadenylation element binding protein 3	7.271	6.084	6.133	6.299	-1.187
7969204	WDFY2	WD repeat and FYVE domain containing 2	9.219	8.031	8.023	7.778	-1.188
7945014	CHEK1	CHK1 checkpoint homolog (S. pombe)	9.277	8.088	7.872	7.844	-1.189
7948444	TCN1	transcobalamin I (vitamin B12 binding protein, R binder family)	6.296	5.104	5.120	4.879	-1.192
8117589	HIST1H3H	histone cluster 1, H3h	6.935	5.743	5.672	5.529	-1.192
7968883	C13orf31	chromosome 13 open reading frame 31	11.216	10.024	10.298	10.920	-1.192
8151890	TP53INP1	tumor protein p53 inducible nuclear protein 1	10.608	9.416	9.307	9.626	-1.192
7979281	WDHD1	WD repeat and HMG-box DNA binding protein 1	8.784	7.592	7.407	7.329	-1.192
7980496	C14orf145	chromosome 14 open reading frame 145	7.465	6.272	6.246	6.310	-1.193
7927215	ALOX5	arachidonate 5-lipoxygenase	10.605	9.412	9.369	9.690	-1.194
7910387	RHOU	ras homolog gene family, member U	10.505	9.307	9.121	9.358	-1.198
8117334	HIST1H4A	histone cluster 1, H4a	7.920	6.722	6.425	6.569	-1.199
7919133	FCGR1B	Fc fragment of IgG, high affinity Ib, receptor (CD64)	11.074	9.874	9.046	10.188	-1.200
8149673	REEP4	receptor accessory protein 4	8.969	7.768	7.573	7.940	-1.201
8090133	CCDC14	coiled-coil domain containing 14	7.951	6.748	6.726	7.416	-1.202
8056837	GPR155	G protein-coupled receptor 155	9.905	8.702	8.396	8.847	-1.203
8117020	MYLIP	myosin regulatory light chain interacting protein	8.324	7.119	6.948	7.115	-1.205
7903358	VCAM1	vascular cell adhesion molecule 1	6.640	5.435	5.254	5.430	-1.206
8001197	NETO2	neuropilin (NRP) and tolloid (TLL)-like 2	10.765	9.559	9.345	9.268	-1.206
8043791	INPP4A	inositol polyphosphate-4-phosphatase, type I, 107kDa	9.999	8.792	8.868	9.097	-1.207
8174654	KLHL13	kelch-like 13 (Drosophila)	5.910	4.703	4.717	4.820	-1.207
7940561	FEN1	flap structure-specific endonuclease 1	8.608	7.400	7.511	7.512	-1.207
7901867	USP1	ubiquitin specific peptidase 1	9.212	8.005	7.801	7.882	-1.208
8028104	HCST	hematopoietic cell signal transducer	11.076	9.867	9.945	9.374	-1.209
7972055	KCTD12	potassium channel tetramerisation domain containing 12	11.955	10.746	10.650	10.841	-1.209
8124440	HIST1H3G	histone cluster 1, H3g	7.636	6.425	6.535	6.032	-1.211
8027247	ZNF93	zinc finger protein 93	7.467	6.255	6.041	5.778	-1.212
8084794	IL1RAP	interleukin 1 receptor accessory protein	7.786	6.574	6.383	6.711	-1.212
8057732	TMEM194B	transmembrane protein 194B	7.804	6.590	6.542	6.698	-1.213
8176193	F8	coagulation factor VIII, procoagulant component	7.820	6.607	6.662	6.386	-1.213
8137252	GIMAP1	GTPase, IMAP family member 1	9.144	7.931	7.669	8.066	-1.213
8035793	ZNF737	zinc finger protein 737	8.462	7.248	6.971	7.677	-1.214
8163839	C5	complement component 5	7.227	6.010	5.691	5.831	-1.217
8143684	PDIA4	protein disulfide isomerase family A, member 4	11.077	9.859	9.679	10.299	-1.217
8102751	SCLT1	sodium channel and clathrin linker 1	8.425	7.207	7.167	7.186	-1.218
8117225	GMNN	geminin, DNA replication inhibitor	8.369	7.150	6.726	6.920	-1.218
7905060	FCGR1A	Fc fragment of IgG, high affinity Ia, receptor (CD64)	11.047	9.826	9.002	10.147	-1.220
8041888	MSH6	mutS homolog 6 (E. coli)	8.773	7.553	7.449	7.582	-1.220
8086880	CDC25A	cell division cycle 25 homolog A (S. pombe)	7.330	6.109	6.261	6.155	-1.221
8151898	C8orf37	chromosome 8 open reading frame 37	7.042	5.820	5.796	5.585	-1.222
8056545	STK39	serine threonine kinase 39	8.236	7.012	6.471	6.612	-1.224
8180029	HLA-DQB2	major histocompatibility complex, class II, DQ beta 2	9.696	8.467	8.687	8.652	-1.228
8165735	CSF2RA	colony stimulating factor 2 receptor, alpha, low-affinity (granulocyte-macrophage)	10.112	8.882	8.887	9.285	-1.230
8176306	CSF2RA	colony stimulating factor 2 receptor, alpha, low-affinity (granulocyte-macrophage)	10.112	8.882	8.887	9.285	-1.230
8148124	MTBP	Mdm2, transformed 3T3 cell double minute 2, p53 binding protein (mouse) binding protein, 104kDa	6.444	5.213	5.335	5.435	-1.231
7968637	CCNA1	cyclin A1	9.185	7.954	7.940	7.647	-1.232
8057887	STK17B	serine/threonine kinase 17b	11.215	9.983	9.784	9.830	-1.232
8122843	ESR1	estrogen receptor 1	8.436	7.204	7.094	6.962	-1.232
8057990	ANKRD44	ankyrin repeat domain 44	8.694	7.460	7.364	7.778	-1.233
8109830	CCDC99	coiled-coil domain containing 99	9.297	8.063	7.476	7.666	-1.234
8040440	GEN1	Gen homolog 1, endonuclease (Drosophila)	9.211	7.976	7.703	8.355	-1.234
8066266	MAFB	v-maf musculoaponeurotic fibrosarcoma oncogene homolog B (avian)	11.138	9.903	9.638	10.298	-1.235
8005603	SLC47A1	solute carrier family 47, member 1	9.315	8.079	7.789	8.223	-1.236
7912257	CLSTN1	calsyntenin 1	8.748	7.513	7.431	7.741	-1.236
8145291	SLC25A37	solute carrier family 25, member 37	6.314	5.075	5.247	5.678	-1.239
7948249	SLC43A1	solute carrier family 43, member 1	9.089	7.848	7.707	7.719	-1.241
7972003	KLF12	Kruppel-like factor 12	6.214	4.972	5.011	4.894	-1.242
8113369	SLCO4C1	solute carrier organic anion transporter family, member 4C1	6.776	5.533	5.898	5.681	-1.243
8035628	NR2C2AP	nuclear receptor 2C2-associated protein	7.963	6.718	6.448	6.234	-1.245
7946275	GVINP1	GTPase, very large interferon inducible pseudogene 1	6.567	5.320	5.181	5.167	-1.246
8089701	ZBTB20	zinc finger and BTB domain containing 20	7.538	6.288	6.442	6.541	-1.250
7956076	CDK2	cyclin-dependent kinase 2	9.010	7.759	7.491	7.375	-1.251
8015526	KAT2A	K(lysine) acetyltransferase 2A	9.132	7.880	7.960	8.164	-1.252
8092640	RFC4	replication factor C (activator 1) 4, 37kDa	10.909	9.656	9.460	9.512	-1.253
7909455	TRAF3IP3	TRAF3 interacting protein 3	7.450	6.194	5.968	6.241	-1.255
7940775	RARRES3	retinoic acid receptor responder (tazarotene induced) 3	7.236	5.980	6.146	6.046	-1.256
8003667	SERPINF1	serpin peptidase inhibitor, clade F (alpha-2 antiplasmin, pigment epithelium derived factor), member 1	8.361	7.102	7.064	6.896	-1.259
8147156	WWP1	WW domain containing E3 ubiquitin protein ligase 1	11.981	10.721	10.733	10.506	-1.261
8095574	DCK	deoxycytidine kinase	10.159	8.897	8.471	8.413	-1.262
8161618	APBA1	amyloid beta (A4) precursor protein-binding, family A, member 1	8.610	7.347	7.282	7.346	-1.264
8023415	TCF4	transcription factor 4	10.279	9.013	8.753	9.066	-1.266
7963750	CBX5	chromobox homolog 5	11.264	9.996	9.819	9.662	-1.268
8124437	HIST1H3F	histone cluster 1, H3f	9.588	8.318	8.055	8.544	-1.270
7900167	CDCA8	cell division cycle associated 8	8.088	6.816	6.578	6.520	-1.272

7937533	AP2A2	adaptor-related protein complex 2, alpha 2 subunit	10.305	9.032	8.892	9.067	-1.272
8063785	C20orf197	chromosome 20 open reading frame 197	6.445	5.171	5.227	5.133	-1.274
8152453	TRPS1	trichorhinophalangeal syndrome I	10.472	9.197	9.230	9.415	-1.275
7938035	TRIM22	tripartite motif-containing 22	10.374	9.097	8.843	9.381	-1.277
8072744	NCF4	neutrophil cytosolic factor 4, 40kDa	11.657	10.379	10.655	10.928	-1.278
7953351	NCAPD2	non-SMC condensin I complex, subunit D2	10.116	8.836	8.675	8.714	-1.280
8139033	AOAH	acyloxyacyl hydrolase (neutrophil)	10.616	9.334	9.317	10.003	-1.282
8156026	CEP78	centrosomal protein 78kDa	8.432	7.149	7.036	6.835	-1.283
7965359	ATP2B1	ATPase, Ca++ transporting, plasma membrane 1	10.447	9.161	9.128	9.590	-1.286
8142765	LRRC4	leucine rich repeat containing 4	8.727	7.441	7.262	7.341	-1.286
7914950	CSF3R	colony stimulating factor 3 receptor (granulocyte)	7.881	6.594	6.980	7.321	-1.287
8005839	TMEM97	transmembrane protein 97	10.463	9.175	8.839	8.615	-1.288
7935270	BLNK	B-cell linker	9.924	8.635	8.119	8.620	-1.289
8170027	DDX26B	DEAD/H (Asp-Glu-Ala-Asp/His) box polypeptide 26B	8.192	6.899	6.838	7.147	-1.293
8114593	APBB3	amyloid beta (A4) precursor protein-binding, family B, member 3	8.530	7.227	7.521	8.127	-1.302
8020183	IMPA2	inositol(myo)-1(or 4)-monophosphatase 2	8.427	7.124	7.192	7.214	-1.303
8014241	SLFN12	schlafen family member 12	7.951	6.647	6.191	6.474	-1.304
7998886	PKMYT1	protein kinase, membrane associated tyrosine/threonine 1	8.194	6.890	6.948	6.843	-1.304
7920057	TDRKH	tudor and KH domain containing	9.118	7.813	7.555	7.461	-1.305
7962312	ABCD2	ATP-binding cassette, sub-family D (ALD), member 2	5.781	4.475	4.686	4.389	-1.306
8026051	RNASEH2A	ribonuclease H2, subunit A	8.519	7.212	7.136	7.135	-1.307
8117106	RNF144B	ring finger protein 144B	10.237	8.927	8.834	9.000	-1.310
8131550	SCIN	scinderin	7.882	6.571	6.572	6.453	-1.310
7940153	FAM111A	family with sequence similarity 111, member A	10.179	8.867	8.699	9.066	-1.312
7969243	CKAP2	cytoskeleton associated protein 2	10.308	8.994	8.561	8.750	-1.315
7957962	SPIC	Spi-C transcription factor (Spi-1/PU.1 related)	10.245	8.929	8.173	8.357	-1.316
7994609	QPRT	quinolinate phosphoribosyltransferase	10.591	9.274	9.518	9.525	-1.317
8066074	DSN1	DSN1, MIND kinetochore complex component, homolog (S. cerevisiae)	9.745	8.427	8.110	8.312	-1.319
7942569	SLCO2B1	solute carrier organic anion transporter family, member 2B1	12.327	11.009	10.801	11.364	-1.319
8120165	CENPQ	centromere protein Q	7.801	6.478	6.121	6.210	-1.323
8173745	CYSLTR1	cysteinyl leukotriene receptor 1	10.276	8.952	8.421	9.258	-1.324
7959052	RFC5	replication factor C (activator 1) 5, 36.5kDa	8.373	7.049	6.673	6.986	-1.324
7935660	DNMBP	dynamin binding protein	9.312	7.987	7.926	8.449	-1.325
7919589	HIST2H3D	histone cluster 2, H3d	10.531	9.205	9.278	9.460	-1.326
8014233	SLFN11	schlafen family member 11	10.223	8.897	8.222	8.967	-1.326
7905881	ADAM15	ADAM metallopeptidase domain 15	9.399	8.070	8.126	7.893	-1.329
8117476	BTN3A3	butyrophilin, subfamily 3, member A3	7.838	6.509	6.473	6.747	-1.329
8070129	DONSON	downstream neighbor of SON	9.456	8.126	8.020	7.653	-1.330
8009913	MYO15B	myosin XVB pseudogene	7.859	6.525	7.136	7.247	-1.334
8008784	PRR11	proline rich 11	9.500	8.166	7.615	7.649	-1.335
8113800	FBN2	fibrillin 2	6.784	5.444	5.490	5.445	-1.340
8082003	EAF2	ELL associated factor 2	8.891	7.551	7.509	7.305	-1.340
8175900	ARHGAP4	Rho GTPase activating protein 4	10.370	9.027	9.036	9.388	-1.343
8124524	HIST1H2AK	histone cluster 1, H2ak	8.648	7.304	7.096	7.374	-1.344
8030374	FCGRT	Fc fragment of IgG, receptor, transporter, alpha	12.167	10.822	10.765	11.149	-1.344
7937823	KCNQ1	potassium voltage-gated channel, KQT-like subfamily, member 1	8.932	7.583	7.601	7.390	-1.349
8138466	MACC1	metastasis associated in colon cancer 1	8.621	7.267	7.603	7.545	-1.354
8124806	NRM	nurim (nuclear envelope membrane protein)	9.755	8.401	8.338	8.005	-1.354
7974341	GNG2	guanine nucleotide binding protein (G protein), gamma 2	9.754	8.399	8.155	8.060	-1.355
8008819	YPEL2	yippee-like 2 (Drosophila)	9.772	8.416	8.418	8.148	-1.356
8020495	CABLES1	Cdk5 and Abl enzyme substrate 1	8.092	6.733	6.446	7.294	-1.358
7898809	EPHB2	EPH receptor B2	9.788	8.428	8.452	8.828	-1.360
8020630	TTC39C	tetratricopeptide repeat domain 39C	8.806	7.446	7.269	7.507	-1.360
7908125	RGL1	ral guanine nucleotide dissociation stimulator-like 1	12.105	10.744	10.626	10.852	-1.360
8003844	GSG2	germ cell associated 2 (haspin)	7.254	5.892	5.845	5.777	-1.362
8008185	ABI3	ABI family, member 3	9.310	7.946	8.075	8.182	-1.364
8174207	NXF3	nuclear RNA export factor 3	8.501	7.136	7.040	7.390	-1.365
8125447	HLA-DQB1	major histocompatibility complex, class II, DQ beta 1	8.718	7.349	7.374	7.505	-1.369
7950082	OC10013331!	transient receptor potential cation channel, subfamily C, member 2-like	7.857	6.486	6.415	6.719	-1.371
8012257	TP53	tumor protein p53	10.434	9.061	9.107	8.886	-1.373
8008802	GDPD1	glycerophosphodiester phosphodiesterase domain containing 1	7.408	6.034	5.702	5.920	-1.374
8157534	CEP110	centrosomal protein 110kDa	7.853	6.476	6.225	6.413	-1.377
8178205	HLA-DQA2	major histocompatibility complex, class II, DQ alpha 2	9.099	7.719	7.718	8.001	-1.381
7976621	VRK1	vaccinia related kinase 1	9.315	7.931	7.596	7.640	-1.384
8087485	UBA7	ubiquitin-like modifier activating enzyme 7	9.798	8.409	8.317	8.833	-1.389
8075785	FOXRED2	FAD-dependent oxidoreductase domain containing 2	9.513	8.122	7.883	8.079	-1.390
7942527	POLD3	polymerase (DNA-directed), delta 3, accessory subunit	9.255	7.863	7.604	7.833	-1.391
7918716	SYT6	synaptotagmin VI	8.839	7.447	7.388	7.363	-1.392
8117598	HIST1H4J	histone cluster 1, H4j	9.510	8.117	7.815	7.365	-1.392
8122222	PDE7B	phosphodiesterase 7B	6.187	4.795	4.791	4.722	-1.393
7934026	DNA2	DNA replication helicase 2 homolog (yeast)	7.195	5.801	5.476	6.058	-1.393
8125463	HLA-DQB2	major histocompatibility complex, class II, DQ beta 2	9.588	8.194	8.319	8.460	-1.394
8013616	SLC46A1	solute carrier family 46 (folate transporter), member 1	9.743	8.348	8.057	8.225	-1.395
8114536	TMEM173	transmembrane protein 173	9.701	8.305	8.080	8.156	-1.395
7937330	IFITM2	interferon induced transmembrane protein 2 (1-8D)	9.711	8.315	8.006	8.416	-1.396
8039180	LILRB5	leukocyte immunoglobulin-like receptor, subfamily B (with TM and ITIM domains), member 5	10.879	9.484	9.360	9.850	-1.396
8059838	HJURP	Holliday junction recognition protein	8.428	7.031	6.756	6.966	-1.397
7923426	UBE2T	ubiquitin-conjugating enzyme E2T (putative)	8.336	6.937	6.205	6.100	-1.399
8115147	CD74	CD74 molecule, major histocompatibility complex, class II invariant chain	13.302	11.902	11.893	12.069	-1.400
8118564	HLA-DQA2	major histocompatibility complex, class II, DQ alpha 2	9.111	7.704	7.719	7.971	-1.407
8082350	MCM2	minichromosome maintenance complex component 2	9.028	7.620	7.563	7.417	-1.408
7934459	NDST2	N-deacetylase/N-sulfotransferase (heparan glucosaminyl) 2	10.831	9.423	9.495	9.543	-1.409
8124391	HIST1H2AB	histone cluster 1, H2ab	7.637	6.226	6.246	6.036	-1.411
8009243	C17orf60	chromosome 17 open reading frame 60	10.914	9.501	9.321	9.832	-1.413
7905088	HIST2H2AC	histone cluster 2, H2ac	10.187	8.773	8.518	8.408	-1.414
8087935	NT5DC2	5'-nucleotidase domain containing 2	10.644	9.229	9.180	9.550	-1.415
8096744	CYP2U1	cytochrome P450, family 2, subfamily U, polypeptide 1	7.431	6.013	5.950	5.913	-1.418
8157524	TLR4	toll-like receptor 4	11.971	10.552	10.283	10.865	-1.419
7902913	CDC7	cell division cycle 7 homolog (S. cerevisiae)	6.517	5.092	5.224	5.162	-1.425
8041867	MSH2	mutS homolog 2, colon cancer, nonpolyposis type 1 (E. coli)	7.856	6.430	6.159	6.709	-1.427
8138289	ETV1	ets variant 1	6.238	4.810	4.668	4.610	-1.428
7952830	NCAPD3	non-SMC condensin II complex, subunit D3	9.417	7.987	7.546	8.176	-1.429
7924712	LIN9	lin-9 homolog (C. elegans)	7.101	5.672	5.484	5.332	-1.430
8081386	NFKBIZ	nuclear factor of kappa light polypeptide gene enhancer in B-cells inhibitor, zeta	8.101	6.670	6.540	7.159	-1.431
7905085	HIST2H3A	histone cluster 2, H3a	10.392	8.961	8.953	9.135	-1.431
7919614	HIST2H3A	histone cluster 2, H3a	10.392	8.961	8.953	9.135	-1.431
8083839	GPR160	G protein-coupled receptor 160	7.754	6.322	6.111	5.786	-1.432
7965094	E2F7	E2F transcription factor 7	7.245	5.812	5.771	5.711	-1.433
8136067	TSPAN33	tetraspanin 33	11.116	9.682	9.541	9.110	-1.434
8077851	HRH1	histamine receptor H1	7.447	6.013	5.827	5.800	-1.435
8166525	POLA1	polymerase (DNA directed), alpha 1, catalytic subunit	8.820	7.385	6.902	7.064	-1.435
7938348	WEE1	WEE1 homolog (S. pombe)	8.399	6.964	6.720	6.701	-1.435

8124385	HIST1H4B	histone cluster 1, H4b	8.541	7.105	7.242	6.525	-1.436
8115234	ANXA6	annexin A6	10.997	9.559	9.268	9.279	-1.438
7917503	GBP3	guanylate binding protein 3	7.418	5.976	5.807	5.972	-1.442
8083709	SMC4	structural maintenance of chromosomes 4	9.628	8.181	7.788	8.126	-1.447
7960771	CD163L1	CD163 molecule-like 1	10.592	9.143	9.497	10.041	-1.449
8124413	HIST1H4D	histone cluster 1, H4d	8.273	6.820	6.507	6.611	-1.453
7964145	TIMELESS	timeless homolog (Drosophila)	8.347	6.894	6.572	6.802	-1.453
8045563	ARHGAP15	Rho GTPase activating protein 15	9.141	7.685	7.498	7.594	-1.455
8040712	CENPA	centromere protein A	8.622	7.165	7.516	7.214	-1.457
7898521	IGSF21	immunoglobin superfamily, member 21	10.118	8.660	8.304	8.507	-1.458
7915955	SPATA6	spermatogenesis associated 6	8.005	6.547	6.324	6.490	-1.458
8121563	MARCKS	myristoylated alanine-rich protein kinase C substrate	11.035	9.574	9.481	9.867	-1.462
7902158	TCTEX1D1	Tctex1 domain containing 1	9.115	7.651	7.460	7.918	-1.464
8137250	GIMAP2	GTPase, IMAP family member 2	9.615	8.150	7.740	8.135	-1.466
8019486	SECTM1	secreted and transmembrane 1	9.539	8.072	7.873	8.755	-1.467
7924733	PARP1	poly (ADP-ribose) polymerase 1	10.846	9.379	9.065	9.253	-1.468
8178399	NRM	nurim (nuclear envelope membrane protein)	9.934	8.465	8.369	8.045	-1.469
8179683	NRM	nurim (nuclear envelope membrane protein)	9.934	8.465	8.369	8.045	-1.469
8132819	IKZF1	IKAROS family zinc finger 1 (Ikaros)	9.323	7.852	7.755	7.511	-1.470
8122818	C6orf211	chromosome 6 open reading frame 211	11.014	9.543	9.087	9.185	-1.472
8137257	GIMAP5	GTPase, IMAP family member 5	9.234	7.761	7.241	7.615	-1.473
8082012	SLC15A2	solute carrier family 15 (H+/peptide transporter), member 2	6.356	4.882	5.013	5.079	-1.474
8117429	HIST1H2BI	histone cluster 1, H2bi	5.993	4.519	4.615	4.298	-1.474
8178811	HLA-DRB4	major histocompatibility complex, class II, DR beta 4	12.831	11.356	11.204	11.523	-1.474
7981530	GPR132	G protein-coupled receptor 132	8.622	7.146	7.221	7.449	-1.476
8157691	SKA2	spindle and kinetochore associated complex subunit 2	11.049	9.572	9.193	8.790	-1.477
8112260	DEPDC1B	DEP domain containing 1B	7.368	5.885	5.525	5.874	-1.483
8178802	HLA-DRB3	major histocompatibility complex, class II, DR beta 3	13.030	11.546	11.482	11.740	-1.484
7999387	EMP2	epithelial membrane protein 2	9.080	7.592	7.484	7.258	-1.487
7902874	LRRC8C	leucine rich repeat containing 8 family, member C	9.745	8.257	8.394	8.349	-1.488
7906757	FCGR2A	Fc fragment of IgG, low affinity IIa, receptor (CD32)	12.634	11.141	10.681	11.289	-1.493
8031646	OC10012825	hypothetical LOC100128252	8.603	7.105	7.234	7.082	-1.498
7993664	CP110	CP110 protein	8.488	6.988	6.642	6.529	-1.500
8035896	TSHZ3	teashirt zinc finger homeobox 3	9.756	8.256	7.989	8.205	-1.500
7903393	S1PR1	sphingosine-1-phosphate receptor 1	7.731	6.228	6.177	6.525	-1.502
8117422	HIST1H4F	histone cluster 1, H4f	9.321	7.816	7.450	7.048	-1.505
7924499	TLR5	toll-like receptor 5	8.414	6.906	6.749	7.241	-1.508
7935403	ARHGAP19	Rho GTPase activating protein 19	8.741	7.233	7.030	7.002	-1.508
8180003	HLA-DRB3	major histocompatibility complex, class II, DR beta 3	12.825	11.314	11.174	11.469	-1.511
8025301	CD209	CD209 molecule	8.477	6.965	6.921	7.281	-1.512
7930148	SFXN2	sideroflexin 2	8.079	6.567	6.275	6.622	-1.513
8156982	SMC2	structural maintenance of chromosomes 2	9.308	7.793	7.469	7.873	-1.515
8117580	HIST1H2AI	histone cluster 1, H2ai	8.271	6.755	6.766	6.552	-1.516
8040578	CENPO	centromere protein O	8.704	7.186	7.100	7.230	-1.517
7995354	ORC6	origin recognition complex, subunit 6	7.718	6.199	5.808	5.932	-1.519
8105436	MAP3K1	mitogen-activated protein kinase kinase kinase 1	10.923	9.404	9.219	9.633	-1.519
8124521	HIST1H4K	histone cluster 1, H4k	9.886	8.365	8.091	7.670	-1.521
7932584	PRTFDC1	phosphoribosyl transferase domain containing 1	7.029	5.508	5.267	5.265	-1.522
8118669	KIFC1	kinesin family member C1	7.661	6.139	6.183	6.054	-1.522
8142497	CTTNBP2	cortactin binding protein 2	7.909	6.387	6.445	6.779	-1.523
7943160	SCARNA9	small Cajal body-specific RNA 9	7.241	5.717	6.125	7.784	-1.524
8129763	FAM54A	family with sequence similarity 54, member A	7.450	5.925	5.773	5.586	-1.524
7958031	C12orf48	chromosome 12 open reading frame 48	7.174	5.646	5.190	5.209	-1.528
8089875	POLQ	polymerase (DNA directed), theta	6.725	5.197	5.159	4.935	-1.529
7945132	FLI1	Friend leukemia virus integration 1	10.795	9.261	9.033	9.018	-1.534
8009301	PRKCA	protein kinase C, alpha	9.376	7.839	7.778	7.503	-1.537
8084100	USP13	ubiquitin specific peptidase 13 (isopeptidase T-3)	8.022	6.484	6.349	6.501	-1.538
8002629	PKD1L3	polycystic kidney disease 1-like 3	6.511	4.972	5.028	4.849	-1.539
7929282	HHEX	hematopoietically expressed homeobox	8.450	6.910	6.898	6.705	-1.539
8125436	HLA-DRB5	major histocompatibility complex, class II, DR beta 5	8.245	6.702	6.699	7.138	-1.543
8151824	RAD54B	RAD54 homolog B (S. cerevisiae)	7.047	5.503	5.159	5.140	-1.544
7941214	POLA2	polymerase (DNA directed), alpha 2 (70kD subunit)	8.766	7.222	6.830	7.272	-1.544
8175177	MBNL3	muscleblind-like 3 (Drosophila)	10.400	8.853	8.821	8.852	-1.547
8171136	P2RY8	purinergic receptor P2Y, G-protein coupled, 8	7.936	6.389	6.299	6.248	-1.547
8177026	P2RY8	purinergic receptor P2Y, G-protein coupled, 8	7.936	6.389	6.299	6.248	-1.547
7901010	KIF2C	kinesin family member 2C	7.842	6.293	6.200	6.240	-1.549
8171381	FANCB	Fanconi anemia, complementation group B	6.976	5.427	5.292	5.091	-1.549
8064716	SIGLEC1	sialic acid binding Ig-like lectin 1, sialoadhesin	10.915	9.365	9.295	9.988	-1.550
7994620	KIF22	kinesin family member 22	8.726	7.173	6.981	7.107	-1.553
8143663	EZH2	enhancer of zeste homolog 2 (Drosophila)	9.359	7.802	7.366	7.586	-1.557
8160346	PTPLAD2	protein tyrosine phosphatase-like A domain containing 2	10.289	8.732	8.348	8.597	-1.558
8138805	CPVL	carboxypeptidase, vitellogenic-like	10.618	9.059	8.751	9.632	-1.559
8118324	C2	complement component 2	9.188	7.622	7.535	7.786	-1.566
8128698	SESN1	sestrin 1	9.859	8.292	8.141	8.284	-1.567
8093500	TACC3	transforming, acidic coiled-coil containing protein 3	8.759	7.191	7.240	7.152	-1.568
8080320	NISCH	nischarin	10.042	8.464	8.644	9.159	-1.578
8149955	PBK	PDZ binding kinase	6.216	4.637	4.544	4.528	-1.579
8124416	HIST1H3D	histone cluster 1, H3d	11.063	9.481	9.282	9.196	-1.582
8113504	C5orf13	chromosome 5 open reading frame 13	8.030	6.443	6.559	6.589	-1.587
8101762	SNCA	synuclein, alpha (non A4 component of amyloid precursor)	10.447	8.860	8.191	8.388	-1.587
8126839	TNFRSF21	tumor necrosis factor receptor superfamily, member 21	10.858	9.269	9.333	9.633	-1.588
7951408	CARD16	caspase recruitment domain family, member 16	7.912	6.323	5.936	6.321	-1.589
8178193	HLA-DRA	major histocompatibility complex, class II, DR alpha	13.315	11.722	11.497	12.031	-1.594
8178095	C2	complement component 2	9.209	7.612	7.505	7.775	-1.597
8179331	C2	complement component 2	9.209	7.612	7.505	7.775	-1.597
7901123	NASP	nuclear autoantigenic sperm protein (histone-binding)	8.475	6.876	6.743	6.818	-1.599
8162601	ZNF367	zinc finger protein 367	8.922	7.321	6.957	6.926	-1.601
8103399	PDGFC	platelet derived growth factor C	9.107	7.504	7.210	8.189	-1.603
8125461	HLA-DQB1	major histocompatibility complex, class II, DQ beta 1	6.900	5.290	5.584	5.358	-1.610
8024792	EBI3	Epstein-Barr virus induced 3	8.409	6.798	6.496	6.927	-1.610
7903565	GPSM2	G-protein signaling modulator 2	8.335	6.724	6.579	6.671	-1.611
7948364	MPEG1	macrophage expressed 1	12.680	11.067	11.113	11.690	-1.613
8160935	FANCG	Fanconi anemia, complementation group G	8.379	6.764	6.802	6.838	-1.614
7957126	KCNMB4	potassium large conductance calcium-activated channel, subfamily M, beta member 4	8.616	7.001	7.018	7.071	-1.616
8066431	ADA	adenosine deaminase	10.095	8.478	8.201	8.555	-1.617
7939173	DEPDC7	DEP domain containing 7	7.683	6.064	5.999	6.120	-1.619
8114780	PCDH12	protocadherin 12	7.272	5.652	5.761	5.743	-1.620
8056102	CD302	CD302 molecule	12.980	11.359	11.072	11.529	-1.621
8113551	MCC	mutated in colorectal cancers	7.715	6.093	6.192	6.324	-1.623
8096602	DAPP1	dual adaptor of phosphotyrosine and 3-phosphoinositides	8.910	7.284	7.330	7.579	-1.626
7964347	TMEM194A	transmembrane protein 194A	9.794	8.168	7.947	8.154	-1.626
8044813	TMEM37	transmembrane protein 37	10.888	9.262	8.471	9.455	-1.626

7929145	HECTD2	HECT domain containing 2	8.605	6.975	6.718	6.834	-1.630
8175393	ARHGEF6	Rac/Cdc42 guanine nucleotide exchange factor (GEF) 6	10.312	8.682	8.606	8.655	-1.631
7971661	MIR15A	microRNA 15a	7.194	5.561	5.697	6.473	-1.633
8045009	GYPC	glycophorin C (Gerbich blood group)	10.947	9.311	9.208	8.669	-1.636
8122637	SASH1	SAM and SH3 domain containing 1	10.073	8.428	8.658	8.472	-1.644
8118556	HLA-DQA1	major histocompatibility complex, class II, DQ alpha 1	11.024	9.380	9.287	9.600	-1.645
8072687	MCM5	minichromosome maintenance complex component 5	10.047	8.401	7.820	8.078	-1.645
7949364	CDCA5	cell division cycle associated 5	7.887	6.238	5.923	5.675	-1.649
7916167	ORC1	origin recognition complex, subunit 1	7.832	6.180	6.017	6.044	-1.651
7951535	KDELC2	KDEL (Lys-Asp-Glu-Leu) containing 2	8.655	7.001	6.620	6.822	-1.654
8150002	FBXO16	F-box protein 16	7.174	5.520	5.387	5.100	-1.654
8003583	KIF22	kinesin family member 22	8.671	7.016	6.914	7.083	-1.655
8135378	PRKAR2B	protein kinase, cAMP-dependent, regulatory, type II, beta	8.245	6.589	6.211	6.160	-1.656
7915787	PIK3R3	phosphoinositide-3-kinase, regulatory subunit 3 (gamma)	8.512	6.854	6.483	6.830	-1.657
7926896	CKS1B	CDC28 protein kinase regulatory subunit 1B	10.878	9.219	8.691	8.696	-1.659
7997712	IRF8	interferon regulatory factor 8	10.743	9.078	8.952	9.532	-1.664
7933707	ZWINT	ZW10 interactor	9.329	7.663	7.308	7.358	-1.666
8055426	MCM6	minichromosome maintenance complex component 6	9.984	8.316	7.790	7.949	-1.668
8011826	C17orf87	chromosome 17 open reading frame 87	10.677	9.005	8.555	9.586	-1.672
8148059	DEPDC6	DEP domain containing 6	9.414	7.742	7.407	7.130	-1.672
7959408	KNTC1	kinetochore associated 1	8.464	6.792	6.457	6.978	-1.673
7907183	SCYL3	SCY1-like 3 (S. cerevisiae)	8.706	7.030	6.628	6.939	-1.676
7964271	PRIM1	primase, DNA, polypeptide 1 (49kDa)	9.685	8.005	7.463	7.353	-1.680
8107194	C5orf30	chromosome 5 open reading frame 30	9.620	7.940	7.624	7.467	-1.680
7973110	RNASE2	ribonuclease, RNase A family, 2 (liver, eosinophil-derived neurotoxin)	7.800	6.116	6.075	6.110	-1.684
8103508	40969	membrane-associated ring finger (C3HC4) 1	10.832	9.146	8.896	9.289	-1.686
8102862	MAML3	mastermind-like 3 (Drosophila)	8.270	6.579	6.438	6.672	-1.691
8089372	KIAA1524	KIAA1524	8.446	6.748	6.400	6.835	-1.698
8112327	CKS1B	CDC28 protein kinase regulatory subunit 1B	11.082	9.384	8.875	8.833	-1.698
8065353	THBD	thrombomodulin	9.999	8.299	8.437	9.083	-1.700
8064844	PCNA	proliferating cell nuclear antigen	10.256	8.556	8.107	8.304	-1.700
8104570	FAM105A	family with sequence similarity 105, member A	10.472	8.770	8.289	8.372	-1.702
8117583	HIST1H2AI	histone cluster 1, H2ai	8.801	7.098	7.118	6.750	-1.703
8101728	FAM13A	family with sequence similarity 13, member A	8.641	6.937	7.082	7.363	-1.704
8179481	HLA-DRA	major histocompatibility complex, class II, DR alpha	13.090	11.383	11.204	11.604	-1.707
8110562	LTC4S	leukotriene C4 synthase	9.248	7.540	7.818	7.323	-1.708
8035838	ZNF724P	zinc finger protein 724, pseudogene	8.033	6.325	6.274	6.884	-1.708
8112478	NAIP	NLR family, apoptosis inhibitory protein	12.173	10.461	10.245	11.101	-1.712
7906061	SYT11	synaptotagmin XI	9.296	7.580	7.573	7.615	-1.716
7988644	ATP8B4	ATPase, class I, type 8B, member 4	11.009	9.285	9.157	9.830	-1.724
7966089	CMKLR1	chemokine-like receptor 1	11.241	9.514	9.677	10.015	-1.726
8160260	BNC2	basonuclin 2	8.709	6.981	6.973	7.358	-1.727
8102371	C4orf21	chromosome 4 open reading frame 21	7.008	5.277	5.320	5.551	-1.731
8117395	HIST1H2BF	histone cluster 1, H2bf	10.424	8.691	7.894	7.723	-1.733
8047288	SGOL2	shugoshin-like 2 (S. pombe)	8.371	6.628	6.102	6.574	-1.743
8178199	HLA-DQA1	major histocompatibility complex, class II, DQ alpha 1	13.060	11.313	11.187	11.565	-1.746
8179489	HLA-DQA1	major histocompatibility complex, class II, DQ alpha 1	13.060	11.313	11.187	11.565	-1.746
8119132	FGD2	FYVE, RhoGEF and PH domain containing 2	8.689	6.941	7.082	7.361	-1.749
8125556	HLA-DPA1	major histocompatibility complex, class II, DP alpha 1	12.100	10.349	10.117	10.590	-1.751
8178891	HLA-DPA1	major histocompatibility complex, class II, DP alpha 1	12.100	10.349	10.117	10.590	-1.751
8056113	LY75	lymphocyte antigen 75	8.740	6.978	7.064	7.725	-1.763
7952601	ETS1	v-ets erythroblastosis virus E26 oncogene homolog 1 (avian)	8.605	6.842	6.830	6.489	-1.763
8116734	LY86	lymphocyte antigen 86	11.200	9.436	8.897	9.647	-1.764
8118548	HLA-DRA	major histocompatibility complex, class II, DR alpha	13.034	11.270	11.025	11.535	-1.764
7929344	GPR120	G protein-coupled receptor 120	8.953	7.187	6.906	7.277	-1.766
7961166	KLRC4	killer cell lectin-like receptor subfamily C, member 4	5.910	4.141	4.229	4.111	-1.769
7939150	PRRG4	proline rich Gla (G-carboxyglutamic acid) 4 (transmembrane)	8.263	6.490	6.620	6.425	-1.773
8112521	NAIP	NLR family, apoptosis inhibitory protein	11.650	9.876	9.704	10.514	-1.774
8177527	NAIP	NLR family, apoptosis inhibitory protein	11.650	9.876	9.704	10.514	-1.774
8127031	MCM3	minichromosome maintenance complex component 3	10.011	8.235	7.938	7.956	-1.777
7951397	CASP1	caspase 1, apoptosis-related cysteine peptidase (interleukin 1, beta, convertase)	10.400	8.620	8.358	8.658	-1.780
8006237	LOC400590	hypothetical LOC400590	9.686	7.899	8.458	8.763	-1.787
7987636	OIP5	Opa interacting protein 5	7.509	5.720	5.798	5.636	-1.789
7926259	MCM10	minichromosome maintenance complex component 10	8.455	6.664	6.263	6.100	-1.790
8104912	SKP2	S-phase kinase-associated protein 2 (p45)	10.093	8.301	8.181	8.024	-1.791
8068593	ETS2	v-ets erythroblastosis virus E26 oncogene homolog 2 (avian)	10.855	9.063	9.061	9.188	-1.792
7924096	NEK2	NIMA (never in mitosis gene a)-related kinase 2	7.258	5.456	5.634	5.511	-1.802
7972157	EDNRB	endothelin receptor type B	9.946	8.142	8.120	8.528	-1.804
8017133	SKA2	spindle and kinetochore associated complex subunit 2	9.877	8.072	7.834	7.001	-1.805
7963770	GPR84	G protein-coupled receptor 84	10.466	8.655	8.242	9.117	-1.811
8117368	HIST1H4C	histone cluster 1, H4c	11.404	9.590	8.769	8.731	-1.814
7975268	ARG2	arginase, type II	8.685	6.868	6.620	6.466	-1.817
8178826	HLA-DQB1	major histocompatibility complex, class II, DQ beta 1	10.566	8.747	8.831	9.079	-1.820
8180022	HLA-DQB1	major histocompatibility complex, class II, DQ beta 1	10.566	8.747	8.831	9.079	-1.820
8012896	PMP22	peripheral myelin protein 22	11.866	10.044	10.138	10.222	-1.821
7914851	CLSPN	claspin	7.642	5.818	5.435	5.728	-1.824
8077731	FANCD2	Fanconi anemia, complementation group D2	8.580	6.755	6.336	6.664	-1.825
8115756	KCNMB1	potassium large conductance calcium-activated channel, subfamily M, beta member 1	8.050	6.224	6.417	6.236	-1.827
8124307	CMAH	cytidine monophosphate-N-acetylneuraminic acid hydroxylase (CMP-N-acetylneuraminate monooxyger	7.464	5.638	5.608	5.682	-1.827
8128329	MMS22L	MMS22-like, DNA repair protein	8.232	6.404	5.875	6.125	-1.828
8058695	BARD1	BRCA1 associated RING domain 1	8.668	6.838	6.520	6.236	-1.830
7915926	STIL	SCL/TAL1 interrupting locus	8.844	7.012	6.755	7.063	-1.832
7942372	FOLR2	folate receptor 2 (fetal)	12.430	10.598	10.302	10.506	-1.832
8138489	CDCA7L	cell division cycle associated 7-like	9.024	7.190	6.685	7.168	-1.834
7971565	LPAR6	lysophosphatidic acid receptor 6	11.344	9.507	9.578	10.595	-1.837
8117330	HIST1H3A	histone cluster 1, H3a	8.385	6.547	6.031	6.163	-1.837
8124166	MBOAT1	membrane bound O-acyltransferase domain containing 1	11.063	9.219	8.700	9.240	-1.843
7970329	GAS6	growth arrest-specific 6	8.184	6.334	6.565	6.420	-1.850
8092726	CLDN1	claudin 1	8.669	6.818	6.626	6.676	-1.851
8163807	PHF19	PHD finger protein 19	8.683	6.828	7.210	6.975	-1.856
8180100	HLA-DPA1	major histocompatibility complex, class II, DP alpha 1	12.335	10.477	10.298	10.795	-1.858
8002969	MAF	v-maf musculoaponeurotic fibrosarcoma oncogene homolog (avian)	10.032	8.164	7.910	8.397	-1.868
7942409	P2RY6	pyrimidinergic receptor P2Y, G-protein coupled, 6	9.267	7.396	7.580	7.635	-1.871
7968563	RFC3	replication factor C (activator 1) 3, 38kDa	9.769	7.887	7.200	7.006	-1.883
8039928	FAM72D	family with sequence similarity 72, member D	8.881	6.979	6.787	7.006	-1.902
7911178	NLRP3	NLR family, pyrin domain containing 3	8.878	6.975	6.830	7.075	-1.903
7940421	PGA3	pepsinogen 3, group I (pepsinogen A)	11.277	9.373	8.619	8.388	-1.905
7957338	SYT1	synaptotagmin I	10.624	8.714	8.386	8.800	-1.909
8092578	ETV5	ets variant 5	11.531	9.613	9.321	9.386	-1.917
8166919	GPR82	G protein-coupled receptor 82	9.867	7.949	7.883	8.671	-1.918
8036136	TMEM149	transmembrane protein 149	10.384	8.465	8.676	8.629	-1.919
7966878	CIT	citron (rho-interacting, serine/threonine kinase 21)	8.357	6.434	6.221	6.354	-1.922

8060813	MCM8	minichromosome maintenance complex component 8	9.823	7.900	7.550	7.745	-1.923
8112615	ENC1	ectodermal-neural cortex 1 (with BTB-like domain)	8.452	6.529	6.034	6.304	-1.923
7994769	CORO1A	coronin, actin binding protein, 1A	12.300	10.377	10.116	9.984	-1.924
8074237	CECR1	cat eye syndrome chromosome region, candidate 1	11.843	9.919	10.054	10.615	-1.924
8137232	GIMAP8	GTPase, IMAP family member 8	8.810	6.878	6.716	7.240	-1.932
8011724	VMO1	vitelline membrane outer layer 1 homolog (chicken)	8.670	6.732	6.505	6.473	-1.937
7965423	BTG1	B-cell translocation gene 1, anti-proliferative	11.099	9.160	8.906	8.908	-1.939
8102389	C4orf21	chromosome 4 open reading frame 21	7.124	5.179	4.958	5.398	-1.945
7986195	SV2B	synaptic vesicle glycoprotein 2B	7.918	5.967	5.726	5.762	-1.951
7940441	PGA5	pepsinogen 5, group I (pepsinogen A)	11.067	9.110	8.333	8.096	-1.957
7909146	FAM72D	family with sequence similarity 72, member D	8.969	7.006	6.820	7.064	-1.963
7904452	FAM72D	family with sequence similarity 72, member D	8.966	7.003	6.793	7.048	-1.963
7991777	C4orf46	chromosome 4 open reading frame 46	9.065	7.101	6.120	6.884	-1.965
7940431	PGA4	pepsinogen 4, group I (pepsinogen A)	11.230	9.263	8.496	8.317	-1.967
7919591	FAM72D	family with sequence similarity 72, member D	8.563	6.595	6.225	6.140	-1.968
8144153	NCAPG2	non-SMC condensin II complex, subunit G2	8.598	6.625	6.313	6.291	-1.974
7986068	BLM	Bloom syndrome, RecQ helicase-like	8.663	6.688	6.109	6.134	-1.974
7961069	CLECL1	C-type lectin-like 1	7.824	5.844	5.558	5.829	-1.980
8101449	HPSE	heparanase	9.533	7.553	7.157	7.851	-1.981
8048717	SGPP2	sphingosine-1-phosphate phosphatase 2	8.589	6.606	7.388	7.402	-1.983
8168146	KIF4A	kinesin family member 4A	7.017	5.025	4.876	5.657	-1.992
8104234	TRIP13	thyroid hormone receptor interactor 13	8.556	6.560	6.110	6.052	-1.996
8006968	GSDMA	gasdermin A	10.562	8.559	7.942	8.109	-2.003
7981068	SERPINA1	serpin peptidase inhibitor, clade A (alpha-1 antiproteinase, antitrypsin), member 1	9.143	7.131	7.102	7.547	-2.012
8021286	C18orf54	chromosome 18 open reading frame 54	6.757	4.727	4.560	4.522	-2.029
7971486	C13orf18	chromosome 13 open reading frame 18	7.908	5.879	5.536	5.628	-2.029
7971866	DIAPH3	diaphanous homolog 3 (Drosophila)	7.448	5.417	5.529	5.538	-2.031
8098611	TLR3	toll-like receptor 3	8.980	6.939	6.740	7.164	-2.041
7898799	C1QC	complement component 1, q subcomponent, C chain	13.102	11.061	10.895	11.374	-2.041
7980438	SPTLC2	serine palmitoyltransferase, long chain base subunit 2	10.200	8.154	8.206	8.294	-2.046
8102560	MAD2L1	MAD2 mitotic arrest deficient-like 1 (yeast)	8.199	6.151	6.026	6.197	-2.048
8130408	IPCEF1	interaction protein for cytohesin exchange factors 1	9.103	7.051	6.609	6.709	-2.052
8006187	ATAD5	ATPase family, AAA domain containing 5	8.266	6.200	5.771	6.352	-2.067
8115397	C5orf4	chromosome 5 open reading frame 4	8.815	6.729	6.458	6.807	-2.086
8045688	TNFAIP6	tumor necrosis factor, alpha-induced protein 6	8.202	6.113	6.029	6.500	-2.089
7916862	WLS	wntless homolog (Drosophila)	11.170	9.079	8.735	9.390	-2.091
8155214	MELK	maternal embryonic leucine zipper kinase	9.130	7.026	6.399	6.492	-2.104
8124394	HIST1H2BB	histone cluster 1, H2bb	7.859	5.752	5.247	5.275	-2.107
8140556	HGF	hepatocyte growth factor (hepapoietin A; scatter factor)	7.530	5.416	5.183	5.087	-2.114
8018849	TK1	thymidine kinase 1, soluble	9.825	7.709	7.153	6.933	-2.116
8091757	TRIM59	tripartite motif-containing 59	7.343	5.226	5.306	5.228	-2.117
8135734	C7orf58	chromosome 7 open reading frame 58	9.410	7.292	7.679	7.756	-2.118
7908351	PLA2G4A	phospholipase A2, group IVA (cytosolic, calcium-dependent)	9.417	7.296	7.208	8.003	-2.121
8179519	HLA-DPB1	major histocompatibility complex, class II, DP beta 1	12.619	10.496	10.552	10.571	-2.123
7910997	EXO1	exonuclease 1	8.520	6.397	6.001	5.914	-2.123
7982358	ARHGAP11A	Rho GTPase activating protein 11A	8.453	6.327	5.541	5.496	-2.126
8146357	MCM4	minichromosome maintenance complex component 4	9.820	7.690	7.012	7.025	-2.130
7988414	GATM	glycine amidinotransferase (L-arginine:glycine amidinotransferase)	11.755	9.623	9.122	9.605	-2.132
8083223	C3orf58	chromosome 3 open reading frame 58	9.311	7.175	7.163	7.094	-2.136
8143781	GIMAP6	GTPase, IMAP family member 6	9.274	7.128	6.757	6.821	-2.146
7901788	NFIA	nuclear factor I/A	9.094	6.945	6.372	6.654	-2.149
8118594	HLA-DPB1	major histocompatibility complex, class II, DP beta 1	12.515	10.362	10.422	10.426	-2.153
8132347	GPR141	G protein-coupled receptor 141	9.483	7.315	7.413	7.590	-2.168
8061471	GINS1	GINS complex subunit 1 (Psf1 homolog)	9.699	7.520	6.786	6.973	-2.180
7947248	KIF18A	kinesin family member 18A	7.388	5.205	4.841	4.980	-2.183
8141459	GAL3ST4	galactose-3-O-sulfotransferase 4	9.104	6.917	7.129	7.018	-2.187
7978272	CIDEB	cell death-inducing DFFA-like effector b	8.697	6.508	6.367	6.496	-2.190
8124534	HIST1H4L	histone cluster 1, H4l	10.901	8.711	8.056	7.659	-2.190
7994109	PLK1	polo-like kinase 1	9.848	7.656	7.048	7.274	-2.193
8145418	CDCA2	cell division cycle associated 2	7.772	5.576	5.492	5.271	-2.197
7982792	RAD51	RAD51 homolog (RecA homolog, E. coli) (S. cerevisiae)	8.616	6.418	5.492	6.114	-2.199
8173287	VSIG4	V-set and immunoglobulin domain containing 4	12.764	10.549	9.985	10.609	-2.215
7951077	SESN3	sestrin 3	11.201	8.979	8.819	8.590	-2.222
8178220	HLA-DPB1	major histocompatibility complex, class II, DP beta 1	13.075	10.852	10.838	10.858	-2.222
7969986	TNFSF13B	tumor necrosis factor (ligand) superfamily, member 13b	10.737	8.502	8.555	8.447	-2.236
8140463	FGL2	fibrinogen-like 2	9.067	6.828	6.542	7.047	-2.239
8117426	HIST1H2BH	histone cluster 1, H2bh	11.438	9.193	8.763	8.842	-2.246
8012605	GAS7	growth arrest-specific 7	10.577	8.326	8.522	8.783	-2.251
8085754	SGOL1	shugoshin-like 1 (S. pombe)	8.719	6.466	5.665	5.331	-2.253
8013671	SPAG5	sperm associated antigen 5	8.537	6.283	5.921	6.531	-2.253
8068478	CHAF1B	chromatin assembly factor 1, subunit B (p60)	8.561	6.306	5.986	6.120	-2.255
8124527	HIST1H1B	histone cluster 1, H1b	8.916	6.656	5.938	6.330	-2.260
7983306	WDR76	WD repeat domain 76	10.156	7.895	7.233	7.255	-2.261
8027862	FFAR2	free fatty acid receptor 2	8.033	5.766	5.704	5.662	-2.267
8069541	SAMSN1	SAM domain, SH3 domain and nuclear localization signals 1	10.126	7.852	7.389	8.187	-2.274
7943892	NCAM1	neural cell adhesion molecule 1	8.153	5.877	5.653	5.843	-2.277
8093858	STK32B	serine/threonine kinase 32B	7.504	5.224	5.757	5.149	-2.280
8102076	CENPE	centromere protein E, 312kDa	8.026	5.745	5.368	5.730	-2.281
7985873	C15orf42	chromosome 15 open reading frame 42	8.449	6.167	5.909	5.880	-2.282
8096808	CCDC109B	coiled-coil domain containing 109B	10.550	8.267	7.631	8.069	-2.283
7919612	HIST2H3D	histone cluster 2, H3d	10.769	8.479	7.902	8.385	-2.289
8151101	MYBL1	v-myb myeloblastosis viral oncogene homolog (avian)-like 1	6.994	4.702	4.509	4.478	-2.292
8024900	UHRF1	ubiquitin-like with PHD and ring finger domains 1	9.274	6.975	6.736	6.389	-2.299
8071036	S100B	S100 calcium binding protein B	9.204	6.904	6.665	6.664	-2.300
8152668	ATAD2	ATPase family, AAA domain containing 2	9.072	6.771	6.123	6.393	-2.300
7929438	HELLS	helicase, lymphoid-specific	7.710	5.395	4.867	4.959	-2.316
7985829	FANCI	Fanconi anemia, complementation group I	9.107	6.783	6.284	6.684	-2.325
7983969	CCNB2	cyclin B2	8.771	6.438	5.704	6.403	-2.333
8141395	MCM7	minichromosome maintenance complex component 7	10.240	7.906	7.481	7.655	-2.334
8107706	LMNB1	lamin B1	8.512	6.169	6.219	6.399	-2.344
8062766	MYBL2	v-myb myeloblastosis viral oncogene homolog (avian)-like 2	9.398	7.053	6.455	6.585	-2.345
7916898	DEPDC1	DEP domain containing 1	7.654	5.307	5.319	5.505	-2.346
8060997	SPTLC3	serine palmitoyltransferase, long chain base subunit 3	8.672	6.321	5.839	6.186	-2.351
8123609	SERPINB9	serpin peptidase inhibitor, clade B (ovalbumin), member 9	10.067	7.715	7.731	7.679	-2.352
8118086	TCF19	transcription factor 19	9.178	6.823	6.817	6.330	-2.355
8177947	TCF19	transcription factor 19	9.178	6.823	6.817	6.330	-2.355
8143441	KIAA1147	KIAA1147	10.145	7.782	7.378	8.038	-2.363
8038899	FPR1	formyl peptide receptor 1	8.850	6.487	6.619	6.559	-2.363
8179228	TCF19	transcription factor 19	9.208	6.841	6.840	6.516	-2.367
8046333	CYBRD1	cytochrome b reductase 1	10.999	8.629	8.593	8.541	-2.370
8071212	CDC45	cell division cycle 45 homolog (S. cerevisiae)	9.099	6.718	6.660	6.626	-2.382
8131339	FSCN1	fascin homolog 1, actin-bundling protein (Strongylocentrotus purpuratus)	11.608	9.226	9.155	9.196	-2.382

7923189	KIF14	kinesin family member 14	7.932	5.548	5.345	5.408	-2.384
8103932	MLF1IP	MLF1 interacting protein	8.466	6.082	5.296	5.275	-2.384
8130374	FBXO5	F-box protein 5	9.811	7.405	7.278	7.034	-2.406
8179564	KIFC1	kinesin family member C1	8.083	5.674	6.036	6.013	-2.409
7898793	C1QA	complement component 1, q subcomponent, A chain	11.127	8.713	8.371	8.639	-2.414
8078619	ITGA9	integrin, alpha 9	9.308	6.889	6.692	6.821	-2.419
8075118	CRYBB1	crystallin, beta B1	9.751	7.331	7.277	6.956	-2.420
8168794	CENPI	centromere protein I	8.726	6.301	5.558	5.543	-2.426
8023497	ATP8B1	ATPase, aminophospholipid transporter, class I, type 8B, member 1	10.267	7.837	7.587	8.074	-2.430
7984540	KIF23	kinesin family member 23	8.916	6.479	6.161	6.275	-2.437
8091260	SLC9A9	solute carrier family 9 (sodium/hydrogen exchanger), member 9	11.776	9.336	9.183	9.847	-2.439
8144036	XRCC2	X-ray repair complementing defective repair in Chinese hamster cells 2	8.643	6.199	5.306	5.629	-2.443
8097857	MND1	meiotic nuclear divisions 1 homolog (S. cerevisiae)	7.243	4.793	4.618	4.420	-2.450
8003204	GINS2	GINS complex subunit 2 (Psf2 homolog)	10.651	8.198	7.011	7.761	-2.453
8097867	KIAA0922	KIAA0922	8.244	5.790	5.611	5.484	-2.454
8073062	APOBEC3B	apolipoprotein B mRNA editing enzyme, catalytic polypeptide-like 3B	9.777	7.309	6.426	7.155	-2.468
7978846	POLE2	polymerase (DNA directed), epsilon 2 (p59 subunit)	8.206	5.732	5.283	5.184	-2.474
8082673	ACPP	acid phosphatase, prostate	9.105	6.631	6.585	6.754	-2.474
8015769	BRCA1	breast cancer 1, early onset	8.709	6.228	6.040	5.944	-2.480
8102643	CCNA2	cyclin A2	9.580	7.099	6.363	6.347	-2.481
7918533	ADORA3	adenosine A3 receptor	10.693	8.205	7.622	8.488	-2.488
8007071	CDC6	cell division cycle 6 homolog (S. cerevisiae)	9.332	6.827	5.736	5.445	-2.504
7953218	RAD51AP1	RAD51 associated protein 1	8.818	6.311	5.951	5.710	-2.507
8040223	RRM2	ribonucleotide reductase M2	9.995	7.479	6.259	6.519	-2.516
8113039	MEF2C	myocyte enhancer factor 2C	12.198	9.678	9.181	9.216	-2.520
8112428	CD180	CD180 molecule	10.704	8.181	7.430	8.450	-2.523
8137240	GIMAP7	GTPase, IMAP family member 7	9.282	6.741	6.656	6.639	-2.541
8100179	NFXL1	nuclear transcription factor, X-box binding-like 1	9.135	6.593	6.535	6.883	-2.541
7909708	CENPF	centromere protein F, 350/400kDa (mitosin)	8.426	5.882	5.767	5.906	-2.544
8084717	ST6GAL1	ST6 beta-galactosamide alpha-2,6-sialyltranferase 1	11.224	8.660	8.215	8.779	-2.564
8124531	HIST1H3I	histone cluster 1, H3i	12.543	9.950	9.612	9.212	-2.593
8092169	TNFSF10	tumor necrosis factor (ligand) superfamily, member 10	9.927	7.325	6.943	7.199	-2.602
8054580	BUB1	budding uninhibited by benzimidazoles 1 homolog (yeast)	9.149	6.543	6.024	6.039	-2.606
7929078	KIF20B	kinesin family member 20B	8.354	5.742	5.254	5.755	-2.612
8098423	NEIL3	nei endonuclease VIII-like 3 (E. coli)	8.149	5.537	5.214	5.175	-2.612
7900699	CDC20	cell division cycle 20 homolog (S. cerevisiae)	9.030	6.418	6.455	6.514	-2.612
8080344	STAB1	stabilin 1	12.477	9.838	10.206	10.734	-2.638
8120838	TTK	TTK protein kinase	7.946	5.297	4.516	4.649	-2.650
8109712	HMMR	hyaluronan-mediated motility receptor (RHAMM)	7.677	5.025	4.746	4.763	-2.652
8067040	NFATC2	nuclear factor of activated T-cells, cytoplasmic, calcineurin-dependent 2	8.339	5.681	5.743	5.770	-2.658
8023361	MRO	maestro	9.782	7.090	6.551	7.433	-2.692
8112376	CENPK	centromere protein K	9.529	6.834	5.781	6.347	-2.695
7982663	BUB1B	budding uninhibited by benzimidazoles 1 homolog beta (yeast)	8.797	6.080	5.208	5.679	-2.717
7989146	MNS1	meiosis-specific nuclear structural 1	8.410	5.680	5.398	5.325	-2.730
8019857	NDC80	NDC80 homolog, kinetochore complex component (S. cerevisiae)	7.963	5.232	5.269	5.354	-2.731
7919642	HIST2H2AB	histone cluster 2, H2ab	10.422	7.682	7.421	7.208	-2.740
7929511	ENTPD1	ectonucleoside triphosphate diphosphohydrolase 1	11.268	8.526	8.456	8.692	-2.742
7898805	C1QB	complement component 1, q subcomponent, B chain	11.796	9.051	8.760	9.194	-2.745
8163629	TNFSF8	tumor necrosis factor (ligand) superfamily, member 8	11.271	8.523	8.453	8.118	-2.748
7982757	CASC5	cancer susceptibility candidate 5	8.849	6.099	5.625	5.845	-2.750
7970513	SKA3	spindle and kinetochore associated complex subunit 3	8.871	6.118	5.480	5.374	-2.753
7974404	CDKN3	cyclin-dependent kinase inhibitor 3	8.436	5.675	5.200	5.385	-2.761
8097356	PLK4	polo-like kinase 4	8.645	5.883	5.356	5.619	-2.762
7947110	E2F8	E2F transcription factor 8	8.934	6.167	5.596	5.787	-2.766
8103728	HMGB2	high-mobility group box 2	8.122	5.338	5.178	5.829	-2.785
8054702	CKAP2L	cytoskeleton associated protein 2-like	8.247	5.453	5.466	5.058	-2.794
8059565	PID1	phosphotyrosine interaction domain containing 1	9.975	7.168	7.518	6.939	-2.807
8079237	KIF15	kinesin family member 15	7.634	4.810	4.748	4.632	-2.824
8056572	SPC25	SPC25, NDC80 kinetochore complex component, homolog (S. cerevisiae)	7.649	4.820	4.413	4.504	-2.829
7982889	NUSAP1	nucleolar and spindle associated protein 1	10.341	7.508	6.866	7.352	-2.833
7906930	NUF2	NUF2, NDC80 kinetochore complex component, homolog (S. cerevisiae)	7.822	4.978	4.735	4.621	-2.845
7960340	FOXM1	forkhead box M1	9.003	6.153	6.022	5.835	-2.851
7909568	DTL	denticleless homolog (Drosophila)	10.242	7.388	6.406	6.438	-2.854
8122827	C6orf97	chromosome 6 open reading frame 97	9.207	6.345	6.191	6.024	-2.862
7914878	CLSPN	claspin	8.008	5.144	4.538	4.596	-2.864
8155930	GCNT1	glucosaminyl (N-acetyl) transferase 1, core 2	10.500	7.627	7.187	8.155	-2.873
7991406	PRC1	protein regulator of cytokinesis 1	9.562	6.688	6.087	6.110	-2.875
8033445	CD209	CD209 molecule	10.566	7.691	7.375	7.790	-2.875
8137244	GIMAP4	GTPase, IMAP family member 4	8.858	5.982	5.638	5.793	-2.876
8124388	HIST1H3B	histone cluster 1, H3b	10.879	7.970	6.773	6.996	-2.909
8167971	MIR223	microRNA 223	8.381	5.440	5.893	5.741	-2.941
8166059	TLR7	toll-like receptor 7	9.925	6.973	6.503	6.605	-2.951
7913869	STMN1	stathmin 1	9.815	6.860	6.083	7.021	-2.955
8145570	ESCO2	establishment of cohesion 1 homolog 2 (S. cerevisiae)	10.310	7.339	6.511	6.608	-2.971
8030563	SIGLEC16	sialic acid binding Ig-like lectin 16 (gene/pseudogene)	11.292	8.315	8.217	8.156	-2.977
8021946	COLEC12	collectin sub-family member 12	11.549	8.567	8.637	8.864	-2.982
8061579	TPX2	TPX2, microtubule-associated, homolog (Xenopus laevis)	9.083	6.096	5.345	5.453	-2.987
8001133	SHCBP1	SHC SH2-domain binding protein 1	9.155	6.157	5.652	5.620	-2.998
7923086	ASPM	asp (abnormal spindle) homolog, microcephaly associated (Drosophila)	8.102	5.071	4.786	5.000	-3.031
7937020	MKI67	antigen identified by monoclonal antibody Ki-67	9.489	6.444	6.167	6.301	-3.045
8025103	EMR1	egf-like module containing, mucin-like, hormone receptor-like 1	9.305	6.247	5.818	6.697	-3.058
7929334	CEP55	centrosomal protein 55kDa	9.633	6.558	6.029	6.271	-3.075
7906377	MNDA	myeloid cell nuclear differentiation antigen	10.344	7.237	6.745	7.250	-3.107
7908376	RGS18	regulator of G-protein signaling 18	8.872	5.761	5.582	5.683	-3.112
8163908	GGTA1	glycoprotein, alpha-galactosyltransferase 1 pseudogene	11.138	8.015	7.498	7.298	-3.124
8112940	SSBP2	single-stranded DNA binding protein 2	10.842	7.718	7.420	7.382	-3.124
8007100	IGFBP4	insulin-like growth factor binding protein 4	12.002	8.854	8.627	8.899	-3.148
8151871	CCNE2	cyclin E2	10.450	7.301	6.070	6.178	-3.149
8123744	F13A1	coagulation factor XIII, A1 polypeptide	13.184	10.034	9.904	10.117	-3.150
8094278	NCAPG	non-SMC condensin I complex, subunit G	9.556	6.378	5.488	5.608	-3.177
8017262	BRIP1	BRCA1 interacting protein C-terminal helicase 1	8.428	5.235	4.405	4.814	-3.193
8034772	ASF1B	ASF1 anti-silencing function 1 homolog B (S. cerevisiae)	10.881	7.683	7.182	7.181	-3.198
8021187	SKA1	spindle and kinetochore associated complex subunit 1	7.976	4.764	4.763	4.397	-3.212
7979307	DLGAP5	discs, large (Drosophila) homolog-associated protein 5	8.367	5.149	4.545	4.987	-3.218
7989647	KIAA0101	KIAA0101	9.149	5.826	4.954	5.386	-3.323
7965873	IGF1	insulin-like growth factor 1 (somatomedin C)	11.513	8.157	8.227	8.824	-3.356
8108301	KIF20A	kinesin family member 20A	8.617	5.253	5.116	5.405	-3.364
7940259	MS4A7	membrane-spanning 4-domains, subfamily A, member 7	10.767	7.380	7.055	8.034	-3.388
8059680	HTR2B	5-hydroxytryptamine (serotonin) receptor 2B	9.781	6.378	6.554	7.092	-3.402
8019842	TYMS	thymidylate synthetase	11.044	7.613	6.163	6.947	-3.431
8089568	CD200R1	CD200 receptor 1	10.296	6.854	6.385	6.092	-3.442
7946579	LYVE1	lymphatic vessel endothelial hyaluronan receptor 1	8.659	5.190	5.395	5.100	-3.468

8132318	ANLN	anillin, actin binding protein	10.006	6.518	5.736	5.810	-3.489
8047677	CD28	CD28 molecule	10.302	6.808	6.149	7.032	-3.494
7940147	FAM111B	family with sequence similarity 111, member B	10.346	6.809	5.695	5.702	-3.537
7968344	ALOX5AP	arachidonate 5-lipoxygenase-activating protein	12.616	9.058	8.988	9.507	-3.558
8117594	HIST1H2BM	histone cluster 1, H2bm	12.084	8.514	7.527	7.731	-3.570
7948455	MS4A6A	membrane-spanning 4-domains, subfamily A, member 6A	10.894	7.281	6.927	7.498	-3.613
7927710	CDK1	cyclin-dependent kinase 1	9.123	5.480	4.303	4.861	-3.643
8046695	ITGA4	integrin, alpha 4 (antigen CD49D, alpha 4 subunit of VLA-4 receptor)	9.836	6.169	5.850	6.607	-3.668
8057677	SLC40A1	solute carrier family 40 (iron-regulated transporter), member 1	11.134	7.445	6.495	7.000	-3.689
8065359	CD93	CD93 molecule	11.406	7.698	7.555	8.247	-3.708
7929258	KIF11	kinesin family member 11	9.529	5.685	5.344	5.495	-3.845
8014974	TOP2A	topoisomerase (DNA) II alpha 170kDa	10.283	6.403	5.966	6.359	-3.879
8112007	EMB	embigin	10.984	7.048	6.438	6.942	-3.936
8155754	MAMDC2	MAM domain containing 2	8.920	4.827	5.058	5.092	-4.093
7904158	OLFML3	olfactomedin-like 3	11.495	6.947	6.812	6.741	-4.548
8105481	GAPT	GRB2-binding adaptor protein, transmembrane	9.475	4.842	5.328	4.747	-4.633
7961151	KLRK1	killer cell lectin-like receptor subfamily K, member 1	8.472	3.727	3.818	3.989	-4.745
8036787	FCGBP	Fc fragment of IgG binding protein	11.204	6.426	6.110	6.815	-4.777

Appendix IX

List of osteoclast genes induced by counter-regulated by GSK-J4 in mature osteoclast.

Probe ID	Gene symbol	Gene Name	m	mr	j4	j5	folds(mr-m)	folds (J4-m)
8079733	KLHDC8B	kelch domain containing 8B	8.582	9.603	9.319	9.647	1.021	0.737
7934434	MYOZ1	myozenin 1	6.981	8.256	7.716	7.853	1.275	0.736
8046646	OSBPL6	oxysterol binding protein-like 6	6.185	7.267	6.919	6.488	1.082	0.734
7975607	ACOT4	acyl-CoA thioesterase 4	6.798	7.881	7.531	7.356	1.083	0.733
7962884	RND1	Rho family GTPase 1	6.020	7.177	6.742	6.294	1.157	0.722
8124448	HIST1H4H	histone cluster 1, H4h	8.704	9.837	9.416	9.630	1.133	0.712
8129848	IL22RA2	interleukin 22 receptor, alpha 2	4.970	6.005	5.642	6.225	1.035	0.672
8131682	ABCB5	ATP-binding cassette, sub-family B (MDR/TAP), member 5	5.683	6.690	6.350	6.688	1.007	0.667
8073015	KDELR3	KDEL (Lys-Asp-Glu-Leu) endoplasmic reticulum protein retention receptor 3	6.345	7.469	6.957	6.450	1.124	0.612
8056491	SCN9A	sodium channel, voltage-gated, type IX, alpha subunit	6.077	7.132	6.610	6.870	1.055	0.533
7902623	DNASE2B	deoxyribonuclease II beta	7.701	8.722	8.054	8.011	1.021	0.352
7948910	SNORD25	small nucleolar RNA, C/D box 25	4.696	3.686	4.631	4.361	-1.010	-0.065
7897877	TNFRSF1B	tumor necrosis factor receptor superfamily, member 1B	10.600	9.534	9.927	9.998	-1.066	-0.673
7948904	SNORD28	small nucleolar RNA, C/D box 28	8.572	7.556	7.876	9.039	-1.016	-0.696
8025498	?A70 // SNOF	small nucleolar RNA, H/ACA box 70 // small nucleolar RNA, H/ACA box 70	11.054	9.971	10.347	10.990	-1.083	-0.707
8009913	MYO15B	myosin XVB pseudogene	7.859	6.525	7.136	7.247	-1.334	-0.723
8093539	WHSC1	Wolf-Hirschhorn syndrome candidate 1	7.758	6.750	7.021	6.717	-1.008	-0.738
7948906	SNORD27	small nucleolar RNA, C/D box 27	6.514	5.488	5.770	6.744	-1.026	-0.744
8170863	SNORA70	small nucleolar RNA, H/ACA box 70	10.994	9.875	10.246	10.976	-1.119	-0.749
8158998	SNORD36C	small nucleolar RNA, C/D box 36C	7.928	6.898	7.178	8.062	-1.030	-0.750

Appendix II - III

Tables showing gene expression values (in base 2 logarithm.) of macrophage. Genes expression values having at least two fold change ($\log_2(\text{values}) \geq 1$) upon IL-4 treatment are shown.

-IL-4: PBS

+IL-4: IL4

j4: IL-4 + GSK-J4

j5: IL-4 + GSK-J5

fold IL-4: Fold change upon IL-4 treatment

fold j4: Fold change upon IL-4 + GSK-J4 treatment.

Appendix IV - IX

Tables showing gene expression values (in base 2 logarithm.) of osteoclasts treated at different time point. Genes expression values having at least two fold change ($\log_2(\text{values}) \geq 1$) upon RANKL treatment are shown.

m: M-CSF

mR: M-CSF + RANKL

j4: M-CSF + RANKL + GSK-J4

j5: M-CSF + RANKL + GSK-J5

fold (mr-m): Fold change upon RANKL treatment

fold (mr-j4): Fold change upon RANKL + GSK-J4 treatment.